

United States
Environmental Protection
Agency

Robert S. Kerr Environmental
Research Laboratory
Ada, OK 74820

EPA/600/2-89/033
July 1989

Research and Development



In-Situ Aquifer Restoration of Chlorinated Aliphatics by Methanotrophic Bacteria



IN-SITU AQUIFER RESTORATION OF CHLORINATED ALIPHATICS BY METHANOTROPHIC BACTERIA

by

Paul V. Roberts, Lewis Semprini, Gary D. Hopkins,
Dunja Grbic-Galic, Perry L. McCarty, and Martin Reinhard

Research Staff:

Constantinos V. Chrysikopoulos, Mark E. Dolan, Franziska Haag,
Thomas C. Harmon, Susan M. Henry, Robert A. Johns, Nancy A. Lanzarone,
Douglas M. Mackay, Kevin P. Mayer, and Robert E. Roat

Department of Civil Engineering
Stanford University
Stanford, California 94305

CR-812220

Project Officer

Wayne C. Downs
Processes and Systems Research Division
Robert S. Kerr Environmental Research Laboratory
Ada, Oklahoma 74820

U.S. ENVIRONMENTAL PROTECTION AGENCY
ROBERT S. KERR ENVIRONMENTAL RESEARCH LABORATORY
OFFICE OF RESEARCH AND DEVELOPMENT
ADA, OKLAHOMA 74820

U.S. Environmental Protection Agency
Region 5, Library (PL-12J)
77 West Jackson Boulevard, 12th Floor
Chicago, IL 60604-3590

DISCLAIMER NOTICE

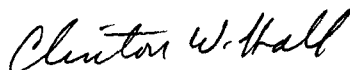
The information in this document has been funded wholly or in part by the United States Environmental Protection Agency under Cooperative Agreement CR-812220 to Stanford University. It has been subjected to the Agency's peer and administrative review, and it has been approved for publication as an EPA document. Mention of trade names or commercial products does not constitute endorsement or recommendation for use.

FOREWORD

EPA is charged by Congress to protect the Nation's land, air, and water systems. Under a mandate of national environmental laws focused on air and water quality, solid waste management and the control of toxic substances, pesticides, noise and radiation, the Agency strives to formulate and implement actions which lead to a compatible balance between human activities and the ability of natural systems to support and nurture life.

The Robert S. Kerr Environmental Research Laboratory is the Agency's center of expertise for investigation of the soil and subsurface environment. Personnel at the Laboratory are responsible for management of research programs to: (a) determine the fate, transport and transformation rates of pollutants in the soil, the unsaturated and the saturated zones of the subsurface environment; (b) define the processes to be used in characterizing the soil and subsurface environment as a receptor of pollutants; (c) develop techniques for predicting the effect of pollutants on ground water, soil, and indigenous organisms; and (d) define and demonstrate the applicability and limitations of using natural processes indigenous to the soil and subsurface environment for the protection of this resource.

This report describes research conducted to develop, evaluate, and demonstrate the efficacy of enhanced biotransformation of chlorinated organic contaminants for in-situ aquifer remediation. The research shows how methanotrophic bacteria can be employed to degrade compounds such as vinyl chloride, 1,2-dichloroethylene isomers, and trichloroethylene, which are widely encountered as ground water pollutants.



Clinton W. Hall
Director
Robert S. Kerr Environmental
Research Laboratory

EXECUTIVE SUMMARY

This project undertook the ambitious task of evaluating the potential of an innovative approach to in-situ aquifer restoration: enhanced biotransformation of chlorinated solvents. The chlorinated solvents investigated included trichloroethylene (TCE), cis- and trans-1,2-dichloroethylene (cis- and trans-DCE), and vinyl chloride (VC). Biotransformation was achieved by creating conditions that promote the growth of a group of bacteria known as methanotrophs, microorganisms that use methane as a source of food and energy under aerobic conditions. The growth of these bacteria can be stimulated by providing methane and oxygen in the proper amounts. These bacteria are able to transform the target chlorinated solvents as secondary substrates through a process termed cometabolism.

This report presents the results of a multidisciplinary investigation that evaluated the technical feasibility of biostimulating native populations of methane-oxidizing bacterial communities to degrade the target chlorinated compounds. The evaluation encompassed a small-scale demonstration of the method's effectiveness under natural conditions at a field site, as well as detailed investigations of the bacterial community's growth and transformation kinetics.

The laboratory studies improved understanding of the growth and transformation kinetics of the microbial population and also characterized the aquifer solids from the field site with respect to important transport properties. These laboratory investigations played an essential role in providing a foundation for designing and interpreting the field demonstration. Mixed cultures of methane-oxidizing bacteria and heterotrophs enriched from samples of the aquifer solids were capable of degrading TCE rapidly and completely under favorable conditions. Pure cultures of methane-oxidizers were isolated that also transformed TCE. It was demonstrated that nutrient media formulations could increase substantially the TCE transformation rates by mixed and pure suspended cultures. Studies with labelled compounds indicated that the transformation by mixed cultures proceeded to form CO_2 and cell mass as the main products, although there was a minor amount of intermediate product of trans-DCE transformation. Column experiments showed that high methane concentrations slowed the transformation of the target compounds through competition for enzyme sites. Sorption experiments showed that the equilibrium relation was approximately linear within the concentration range studied, and sufficiently strong to account for retardation factors on the order of two to ten for the various target organic compounds.

In the field experiments, biostimulation was accomplished by feeding the native population methane and oxygen. Methane utilization commenced rapidly, within ten days in the first biostimulation at the test site, and within one day in subsequent biostimulation episodes. Biotransformation of the target organic compounds ensued immediately after commencement of methane utilization, and reached steady state values within approximately two weeks. The extents of transformation at steady state were as follows: approximately 95% for VC, 85% for trans-DCE, 40% for cis-DCE, and 20% for TCE. These amounts of transformation were achieved in a relatively small biostimulated zone, with travel distances of 1 to 4 meters and residence times of 8 to 25 hours. Mathematical modeling of the transport and transformation processes confirmed that the behavior observed in the field demonstration was entirely consistent with the results of the laboratory research and theoretical expectations. The excellent agreement between the observed behavior and model predictions strengthens confidence in the validity of the results and conclusions.

This research has confirmed that biostimulation of a native population of methanotrophs is capable of substantially enhancing the transformation of halogenated aliphatic contaminants. The transformation rates are moderately high, with half lives on the order of several hours to several days under the conditions

that could be created and maintained in the subsurface environment. Transformation rates of this magnitude are substantially greater than the rates of most natural degradation processes in the subsurface, and if achieved over an extensive domain, would lead to complete degradation over the time spans corresponding to typical aquifer residence times.

Biostimulation of natural methanotrophic bacteria to achieve biotransformation of halogenated alkenes deserves full consideration as an alternative means of groundwater remediation in cases where this group of chemicals constitutes a major part of the contamination. This technology has been demonstrated to be effective in continuous operations in a real subsurface environment at small scale, and is ready for demonstration at a real contamination site where conditions are favorable.

CONTENTS

Foreword	iii
Executive Summary	iv
Figures	ix
Tables	xv
Acknowledgments	xvii
 1. Introduction	 1
Background	1
Research objectives	10
Report organization	11
2. Summary and Conclusions	12
Field demonstration methodology	12
Site characterization	13
Field demonstration of biostimulation and biotransformation	13
Identification of intermediate product	14
Sorption	15
Growth and transformation rates	15
Mathematical modeling	16
Project integration	17
3. Recommendations	18
Recommendations for process research	18
Recommendations for application	19
4. Field Experiment Methodology and Site Characterization	21
Experimental methodology	21
Characterization of the field site	24
Geologic characteristics	25
Site instrumentation	36
The automated Data Acquisition and Control system	39
Analytical system performance	41
Summary	44
5. Results of Tracer Tests	45
Natural gradient tracer tests	45
Induced gradient tracer tests	47
Pulsed injection	61
Summary	63
6. Results of Biostimulation and Biotransformation Experiments	65
Results of the first season of field testing	67
Results of the second season of field testing	73
Results of the third season of field testing	82
7. Formation and Fate of trans-Dichloroepoxide	91
Chemical synthesis of trans-DCO	91
Results	92
Summary	90
8. Sorption	96
Introduction	96
Moffett solids	96
Moffett solids sorption studies	102
Summary	108

9.	TCE Transformation by Mixed and Pure Groundwater Cultures	109
	Introduction	109
	Methods	109
	TCE Degradation experiments	110
	Results	113
	Conclusions	125
10.	Batch Exchange Soil Column Studies of Biotransformation by Methanotrophic Bacteria	126
	Introduction	126
	Materials and Methods	126
	Results	131
	Discussion	143
	Conclusions	145
11.	Continuous Flow Column Studies	147
	Introduction	147
	Methods	148
	Results	151
	Summary	159
12.	One-Dimensional Solute Transport in Porous Media with Well-to-Well Recirculation	162
	Background	162
	Model formulation and solution	163
	Parameter estimation methodology	165
	Application to field experiments	166
	Summary	168
13.	Biostimulation and Biotransformation Modeling	172
	Introduction	172
	Model development	172
	Model simulations of biostimulation experiments	177
	Model simulations of biotransformation experiments	188
	Discussion	194
14.	In-situ Biotransformation Methodologies	197
	Prototype scenarios	197
	Contamination characterization	200
	Comparison of laboratory and field results	200
	Model simulations of restoration scenarios	203
	References	205

FIGURES

<u>Number</u>	<u>Page</u>
1.1 Oxidation of methane by methanotrophs and the initial transformation step in TCE oxidation	4
1.2 Initial oxygenation of TCE by methanotrophs and the transport of the epoxide from the cell	6
1.3 Degradation of chlorinated alkenes by mixed methane-grown microbial enrichments from soil	7
1.4 Anaerobic transformation pathways for selected chlorinated aliphatic compounds	8
1.5 Possible systems for biologically treating a contaminated aquifer	10
4.1 Vertical section of the test zone	22
4.2 Location of the field site, SU-39, at the Moffett Naval Air Station, Mountain View, California	24
4.3 Map of the well field installed at the field site	26
4.4 Fence diagram constructed from inspection of cores and well logs	26
4.5 Particle size distribution of the aquifer core samples based on standard sieve analysis	27
4.6 Automated regression match of the leaky aquifer model to pump test observation well response	29
4.7 Schematic of the injection system	38
4.8 Chlorinated organics delivery system	38
4.9 Schematic of the automated Data Acquisition and Control system	39
4.10 Daily variations in 1,1,1-TCA concentrations due to diurnal temperature fluctuation	42
5.1 Results from the Tracer2 natural gradient tracer test	46
5.2 Results from the Tracer3 natural gradient tracer test	46
5.3 Bromide tracer breakthrough and elution in the Tracer4 experiment	49
5.4 Bromide tracer breakthrough and elution in the Tracer8 experiment	49
5.5 Initial breakthrough of bromide in the Tracer8 experiment	50
5.6 DO breakthrough in the Tracer4 experiment	52

<u>Number</u>	<u>Page</u>
5.7	DO and bromide breakthroughs at the S2 well in the Tracer8 experiment52
5.8	Normalized breakthrough of bromide and TCE at the S1 well in the Tracer5 experiment54
5.9	Breakthrough and elution in the Tracer5 experiment54
5.10	Normalized breakthrough of bromide, trans-DCE, cis-DCE, and TCE at the S1 well in the Tracer11 experiment56
5.11	Normalized breakthrough of TCE during the Tracer8 experiment56
5.12	Response at the S1 and S2 wells to the two-step vinyl chloride addition57
5.13	RESSQ simulations of the injected fluid fronts which develop under induced flow conditions of the tracer experiments with no regional flow60
5.14	RESSQ simulations of the injected fluid fronts which develop under induced flow conditions of the tracer experiments with a regional flow of 300 m/yr60
5.15	Fit of the 1-D advective-dispersion transport model to the breakthrough of DO at the S2 observation well during the Tracer4 test61
5.16	Comparison of predicted and observed effects of dissolved oxygen pulsing63
6.1	Dissolved oxygen (DO) concentration response at the observation wells and extraction well due to biostimulation of the test zone68
6.2	Methane and DO response at the S2 observation well due to the biostimulation of the test zone69
6.3	The response at the S2 observation well resulting from 8- and 4-hr alternate pulses of DO and methane69
6.4	The response at the S1 observation well resulting from 8- and 4-hr alternate pulses of DO and methane70
6.5	Steady-state normalized TCE fractional breakthroughs during the first season's biotransformation experiment, Biotrans471
6.6	Normalized bromide tracer breakthrough for the steady-state period shown in Figure 6.571
6.7	Response at the S1 well of methane, DO, and trans-DCE in the second season's biostimulation-biotransformation experiment, Biostim275
6.8	Response at the S2 well of trans-DCE, cis-DCE, and TCE in the second season's biostimulation-biotransformation experiment, Biostim275
6.9	Fractional breakthrough at the S2 well of trans-DCE, cis-DCE, and TCE under steady-state biotransformation conditions at the end of Biostim2 experiment77
6.10	Production of trans-DCE oxide (epoxide), an intermediate of trans-DCE biotransformation in the Biostim2 experiment77

<u>Number</u>	<u>Page</u>
6.11 Response at the S1 well of TCE and cis-DCE to the reduction (100-200 hrs) and termination (275-475 hrs) of methane addition	78
6.12 Response at the S1 well of trans-DCE and trans-DCE oxide (epoxide) to the reduction (100-200 hrs) and termination (275-475 hrs) of methane addition	79
6.13 Steady-state fractional breakthroughs of the chlorinated organics during the peroxide addition experiment (0-553 hrs) and methane reduction (553-750 hrs) experiments	80
6.14 Decreases in normalized concentration of vinyl chloride, trans-DCE, and cis-DCE at the S2 well in response to biostimulation in the third season	84
6.15 Transient responses of vinyl chloride and trans-DCE at the S1 well due to methane pulsing	85
6.16 Transient responses of vinyl chloride and trans-DCE at the S3 well due to methane pulsing	85
6.17 Decreases in cis-DCE and trans-DCE concentration during the first 380 hrs of biostimulation in the third season	87
6.18 Methane and trans-DCE concentrations at the S1 well for periods of methane (0-350 hrs) and formate (350-500 hrs) addition	87
6.19 Response of trans-DCE and cis-DCE to injection of: 1) methane, 2) formate, 3) methane, 4) methanol, and 5) no electron donor	88
7.1 Pseudo-first-order plots for trans-1,2-DCE epoxide hydrolysis at pH values of 5.0, 7.9, and 10.6	93
7.2 k_{obs} as a function of pH	94
7.3 Concentrations of trans-DCO at observation wells S1, S2, S3, and the extraction well in the Biostim2 experiment	95
8.1 Location of cores used in laboratory sorption studies	97
8.2 Particle size distribution corresponding to the synthesized bulk samples; observed in aquifer solids from core SU-39-6	97
8.3 BET plots for nitrogen and krypton adsorption by silica standard, and nitrogen adsorption by Moffett 20-40 fraction	99
8.4 Nitrogen adsorption/desorption isotherm for Moffett 20-40 fraction	101
8.5 Combined nitrogen adsorption and mercury intrusion cumulative pore size distribution for Moffett 20-40 fraction	101
8.6 Flame-sealed ampule method for batch sorption studies	103
8.7 Sorption isotherm at increasing times for Moffett bulk solids and TCE	103
8.8 Increase of apparent K_d with time for sorption of TCE on bulk and synthesized bulk solids	105

<u>Number</u>	<u>Page</u>
8.9	One-day and thirty-day apparent K_d values for Moffett size fractions and TCE 105
8.10	Sorption isotherms and K_d values for vinyl chloride, cis-, and trans-DCE and Moffett synthesized bulk; determined by headspace variation of flame-sealed ampule method 106
8.11	Sorption rate of TCE by synthesized bulk, showing diffusion model fit 108
9.1	Diagram of LSC assay 112
Plate 9.1	Scanning electron micrographs of ethylene-oxidizing cultures 115
Plate 9.2	Scanning electron micrographs of methane-oxidizing cultures 116
Plate 9.3	Transmission electron micrographs of the methane-oxidizing mixed cultures 117
Plate 9.4	Transmission electron micrographs of pure culture <i>Methylomonas</i> MM2 118
9.2	Effects of methane concentration on percent TCE transformed into the nonvolatile aqueous, CO_2 , and cell fractions by mixed culture MM1 (dry weight = 0.40 mg/ml) 120
9.3	Effects of methane concentration on percent TCE transformed into the nonvolatile aqueous, CO_2 , and cell fractions by mixed culture MM2 (dry weight = 0.33 mg/ml) 121
9.4	Effects of methane concentration on percent TCE transformed into the nonvolatile aqueous, CO_2 , and cell fractions by <i>Methylomonas</i> MM2 (dry weight = 0.12 mg/ml) 121
9.5	Biomass concentration/mass transfer limitation study 123
10.1	Column design 127
10.2	Experimental design for sample mixing and column feeding 128
10.3	Dissolved oxygen concentration versus time for the control column (oxygen and TCE) 132
10.4	Methane concentration versus time for column 4 132
10.5	TCE degradation and concentration in the initial effluent from the control column (oxygen and TCE) 133
10.6	TCE degradation in column 6 (low methane plus nutrients) 134
10.7	TCE concentration in the initial effluent from column 6 (low methane plus nutrients) 134
10.8	TCE degradation in column 3 (high/low methane plus nutrients) 135
10.9	TCE degradation in column 5 (high/low methane no nutrients) 135
10.10	TCE degradation in column 4 (pulse high/low methane plus nutrients) 136
10.11	The 1,2-DCA degradation and concentration in the initial effluent from column 7 (1,2-DCA: low methane plus nutrients) 137

<u>Number</u>	<u>Page</u>
10.12	Percent degradation for TCE and 1,2-DCA in columns 6 and 7, respectively (low methane plus nutrients for both TCE and 1,2-DCA) 137
10.13	Vinyl chloride removal efficiency in biostimulated column versus control column 138
10.14	Methane utilization versus VC removal in a methanotroph enriched column 139
10.15	Effect of hydrogen peroxide addition on methane and oxygen consumption in batch exchange soil columns 141
10.16	Mass balance of ^{14}C -labeled TCE in batch exchange soil columns with fourteen days between exchanges of pore liquid 142
11.1	Design of the continuous flow column 149
11.2	Results of column transport experiments and model simulations 153
11.3	The results of the first biostimulation-biotransformation experiment 155
11.4	The net methane and DO consumption in the biostimulation experiment 156
11.5	Fractional transformation of TCE during methane variation experiments 158
11.6	Labeled CO_2 produced during methane variation experiments 158
11.7	Methane stimulation experiment with trans-DCE 160
11.8	trans-DCE epoxide concentration history 160
12.1.	Comparison of the approximate analytical, semi-analytical, and case of no recirculation solutions: $V = 0.5 \text{ m/d}$, $D = 0.02 \text{ m}^2/\text{d}$, $R = 1$, $\bar{C}_p = 1.0 \text{ mg/l}$, $x = 2.0 \text{ m}$, $l = 6.0 \text{ m}$, $t_p = 40.0 \text{ days}$, and $q = 0.1$ 166
12.2.	Bromide concentration breakthrough data of experiment Tracer8 observed at S1 (squares), and simulated concentration history (solid curve) 169
12.3.	Bromide concentration breakthrough data of experiment Tracer8 observed at S2 (squares), and simulated concentration history (solid curve) 169
12.4.	Bromide concentration breakthrough data of experiment Tracer11 observed at S1 (squares), and simulated concentration history (solid curve) 170
12.5.	Bromide concentration breakthrough data of experiment Tracer11 observed at S2 (squares), and simulated concentration history (solid curve) 170
12.6.	Curve matching with the two-parameter (V and D) classical advection-dispersion model to Tracer8 data observed at (a) S1, (b) S2, and with C_p as an additional fitting parameter, (c) S1, and (d) S2 171
13.1	Arrival of fluid at distances along a direct path from the injection to observation wells under hydraulic conditions of the field experiment based on simulations using RESSQ 178
13.2	Breakthrough of bromide, methane, and DO at the S1 observation well and the fit to equation (13-4) 178

<u>Number</u>		<u>Page</u>
13.3	Model simulation and observed methane and DO response at the S2 observation well in the Biostim1 experiment	181
13.4	Snapshots of the predicted distribution of methane-utilizing biomass during Biostim1 experiment	181
13.5	Model and field response at the S2 well resulting from the change from short to long alternating pulse cycles	183
13.6	Model and field response at the S1 well resulting from the change from short to long alternating pulse cycles	183
13.7	Predicted biomass concentration at the node 2.2 meters from the injection well due to biostimulation with short and long pulse cycles	185
13.8	Snapshot of the predicted spatial distribution of DO and methane during a DO pulse cycle after a steady-state biomass is achieved	185
13.9	Predicted steady-state biomass distributions achieved at two different pulse cycle lengths	186
13.10	Simulated and observed DO and methane response at the S1 observation well during the Biostim2 experiment	186
13.11	Simulation and field response of trans-DCE, cis-DCE, and TCE at the S1 well during the second season's biostimulation experiment (Biostim2)	189
13.12	Simulations and field response of vinyl chloride, trans-DCE, and cis-DCE at the S2 well during the third season's biostimulation experiment (Biostim3)	191
13.13	Simulation of vinyl chloride response at the S2 well using the equilibrium sorption model	191
13.14	Simulation of the aqueous- and sorbed-phase vinyl chloride concentrations at the S1 well using the non-equilibrium sorption model	193
13.15	Simulation of the aqueous vinyl chloride response at the S1 well using the equilibrium sorption model	193
13.16	Simulation of the trans-DCE response at the S1 well to methane pulsing and formate substitution for methane	194
14.1	Two possible bioremediation systems	198
14.2	Simulation of the aqueous phase concentration (boxes) and sorbed phase concentration (crosses) of vinyl chloride at the S2 well resulting from a two step addition of vinyl chloride	202
14.3	Comparison of bioremediation versus pump-and-treat of rapidly degrading, moderately sorbed compounds, such as trans-DCE, based upon the scheme illustrated in Figure 14.1a	204
14.4	Comparison of bioremediation versus pump-and-treat remediation of TCE contamination with and without biostimulation based upon the scheme illustrated in Figure 14.1b	204

TABLES

<u>Number</u>	<u>Page</u>
1.1 Biological Processes and Environmental Conditions Under Which Different Compounds May Be Transformed by Bacteria	3
4.1 Sequence of Experiments and Processes Studied in the Field Evaluation	23
4.2 Parameter Estimates from Regression Analysis Using the Leaky-Aquifer Model	29
4.3 Comparison of Aquifer Parameters Derived from Leaky-Aquifer and Constant-Pressure Models	30
4.4 Groundwater Chemistry: Major Ions and Other Parameters	32
4.5 Trace Chemical Composition of the Groundwater from the SU-39 Site	33
4.6 Organic Carbon Content of Moffett Aquifer Solids	35
4.7 Summary of Analytical Methods and Detection Limit	41
4.8 Summary of Analytical and Injection Performance	41
4.9 Comparison of Variability of Absolute and Normalized Concentration Data for Observation Well S2	43
5.1 Estimates of Regional Velocities Based on the Results of the Natural Gradient Tracer Experiments	47
5.2 Comparison of Bromide Tracer Tests Under Induced Gradient Conditions	48
5.3 Summary of Induced Organic Tracer Tests Performed	53
5.4 Residence Times and Retardation Factors for the Chlorinated Organic Compounds Based on the Time Required to Achieve 50% Fractional Breakthrough	58
5.5 Residence Times and Retardation Factors for the Chlorinated Compounds Based on Center-of-Mass Estimates	58
6.1 Experiments and Processes Studied	65
6.2 Tracer8 Experiment - Percentage Breakthrough of the Organic Solutes and Bromide at the Observation Wells	74
6.3 Percentage Biotransformation in the Second Season's Biostimulation-Biotransformation Experiments	81

<u>Number</u>		<u>Page</u>
6.4	Tracer12 Experiment Percentage Breakthrough of Chlorinated Solutes and Bromide at the Observation Wells	83
6.5	Percentage Biotransformation – Third Field Season	89
8.1	Mass Fraction of Particle Sizes Used to Prepare Synthesized Bulk Samples	98
8.2	Specific Surface Area and Internal Porosity for Moffett Field Size Fractions	100
8.3	Partitioning Coefficients and Aqueous Solubilities of the Solutes Studied with Moffett Bulk and Synthesized Bulk Solids	106
9.1	TCE Transformation Rates	119
9.2	Rate Coefficients for Methane-Oxidizing Mixed Cultures	119
9.3	Mixed Culture TCE Transformation Rates	122
9.4	<i>Methylomonas</i> MM2 TCE Degradation Rates	124
9.5	Mixed Culture MM1 TCE Degradation Rates	124
10.1	The Original Experimental Design	131
10.2	The Distribution of ¹⁴ C in the Initial Effluent Removed from Column 6 after ¹⁴ TCE Addition to the Influent Was Stopped	139
10.3	Feed Conditions for Peroxide Study	140
11.1	Experiments and Processes Studied	152
11.2	Model Results: Mobile-Immobile Zone Model	153
11.3	TCE Biostimulation Results	161
11.4	trans-DCE Biostimulation Results	161
12.1	Estimated Transport Parameters for the Bromide Breakthrough Data of Experiments Tracer8 and Tracer11	167
12.2	Estimated Transport Parameters Obtained by the Classical A–D Model for the Bromide Breakthrough Data of Experiment Tracer8	168
13.1	Basic Features of the Non-Steady-State Biotransformation Model	173
13.2	Input Parameters Used in the Biostimulation Model Simulations	179
13.3	Model Setup Parameters	180
13.4	Comparison of Adjusted Model Parameters for the Biostimulation Experiments (Well S2)	187
13.5	Model Parameters for Simulation of Chlorinated Organics in Biostim2	189
13.6	Model Parameters for Simulation of Chlorinated Organics in Biostim3	192

ACKNOWLEDGMENTS

The authors thank the personnel of the U.S. Navy, especially the Public Works Department at the Moffett Naval Air Station for allowing the Field Site to be located on their base. They have cooperated fully in helping us solve the many logistical problems associated with performing a field study of this type. Public works officer, John Heckman, has been especially helpful in this regard.

We would also like to thank the staff at the Oakland Office of the California Regional Water Quality Control Board for permitting us to perform these experiments. Thomas Berkins, Steve Morse, and Steve Ritchie have provided helpful suggestions which have aided in the design of the experiments.

Members of the Kerr Laboratory of EPA have also provided input to the experimental design and the characterization of the test zone, and have conducted laboratory studies which have helped to guide the field experiments. John Wilson, Michael Henson, and Barbara Wilson provided helpful technical information. We also thank Jack Keeley and William Dunlap, who served as Project Officers during the early stages of this work.

Graduate students and postdoctoral students, who have made significant contributions to the development and characterization of the field site include, in addition to those listed as authors, the following: William Ball, Christoph Buehler, Helen Dawson, Meredith Durant, and Barton Thompson.

SECTION 1

INTRODUCTION

Lewis Semprini, Dunja Grbić-Galić, Perry McCarty, and Paul Roberts

The in-situ remediation of aquifers contaminated with halogenated aliphatic contaminants, commonly known in water supply as chlorinated solvents, is a promising alternative in efforts to protect groundwater quality. Chlorinated aliphatic compounds are frequently observed in groundwater. In a survey of 945 water supplies, Westrick et al. (1984) found trichloroethylene (TCE), tetrachloroethylene (PCE), cis- and/or trans-1,2-dichloroethylene (cis-, trans-DCE), and 1,1-dichloroethylene to be the most frequently appearing compounds other than trihalomethanes. Approaches for the restoration of aquifers contaminated by these compounds based on extracting the contaminated groundwater by pumping and subsequently treating at the surface have been shown to be effective, but often entail great expense and also a risk of transferring the contaminants to another medium, i.e., the atmosphere. To circumvent these difficulties, in-situ treatment of the contaminants has become a potentially favorable alternative, with investigations centering on promoting biotransformation of the contaminants.

Our group at Stanford University has assessed under field conditions the capacity of native microorganisms, i.e., bacteria indigenous to the subsurface environment, to metabolize halogenated synthetic organic contaminants, when proper conditions are provided to enhance microbial growth. Specifically, the growth of methanotrophic bacteria was stimulated in a field situation by providing ample supplies of dissolved methane and oxygen. Under biostimulation conditions, the transformation of representative halogenated organic contaminants, such as trichloroethylene (TCE), cis-1,2-dichloroethylene (cis-DCE), trans-1,2-dichloroethylene (trans-DCE), and vinyl chloride (VC), was assessed by means of controlled addition, frequent sampling, quantitative analysis, and mass balance comparisons.

The field demonstration study was conducted at Moffett Naval Air Station, Mountain View, CA, with the support of the Kerr Environmental Research Laboratory of the U.S. Environmental Protection Agency, and with the cooperation of the U.S. Navy. To provide guidance for and confirmation of the field work and to obtain a more basic understanding of key microbial and physical processes, laboratory experiments were also performed at Stanford University's Water Quality Control Research Laboratory.

This report summarizes the results of both the field study and the associated laboratory studies.

BACKGROUND

The in-situ restoration of aquifer contaminated with hydrocarbons is not a new idea. Raymond (Raymond, 1974; Raymond et al., 1976) pioneered the development of the process for the in-situ reclamation of aquifers contaminated by liquid fuels. This work indicated that by promoting the proper conditions in the subsurface (i.e., by the addition of oxygen and nutrients), a native population of microorganisms was stimulated that degraded the hydrocarbon contaminants. The microorganisms used the hydrocarbon contaminants as primary substrates for growth.

In-situ bioremediation of aquifers contaminated by halogenated aliphatic compounds requires a somewhat different approach, since in most cases the halogenated aliphatic compounds cannot be

utilized by native microorganisms as primary substrates for growth. However, they can be degraded as secondary substrates by microorganisms which utilize another primary substrate for growth. The in-situ bioremediation of aquifers contaminated with organic compounds has been thoroughly reviewed recently (Lee et al., 1988; McCarty, 1988; and Wilson et al., 1986). These articles review the basic microbial, chemical, and physical processes that affect in-situ bioremediation and provide an adequate overview of the basic information on in-situ bioremediation, so that information is not repeated here.

Substrate Utilization Concepts

In this work, the evaluation of the in-situ restoration of aquifers contaminated with chlorinated aliphatic compounds was studied. McCarty (1988) reviewed biological processes and environmental conditions under which different organic compounds are transformed. Contaminants may be transformed as 1) primary substrates for growth, or 2) by co-metabolism or secondary substrate transformation.

Primary Substrate Utilization--

When the contaminant is utilized as a primary substrate, it is a source of energy and carbon for the microorganisms. Under these conditions in-situ biotransformation may be promoted by supplying the appropriate electron acceptor and nutrients to the subsurface.

Secondary Substrate Transformation--

The cells grown on the substrate can sometimes degrade other compounds, called secondary substrates, even though the secondary substrates do not afford sufficient energy to sustain the microbial population (McCarty et al., 1981). However, when the contaminants themselves do not act as a suitable substrate for cell growth, it is sometimes possible to grow a bacterial population by providing an easily metabolized substance, called the primary substrate. To transform contaminants as secondary substrates, both the primary substrate and the electron acceptor must be added to the treatment zone, if one or the other is not present naturally. This results in an even more complex system than when contaminants are degraded as primary substrates.

Cometabolism is one form of secondary substrate transformation in which enzymes produced for primary substrate oxidation are capable of degrading the secondary substrate fortuitously (Brock et al., 1984). We will use the more general term, "secondary substrate transformation," in this report to describe the biotransformation of the chlorinated aliphatics, although the specific transformations dealt with in this work are thought to result from cometabolism.

Transformation Overview--

Table 1.1 summarizes environmental conditions and biological processes under which different compounds may be transformed. Transformations as primary substrates and by co-metabolism (secondary substrate transformation) are presented. While a few chlorinated compounds can be used as primary substrates for growth, the majority are transformed as secondary substrates. Less chlorinated compounds are shown to be more easily transformed by oxidation processes, while more highly chlorinated compounds are more easily transformed by reduction processes.

The transformation of the chlorinated organics by methanotrophic bacteria is an oxidation process. As shown in Table 1.1, TCE can be transformed by either oxidative or reductive processes. One of the advantages of the oxidation process is that complete mineralization of the contaminant can result, whereas the reductive process often produces less chlorinated compounds, some of which are more difficult to degrade under reducing conditions.

The present work, to our knowledge, was the first attempt to demonstrate in-situ bioremediation of chlorinated organics as secondary substrates. The success of this venture depended largely upon the existence of a microbial community indigenous to the subsurface environment, that is capable of metabolizing organochlorine compounds as secondary substrates.

TABLE 1.1. BIOLOGICAL PROCESSES AND ENVIRONMENTAL CONDITIONS UNDER WHICH DIFFERENT COMPOUNDS MAY BE TRANSFORMED BY BACTERIA

<u>Primary Substrates</u>	
Aerobic and anaerobic:	Glucose, acetone, isopropanol, acetate, benzoate, phenol
Aerobic primarily:	Alkanes, benzene, toluene, xylene, vinyl chloride, 1,2-dichloroethane, chlorobenzene
<u>Co-Metabolism (Secondary Substrates)</u>	
Oxidations:	Trichloroethylene, dichloroethylene, dichloroethane, vinyl chloride, chloroform
Reductions:	1,1,1-Trichloroethane, trichloroethylene, tetrachloroethylene, dichloroethylene, dichloroethane, carbon tetrachloride, chloroform, DDT, lindane, polychlorinated biphenyls

Source: McCarty (1988).

Methanotrophic Bacteria

Wilson and Wilson (1985) reported the transformation of trichloroethylene by aerobic microbial communities from soil which were grown on natural gas. Since the main constituent of natural gas is methane, this experiment focused attention on methanotrophs, a physiological group of aerobes which utilize methane (and a limited number of other C1 compounds) as their carbon and energy sources.

Characteristics and Occurrence--

Methanotrophs have been studied extensively, not only owing to their growth substrate specificity and the resulting specialized ecological niche they occupy in the environment, but also because of their capability to cometabolically oxidize a whole range of various organic non-growth substrates.

The characteristics of methanotrophs (and methylotrophs as a broader physiological group) have been summarized in numerous reviews (Quayle, 1972; Anthony, 1975; Colby et al., 1979; Wolfe and Higgins, 1979; Hanson, 1980; Higgins et al., 1981; Hou, 1984a).

In nature, methanotrophs can be found in boundary regions between anaerobic habitats, which are the sources of methane, and the aerobic ones from which oxygen for respiration and methane oxygenation can be extracted. One could expect these bacteria to be present in subsurface environments, where aerobic and anaerobic "pockets" frequently coexist in relatively small areas. This expectation was confirmed in our field investigations.

Since the supplies of their major carbon and energy sources, as well as of oxygen, are frequently uncertain, numerous methanotrophs have developed the capability of forming resting stages (exospores or cysts) which enable them to survive the periods of famine (Hou, 1984a). This ability makes them excellent candidates for subsurface existence.

Depending on fine intracellular membranous structures and the type of carbon assimilation pathway, methanotrophs can be divided into two broad groups: type I, with ribulose monophosphate biosynthetic pathway and bundles of vesicular membranous discs distributed throughout the cell; and type II, with serine biosynthetic pathway and paired membranes aggregated at the periphery of the cell, running throughout it parallel with its outer membrane. There are discrepancies from these two general descriptions, and microorganisms can be found which combine characteristics of both types.

Enzymes--

Regardless of the type, energy generation from the major substrate, methane, is initiated through the activity of a powerful enzyme, methane monooxygenase (MMO). MMO incorporates one atom from the oxygen molecule into methane to create methanol. The other oxygen atom needs to be reduced to water, and therefore, the MMO enzyme requires a reduced electron/proton carrier (a requirement typical for monooxygenases in general).

The enzymes that catalyze subsequent oxidations include methanol dehydrogenase, which catalyzes formation of formaldehyde from methanol; formaldehyde dehydrogenase, which converts formaldehyde to formate; and formate dehydrogenase, which produces CO_2 (upper row in Figure 1.1). Formaldehyde is a branching point in methanotrophic metabolism, since it is used not only for energy generation, but can be channeled into biosynthesis as well.

Tonge et al. (1975) first isolated and partially purified a MMO (from *Methylosinus trichosporium*, a type II obligate methanotroph); it consisted of three components (one soluble and two particle-bound), contained both iron (cytochrome c) and copper as cofactors, and could oxidize ethane, propane, butane, and carbon monoxide in addition to methane. Subsequently, it was shown that cell-free systems derived from resting cell suspensions of methane-grown methanotrophs epoxidized alkenes to the corresponding 1,2-epoxides, and hydroxylated alkanes to the corresponding secondary alcohols and methyl ketones; the MMO activity resided mainly in the particulate fraction of methanotrophs (Patel et al., 1979). Stirling et al. (1979) demonstrated hydroxylation of mono- and dichloromethane by the MMO from this bacterium.

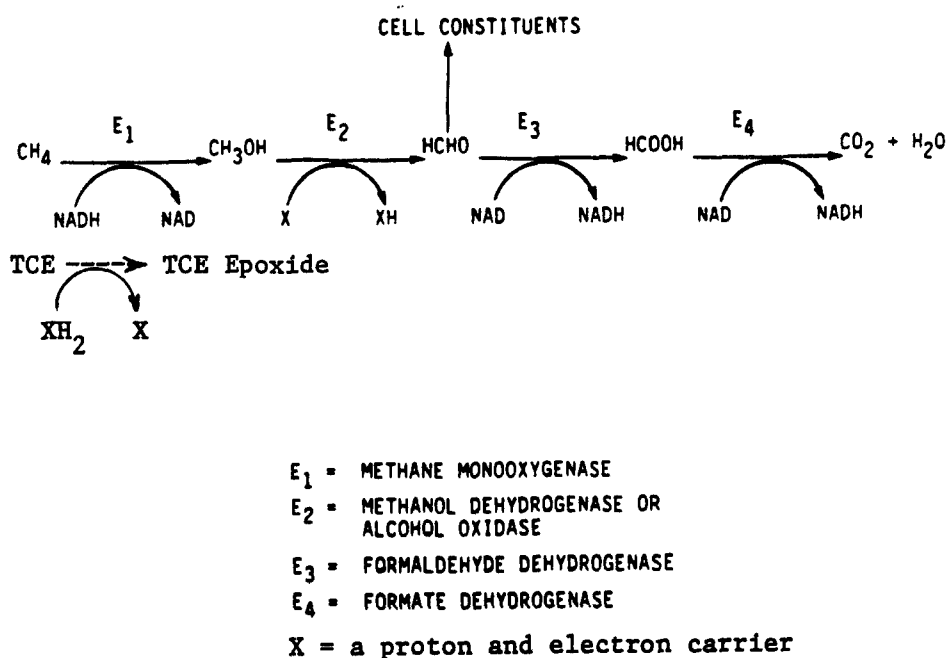


Figure 1.1. Oxidation of methane by methanotrophs and the initial transformation step in TCE oxidation (adapted from Hou, 1984a, and Henry and Grbić-Galić, 1986).

In addition to these particulate fraction activities, a soluble MMO system was purified from *Methylococcus capsulatus* (Bath), a type I obligate methanotroph, and shown to catalyze the oxygenation not only of methane, but also of chlorinated and iodinated methanes, as well as nonhalogenated alkanes, alkenes, ethers, cyclic compounds, alicyclics, and aromatics (Colby et al., 1977). This enzyme was also resolved into three components: "A", containing iron and acid-labile sulfide; "B", a protein of undefined function; and "C", a flavoprotein containing non-heme iron and acid-labile sulfur, which could accept electrons from NADH. Later, Stirling and Dalton (1979) found a soluble MMO in *Methylosinus trichosporium* as well; this enzyme also had a very broad substrate specificity. *Methylobacterium* sp. CRL-26, a facultative methanotroph, was demonstrated to contain both a particulate and a soluble methane monooxygenase activity; the soluble MMO oxidized alkenes, including methylated and brominated alkenes, CO, ethers, cyclic and aromatic hydrocarbons; and hydroxylated alkanes (C2 to C8), chloro-, fluoro-, bromo-, and nitro-methanes, and nitro-alkanes (Patel et al., 1979, 1982; Patel, 1984).

The dispute about the importance and specificity of particulate versus soluble MMO has not been resolved yet, but it seems the expression of the two enzyme classes depends on the growth conditions. For example, particulate MMO activity is associated with low oxygen tension and copper excess, whereas soluble MMO seems to be expressed when oxygen is plentiful but copper is limiting (Hou, 1984a).

From the above discussion, it becomes obvious that MMO is a remarkable enzyme with an unusually broad substrate specificity. Yet, methanotrophs, especially the obligate ones, can grow only on a very limited range of compounds. The process which attacks the non-growth substrates is termed cometabolism (first suggested by Horvath, 1972), and results only in a partial change of the compounds.

Competition between the growth substrate and the non-growth substrate for the active site of the relevant enzyme is very likely to happen, and can greatly influence the transformation of the non-growth compound. If the transformation occurs in a complex natural microbial community, which consists of various populations (e.g., methanotrophs and heterotrophs) working together, complete degradation of a cometabolic substrate can be achieved if its early transformation products can be further transformed by subsequent members of the food chain. This seemed to be the case in the experiment described by Wilson and Wilson (1985), where TCE was completely degraded by a microbial community from soil. The phenomenon warranted further investigation, because of its potential applicability.

TCE Transformation--

Parallel investigations on the capability of methanotrophic- heterotrophic communities to degrade TCE were started in 1985 in the Kerr Research Laboratory (EPA, Ada, Oklahoma), in the Environmental Engineering and Science Program (Civil Engineering, Stanford University), in the Environmental Sciences Division of Oak Ridge National Laboratory (Oak Ridge, Tennessee), and in a consulting company, Cambridge Analytical Associates (Bioremediation Systems Division), Boston, Massachusetts. Henry and Grbić-Galić (1986) at Stanford University suggested a possible mechanism of initial transformation of TCE (Figure 1.1, second row; Figure 1.2) which was based on the well-known capability of methanotrophs to epoxidize alkenes (Hou et al., 1979a; Hou, 1984b) and which involved epoxidation of the TCE molecule by methane monooxygenase, and subsequent transport of the epoxide intermediate out of the methanotrophic cell, where it could be subjected to various other transformations.

The suggested mechanism was accepted by Little et al. (1987a, b; 1988) at Oak Ridge National Laboratory, who used it to explain transformation of TCE by pure cultures of methanotrophs, and incorporated it into the general pathway of TCE transformation by methanotrophic-heterotrophic mixed cultures, involving epoxidation of TCE by methanotrophs, abiotic hydrolysis of the epoxide to nonvolatile products, and subsequent heterotrophic degradation of the products to CO₂, chloride, and water. The details of the pathway are still being investigated by the research group at Stanford, using pure cultures of methanotrophs and mixed methane-grown cultures. There seem to be differences in transformation intermediates depending on the microbial groups involved.

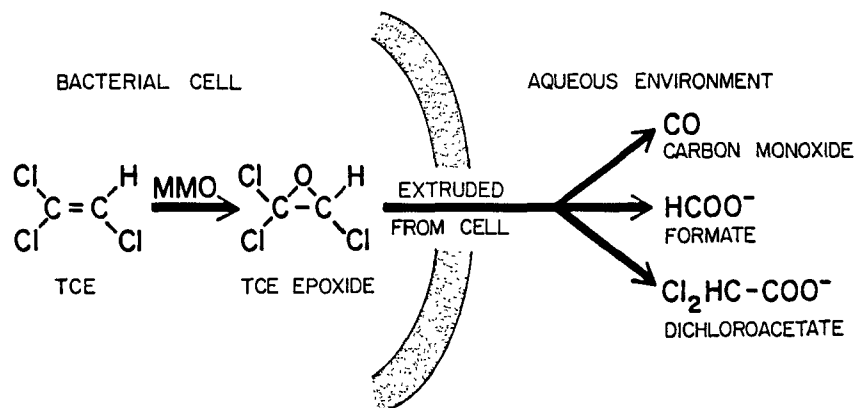


Figure 1.2. Initial oxygenation of TCE by methanotrophs and the transport of the epoxide from the cell (from Henry and Grbić-Galić, 1986).

Fogel et al. (1986) at Cambridge Analytical showed that methane-grown enrichments from fresh-water sediments could degrade TCE, cis- and trans-1,2-dichloroethylene, vinyl chloride, and vinylidene chloride. Early degradation products were water-soluble intermediates; the authors theorized that these intermediates could be further mineralized to CO_2 and other inorganic products. The more highly chlorinated (and therefore highly oxidized) compound, tetrachloroethylene (PCE), was not transformed.

Henson et al. (1987, 1988) at Kerr Research Laboratory demonstrated that a range of halogenated methanes, ethanes, and ethylenes (except PCE) could be completely degraded by mixed methane-utilizing cultures derived from soil (Figure 1.3). However, the details of the methanotrophic transformation process still remained unclear. Important questions remained regarding competition between methane and TCE for the MMO active site, nutritional requirements of mixed cultures and methanotrophs themselves, and other important aspects of this microbial activity. Many of these questions have been resolved during our work on this project, and will be described and explained in the subsequent sections.

Secondary Transformation of TCE by Other Groups of Bacteria

In addition to methanotrophs, other microbial groups show capabilities of transforming halogenated alkenes as non-growth substrates. Henson et al. (1987) used propane as the growth substrate to enrich TCE-degrading mixed cultures from soil. Henry et al. (1988) obtained ethylene-grown cultures which could degrade TCE, but at much lower rates than methanotrophs.

An entirely different group of microorganisms--pseudomonads--were shown by Pritchard and coworkers at Environmental Research Laboratory, EPA, Gulf Breeze, Florida (Nelson et al., 1986, 1987, 1988) to transform TCE while growing on aromatic compounds (toluene or phenol); the microorganisms were enriched from freshwater samples. Some of the laboratory strains of pseudomonads capable of growing on toluene showed similar activity. Depending on the microbial strain, either a dioxygenase (toluene dioxygenase), or a monooxygenase is involved in the TCE oxidation process.

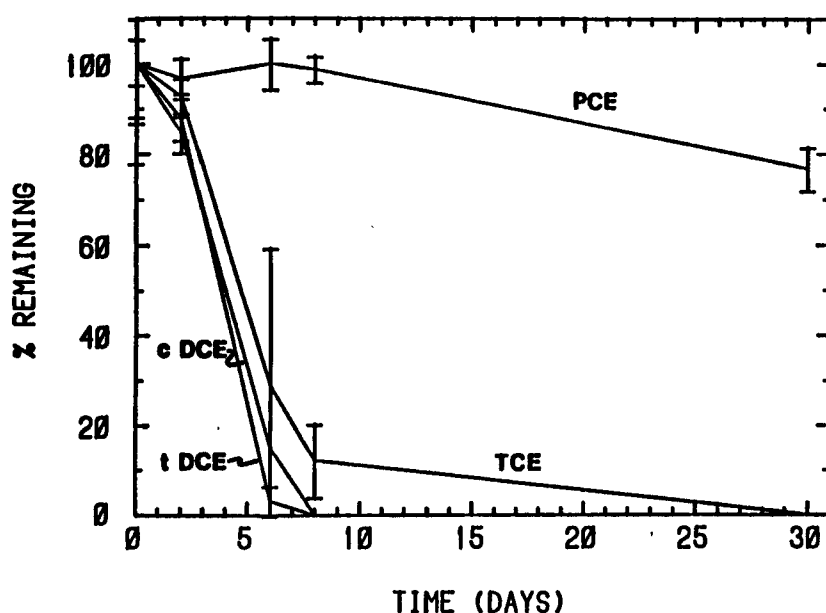


Figure 1.3. Degradation of chlorinated alkenes by mixed methane-grown microbial enrichments from soil (from Henson et al., 1987).

It could be theorized that numerous and diverse microorganisms, if only they contain an oxygenase with relatively broad substrate specificity, could transform halogenated aliphatic compounds. If this were true, this transformational capability could be quite widespread in natural habitats, which would open exciting possibilities for bioreclamation of environments contaminated by chlorinated solvents. This hypothesis warrants further investigation aimed at understanding the active microorganisms, including their physiology, environmental and nutritional requirements, adaptability, and biotic-abiotic interactions, before full advantage can be taken of cometabolism for purposes of aquifer restoration.

Anaerobic Transformations of Halogenated Aliphatic Compounds

Halogenated compounds that are common groundwater contaminants are frequently transformed by both abiotic and biotic processes. Such transformations generally occur most readily under active anaerobic conditions that result from simultaneous contamination with other organic chemicals that are readily susceptible to anaerobic transformations, especially methane fermentation. These reductive transformations can be of significance to the methanotrophic process for in-situ biodegradation that is the subject of this report. Anaerobic transformations lead to the formation of less halogenated compounds that are most readily degraded by methanotrophs. Thus, a brief review of anaerobic transformations is in order.

The occurrence of reductive transformation of halogenated aliphatic compounds in groundwater was first demonstrated in 1981 (Bouwer et al., 1981). Since then, several investigations have elucidated this process so that the environmental conditions required and the transformation products to be expected are now much better understood. In general, anaerobic transformations of halogenated alkanes and alkenes lead to the production of a wide variety of less-halogenated products (Bouwer and McCarty, 1983; Gossett, 1985; Parsons and Lage, 1985; Vogel and McCarty, 1985, 1987; Barrio-Lage et al., 1986; Belay and Daniels, 1987), and the rates of transformation are faster under conditions where methane is formed. Methane-producing bacteria (methanogens as opposed to methanotrophs) are implicated in

many of these transformations (Belay and Daniels, 1987), but other anaerobic bacteria can participate in them as well.

Anaerobic transformations of halogenated solvents follow pathways illustrated in Figure 1.4. Compounds such as tetrachloroethene (PCE) and trichloroethene (TCE) are sequentially reduced to form 1,2-dichloroethene (both cis- and trans-isomers), and then vinyl chloride. Vinyl chloride can also be transformed anaerobically, but the rate is very slow. Another common solvent, 1,1,1-trichloroethane (TCA), can be transformed abiotically into 1,1-dichloroethene and acetic acid (Vogel and McCarty, 1987). TCA can also be reduced biotically to 1,1-dichloroethane (1,1-DCA), and then into chloroethane. However, 1,1-DCA is relatively stable and the rate of transformation into chloroethane is slow.

As reported by others, the reduced products such as 1,2-dichloroethene and vinyl chloride are much more readily biodegraded by methanotrophs than the parent compounds, PCE or TCE. Thus, it may be desirable to have the anaerobic transformations occur first in an aquifer before remediation with methanotrophic bacteria is considered. Indeed, there may be circumstances under which it is desirable to encourage the reductive process. In other cases, one may simply take advantage of naturally occurring reductions that occur in aquifers under the proper conditions.

Implementation of Secondary Substrate Transformation for Bioremediation

Our study evaluated an oxidation process in which methanotrophic bacteria initiate the transformation of the chlorinated aliphatics. In this case, methane and oxygen must both be added to the treatment zone in order to enhance selectively a native methanotrophic population that transforms the chlorinated organics as secondary substrates.

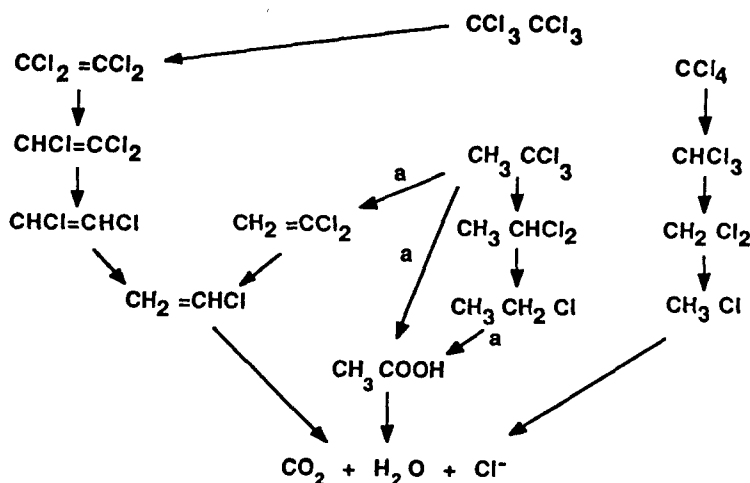


Figure 1.4. Anaerobic transformation pathways for selected chlorinated aliphatic compounds [after Vogel et al. (1987) and McCarty (1988)]. Arrows with "a" indicate abiotic transformations; other arrows represent biotic transformations.

Rate Concepts--

Numerous models have been developed to describe the rate of biotransformation of halogenated organics as secondary substrates. One of the simplest models used when the contaminant concentration is low is given by McCarty (1984):

$$dC_2/dt = - (k/K_s)X_a C_2 \quad (1-1)$$

where C_2 is the concentration of the secondary substrate, X_a is the microorganism concentration, and k/K_s is a ratio of constants that is equivalent to a second-order rate constant. The k value (time^{-1}) represents the maximum specific substrate utilization rate per unit mass of microorganisms per unit time, and K_s is the half velocity constant (mass/volume) which represents the organisms' affinity for the substrate. At low substrate concentrations, the rate of transformation depends on the concentrations of both microorganisms and contaminant.

Biostimulation--

The basic objective of enhanced in-situ bioremediation by secondary substrate transformation is to increase transformation rates in the treatment zone by stimulating a large bacterial population. Equation (1-1) illustrates how this may be accomplished. One means is to increase the concentration of the microbial population of interest. This process, referred to as biostimulation, is accomplished by adding the appropriate electron donor and electron acceptor. In the field experiment the biostimulation of a naturally occurring methanotrophic population required the addition of methane and oxygen.

Enhanced transformation rates might also be achieved through the addition of minor nutrients, adjusting chemical conditions, such as pH, or physical conditions such as temperature. Selection of a specific type of native methanotroph or inoculating the treatment zone with a type that rapidly transforms the chlorinated organics is another means of increasing rates. The information required for such methods of enhancement was not available, and therefore was not evaluated in our field study. Some of the laboratory studies performed as part of this research work focused on obtaining this information.

A third factor which affects the rates of transformation is the contaminant concentration. Physical processes such as sorption onto the aquifer solids act to lower aqueous concentrations, thus decreasing transformation rates, especially in the case where only aqueous-phase transformation occurs. If biotransformation rates are rapid compared to desorption rates from the aquifer solids, the rate at which both the aqueous and sorbed contaminants are transformed may be reduced. To account for this effect, laboratory sorption studies using aquifer solids from the test zone were performed as an important component of this work.

Approaches to Treatment--

The enhanced in-situ biotransformation approach taken in this work required creating an in-situ treatment zone in an aquifer that represented conditions of a real contamination incident. Conceptual models for in-situ treatment systems are given by Lee et al. (1988) and McCarty (1984). The conceptual model of McCarty (1984) is shown in Figure 1.5. Several different forms of biological treatment are shown: 1) surface treatment, 2) a well bore reactor, and 3) treatment in the contaminated aquifer. Our evaluation represented treatments near the well bore and in the contaminated aquifer.

The process evaluated, however, is not limited to subsurface treatment. Surface bioreactors can also be integrated with in-situ treatment. Since in-situ treatment would most likely require the extraction of contaminated groundwater, surface treatment in combination with in-situ treatment would most likely be used in practice.

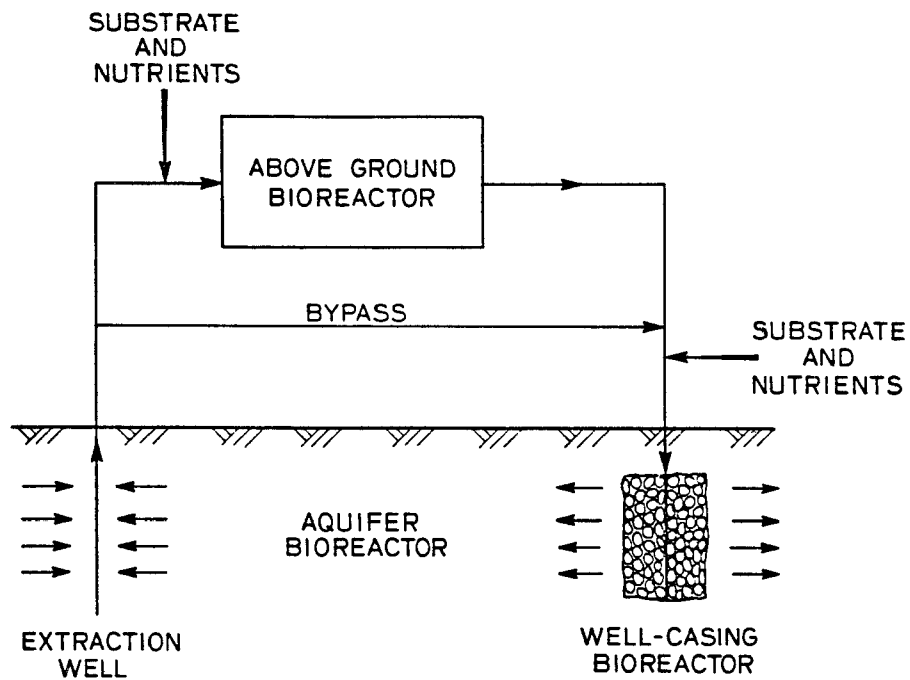


Figure 1.5. Possible systems for biologically treating a contaminated aquifer (McCarty, 1984).

RESEARCH OBJECTIVES

The overall objective of this work was to assess the efficacy of the proposed method for enhancing the in-situ degradation of the halogenated aliphatic compounds. The specific objectives of this research project were to:

- 1) Demonstrate whether the proposed method of promoting the biodegradation of chlorinated aliphatic compounds is effective under controlled experiments performed in-situ, in an aquifer representing conditions typical of groundwater environments;
- 2) Quantify the rate of decomposition, and identify intermediate transformation products, if any;
- 3) Bracket the range of conditions under which the method is effective, and establish criteria for dependable treatment of a real contamination incident;
- 4) Determine factors that affect biodegradation rates by means of basic microbiological studies on methanotrophic bacteria in the laboratory;
- 5) Quantify the sorption of the chlorinated aliphatics on the aquifer solids in controlled laboratory experiments; and
- 6) Simulate the in-situ biodegradation process using a mathematical model that incorporates key biological and transport processes, and adapt suitable models for this purpose.

In order to meet these objectives a combined field, laboratory, and modeling study was performed. The field studies focused on objectives 1, 2, and 3, while the laboratory studies focused on objectives 2, 3, 4, and 5. The modeling effort of objective 6 permitted comparisons between the field and laboratory results.

REPORT ORGANIZATION

In keeping with EPA's required format, overviews of the report's contents and findings are provided in the Executive Summary (preceding the Table of Contents), and in the Summary and Conclusions (Section 2) and the Recommendations chapter (Section 3).

Section 4 presents the methodology of the field experiments that was developed to provide a convincing and objective demonstration of the proposed method. Details of the Automated Data Acquisition and Control system used to continuously monitor the field experiments are presented in this section. The geologic, hydrogeologic, chemical, and microbiological characteristics of the field site are also summarized.

Section 5 presents the results of tracer experiments performed in the test zone. The results of tracer tests under natural gradient and induced gradient conditions are presented. These tests characterized the transport of the chemicals of interest in subsequent biostimulation and biotransformation experiments and quantified the solute residence times.

Section 6 presents the results of biostimulation and biotransformation experiments conducted at the field site; this section contains the principal findings of the field demonstration phase of the project. In Section 6, the response of the natural methanotrophic community following biostimulation with methane and oxygen, and the resulting transformations of the target organochlorine compounds are described. Section 7 deals with the chemistry of the single transformation intermediate identified in the field work.

Section 8 presents the results of laboratory experiments that quantified the sorption characteristics of the aquifer solids and other properties affecting transport. The laboratory studies of microbial growth and transformation of the target compounds are summarized in Sections 9-11. Research conducted with enriched and pure cultures are covered in Section 9. Column studies using aquifer solids from the Moffett site are presented in Sections 10 (batch columns) and 11 (continuous-flow columns).

A new mathematical modeling approach for simulating transport with recycle of extracted solutes is presented in Section 12. The simulation of the transport, biostimulation, and biotransformation observed in the field demonstration are presented in Section 13, together with the development of the mathematical models employed. An orientation toward practical application of this bioremediation approach is offered in Section 14, which describes a scenario for application to aquifer remediation.

SECTION 2

SUMMARY AND CONCLUSIONS

Paul Roberts, Dunja Grbić-Galić, Perry McCarty, Gary Hopkins, and Lewis Semprini

This project demonstrated conclusively the efficacy of enhanced in-situ biotransformation of chlorinated alkenes by microbial communities comprising methanotrophic and heterotrophic bacteria. It proved easy to stimulate the growth of the native population of methanotrophic bacteria by providing oxygen and methane in the proper amounts. Once stimulated, the mixed methane-grown communities metabolized the target chlorinated compounds at rates that ranged from moderately rapid (with a half life on the order of a few days) to very rapid (with a half life of less than one day). In most cases, transformations appeared to progress completely to stable, harmless end products, although in one instance a transitory intermediate product was identified.

The project was organized as a multidisciplinary effort, which encompassed evaluations at a small-scale field demonstration site, as well as detailed studies in the laboratory. The major conclusions of the various aspects of the research, and their interrelationships, are summarized below.

FIELD DEMONSTRATION METHODOLOGY

An effective methodology was developed to evaluate objectively and quantitatively the efficacy of the bioremediation approach for stimulating the growth of the desired bacterial population and transforming the target organic compounds under natural conditions at a field site. The methodology entails creating a flow field dominated by pumping from an extraction well, while introducing solutes in known amounts at a nearby injection well and measuring concentrations regularly at the injection, extraction, and intermediate observation points (Section 4). Interpretation of biotransformation behavior could then be made by qualitative examination of the concentration histories of the various solutes at the several monitoring points, comparing results under biostimulation conditions with results obtained under similar conditions in the absence of biostimulation measures (Section 6). These interpretations could then be substantiated by quantitative mass balances.

A custom-designed, automated data acquisition and control system (Section 4), constructed by the project team for this purpose, provided continuous records of accurate data over sustained periods that enabled us to compute mass balances with relative errors of only a few percent.

Incorporating experimental controls and quantitative mass balances to the extent possible is an absolute prerequisite for meaningful experimentation in the field as well as in the laboratory. Only field and laboratory experimentation of this kind can provide a reliable engineering scientific basis for evaluating and designing in-situ bioremediation strategies.

SITE CHARACTERIZATION

The site chosen for the field demonstration, at Moffett Naval Air Station, offered a near-ideal combination of characteristics (Section 4). The site was representative of a typical situation of groundwater contamination in the San Francisco Bay area and elsewhere, in which a shallow sand-and-gravel aquifer is contaminated by chlorinated aliphatic compounds widely used as solvents. Drilling logs revealed that the aquifer at the test site consisted of a layer of silt, sand, and gravel, approximately 1.2 m thick, at shallow depth (approximately 5 m below the ground surface), well confined above and below by a silty clay layer of low permeability. The formation groundwater was also of appropriate composition for the field experiments. The water was moderately saline and was substantially contaminated by chlorinated organic compounds, mainly 1,1,1-trichloroethane, but was devoid of the chlorinated alkenes (TCE, 1,2-DCE, and VC) chosen as target compounds for this study.

Sustained pump tests showed that the transmissivity was sufficiently high (approximately 100 m²/day) to permit extracting water at the design rate (approximately ten liters per minute) without excessive drawdown at the extraction well. Natural gradient tracer tests showed that the local groundwater velocity was approximately two meters per day. Preliminary mathematical modeling of the flow field, imposing a forced gradient on the natural flow field to simulate injection/extraction operations, showed that injection and extraction rates of approximately one liter per minute and ten liters per minute, respectively, would be sufficient to satisfy the two main requisites for the field experiment from the hydraulic point of view: 1) complete permeation by injected fluid of the aquifer in the observation zone between the injection and extraction points (i.e., minimum dilution by native groundwater in that zone); and 2) complete recovery of the injected fluid at the extraction well (to assure accurate mass balances).

Extensive tracer tests (Section 5) undertaken to quantify transport velocities and residence times in the test zone confirmed that the aquifer was permeated virtually completely by the injected fluid in the observation zone, as evidenced by complete breakthrough of bromide tracer at the observation wells, under the chosen experimental conditions. Further, the overall mass balances, comparing the amounts of tracer injected and extracted, demonstrated that the tracer recovery in the extracted water was essentially complete. This was necessary to assure the validity of the experimental approach.

The hydraulic residence times between the injection well and the three observation wells in the test zone, quantified by tracer tests under the forced gradient conditions, were found to be in the range of 8 to 27 hrs; the residence time between the injection and extraction well was 25 to 40 hrs, depending on the pumping rate. These residence times were later found to be suitable for quantifying the transformation rates of interest in this work. The retardation factors for the organic solutes, evaluated from relative mobility data obtained in the field, were in the range of two to twelve.

FIELD DEMONSTRATION OF BIOSTIMULATION AND BIOTRANSFORMATION

The biostimulation and biotransformation evaluations conducted in the field (Section 6) were consistent in all major respects with expectations based on the laboratory results and theory.

It was confirmed that a native population of methane-oxidizing bacteria could be stimulated by introducing dissolved methane and oxygen into the aquifer in proper amounts, without any other supplementary nutrients. Within ten days, the population of methane utilizers had grown to the point of utilizing substantial amounts of methane, and within another five days methane utilization was complete. Clogging of the injection well and borehole could be controlled effectively by alternately pulsing methane and oxygen, a strategem which also served to spread the microbial growth more uniformly over a larger domain around the injection point. The ratio of oxygen consumption to methane consumption was 2.5 g/g, which is consistent with literature data and laboratory results on methanotrophic growth.

Transformation of the organic target compounds ensued immediately following the beginning of methane utilization, increasing with time as the bacterial population grew, and ultimately reaching a steady-state value that differed among the compounds. The steady-state transformations observed during the final year's field work, quantified by normalization to the bromide fractional breakthrough, were as follows: TCE, 10 to 29%; cis-DCE, 33 to 45%; trans-DCE, 85 to 90%; and VC, 90 to 95%. Of the values cited, the lower end of the range represents the nearest observation point (1 m distant, 8 h residence time), whereas the upper end of the range represents more distant observation points with longer residence times (2 to 4 m; 16 to 27 h). The injected concentrations of the target compounds were in the range of 50 to 100 µg per liter. A chlorinated alkane present as a background contaminant, 1,1,1-trichloroethane (TCA), was not degraded to any appreciable extent.

GC analysis of water samples during active biotransformation of trans-DCE provided evidence of an intermediate transformation product identified in laboratory studies (Section 7) to be the epoxide of trans-DCE, which was present in amounts equivalent to a few percent of the parent compound. No other intermediate products were identified.

Termination of the methane feed was followed by cessation of transformation activity on approximately the same time scale as that of organic transport. This suggested that the microbial population remained active in the absence of methane for only a short time before ceasing to transform the target organic compounds (Section 6). However, the concentration oscillations in response to the alternate pulsing of methane and oxygen suggested methane inhibition. Close examination of the concentration variations indicated that the organic compounds were transformed more fully when the methane concentration was lower.

Substitution of either formate or methanol for methane effectively diminished the effects of methane inhibition and increased transformation rates of organic compounds (trans- and cis-DCE) temporarily (Section 6). However, the substitute electron donors could not sustain growth of the active microbial population indefinitely, which was demonstrated by the decrease in transformation activity after approximately 50 to 100 hrs without methane.

After a prolonged period without methane feed, the population of active methane utilizers declined substantially. However, even after eight months without methane feed an appreciable fraction of the population grown during biostimulation continued to survive. When the test zone was restimulated after the eight-month starvation period, methane utilization commenced immediately and continued to increase until utilization was complete within three days.

Employing peroxide as a means of increasing the electron acceptor dose permitted operating at a higher rate of methane feed and increased biological growth, but did not enhance the rate of transformation of the target organic compounds.

Overall, the field results confirmed the existence of a natural population of methane oxidizers that could be stimulated by introducing methane and oxygen. Moreover, it was demonstrated that quantitative comparisons could confirm the extent of transformation within five percent. Finally, it was observed that substantial transformation of TCE, cis- and trans-DCE, and VC occurred within a distance of a few meters and residence times on the order of several days.

IDENTIFICATION OF INTERMEDIATE PRODUCT

The intermediate product observed in the field work was definitely identified as the epoxide of trans-DCE, namely trans-1,2-dichlorooxirane (1,2-DCO) in the laboratory (Section 7). The compound was synthesized and purified to provide a standard for quantitative analysis. The compound was found to degrade via a hydrolysis mechanism, with a half-life of approximately 4 days at 18°C.

SORPTION

The retardation factors quantified from the field data were consistent with the results of laboratory studies of sorption (Section 8). The sorption of the organic solutes by aquifer core samples from the Moffett site confirmed that sorption equilibrium was approximately linear, justifying the use of a distribution coefficient for interpreting and reporting the sorption equilibrium data. Sorption was strongest for TCE and weakest for VC, among the compounds studied. The retardation factors calculated from the laboratory sorption data agreed closely with those estimated from the transport experiments conducted in the field. The extent of sorption was approximately equal for all grain size fractions, but equilibrium was reached much more slowly in large grains than in small ones. This finding illustrates that the deviations from sorption equilibrium owing to rate limitations may be an important factor influencing transport and biotransformation behavior. The slow rates of adsorption and desorption need to be taken into account by incorporating the appropriate rates into transport and biotransformation models used for simulation and design.

GROWTH AND TRANSFORMATION RATES

Biotransformation studies of several kinds were conducted to characterize the populations of methanotrophic bacteria at the field site. These included studies with enriched mixed cultures and isolated pure cultures grown on nutrient media (Section 9), as well as experiments with the natural population grown on aquifer solids under conditions simulating the field experiments, in batch exchange soil columns (Section 10) and a continuously fed column (Section 11).

The experiments with mixed cultures enriched from Moffett samples (Section 9) evaluated the ability of populations grown on several substrates--methane, propane, and ethylene--to transform TCE as the target compound. Methane oxidizers transformed TCE about one hundred times faster than ethylene oxidizers; propane oxidizers showed no ability to transform TCE. The transformation of TCE in both the methane- and ethylene-oxidizing mixed cultures was complete, although about five percent (methane-grown cultures) to ten percent (ethylene-grown cultures) of the original TCE remained in a nonvolatile aqueous fraction that has yet to be completely differentiated. Pure cultures of both methane- and ethylene-oxidizing organisms were isolated from the corresponding mixed cultures, and were shown to be capable of transforming TCE. Acetylene inhibited both methane oxidation and TCE transformation, implying that the methane monooxygenase (MMO) enzyme was responsible for both processes. Experiments with varying methane concentration revealed that high methane concentration slows or stops the transformation of TCE, presumably through the competition between methane and TCE for the MMO enzyme active sites. The properties of the various cultures enriched from the Moffett aquifer material differed somewhat with respect to transformation rates and the effects of environmental variables on rates. In some, but not all, cultures, TCE concentrations above 10 mg/l were found to inhibit the rates of both methane oxidation and TCE transformation. Cultures containing storage compounds (PHB granules) were able to transform TCE as rapidly in the absence of methane as in the presence of low methane concentrations. This observation suggests the importance of the availability of reducing power in sustaining the normal functions of MMO. Extremely high concentrations of oxygen exercised a slight inhibitory effect as well.

Batch experiments with cultures grown on Moffett solids (Section 10) largely confirmed the results of the experiments with cultures grown on nutrient media, and served to demonstrate the applicability of the results to the specific case of the aquifer at the Moffett site. The ability to conduct concurrently a number of parallel experiments, including controls, enabled the project team to evaluate the effects of parameters such as methane concentration, nutrient requirements, and the choice of electron acceptor and electron donor, under conditions simulating the real subsurface environment.

The experiments showed conclusively that a population of the native methanotrophic community could be stimulated in a porous medium consisting of Moffett aquifer material, without the addition of microbial seed or nutrients. The subsurface environment contained sufficient nitrate and phosphate as a

nutrient source; the column experiments showed that transformation rates were not enhanced by supplying additional nitrogen and phosphorus.

Columns fed with methane and oxygen began to utilize the methane within 7 days, and partial TCE transformation ensued within 80 days, reaching approximately 20% after a year. No significant amounts of intermediate transformation products of TCE were found. Mass balances on columns previously saturated with sorbed TCE and then purged with water for prolonged periods, with and without biostimulation, showed that the TCE was removed from the solids twice as fast by the combination of biodegradation and desorption as by desorption alone. In similar experiments conducted with 1,2-dichloroethane (DCA), the compound degraded to about the same extent as TCE, but concentrations responded more rapidly, as DCA was less strongly sorbed. Vinyl chloride (VC) degraded still more rapidly than DCA, being removed about one-half as fast as methane itself. Within two days, VC degradation was essentially complete.

The concentration observations generally support the hypothesis of enzyme competition, and showed that methane should not be present at too high a concentration. It was further demonstrated that methane does not have to be added continuously for TCE degradation to proceed; TCE transformation persisted for several days after methane depletion, and indeed seemed to be more rapid at very low methane concentrations.

The rate of TCE transformation by suspended mixed and pure methanotrophic cultures increased by an order of magnitude when the growth medium contained the complexing agent EDTA, compared to a growth medium containing nutrients but no EDTA (Section 9). The field results (Section 6) also suggest that TCE degradation can be increased by intermittently supplying an alternative source of reducing power (e.g., a single-carbon compound such as formate or methanol), to maintain transformation activity in the absence of methane. Use of a high concentration of hydrogen peroxide (85 mg/l) as an alternative source of oxygen (electron acceptor) proved to be inhibitory to both methane utilization and TCE transformation (Section 10). The batch growth and transformation experiments allowed evaluation of alternative strategies and operation modes for the field experiments. Results from these efforts helped reconcile microbiological theory and research conducted with cultures grown on nutrient media, on the one hand, with the growth and transformation behavior observed in an aquifer environment, on the other.

The continuous flow column experiments (Section 11) simulated closely the conditions of the field experiment. The experiments were conducted with continuous feed of methane and oxygen (unlike the batch column experiments, Section 10), with a hydraulic residence time of one day, corresponding approximately to the travel times between the injection well and the observation wells at the field site. In the initial biostimulation with methane and oxygen, substantial methane utilization commenced 20 days after beginning the methane feed, increasing rapidly over the next 5 days to the point where methane was completely utilized. The mass ratio of oxygen consumption to methane consumption was approximately 2.5:1. Following attainment of complete methane utilization, transformation of TCE began, ultimately reaching approximately 20%. The extent of transformation of TCE was not improved by raising the influent methane concentration from 4.5 to 6.5 mg/l. On the other hand, TCE transformation did increase substantially (from 22% to 29%) by temporarily ceasing the methane input for a period of up to 20 days. The extent of trans-DCE transformation under similar conditions was much greater than that of TCE (85% vs 22%). Transformation of trans-DCE in the continuous column persisted unabated for more than 40 days after cessation of methane input.

MATHEMATICAL MODELING

A non-steady-state model developed for simulating the results of the field experiments proved useful in interpreting field data and comparing with laboratory results (Section 13). The model incorporated advection, dispersion, sorption with and without rate limitation, and the microbial processes of substrate utilization, growth, halogenated aliphatic transformation, and competitive inhibition. The transport was simplified by assuming one-dimensional, uniform flow, as a computational compromise to permit more rigorous representation of the biological processes. Input parameters were estimated based

on the results of the laboratory research, or on values from the literature. Only the initial population of methane-utilizing bacteria was allowed to vary as an unconstrained fitting parameter.

The model was able to simulate the dynamic behavior of the system very closely, including the concentration oscillations stemming from the pulsed addition of methane and oxygen. The observed transient responses of the target organic compounds were matched closely by the model simulations, using rate parameters that were consistent with the values inferred from rate experiments conducted in the laboratory. Model simulations of the effects of competitive inhibition and rate-limited sorption and desorption also agreed well with the observed behavior, showing substantial attenuation of the organic solute concentrations.

PROJECT INTEGRATION

The coordination between concurrent laboratory and field work proved extremely beneficial. This arrangement facilitated the cooperation between researchers from the relevant disciplines--microbiology, biochemistry, organic chemistry, process engineering, and hydrology--in a manner that assured proper consideration of all of the crucial factors in designing and interpreting the experimental program. This interactive mode also promoted a flexible approach to periodically reevaluating research priorities in the various research tasks: laboratory work could be redirected to address relevant mechanistic questions raised in the field work, and the field demonstration could be modified to take advantage of potential improvements suggested by the laboratory research. For example, the field demonstration program was modified to evaluate the transformation of the DCE isomers and VC after laboratory experiments had shown that these compounds were transformed more rapidly than TCE.

Moreover, the results and conclusions from laboratory research and field work were in general agreement. This provided greater confidence in describing the governing mechanisms and relevant processes than otherwise would have been possible. For example, the column experiments agreed with the results of the field biostimulation and biotransformation in virtually every respect. In particular, the column experiments (Sections 10 and 11) and the field observations of biostimulation and biotransformation (Section 6) agreed remarkably well. The areas of close agreement encompassed the delay in the onset of methane utilization during the initial stage of biostimulation (20 vs 10 days), the observed ratio of oxygen consumption to methane consumption (2.8 vs 2.5 g/g), and the extents of transformation of TCE (approximately 20%), trans-DCE (approximately 85%), and VC (approximately 95%). The batch column results confirmed the field results with respect to the effects of variable methane concentration, and replacement of oxygen with peroxide. However, the laboratory and field tests differed with respect to the effect of terminating the methane feed. The laboratory column experiments indicated that transformation of the halogenated organic compounds persisted for weeks, whereas the field observations exhibited a much more rapid decline in secondary substrate transformation. The laboratory results from the sorption equilibrium and rate experiments were consistent with the parameters estimated from the dynamic tests conducted in the field, which confirmed that sorption is a major factor governing the mobility and availability of organic contaminants in an aquifer. Thus sorption considerations need to be taken into account in evaluating aquifer restoration strategies.

In establishing such connections between laboratory investigations of processes and field investigations of behavior under natural conditions, mathematical modelling was an essential tool in facilitating the transfer of information. In developing appropriate models, it was essential to strike a judicious compromise between the competing goals of accurate process representation and computational feasibility. The mathematical model chosen for the present application stressed relatively complete representation of the relevant biological processes, and compensated with a highly simplified model for advective/dispersive transport. The rate parameter values estimated from the mathematical model simulations of the field data agreed well with the growth rates and TCE transformation rates observed in the laboratory.

SECTION 3

RECOMMENDATIONS

Paul Roberts, Dunja Grbić-Galić, Perry McCarty, Gary Hopkins, and Lewis Semprini

This project has focused on evaluating the potential of aquifer restoration by enhancing the biotransformation of halogenated alkenes, e.g. TCE, cis- and trans-DCE, and VC, through the biostimulation of a community of methane-oxidizing bacteria.

The laboratory research improved the understanding of the processes of microbial growth and transformation, as well as their interrelationships with other processes. It also provided the scientific basis for employing these processes in the subsurface environment. One group of recommendations identifies directions for extension of this kind of applied research to further strengthen our understanding of this potentially useful microbial community, as well as other subsurface phenomena related to aquifer restoration.

The demonstration of the methodology under field conditions confirmed the efficacy of the biostimulation approach. Accordingly, another group of recommendations points out steps toward applying this technology for large-scale cleanup, and for further refining methodologies for field evaluations.

RECOMMENDATIONS FOR PROCESS RESEARCH

1. There is a need to further clarify the roles of the various organisms in the methanotrophic community, including the heterotrophic members. Achieving this goal requires further investigation into the physiology and metabolism of the various organisms, focusing on both enriched mixed cultures and pure cultures. The aim of this research is to be able to specify completely and unambiguously the optimum conditions for growth and secondary substrate transformation. The formation and function of the methane monooxygenase enzyme needs to be elucidated more completely, as does the phenomenon of competition between methane and other compounds for enzyme sites. The potential for sustaining enzyme activity for prolonged periods in the absence of methane, by adding sources of reducing power such as formate or methanol or by biostimulating in such a manner as to create internal sources, deserves further attention as a means of enhancing the degradation of the targeted chlorinated organics.
2. It is essential to delineate the degradation pathways of halogenated compounds more fully, and to reach quantitative understanding of the transformation rates. The roles of abiotic transformation reactions of the epoxide intermediates, such as hydrolysis, need to be appreciated more fully, as well as the biotransformation processes. The kinetics of the individual transformation processes and the influence of environmental factors on the relative rates of alternative transformation processes must be thoroughly comprehended to enable confident prediction of the intermediate and final products. Further, it is crucial to understand the effects of both abiotic and biotic processes in mediating the geochemical conditions that, in turn, govern which processes can transform the contaminants at appreciable rates. Future research should be committed to understanding the interrelations among geochemical conditions and chemical and biological transformations.

3. It is necessary to continue research on the sorption of the targeted organic compounds on real aquifer solids. Biotransformation processes cannot be adequately understood without sufficient understanding of other processes that govern solute transport, distribution, and local chemical conditions in the subsurface environment. Sorption is a major factor influencing the organic contaminants' relative mobility and distribution between the solids and the pore water, and is an important factor to consider in evaluating the prospects for successful in-situ biotransformation. Research must be continued to provide sufficient insight into the sorption equilibrium, the distribution of the sorbed solute within the solid phase, and the relative rates of sorption and desorption, and to demonstrate the validity of the principles for the full spectrum of prospective target chemicals. These insights should permit accurate formulation of expressions representing the sorption/desorption phenomena in mathematical models used to predict transport and transformation. Research in this direction is crucial to successful application of bioremediation technology in the usual situation in which the contamination is largely associated with the solids rather than in solution.
4. It is also essential to verify more conclusively the accuracy of the mathematical model formulation of the biotransformation process, and to refine this formulation if necessary. In particular, the questions related to prolonged transformation activity in the absence of methane and to competition for the enzyme and methane inhibition of cometabolic transformation need to be clarified, and appropriate rate models must be developed.
5. Research and development should be undertaken to adapt the methanotrophic biotransformation technology for application to remediation in the vadose zone. There is every reason to believe that this modification is possible, as it is inherently easier to introduce methane and oxygen in the gas phase than in solution.

RECOMMENDATIONS FOR APPLICATION

6. The approach evaluated here merits full consideration for application to real aquifer remediation cases. This technology should be considered as an alternative where the contamination consists in large part of the compounds for which methanotrophic transformation has been shown effective in the demonstration phase of the present work: namely, VC, trans- and cis-DCE, and possibly TCE. An initial application where the rapidly degraded compounds trans-DCE and VC are present as major contaminants would be ideal. The success of such applications of course will depend on the prevailing conditions and the complexity of the situation. Candidate scenarios for early application of this innovative technology should be well characterized with respect to hydrology, geochemistry, and contaminant distribution. The candidate sites should be reasonably homogeneous, and the contaminant distribution should be well-defined and reasonably uniform throughout an extensive domain; however, it is not essential to restrict the application to a shallow zone such as that investigated at the Moffett site; indeed a deeper zone would be favorable because it would permit operation at higher pressures and correspondingly higher concentrations of oxygen and methane. Any application should be preceded by thorough characterization: not only the usual coring, water sampling and analysis, field hydrogeology and geochemistry, but also supporting studies of the kind illustrated by the laboratory tasks of this research: i.e., batch and continuous column studies of biotransformation rates conducted with core materials from the site and quantification of sorption equilibrium and rates. Such laboratory studies should be continued concurrent with the aquifer restoration operation to aid in evaluating its effectiveness and to assess the experience for generalization to subsequent operations of this kind.
7. Additional development and optimization should be conducted at small scale at a well-instrumented site; the Moffett site is ideally suited for this purpose. Specific tasks to be undertaken in the near term include the following: a) determine whether TCE transformation can be further enhanced by the addition of a chelated mineral or EDTA directly to the test zone; b) evaluate the efficacy of substituting a primary substrate other than methane, such as methanol, once the methanotrophic population has become established; and c) assess alternative methods of methane addition that

would circumvent or minimize enzyme competition by avoiding high methane concentrations in the biostimulated zone (for example by adding methane and oxygen at different locations and allowing them to blend in the aquifer). This additional applied research should be undertaken prior to, or concurrent with, any large-scale application of the methanotrophic approach for aquifer bioremediation.

8. Further development of mathematical models incorporating all processes and phenomena relevant to bioremediation of large-scale subsurface domains is necessary to support aquifer remediation for different treatment scenarios, designs, and operating policies. Models for this purpose will have to account better for the possible effects of aquifer heterogeneity--in physical, chemical, and biological terms--and ultimately will have to be modified to extend to two and three dimensions.
9. A national survey of contamination sites should be undertaken to establish a data base on the ubiquity of methanotrophic communities to permit evaluation of the potential for widespread application of aquifer remediation with natural populations.
10. For application to cases where such natural populations are absent, methodologies should be developed and demonstrated to achieve colonization of the subsurface environment with introduced cultures. Criteria should be elaborated for the preparation of these seed cultures.
11. A technoeconomic evaluation should be undertaken to evaluate the cost-effectiveness of the bioremediation technology described in the present work. The technoeconomic evaluation should encompass a range of scenarios chosen to represent typical conditions at real contaminated sites, and should combine the practical experience of consultants with operations experience in aquifer remediation with the scientific insights embodied in the applied research developed from the present study. This evaluation will serve to assess the promise of the proposed alternative in the overall context of the national remediation effort, and will help identify the kinds of scenarios for which the methanotrophic bioremediation is best suited.
12. The methanotrophic biotransformation approach deserves further development and evaluation as a means of surface treatment, alone or in combination with subsurface application of the same technology.

SECTION 4

FIELD EXPERIMENT METHODOLOGY AND SITE CHARACTERIZATION

Gary Hopkins, Lewis Semprini, Douglas Mackay, Paul Roberts, and Robert Johns

This section will discuss the experimental methodology used in the field evaluation. Results of the detailed site characterization will be presented and the field site instrumentation will also be described.

EXPERIMENTAL METHODOLOGY

The experimental methodology developed to meet the goals of the field study was as follows:

- A. Select a representative demonstration site based on available information regarding regional hydrology and geochemistry, and considering practical and institutional constraints;
- B. Characterize the site by means of coring, pump tests, sampling and analysis of the native groundwater;
- C. Construct a system of wells for injection, extraction, and monitoring of water at the demonstration site;
- D. Design and install an automated system for sampling and analysis of the groundwater at the demonstration site;
- E. Determine the velocity and direction of groundwater flow under natural gradient conditions, by means of bromide tracer tests;
- F. Assess the mobility of the chlorinated aliphatics, relative to bromide tracer, at the demonstration site and quantify residence times in the system under injection/extraction conditions.
- G. Stimulate the growth of native methane-oxidizing organisms by injecting dissolved methane and oxygen (biostimulation mode); and
- H. Assess the transformation of the chlorinated aliphatics under biostimulation conditions.

This methodology provided a staged approach for evaluating the proposed technology. The initial phases of the study (A-E) focus on selecting the field site and characterizing its physical, chemical, microbiological and hydraulic properties. The later phases of the experiment involve biostimulating methane-oxidizing bacteria in the test zone and evaluating the degree of transformation of specific contaminants of interest.

The information obtained during the early phases of the experiments was critical to the success of subsequent evaluation experiments, which were dependent on the ability to run controlled experiments in the subsurface. The hydraulic information obtained in pump tests and tracer experiments was required in designing a fluid injection and extraction system used to create the in-situ treatment zone. The chemical, physical and microbiological characteristics of the test zone also indicated whether favorable conditions existed for the biostimulation of a native population of methane-oxidizing bacteria. These data were necessary for determining whether a controlled evaluation of the proposed technology could be performed at the selected site.

The basic approach of the evaluation experiments was to create a test zone in the subsurface. This was accomplished in our experiments as follows. A series of injection, extraction, and monitoring wells were installed within a shallow confined aquifer, as shown in Figure 4.1. An induced flow field was created by the injection and extraction of fluid. The chemicals of interest for a specific experiment were metered into a stream comprising 10 to 15% of the extracted groundwater and then reinjected. The concentrations of the specific chemicals were monitored at several locations, including the injected fluid, the three monitoring wells, and the extracted fluid. The spatial and temporal responses of the chemicals in the test zone were determined by frequent monitoring, using an automated data acquisition and control system located at the test site.

The sequence of field experiments using this approach is outlined in Table 4.1, where the row numbers are referenced as Stages 1 through 5 in the following text. The initial experiments (Stage 1) studied the transport of bromide ion as a conservative tracer. The experiments determined fluid residence times in the system, the amount of dispersion, and the recovery of the injected fluid at the extraction well. In later experiments (Stages 2 and 3), bromide, dissolved oxygen and the target chlorinated compounds were injected simultaneously. The retardation factors of the different chemicals with respect to bromide, owing to sorption, were determined. The transformation of the chlorinated aliphatic compounds in these experiments was evaluated based on comparisons with the bromide tracer by comparing the steady-state fractional breakthrough achieved at the monitoring wells. These Stage 3 tracer experiments therefore served as quasi controls, permitting a comparison of the observed responses before and after the test zone was biostimulated. Results of these transport experiments are presented in Section 5.

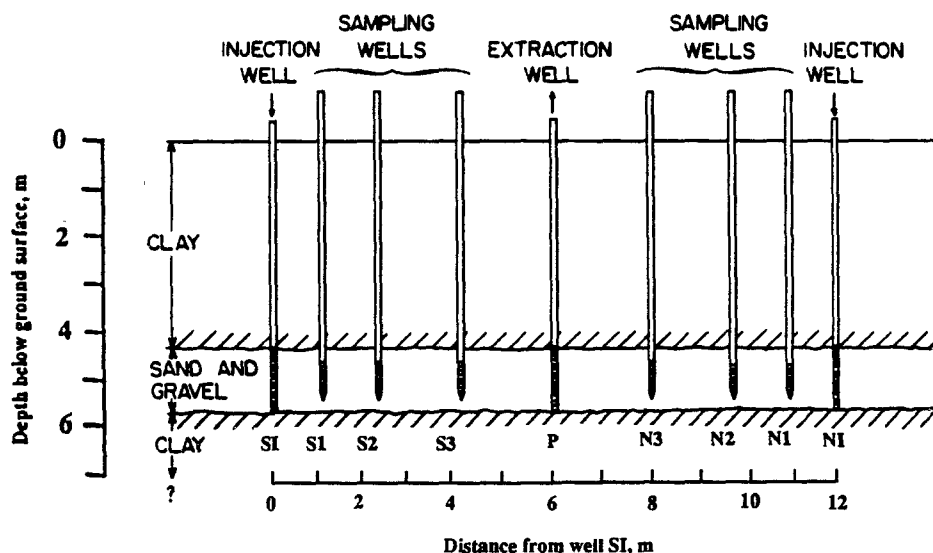


Figure 4.1. Vertical section of the test zone.

TABLE 4.1. SEQUENCE OF EXPERIMENTS AND PROCESSES STUDIED IN THE THE FIELD EVALUATION

Injected Chemicals	Process Studied
1) Br ⁻	Advection/Dispersion
2) Br ⁻ + O ₂	Retardation/Dispersion (TCA - Elution)
3) Br ⁻ + TCE ^a + O ₂	Retardation (Transformation)
4) CH ₄ + O ₂ + (nutrients) + TCE ^a	Biostimulation + Biotransformation
5) Transient experiments	Biotransformation + Competitive Inhibition

^aTCE, cis-DCE, trans-DCE, vinyl chloride.

The biostimulation and biotransformation experiments were performed in Stage 4. Biostimulation involved the addition of methane, oxygen, and nutrients (if required), to stimulate the growth of methane-consuming bacteria in the test zone. The transient response of the different chemical components was monitored, as previously discussed. This experiment determined: 1) how easily the methane-oxidizing bacteria were stimulated and whether nutrients were required, 2) stoichiometric requirements of oxygen to methane, 3) information on the kinetics and the rate of growth, and 4) the areal extent over which biostimulation was achieved.

Biotransformation in response to biostimulation was directly demonstrated by measuring the simultaneous decrease in concentration of the chlorinated aliphatics at observation locations. In the second and third seasons of testing, the chlorinated organics were continuously added after quasi-steady-state conditions were achieved in Stage 3 of the experiments. Thus, the degree of biotransformation was assessed as concentration decreased to steady-state values during transport through the biostimulated zone.

The final stage of the experiments (Stage 5) involved transient experiments to determine how changes in operating conditions affected biotransformations. Transient experiments included terminating methane addition, substituting formate and methanol for methane, and adding hydrogen peroxide instead of oxygen into the test zone. The transient responses of the chlorinated organics to these changes were monitored at observation locations. Results of Stages 4 and 5 are presented in Section 6.

The extents of biotransformation of the chlorinated organics were determined using several methods: 1) comparisons of steady-state fractional breakthrough concentrations at monitoring points, 2) comparisons of steady-state breakthroughs obtained before (Stage 3) and after biostimulation, and 3) complete mass balances on the amounts injected and extracted. In methods 1 and 2 the steady-state fraction (normalized) breakthroughs were calculated by dividing the compound's observed concentration by the injection concentration. Steady-state conditions were operationally defined as an experimental period of several days to a week during which concentrations remained essentially constant. This period followed a transient period, in which concentrations were changing in response to a stimulus, such as a change in input concentration.

Estimates of the degree of biotransformation for methods 1 and 2 were made using equation 4-1:

$$\text{Percent biotransformed} = (1 - C_{f,org}/C_{f,br}) \times 100\% \quad (4-1)$$

where for method 1, $C_{f,org}$ is the mean steady-state fractional breakthrough of the organic solute after biostimulation and $C_{f,br}$ is the mean steady-state fractional breakthrough of bromide over the same time interval. For method 2, the fractional breakthrough of the organic solute before biostimulation is substituted for fractional bromide breakthrough in equation 4-1.

The field evaluation described above consisted of a series of stimulus-response experiments. In order to perform these experiments, a test zone with controlled hydraulic conditions was created in the subsurface through the injection and extraction of groundwater. The stimulus in the experiments was achieved by injecting known quantities of the chemicals of interest in a controlled manner into the test zone. The response was measured in terms of the chemical concentrations of fluid samples taken at observation wells and the extraction well.

In order to perform controlled field experiments, the site was carefully characterized with respect to its physical, chemical, and biological properties. The site was instrumented to permit injection and monitoring of the chemical concentrations of interest.

CHARACTERIZATION OF THE FIELD SITE

Field Site Description

After a reconnaissance study of several sites, a location at the Moffett Naval Air Station, Mountain View, Ca., was chosen (Figure 4.2). The site, designated SU-39, located on the lower part of the Stevens Creek alluvial fan, is approximately 3 km south of the southwest extremity of San Francisco Bay. The surface elevation at the site is 8.5 m above mean sea level.

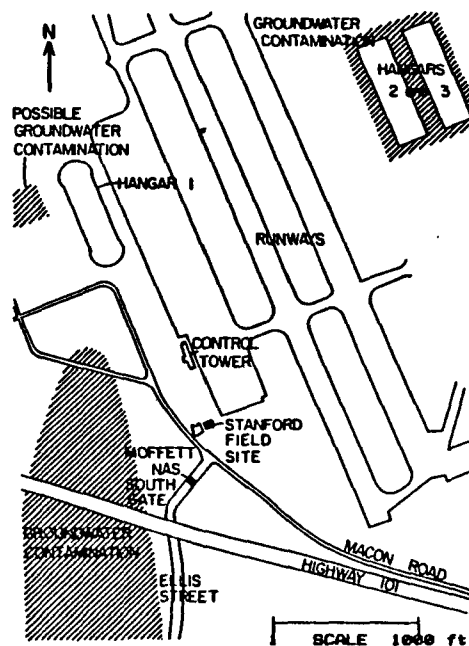


Figure 4.2. Location of the field site, SU-39, at the Moffett Naval Air Station, Mountain View, California.

The experimental site is located in a region where the groundwater is contaminated with several organic solutes for which this bioremediation method might be applied. The area of groundwater contamination shown in Figure 4.2 represents the 1 mg/l TCE contour of the "A" Aquifer delineated in January, 1983 (Canonie Engineers, 1983). The plume contains 1,1,1-trichloroethane (TCA) and trichloroethylene (TCE) at concentrations up to 100 mg/l, measured at points 700 and 1000 m from the SU-39 site. Thus, if effective, the treatment method may have direct use in the area where it was evaluated.

GEOLOGIC CHARACTERISTICS

The geologic characteristics of the test zone were examined using core samples and drilling well logs. Figure 4.3 shows the location of the wells installed at the test site. A series of exploratory wells (1, SI, 3, 4, 5, 6) were installed in July 1985, using the hollow stem auger drilling method. Cores were obtained using 2" pitcher barrels that were pushed ahead of the drill bit. The 6 test drillings identified a shallow, confined aquifer which is known as the "A" Aquifer, the shallowest of several in the region. Well logs indicate that the aquifer is confined between silty clay layers, and is approximately 1.2 m thick; the top border is located 4.4 to 4.6 m below the ground surface, and the bottom ranges from 5.3 to 5.7 m below the surface.

Figure 4.4 is a fence diagram constructed from cores and well logs of the fully penetrating wells SI, P, NI, 5, and 6. Well SI is the injection well and P is the extraction well used in the experiments. The well logs generally show similar lithologic profiles. The uppermost 0.5 m consists of silty sand with pebbles up to 8 cm in diameter. This surface layer is underlain by approximately 4 m of silt and clay of a brownish-black to olive gray color, indicating that the sediment contains organic material. The bottom of this sequence of the upper confining layer is marked by a clayey sand that commonly separates the silt and clay overburden from the underlying aquifer.

The aquifer consists of fine- to coarse-grained sand and appears poorly sorted in most cores. The aquifer, as indicated by the slotted well screens in Figure 4.4, is located 4.3 to 5.8 m below the surface. Gravel lenses with pebbles up to 2.5 cm in diameter occur in some cores within the sand layers. Due to the presence of gravel, intact cores were difficult to obtain. Cores were often lost over the depth interval from 4.7 to 5.2 m below the surface. This zone is considered to have the highest gravel fraction.

The aquifer thickness and composition differs spatially. Along the north-south series of wells (SI, P, NI) the aquifer is composed of a mix of sands and gravels, of fairly uniform thickness. However, profiles in the areas of wells 5 and 6, to the east, show less gravel and more sand, indicating some aquifer thinning compared to the SI through NI region. Cores obtained from wells farther east (not shown) showed that the permeable layer in that location consisted primarily of sand, with no gravel present.

A layer of dark greenish-gray silty clay underlies the aquifer (top at 5.9 m below the surface). While no well was drilled through this clay/silt layer at the project site, other studies in the vicinity have shown that this layer is approximately 7 m thick and is underlain by another aquifer (Canonie Engineers, 1983).

The particle size distributions of aquifer cores are shown in Figure 4.5. Core samples taken from wells 4 and 6 at a depth of 5.5 m and 5.3-5.5 m, respectively, exhibit similar distributions of particle sizes, with a large fraction of the solids being coarse to medium sands and gravel. The core sample from well 5 at a depth of 4.1-4.3 m has a greater fraction of fine sand and silt, which is consistent with well log observations. Petrographic analysis shows that the aquifer solids consist of rock fragments of the parent rock of the Santa Cruz Mountains. These include graywackes, cherts, and volcanics of eugeosynclinal (slope) origin (Franciscan Series).

The observations at the test site are consistent with geologic studies in the region. The inter-layering of coarse and fine sediments in the Santa Clara Valley results from changes in sea level caused by world-wide climate fluctuations (Atwater et al., 1977). During times of high sea level (warm periods), fine-grained estuarine sediments were deposited in the valley, resulting in the clay and silt aquitards. During

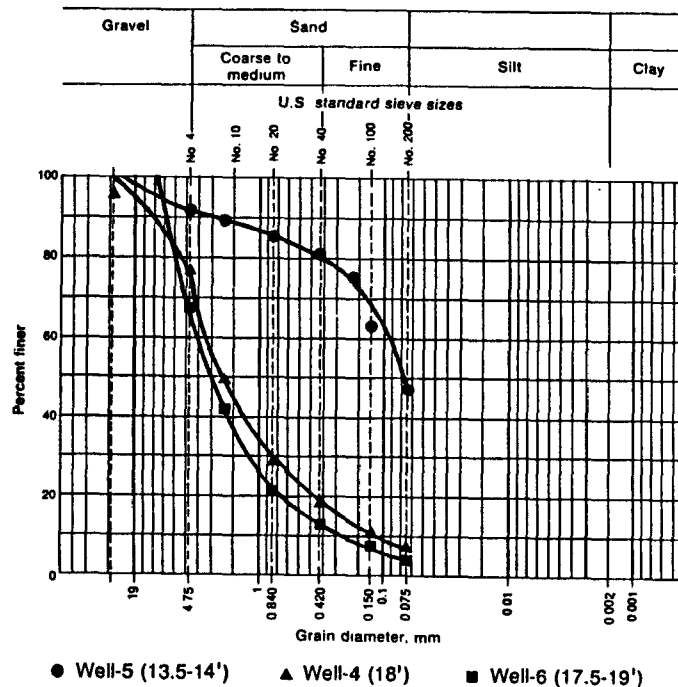


Figure 4.5. Particle size distribution of the aquifer core samples based on standard sieve analysis.

times of low sea level (glaciation in northern latitudes), these sediments were covered by coarser-grained alluvial deposits that form the aquifers. At the study site, the aquifer consists of alluvial sediments deposited during the last 5000 years. The aquifer is spatially heterogeneous, with the composition varying appreciably over short distances. The test zone appears to have the structure of a buried stream channel, containing sand and gravel in some areas and only sand in others. This structure is common in alluvial aquifers, which are characterized by deposition from multiple channels with constantly shifting loci of deposition, resulting in discontinuous lenses of sand and gravel (Press and Siever, 1974).

Hydraulic Characteristics

Maps of the regional piezometric surface of the "A" Aquifer have been reported by Canonie Engineers (1983). The hydraulic gradient is northward at about 4.5 m per km. Piezometric measurements that were made with the original wells of the test zone indicated that the aquifer was confined with a piezometric surface 2.5 m above the top confining layer (6.4 m above mean sea level). The magnitude and direction of the gradient in the test zone was in the range of regional values. The original gradient estimates had a large level of uncertainty due to the short spatial resolution. Wells 11, 12, 13, installed in August 1986, provided a more accurate estimate of the local gradient due to the greater distances between wells. A gradient of 0.0032 in a northerly direction was estimated using these wells.

A series of pump drawdown tests was performed to characterize hydraulic properties of the aquifer. The tests determined the transmissivity, which permitted estimates of the hydraulic conductivity and the natural gradient groundwater velocity. The possible influence of leakiness, barriers, and abnormalities was also examined.

The drawdown tests were conducted using a Hydrologic Analysis System Model SE 200A well test device (In-Situ, Inc.) that consisted of a central mini-computer and downhole pressure transducers. Six

transducers were placed in the wells (SI, P, NI, P1, EI, 6) during the tests. Nine tests were conducted, varying in duration from 30 to 3500 min. Water was extracted at a steady rate from well P while the drawdown versus time was recorded in the extraction well and the observation wells. In one test, test 8, well EI was used as the extraction well. Pressure transducer measurements, accurate to ± 0.3 cm, were recorded as frequently as every second.

A preliminary analysis of the pump tests was made using the graphical semi-log technique and the log-log-type curve-matching method (Semprini et al., 1988). The graphical analysis of the pump tests pointed to the following conclusions: (1) the pump test response matched that of a confined leaky aquifer system; (2) the aquifer had an average transmissivity of $140 \text{ m}^2/\text{day}$, a storativity of 0.00013, and an r/B value of 0.05; and (3) the presence of directional anisotropy was not clearly indicated. The study also recommended the use of unbiased statistical methods in analyzing the pump tests.

A multiple non-linear regression method based on a technique presented by Golub and Pereya (1973), entitled VARPRO (Stanford Computer Science Department, 1973), was used subsequently for automated analysis of the pump test data. VARPRO computes a weighted least-squares fit of the observed data to the chosen aquifer model using a modified version of the Levenberg-Marquardt algorithm. The Laplace space solutions of the well functions were used to represent the aquifer model in the regression analyses; the Stehfest algorithm was used to invert the Laplace space solutions. Details of the methods used are presented by Johns et al. (1989).

The Theis model was the first model evaluated using the non-linear regression method. There was a poor match between observations and the Theis model due to the nearly steady-state drawdown condition reached at late times.

The second model evaluated was that for leakage across the confining layer (Hantush and Jacob, 1955). Figure 4.6 illustrates the excellent agreement between the field data and the leaky aquifer model for observation wells NI and SI. The goodness of fit to the leaky aquifer model is indicated by the low weighted residual variance, only $3.5 \times 10^{-4} \text{ m}^2$. Subsequently, all the observation well data from tests 5, 6, and 7 were regressed to this model. The parameter estimates obtained are summarized in Table 4.2. Values of transmissivity, storativity, and r/B are in the range obtained by the visual log-log matching of the type curves. The regressions, however, showed larger spatial differences with greater variations in transmissivity estimated using the regression fits, compared to visual fitting.

Recharge from a nearby boundary is another phenomenon which could provide pressure support to the "A" aquifer. A solution for a well in a semi-infinite aquifer with a recharge boundary was generated from the superposition of a pumping well and an image injection well. The resulting regression of the field observations yielded an excellent match to the recharge boundary model. Table 4.3 presents a comparison of the parameter and variance estimates for both the leaky-aquifer and constant-pressure models and their fits to the field observations. The variance and transmissivity values for the recharge boundary model and leaky aquifer model are essentially identical. Therefore, it is not possible to distinguish on a statistical basis which of the two alternative explanations is a more likely cause for the deviation from the Theis model.

Average transmissivity values in the western portion of the well field range from $130 \text{ m}^2/\text{d}$ at well NI to $151 \text{ m}^2/\text{d}$ at well SI. Lower average values were noted to the east, ranging from $74 \text{ m}^2/\text{d}$ to $112 \text{ m}^2/\text{d}$ in wells 6, EI, and P1. Aside from this west-east trend there is also a trend from south to north, illustrated by both the decrease from well SI to well NI in the western segment and the decrease from well 6 to well P1 in the eastern segment. Superimposing these two variations suggests an overall southwest to northeast trend in transmissivity, with values decreasing from $151 \text{ m}^2/\text{d}$ in the southwest to $74 \text{ m}^2/\text{d}$ in the northeast. The decline in transmissivity values towards the northeast suggests a decrease in conductivity and/or aquifer thickness in this direction. The average r/B values are greater in the east compared to the west, with respective values of 0.33 and 0.10. This observation is consistent with the decrease in transmissivity to the east.

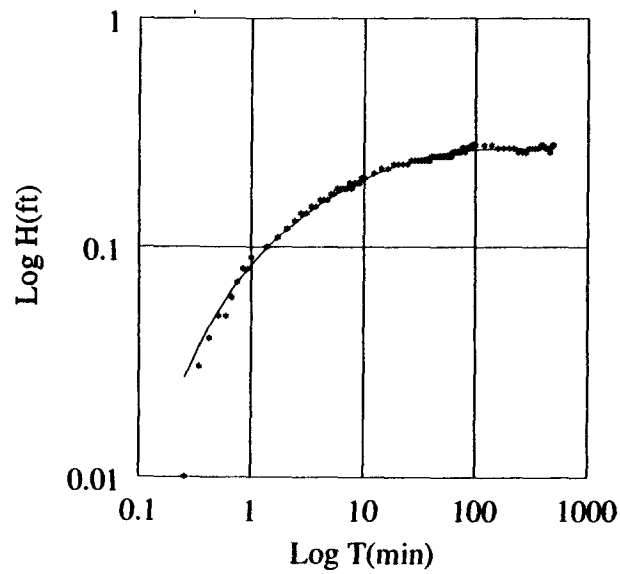


Figure 4.6. Automated regression match of the leaky aquifer model to pump test observation well response.

TABLE 4.2. PARAMETER ESTIMATES FROM REGRESSION ANALYSIS USING THE LEAKY-AQUIFER MODEL

	Well	Transmissivity (m ² /d)	Storativity	r/B
Test 5	Nl	132	0.0011	0.10
	Sl	165	0.0019	0.10
	6	159	0.0034	0.20
	El	*	*	*
	P1	*	*	*
Test 6	Nl	131	0.0011	0.06
	Sl	148	0.0019	0.07
	6	104	0.0025	0.25
	El	*	*	*
	P1	*	*	*
Test 7	Nl	127	0.0015	0.11
	Sl	141	0.0026	0.13
	6	72	0.0043	0.31
	El	90	0.0022	0.33
	P1	74	0.0024	0.42

* Noisy data, regression routine did not converge.

TABLE 4.3. COMPARISON OF AQUIFER PARAMETERS DERIVED FROM LEAKY-AQUIFER AND CONSTANT-PRESSURE MODELS

Well S1, Test 7	Transmissivity (m ² /d)	Storativity	Variance (m ²)
Leaky-Aquifer Model	140.6	0.003	0.00035
Constant-Pressure Model	143.1	0.002	0.00036

The higher transmissivity in the west is consistent with site geology as indicated in the fence diagram, Figure 4.4. More gravel was found in the western section (SI, P, NI), while more sand and clay lenses were found in the eastern section. Although quantitative areal variations cannot be estimated with the models used in this study, the agreement between the well-site geology and the areal trends in the regression-matched pump test results suggests spatial variations in the parameters.

The average storativity value determined from the leaky aquifer model for the test zone is 0.0023, with a standard deviation of 40%. However, despite the large variability in the storativity parameter, none of the estimates were even within an order of magnitude of the storage values expected for phreatic conditions (10^{-1}). Thus, it is clear that confined conditions were observed for the duration of the tests.

Choosing between leakage or a recharge boundary as a model for the aquifer at this test site is difficult; both models fit the pump test data extremely well. Thus, the solution to the model identification problem considered here appears to be non-unique. Subjective criteria, such as the geologic description at the well site, must be used to evaluate which aquifer model is more likely correct. For example, the recharge boundary model estimates the boundary to be 31 m from the pumping well; however, the nearest natural recharge source, Stevens Creek, is located 350 m from the pumping well. Thus, geologic support for a recharge boundary within 35 m of the test site is questionable. Reviewing other studies in the Santa Clara Valley (Harding Lawson Associates (HLA), 1986), there is evidence to support leakage across the aquitard below the "A" aquifer. This gives strong indications that a leaky aquifer model is better suited for the Moffett Field test area.

The leakage parameter estimates from the leaky aquifer model ranged from 0.06 to 0.42, with an average value of 0.19. Using these results, the fraction of fluid leaking across the aquitard was determined at the 6-m radius for the best, worst, and average cases. For the best case, $r/B = 0.06$ ($B = 100$ m), essentially none of the injected or extracted fluid crosses the aquitard. For the worst case, $r/B = 0.33$ ($B = 18$ m), only 10% of the fluid crosses the aquitard. On the average, $r/B = 0.12$ ($B = 50$ m), only 1% of the fluid crosses the aquitard. Since the well layout for the experiments puts all process and observation wells within this 6-m radius, leakage through the aquitard within the process area should be negligible. Thus, despite the low-to-moderate leakage coefficient determined in the regression analysis, the small scale of the pilot area and the high aquifer transmissivity result in minimal leakage at the test site.

The high transmissivity results in an estimated hydraulic conductivity of 100 m/d (based on an aquifer thickness of 1.4 m). The hydraulic conductivity is in the range of values given by Bouwer (1978) for coarse sand (20-100 m/d), gravel (100-1000 m/d), and sand-gravel mixes (20-100 m/d), which is consistent with the aquifer cores as indicated by the particle size distributions shown in Figure 4.5.

The long-term pump tests show that steady-state drawdowns were achieved, and that the aquifer was capable of supplying water at the rates required for the experiments, with less than a one-meter draw-down at the extraction well. The long-term pump tests did not detect any abrupt barriers to flow.

The pump tests indicated that the site had several favorable hydraulic features: 1) high transmissivity would permit the required pumping and injection of fluids into the test zone; 2) loss of permeability by clogging, which might result from biological growth or chemical precipitation, would be limited, owing to the original high permeability; 3) vertical leakage is insignificant, because the test zone is fairly well bounded above and below; and 4) the aquifer is capable of supplying groundwater at rates required for the experiments with less than one meter of drawdown at the extraction well.

One potential problem with the high hydraulic conductivity is that the velocity of the groundwater under natural gradient conditions is high. A velocity of 1 m/d was estimated based on the hydraulic conductivity of 100 m/d, the measured hydraulic gradient across the field of 0.0032, and an estimated porosity of 0.33. This high groundwater velocity limits the control of fluid residence times, since the induced flow field must be operated in such a manner as to overcome the natural flow in order to assure capture of the injected solutes.

Chemical Characteristics

Samples of the groundwater from the A-aquifer were obtained during the pump test program to determine the background concentrations of inorganic and organic components. The analyses provided information on the quality of the groundwater in the area of the test zone and determined whether the aquifer was contaminated with chlorinated aliphatics of interest.

Inorganic Composition--

Table 4.4 presents the major anions and cations, along with other parameters. The charge balance, as well as the measured and calculated TDS, confirms that all of the major ions have been identified. The major cations, in decreasing milliequivalent concentrations, are as follows: calcium > magnesium > sodium > potassium. The major anions are, in declining order: sulfate > bicarbonate > chloride > nitrate. The groundwater hardness is 920 mg/l, based on the calcium and magnesium concentrations, and would be classified as very hard water. Bicarbonate is the major form of alkalinity at the measured groundwater pH of 6.5. The dissolved oxygen content of the groundwater is below 0.2 mg/l.

The analysis of the major chemical components indicates that the test zone is suitable for the experiments. The chemical composition, including the pH, is suitable for the microbial growth. However, because the concentration of dissolved oxygen in the groundwater is very low, all of the oxygen required for microbial growth must be added to the test zone. The presence of high nitrate and low ammonia concentrations indicate that the aquifer is not strongly anaerobic. Thus, major problems associated with the change in the oxidation state by the addition of oxygen were not anticipated, at least from the microbiological point of view. The high calcium concentration was a potential problem, e.g., the precipitation of sulfates and carbonates with changes in fluid chemistry. The chemical composition of the groundwater indicates that the pore water concentrations are close to the solubility limits of gypsum (CaSO_4) and calcite (CaCO_3). Owing to the high sulfate concentration, the groundwater is not considered of drinking water quality; the poor quality of the formation water facilitated obtaining regulatory approval to perform the experiments.

Trace Chemical Analysis--

Analysis for trace element composition was performed by Inductively-Coupled Argon Plasma Spectrometry at the Robert S. Kerr Environmental Research Laboratory (Bledsoe, 1985, unpublished data). Table 4.5 shows that concentrations of all inorganic elements were below 1000 $\mu\text{g/l}$, and in most cases below the detection limit of the analysis. Concentrations were below levels that would be considered toxic to microorganisms, and indicate that the addition of trace nutrients may be required to promote effective microbial growth.

Analyses were conducted to determine the type and concentrations of trace organic compounds at the field site. Four volatile organic compounds were detected, as shown in Table 4.5. The highest concentrations in the native groundwater were found for 1,1,1-trichloroethane (TCA), which is present at an

TABLE 4.4. GROUNDWATER CHEMISTRY: MAJOR IONS AND OTHER PARAMETERS

MAJOR IONS	<u>Concentrations</u>		<u>Milliequivalents</u>
	(mg/l)	(mg/l)	Calculated from Lab 1 results (meq/l)
CATIONS	<u>Lab 1^a</u>	<u>Lab 2^a</u>	
Na ⁺	53.	44.	2.3
K ⁺	2.6	1.5	<0.1
Ca ⁺⁺	200.	216.	10.0
Mg ⁺⁺	100.	93.	8.2
NH ₄ ⁺	<0.1	nd	<0.1
TOTAL	356.	355.	20.5
ANIONS	<u>Lab 1^a</u>	<u>Lab 3^a</u>	
Cl ⁻	42.	39.	1.2
Br ⁻	0.6	<0.2	<0.1
HCO ₃ ⁻	270.	227.	4.4
NO ₃ ⁻	6.9	14.9	0.2
PO ₄ ³⁻	0.1	<0.1	<0.1
SO ₄ ²⁻	750.	699.	15.6
TOTAL	1070.	980.	21.4
CHARGE BALANCE ERROR = 2%			

OTHER PARAMETERS

Total Dissolved Solids (TDS, mg/l)

Measured = 1456 ± 15 (by gravimetric analysis)
 Calculated = 1426 (from major ion analyses)
 Estimated = 1000-1400 (from specific conductance)

pH = 6.5 (measured in the field)

DO < 0.2 mg/l

Temperature = 18°C (measured in the field)

^a Major ion analyses conducted by different laboratories. Lab 1, Lab 2, and Lab 3 refer to Sequoia Analytical Laboratory, Kerr Environmental Research Laboratory, and Stanford University Civil Engineering Laboratory, respectively.

TABLE 4.5. TRACE CHEMICAL COMPOSITION OF THE GROUNDWATER FROM THE SU-39 SITE

TRACE INORGANIC CONSTITUENTS ^a		
Element	DISSOLVED (µg/l)	TOTAL (µg/l)
Fe	nd	540
Mn	300	310
B	150	200
Zn	10	30
Sr	67	76
Ba	20	20
Al	<100	<100
As	<30	<30
Be	<3	<3
Ag	<10	<10
Cd	<3	<3
Co	<10	<10
Cr	<10	<10
Cu	<10	<10
Hg	<30	<30
Li	<10	<10
Mo	<10	<10
Ni	<10	<10
Pb	<20	<20
Ti	<100	<100
Se	<30	<30
Tl	<20	<20
V	<10	<10

TRACE ORGANIC CONSTITUENTS ^b	
Chemical	Concentration (µg/l)
1,1-dichloroethylene (1,1-DCE)	14
1,1-dichloroethane (1,1 DCA)	0.5
1,1,2-trichloro-1,2,2-trifluoroethane (Freon 113)	9.4
1,1,1-trichloroethane (TCA)	97.4 ± 30

^a Determined by Inductively-Coupled Argon Plasma Spectrometry; when results were below detection limit (d.l.), the results are listed as less than (<) the d.l. for the method.

^b Determined by gas chromatography or gas chromatography/mass spectrometry. Values listed are averages of duplicate determinations, except for TCA. TCA analyses were conducted on seven samples taken during the period 7/9/85-11/10/85; the TCA concentrations in the samples ranged in concentration from 56 to 131 µg/l.

average concentration on the order of 100 µg/l, varying over a range of 56-131 µg/l for analyses conducted over several months. Trace amounts of other halogenated compounds are present, as shown in Table 4.5. The organic solutes chosen as targets in the biostimulation experiments (Section 6)--trichloroethylene (TCE), cis- and trans-1,2-dichloroethylene (cis- and trans-DCE), and vinyl chloride (VC)--were not detected in the native groundwater samples.

Analyses were as performed for purgeable aromatics. No such compounds (e.g., benzene, xylene, toluene, chlorinated aromatics), were detected. Total (non-purgeable) organic carbon was determined to be approximately 2 mg/l, within the range of 0.1-10 mg/l reported for groundwaters due the presence of natural humic and fulvic acids (Freeze and Cherry, 1979).

These analyses showed that the native groundwater in the test zone had the following important characteristics with respect to chlorinated compounds:

- 1) The groundwater was contaminated with halogenated organics at low concentrations. This was considered an important criterion for obtaining regulatory approval to conduct the experiments. The concentrations were low, however, and would not be toxic to the native bacteria.
- 2) The concentrations of the target organic compounds (TCE, cis-, and trans-DCE, VC) were below the detection limit. Thus, controlled experiments could be performed by adding small but measurable quantities of the target compounds to the test zone.

The results of the initial inorganic and organic analyses indicated that the groundwater was of a suitable chemical composition for performing the experiments. The chemical composition would not inhibit the stimulation of the methanotrophic bacteria, and it appeared feasible to inject and transport dissolved oxygen in the test zone without undue consumptive losses.

Aquifer Solids Analysis

Core samples of the aquifer material were obtained in order to characterize the aquifer material's physical, chemical, and microbiological properties. Some of the core material was to be used for microbiological studies in the laboratory. Aseptic procedures as outlined by Wilson et al. (1983) were used for obtaining the core samples and transferring the materials to storage containers.

Microbial Enumeration--

The acridine orange-epifluorescence procedure of Ghiorse and Balkwill (1983) was used to enumerate the active bacteria attached to solid samples from the test zone. The analysis indicated that the microorganisms were typically attached to particles of organic matter. The bacterial numbers per gram of dry solids varied from 2×10^6 to 39×10^6 , within the range of values of 1×10^6 to 50×10^6 obtained in subsurface investigations of Ghiorse and Balkwill (1983), Wilson et al. (1983), and Webster et al. (1985). No apparent trend with depth was indicated, but the highest value was observed in the sand and gravel zone, 5.2-5.4 m below the surface. The higher bacteria counts may be associated with the high permeability of this zone and a correspondingly greater flux of nutrients.

The presence of methanotrophic bacteria was not established using this enumeration procedure, since the method is not type-specific. The presence of methane-consuming bacteria on aquifer solids was, however, demonstrated in column experiments which were discussed by Wilson et al. (1987). In these studies, columns were packed with core solids obtained from well S1. After exchanging the pore water with water containing methane and oxygen, oxygen and methane consumption was observed. Results of mixture culture and soil column studies, presented in Sections 9-11, also demonstrated the presence of methane-consuming bacteria. These studies and the bacteria enumeration study indicated that the test zone had an indigenous microbial population that could be successfully biostimulated.

Organic Carbon Content--

The organic carbon content of the Moffett aquifer material was determined by measurement on a Dohrmann DC-80 organic carbon analyzer following pretreatment consisting of acidification with H_3PO_4 and heating under vacuum to remove carbonate, addition of $\text{K}_2\text{S}_2\text{O}_8$, and autoclaving at 121°C for 4 hrs in sealed ampules to oxidize the organic matter to CO_2 (Ball et al., 1989). The ampules were then broken into the oxygen stream of the DC-80 analyzer, and the CO_2 production was quantified by a Horiba nondispersive IR spectrometer. Coarse-grained samples were preground for 10 seconds in a tungsten carbide mill to facilitate complete removal of inorganic carbon and complete recovery of the organic carbon.

Results are summarized in Table 4.6. For the bulk material, the average value was 0.11% carbon, with no significant influence of pregrinding. The organic matter appeared to be concentrated in the clay fraction, which had an organic carbon content six times that of the bulk material, whereas the coarse-grained fractions have organic carbon contents as much as 40% less than the bulk average.

Based on these measurements, it appeared likely that the Moffett aquifer material would exhibit substantial sorption capacity, significantly greater than observed at the Borden site in our previous field experiment (Roberts et al., 1986; Curtis et al., 1986), where the organic carbon content was measured as 0.02%.

TABLE 4.6. ORGANIC CARBON CONTENT OF MOFFETT AQUIFER SOLIDS

Size Fraction	Organic Carbon Content ^a Percent. mean \pm std. dev.	
	ground	not ground
Bulk	0.112 \pm 0.020 ^b	0.110 \pm 0.014
Clay-top		0.649 \pm 0.039
Clay-bottom		0.638 \pm 0.090
U.S. Std. Mesh		
<200		0.161 \pm 0.014 ^c
-100+200	0.113 \pm 0.009	
-60+100	0.087 \pm 0.005	
-40-60	0.100 \pm 0.008	
-20+40	0.062 \pm 0.005	
-8+20	0.095 \pm 0.009	
-4+8	0.082 \pm 0.007	

^a 4 replicates, unless otherwise noted.

^b 3 replicates.

^c 6 replicates.

SITE INSTRUMENTATION

The Well Field

Figure 4.1 presents a vertical section of the test zone and the well field used in the experiments. The well field was originally designed to permit simultaneous experiments by creating two test zones through the injection of fluids at both the south (SI) and north (NI) injection wells, and extraction at the central extraction well (P). The operation of the extraction well was intended to dominate the regional flow field in the study area in an approximation of radial flow. The injection wells were located 6 m from the extraction well. The monitoring wells were located 1.0, 2.2 and 4.0 m from the injection wells. This spacing was chosen to result in roughly equivalent fluid residence times between monitoring wells if radial flow conditions existed.

The extraction and injection wells were constructed of 2" PVC wellstock which is slotted over a 1.5-m screened section. The screened section was positioned 4.3 to 5.8 m below the surface in order to fully penetrate the aquifer. After installation with a hollow stem auger, the borehole around the screened section was back filled with sand (Monterey #8). The internal volume of each injection well was reduced by 60% by inserting a 1.5-m length of 1.75"-OD PVC hollow bar with a packer attached at the top. The hollow bar had twenty 1/8" holes drilled along its length to distribute flow and was plugged at the bottom. The injection solution was delivered via a 1/4"-OD stainless steel (SS) tubing connected to the top of the PVC hollow bar packer.

The monitoring wells were 1.75"-OD stainless steel well casing with a 0.6-m screened drive point (Johnson Wirewound #35 slot). The wells were installed with minimal disturbance of the aquifer by augering to a depth of 4 m and hand-driving the wellpoint to a depth of 4.7 to 5.3 m (± 1 cm). The 0.6-m screen section was placed to intercept what was considered to be the most permeable zone consisting of sands and gravels. A 1/4"-OD stainless steel tube containing a series of orifices along the slotted interval was placed into the sandpoint. The sandpoint was filled with 3-mm glass beads to the top of the screen, which reduced the internal pore volume by 60% and produced a porosity of 38%. A packer was then slid over the 1/4" sampling tube.

The Automated Data Acquisition and Control System as well as the injection system were housed in a control shed adjacent to the well field. Samples from the test zone were pumped to the surface with a Cole-Parmer, multihead peristaltic pump, located in the control building. In order to prevent losses by volatilization and sorption, the fluid injection and sampling lines were fabricated with 1/4"-OD stainless steel tubing. The total maximum volume of the sampling lines and the tubing to the well screen was approximately 300 ml.

The Extraction System

The groundwater extraction system was designed to maintain a very constant rate of fluid withdrawal and permit changes in rates, if desired. The central extraction well was equipped with a shallow well jet pump, essentially a combination of centrifugal and eduction systems. The inlet to the suction pipe was located at a depth of 5.1 m, the center of the screened section. The extracted water was delivered to the instrument/control house where the flow rate was controlled using a pressure regulator and needle valve. Flow rate was measured by an electronic paddle-wheel sensor backed-up by a standard rotameter. Induced gradient conditions were created by extracting groundwater at a rate approximately 7 to 8 times greater than the injection rate. This was required in order to dominate the regional groundwater flow. Extraction rates ranged from 8 to 10 l/min in the experiments. Results of induced gradient bromide tracer tests and modeling studies, described in Section 5, were used to determine the injection and extraction rates.

In order to meet discharge requirements, the excess extracted water was air stripped before it was discharged to a storm sewer. The air stripper was an 8"- ID column packed to a depth of 1.4 m with 5/8" polypropylene Flexrings (Koch). The air stripper was composed of glass segments (Corning) which were

easily acid cleaned to remove carbonate deposits that resulted from air stripping. Air flow was provided by a 600 SCFM high-pressure blower. The air stripper removed more than 95% of the measurable chlorinated aliphatics, and was capable of achieving the discharge requirement of 5 µg/l for each compound.

The Injection System

The chemical injection system was designed to achieve: 1) constant injection rates, 2) constant chemical concentrations, 3) alternate pulse injection of the groundwater containing methane or oxygen, and 4) sampling with minimal disturbance of the system. The system was also designed to automatically shut down when injection water was not being supplied due to a system malfunction.

Figure 4.7 is the schematic of the injection system. The extraction water before air stripping was used as the injection supply water. This greatly reduced the buildup of carbonates in the system. A gear pump pumped the supply water through a nominal 5µ polyester filter and a UV disinfection unit (rated at 4.5 log reduction of *E. coli* at 4 l/min). Rotameters metered the water at a rate of 2 l/min into each of two counter current gas sorption columns, one for oxygen and the other for methane.

The countercurrent sorption columns, fabricated from 4"-OD plexiglass, were 40" long and were packed to a depth of 34" with 1/2" ceramic berl saddles(Koch). Methane and oxygen, as pure gases, were introduced into each of the columns at 330 ml/min. At this flow rate, the columns achieved effluent concentrations ranging from 16 to 20 mg/l for methane and 33 to 38 mg/l for oxygen, about 75% to 80 % of the saturation values. The columns had overflow drains equipped with syphon-type gas traps to keep the gas from flowing out the bottom of the columns, thus decreasing the explosive hazards of working with pure oxygen and methane. Excess gas was vented outside of the instrument/control house.

The injection system also included solenoids and a pulse timer that permitted the alternate injection of groundwater containing either methane or oxygen. This system was adapted in order to avoid biological clogging near the injection well by keeping the electron donor and acceptor separated in that region. This was accomplished by installing a timing clock (not shown in Figure 4.7), that controlled the two pulse solenoids connected to the effluent of the two gas sorption columns. The interval over which each pulse cycle length could be varied ranged from a fraction of an hour up to a full day. By adjusting the pulse cycle duration, the ratio of the amount of methane to oxygen injected could also be regulated.

The groundwater containing either methane or oxygen was pumped by a gear pump to a rotameter and mixer, where the spike solutions containing the chlorinated organics were added. The in-line mixer was a low volume (approximately 20 ml), magnetically stirred mixer. Each spike solution was added as an independent stream to avoid any combined solubility problems. Inorganic spike solutions (bromide tracer, hydrogen peroxide) were made up as batches and pumped into the injection stream via a peristaltic pump.

The system for delivering spike solutions of the chlorinated organics was designed to: 1) maintain constant injection concentrations; 2) change the injected concentration, if desired; 3) add an aqueous spike solution free of any co-solvent such as methanol; and 4) permit the addition of several chlorinated organics, simultaneously. Figure 4.8 shows the solution preparation system, which consisted of a refillable water reservoir, a solute saturation flask, and a multichannel peristaltic pump to inject the spike solutions at the desired flow rates. A separate saturation flask was used for each chlorinated organic compound. Water was drawn from the refillable reservoir through the solute saturation flask via the peristaltic pump. The solute saturation flask, containing a sufficient quantity of pure chlorinated organic solute to have an immiscible phase present, was mixed by a magnetic stirrer to form a saturated aqueous solution of the chlorinated organic. The flask was immersed in a water bath maintained at 21°C.

The flow rate of the solute-saturated spike was controlled by selecting the diameter of the peristaltic pump tube and the pump's motor speed. Stainless steel tubing, 1/16", was connected to the peristaltic pump tube and to transport the solute spike to the in line mixer shown in Figure 4.7.

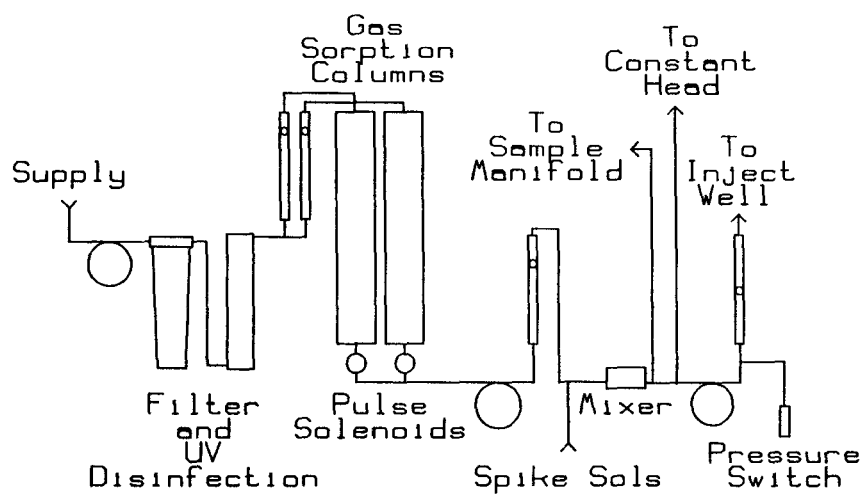


Figure 4.7. Schematic of the injection system.

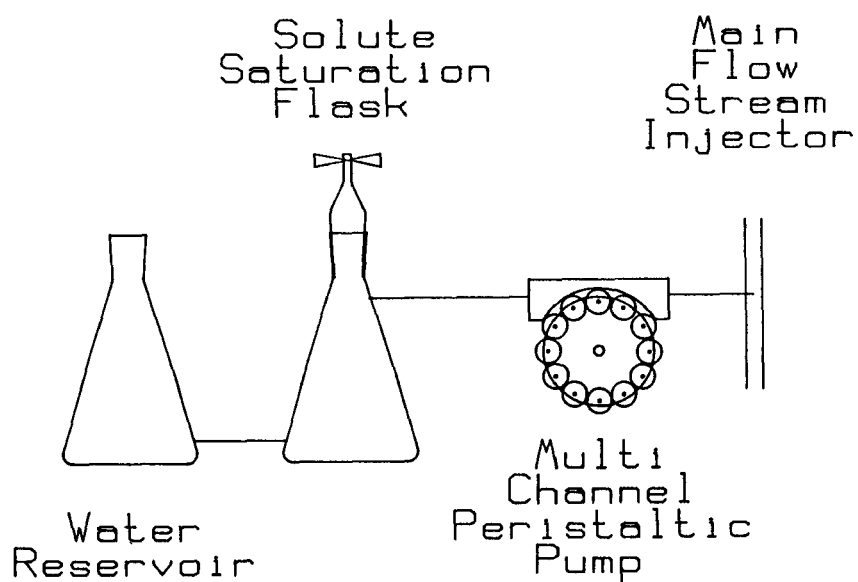


Figure 4.8. Chlorinated organics delivery system.

Upon leaving the mixer the bulk of the injection solution was pumped by a gear pump through the injection rotameter and to the injection well. A pressure switch, connected to the rotameter influent, automatically shut down the three gear pumps and the multichannel peristaltic pump if the rate of injection water supply decreased significantly due to an upstream malfunction. The switch also sent a signal to the automated data acquisition system to alert the field operator of the shut-down.

The side stream of the injected solution was connected to the sampling manifold via a 1/4" SS tube. This side stream flow occurs only when the injected fluid is sampled. The flow from the third side stream goes to a constant head reservoir that overflows into the air stripper. The constant head reservoir keeps the system balanced, maintaining constant injection rates during periods when the injected fluid is being sampled.

THE AUTOMATED DATA ACQUISITION AND CONTROL SYSTEM

Data Acquisition and Control system (DAC) was devised at the test site to implement the field experiments. The system permits the continuous measurement of the experiment's principal parameters: the concentrations of the bromide tracer, methane, halogenated aliphatic compounds of interest, dissolved oxygen, and pH.

Figure 4.9 is a schematic representation of the DAC system. The following instruments were operated by the DAC system, an ion chromatograph (IC) for the bromide tracer analysis, a gas chromatograph equipped with a electron capture (GC-ECD) and a Hall detector (GC-Hall) for the chlorinated organics analysis, a gas chromatograph equipped with a flame ionization detector (GC-FID) for the methane analysis, a dissolved oxygen meter, and a pH meter. The ion and gas chromatographs were fabricated as part of the automated system at the field site.

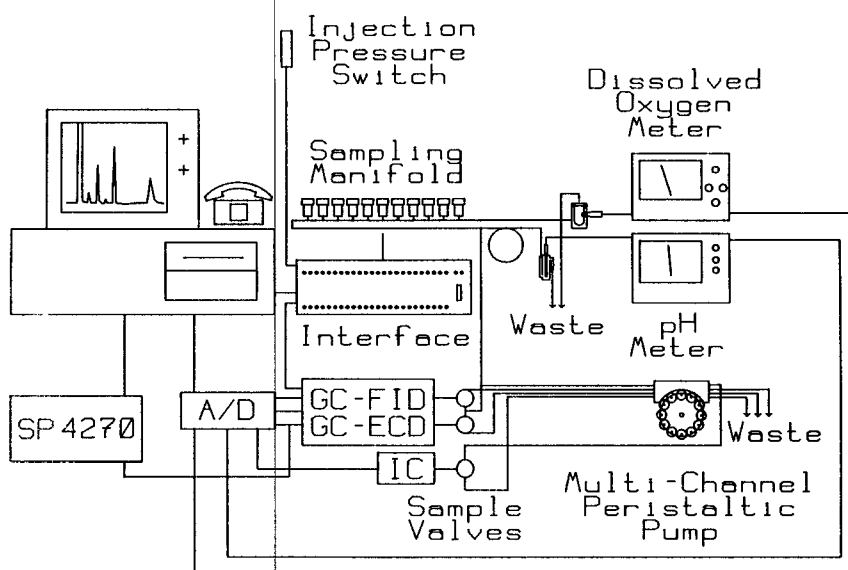


Figure 4.9. Schematic of the automated Data Acquisition and Control system.

The system was driven by a 6 Mhz microcomputer. The computer is equipped with a Techmar Lab Master A/D board for transforming analog to digital response. The system also includes a Techmar Mega-Function board, CGA composite monitor, 20 Mb hard disk, and modem. The program controlling the analytical system was written and compiled with Microsoft's Quick Basic.

The DAC system was run in either manual or automated mode. In manual mode, the operator could 1) select individual sample locations, 2) create a sample table for automated sampling mode, 3) calibrate instruments, 4) produce real-time graphics of current experiments, or 5) analyze stored data and recalculate erroneous data (such as misidentified chromatographic peaks).

The DAC system functioned in automated mode as follows. The DAC system selected from a pre-programmed table the location of the next sample. The multihead Cole Parmer peristaltic pump, used for sampling, was activated through the interface. The sampling manifold was flushed with rinse water (activated carbon treated, nominal 1 μ m filtered, deionized water) for 30 sec at a flow rate of 200 ml/min. The electrically driven solenoid, for the selected sampling location, was opened and pumping was initiated. Pumping was continued for a preset time (approximately 4 min), to obtain a representative sample.

The sample was split into two streams, one flowed through a cell containing the DO probe and the other through a cell containing a pH probe. After pumping at the sampling location for the desired time, the DAC stopped the sampling pump and collected readings from the DO meter and the pH meter. Analog signals were converted to digital output through the Lab Master A/D board.

The DAC then started processing the IC, GC-ECD, GC-Hall and FID analyses. The sample manifold solenoid was held open and the sample was pulled through the chromatograph sample loops by a multi-channel Technicon pump. The sample lines and loops were fabricated of either stainless steel or glass to minimize sample losses due to sorption.

All the analyses were performed simultaneously, with the DAC controlling the analysis and the collection of the data through the Lab Master A/D board. A Spectra-Physics 4270 integrator, which was added to the system in the spring of 1987, processed the output from the GC-ECD, and the GC-Hall analysis. An integrator programmed into the DAC system as a subprogram was used to process the output from the IC and GC-FID.

The data were stored in the systems data base both as integrated peak areas and as computed concentrations. The storage as integrated peaks permitted recalculation of concentrations if a calibration was in question or a peak was misidentified. The stored concentrations could then be plotted by the DAC system providing real time monitoring capabilities.

Upon completion of the analysis, the DAC the system automatically proceeded to the next sample. System interprets could be made at this time in order to enter manual operation.

The system calibrations were performed in manual operation using external standards. The external standards for the GC calibrations required the preparation of a solution containing known concentrations of the compounds of interest in a 100 ml (Spectrum) gas-tight syringe. The syringe solution was first saturated with methane. The chlorinated organics were when added to the syringe solution as standards dissolved in methanol. The standard syringe solution was processed in the same manner as a field sample. This was accomplished by attaching the syringe to the GC sample valves, where the sample manifold normally was connected. The standard solution was then pulled through the sampling loop by the Technicon Pump, in the same manner as the field sample. Similarly, the IC is calibrated with a standard solution fed at the point where it normally connects to the sample manifold. During normal operation the system was calibrated several times a week. The system was also calibrated after maintenance of the analytical equipment.

ANALYTICAL SYSTEM PERFORMANCE

The DAC system proved capable of sustained and reliable operation, and permitted continuous operation and oversight capabilities that would have been unachievable in a manual mode. During 1987, for example, the DAC system collected data over 85% of the year and processed approximately 9,300 samples, yielding approximately 93,000 individual data points. The detection limits for the various analyses are summarized in Table 4.7. The detection limits are generally two orders of magnitude lower than the injected concentrations of the field experiment.

In order to evaluate in the analytical system and the injection system, the average injection concentrations, standard deviations, and coefficients of variation of injection concentrations for one experiment are summarized in Table 4.8. The compounds tabulated in Table 4.8 are broken into four groups based upon type of analysis.

TABLE 4.7. SUMMARY OF ANALYTICAL METHODS AND DETECTION LIMIT

Component	Method of Measurement	Detection Limit
Dissolved Oxygen	Probe	0.1 mg/l
pH	Probe	NA
Anions (Br, NO ₃)	Ion Chromatography	0.5 mg/l
Organic Solutes		
(Freon 113, TCA, TCE)	Gas Chromatography-ECD	0.5 µg/l
(trans-, cis-DCE)	Gas Chromatography-ECD	5 µg/l
(trans-, cis-DCE, vinyl chloride)	Gas Chromatography-Hall	0.5 µg/l
Methane	Gas Chromatography-FID	0.2 mg/l

TABLE 4.8. SUMMARY OF ANALYTICAL AND INJECTION PERFORMANCE

Compound	Mean	Standard Deviation	Number of Observations	Coefficients of Variation (%)
Freon 113	4.3	0.8	169	18.4
trans-DCE	121	19.8	167	16.3
cis-DCE	140	23.3	164	16.6
TCA	46.0	10.8	169	23.6
TCE	47.3	6.9	169	14.5
DO	35.0	2.4	61	6.9
Methane	16.9	2.3	27	17.6
Bromide	45.9	3.0	81	6.5
Nitrate	56.8	3.3	82	5.8
pH	6.5	0.2	89	NA

The first group are compounds measured by the GC-ECD, including the three spiked chlorinated solutes, trans-1,2-dichloroethylene (t-DCE), cis-1,2-DCE (c-DCE), and TCE. The concentrations range from 4 µg/l for Freon as a background contaminant to 140 µg/l for cis-DCE. The coefficients of variation fall within expected bounds for all cases, and do not exceed 25%. In the ECD group, the compounds native to the groundwater, Freon 113 and TCA, show the greatest coefficient of variation. This is probably due to unequal gas flows through the two gas sorption columns, which strip a fraction of these recycled compounds.

The second group consists of methane and DO, which were alternately pulse-injected at a ratio of 1:2 (methane:oxygen). In actual operation methane gas flow was stopped while an oxygen pulse was being injected. This may contribute to some variability in the measured methane concentrations. Nonetheless, the coefficient of variation achieved for the methane analysis, 18%, conforms to the precision expected for this type of GC analysis. The dissolved oxygen measurements are very consistent, as indicated by the low coefficient of variation of 6.9%.

The third group of compounds consists of the anions, which are measured by IC. Bromide was added as a conservative tracer, whereas nitrate was native to the groundwater. The IC data were very reproducible, with standard deviations of approximately 6 to 7%. The final parameter measured was pH, which was also very reproducible, with a precision of ± 0.2 pH unit.

The compounds that were measured by GC analysis were found to have the greatest variability. Daily changes in temperature at the site, which caused diurnal variations in measured concentrations, is one reason for this. In Figure 4.10, minimum values in TCA concentrations are shown to occur at about 4 AM while maximum values occur at 3 PM. This is in response to nightly cooling and warming in the afternoon. Although considerable effort was made to reduced these variations, they could not be completely eliminated.

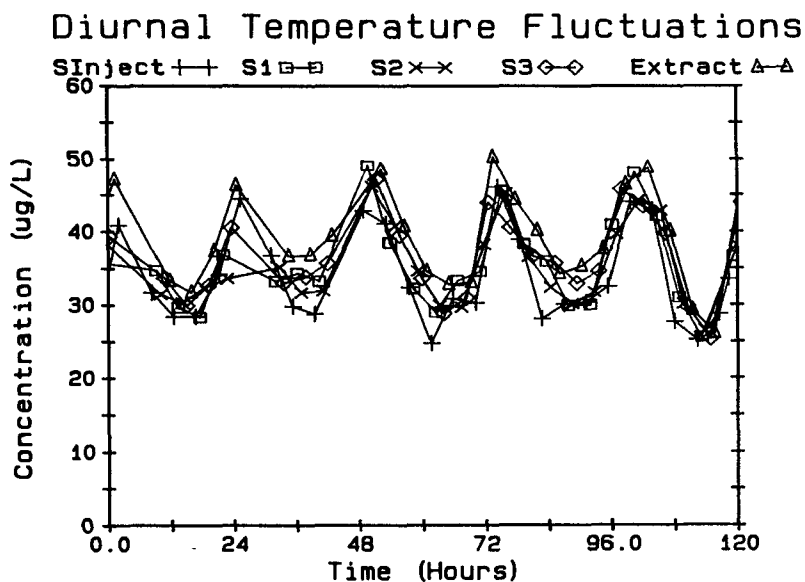


Figure 4.10. Daily variations in 1,1,1-TCA concentrations due to diurnal temperature fluctuations.

Normalizing Data

In the analysis of the experimental results, the concentrations at the observation locations were normalized to the injected concentrations. This was done to: 1) provide an easy means of showing the fractional breakthrough at observation locations of the injected chemicals; and 2) show the degree of biotransformation that was achieved during transport through the biostimulated zone. In addition, normalization provided a means of reducing some of the variability that resulted from temperature variations in the analytical system. This was accomplished by normalizing to the last injected concentration obtained prior to the particular measurement being normalized.

Table 4.9 presents a raw data set and a normalized data set from one experiment. Concentrations at the observation location had achieved near-steady-state fractional breakthroughs during the period analyzed. The coefficient of variation of the normalized data is lower than that of the raw data. A 40% reduction in the coefficient of variation was achieved by the normalization. This results mainly from reducing the daily variations caused by temperature fluctuations.

TABLE 4.9. COMPARISON OF VARIABILITY OF ABSOLUTE AND NORMALIZED CONCENTRATION DATA FOR OBSERVATION WELL S2

Chemical	Mean Concentration (µg/l)	Standard Deviation ^a (µg/l)	Coefficient of Variation ^b (%)	Number of Observations
VC	41.9	5.2	12.3	18
trans-DCE	50.9	8.6	16.9	39
cis-DCE	96.7	14.2	14.7	39
TCE	33.8	4.7	13.9	39

Chemical	Normalized Concentration	Standard Deviation	Coefficients of Variation ^b (%)	Number of Observations
VC	0.91	0.082	9.0	18
trans-DCE	0.95	0.098	10.3	39
cis-DCE	0.99	0.092	9.4	39
TCE	0.96	0.082	8.5	39

^a Standard deviation of individual measurements.

^b Coefficient of variation of individual measurements.

The coefficients of variation of the normalized concentrations at the observation locations are less than 10%. When the data are used to estimate the degree of transformation achieved, based on equation 4.1, the mean value and the standard error of the mean are used. The standard error of the mean reflects the large number of samples used in the estimate, where the standard deviation is divided by the square root of the number of observations. Thus, for example, the standard error of the mean of the cis-DCE concentration given in Table 4.9 is $14.2/39^{0.5} = 2.3 \mu\text{g/l}$. This is a very small standard error, compared to the average value of 96.7 µg/l. This illustrates the advantage of the DAC system: the large number of precise observations minimize the relative errors associated with the mean estimates.

SUMMARY

A field site was selected for the demonstration that offered a suitable combination of attributes from the standpoint of hydrogeology, geochemistry, logistics, and institutional acceptability. A shallow, confined aquifer was tested and shown to have adequate permeability and acceptable chemical composition. The well test data also provided a basis for preliminary design of the injection/extraction system. The general approach to the experimental program is also summarized.

The quality assurance checks demonstrated that the automated data acquisition was capable of providing a large number of measurements with high precision. This ability permitted the field experiments to be performed as a series of stimulus-response tests, with the response of the system to the stimulus precisely monitored. The injection system used in the field experiments delivered controlled amounts of the chemicals, which was required in these experiments. Coefficients of variation in the mean observed concentrations were less than 15%. Normalization reduced the coefficient of variation to less than 10%.

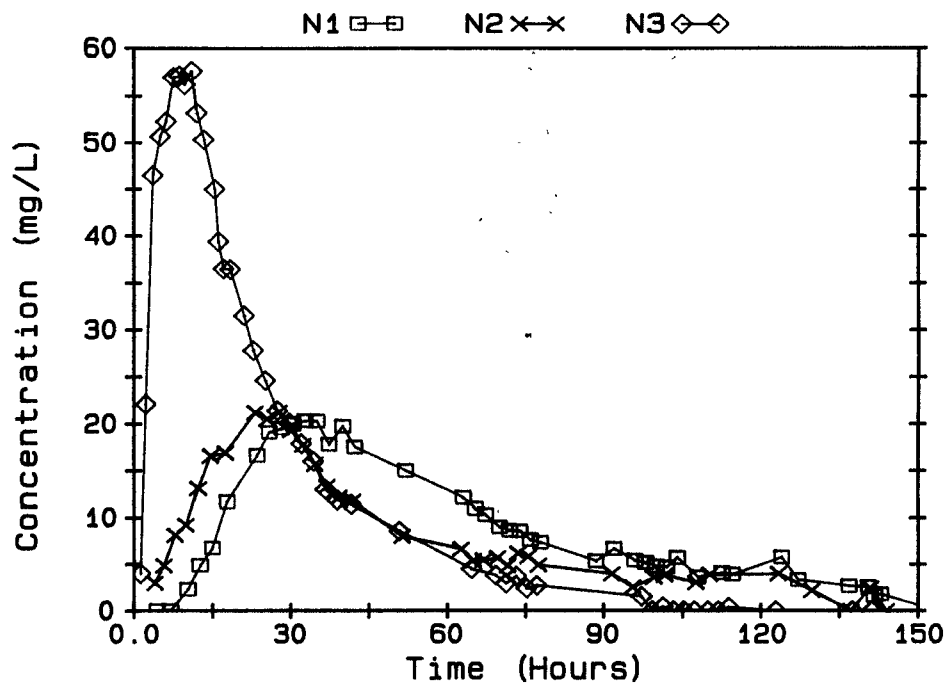


Figure 5.1. Results from the Tracer2 natural gradient tracer test.

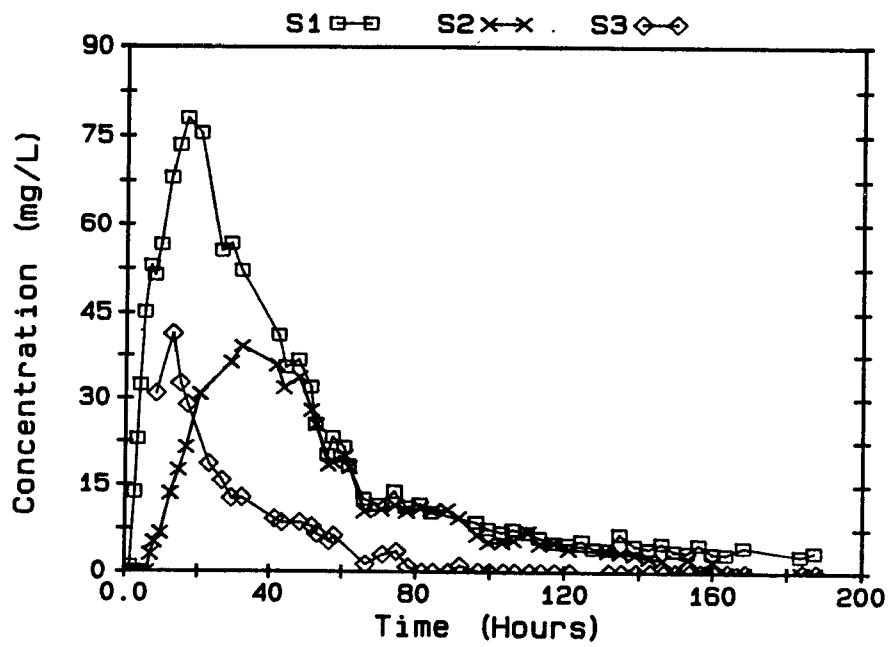


Figure 5.2. Results from the Tracer3 natural gradient tracer test.

SECTION 5

RESULTS OF TRACER TESTS

Lewis Semprini, Gary Hopkins, and Paul Roberts

Tracer tests were performed under both natural gradient and induced gradient conditions to characterize fluid and contaminant transport in the test zone. Natural gradient tracer tests were conducted to determine the direction and magnitude of groundwater flow. Induced gradient tracer tests provided information on the transport of chemicals that were used in the later biostimulation and biodegradation experiments.

NATURAL GRADIENT TRACER TESTS

Two natural gradient tracer tests were conducted, Tracer2 and Tracer3. The tests were performed as follows: a slug of 460 liters of bromide tracer was injected over a period of 3 to 4 hrs into a well along the main line of wells S1 through N1, and then allowed to drift under natural gradient conditions. Responses at monitoring wells encompassed both the breakthrough and the elution of the bromide tracer. In the Tracer2 test (Figure 5.1), well P was used to inject the tracer and wells N3, N2, and N1 were used as monitoring wells. In the Tracer3 test (Figure 5.2), well S1 was used to inject the tracer, and all the wells along south to north legs were monitored.

The experiments indicated that the groundwater flow was primarily in a northerly direction. Figures 5.1 and 5.2 show responses at the monitoring wells for the Tracer2 and Tracer3 tests, respectively. The response curves are skewed in shape, with a sharp rise in concentration followed by a gradual decrease, or tailing, to background concentrations. The areas under the response curves are seen to decrease as the distance from the injection well increases, especially for the Tracer3 test. The maximum concentrations are significantly lower than the injected concentrations. The decrease in area with distance and the low maximum concentrations suggest either a flow direction that deviates slightly from being parallel to the line of the observation wells and/or a large amount of lateral dispersion.

Table 5.1 summarizes the results from the natural gradient tracer tests. The skewed shape of the response curves are indicated by the greater time associated with the center of mass of the response curves compared to the time to the maximum observed concentration. The groundwater velocity estimates based on the time corresponding to the center of mass of the response curve are in good agreement for the Tracer2 test. An average value of 2.5 m/d was obtained. The results obtained from the Tracer3 test are more variable, with values increasing with increased distance from the injection well to the observation well. The higher velocities are associated with a decrease in area under the response curves.

The rapid transport in the test zone is typified by the initial response at the S3 monitoring well, which precedes that of the S2 well, even though the latter well is located closer to the injection well for this test. This earlier breakthrough is reproduced in all the tracer experiments performed to date. These data suggest that the aquifer is quite heterogeneous. The high permeability zones rapidly convey the tracer to the distant wells, while the responses at observation wells closest to the injection well represent contributions from a range of permeability zones. The observation wells are not fully penetrating. Thus, if there were layering and vertical structure in the test zone, the monitoring wells may be sampling different zones,

TABLE 5.1. ESTIMATES OF REGIONAL VELOCITIES BASED ON THE RESULTS OF THE NATURAL GRADIENT TRACER EXPERIMENTS

	Well	Distance from the Inj. Well (m)	Time Max. Conc. (hrs)	Time Center of Mass (hrs)	Velocity ^a (m/d)	Area Under Response Curve (mg-hr/l)
Tracer2	N3	2.0	8.8	17.9	2.6	1555
	N2	3.8	27.8	38.6	2.4	1059
	N1	5.0	32.8	50.5	2.4	1250
Tracer3	S1	1.0	16.4	32.9	0.7	3658
	S2	2.2	32.5	44.3	1.2	2131
	S3	3.8	12.9	20.0	4.8	1019

^a Velocity based on center of mass.

especially along the south experimental leg, where the variations in estimated velocity are great. Moreover, the extensive tailing in the response curves would suggest multi-permeability zones, as discussed by Molz et al. (1986a).

The results of the two natural gradient tests indicate a fairly high groundwater velocity at the site: approximately 2.4 m/d. The velocity is higher than the 1 m/d value obtained from the measured gradient and hydraulic conductivity estimated from pump tests, but nonetheless of the same order of magnitude. The hydraulic conductivity, however, is based on an aquifer thickness of 1.5 m. If the thickness were less, higher estimates of groundwater velocity would result.

INDUCED GRADIENT TRACER TESTS

Induced gradient tracer tests were performed using bromide as a conservative tracer, DO as a potentially reacting tracer, and the chlorinated organics studied in later biotransformation experiments. The hydraulic conditions approximated closely those of the later biostimulation-biotransformation experiments. The bromide tracer tests provided information on the (1) fluid residence times, (2) degree of breakthrough at observation locations, (3) dispersion, and (4) extent to which the injected fluid was captured by the extraction well. The chlorinated organic transport experiments provided information on (1) the extent of retardation of chlorinated solutes due to sorption onto the aquifer solids, (2) the rate processes affecting sorption and desorption, and (3) whether transformation occurred before the test zone was biostimulated. While providing information on transport, the experiments also served as quasi-controls before the test zone was biostimulated.

The southern experimental leg of wells—including injection well SI, observation wells S1, S2, S3, and extraction well P—were used in these experiments and all subsequent biostimulation and biotransformation experiments. By injecting and extracting groundwater in this configuration, the induced flow was in the same direction as the natural groundwater flow, thus promoting effective capture of the injected groundwater by the extraction well.

The induced gradient tracer tests were performed with continuous chemical addition, using the system described in Section 4. Fluid extraction rates ranged from 8 to 10.5 l/min, while injection rates ranged from 0.7 to 1.5 l/min. The injection and extraction rates used in the different experiments are presented in Table 5.2.

TABLE 5.2. COMPARISON OF BROMIDE TRACER TESTS UNDER INDUCED GRADIENT CONDITIONS

Test ^a Season		TR4 1	TR5 1	TR8 2	TR11 3	TR12 4
Injection Rate (l/min)		1.1	0.66	1.36	1.5	1.5
Extraction Rate (l/min)		8.0	8.0	10.0	10.0	10.0
Percent Steady-State Breakthrough						
	Well S1	95	94	100	102	100
	Well S2	95	72	98	100	99
	Well S3	80	57	84	96	95
	Extraction	9	5	13	14	15
Time to 50% Break- through (hrs)						
	Well S1	8	9	7.5	9	8
	Well S2	20	17	16	23	21
	Well S3	20	7	20	27	26.5
	Extraction	26	20	30	40	42
Percentage Recovered at the Extraction Well		66	59	105	94	ND

^a TR4 = Tracer4 experiment, etc.

The induced-flow tracer tests were conducted in each of the field seasons. The first season's tests included studies with bromide, TCE, and DO. The second season's studies included bromide, TCE, trans-DCE, and cis-DCE; vinyl chloride was included in the third field season as well.

Bromide tracer tests provided the initial information on the transport characteristics of the test zone. Bromide tracer results from the Tracer4 test (first season), and the Tracer8 test (second season) are shown in Figures 5.3 and 5.4, respectively. Concentrations are normalized to the injected concentration for both experiments. Bromide was injected for 107 hrs in the Tracer4 test and for 190 hrs in the Tracer8 test. Both sets of data show a tightly spaced temporal response with approximately eight samples at each observation point per day. The tracer breakthrough at observation locations, due to constant bromide injection and its elution from the test zone after its addition was stopped, is apparent. The normalized concentration values of the Tracer8 test are shown to have less variability compared to the Tracer4 test. This results from an experimental modification for adding the bromide tracer that resulted in a more constant rate of bromide addition in the Tracer8, and subsequent, experiments.

The steady-state fractional breakthrough at observation locations and the time required to achieve 50% of this breakthrough are summarized in Table 5.2 for several key tracer tests. Comparing the Tracer4, Tracer5, and Tracer8 experiments, the highest degree of fractional breakthrough was observed in the Tracer8 experiment, while the lowest was observed in the Tracer5 test. The higher degree of breakthrough results from the factor of 2 increase in the injection rate in the Tracer8 test compared to the Tracer5 test. Breakthroughs of less than 100% result from dilution by the native groundwater. This dilution is most apparent at the extraction well as a result of the greater rate of extraction compared to injection. The S3 observation well, farthest from the injection well, always showed some dilution of the injected fluid by native groundwater.

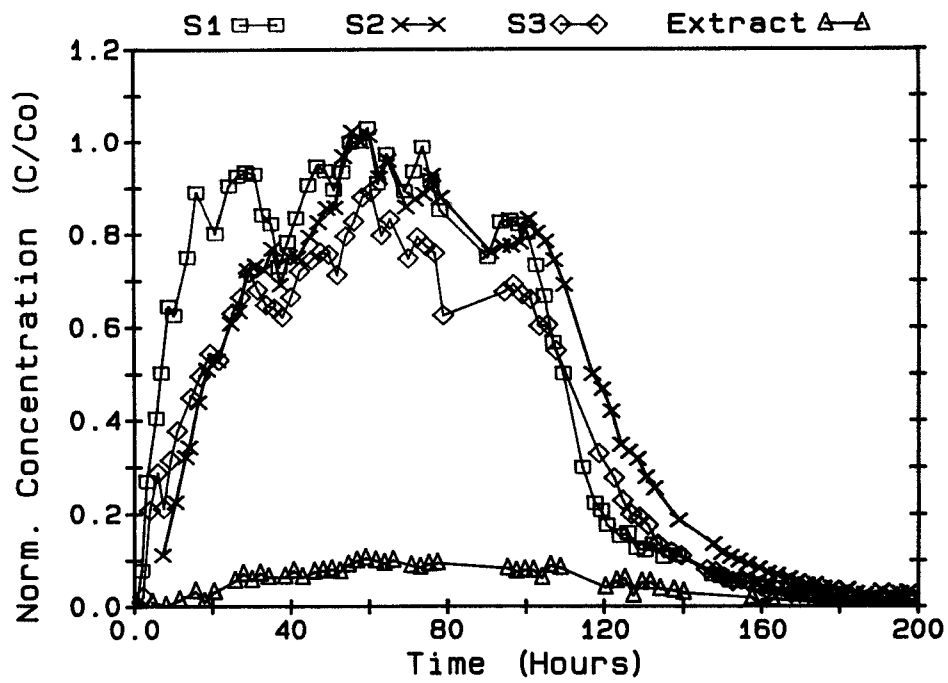


Figure 5.3. Bromide tracer breakthrough and elution in the Tracer4 experiment.

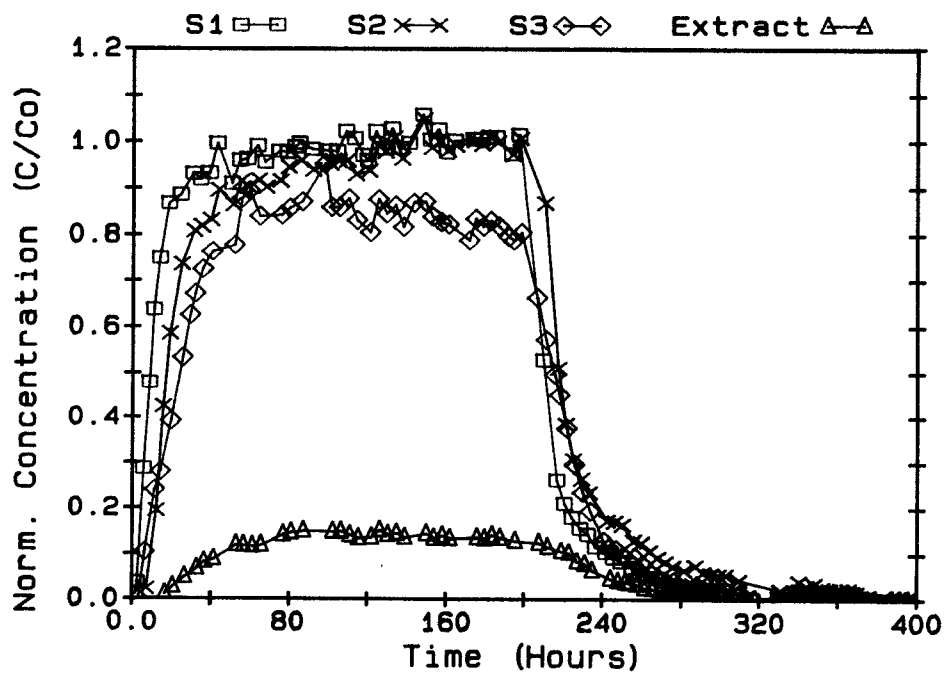


Figure 5.4. Bromide tracer breakthrough and elution in the Tracer8 experiment.

The mean fluid residence time is approximately 8 hrs to the S1 well, and 18 hrs to the S2 well. The mean fluid velocity based on transport times to both wells is approximately 3 m/d. The time required to achieve 50% breakthrough does not change significantly between the Tracer4 and Tracer8 experiment, despite the different injection and extraction rates. This result indicates the strong influence of the natural groundwater flow (1 to 2 m/d) on transport in the test zone. Due to the dilution and more dispersed response at the S3 well, the 50% breakthrough time is probably less representative of the mean residence time, which is also more variable at that well.

Figure 5.5 shows the initial breakthrough of the bromide tracer during the initial 200 hrs of the Tracer8 test. The initial breakthrough at the S3 observation well, located 3.8 m from the injection well preceded that at well S2, 2.2 m from the injection well. This response indicates the short-circuiting of flow or, since the observation wells are only partially penetrating, the possible existence of vertical variations in permeability. As time proceeds, the fractional breakthrough at the S2 well surpasses that of the S3 well, and eventually reaches 100%, while at steady state, the S3 well only achieves 84% breakthrough. Due to the behavior of the S3 well in these tracer tests, less emphasis is placed in its response in the interpretation of the results of later biostimulation and biodegradation experiments.

The bromide breakthrough observed during the Tracer8 test shows a relatively rapid increase to 80% fractional breakthrough at the S1 and S2 wells, followed by a much slower approach to 100% breakthrough. This gradual increase at later time results in part from a gradual increase in the injected bromide concentration, due to the recycling of bromide in the extracted water. The recycle also resulted in some extended tailing in the elution part of the tracer test. In Section 12 of this report, an analytical model is presented that takes into account advective and dispersive transport, as well as recycle, in a uniform flow field. The analytical model's fit to these tracer data are presented in Section 12.

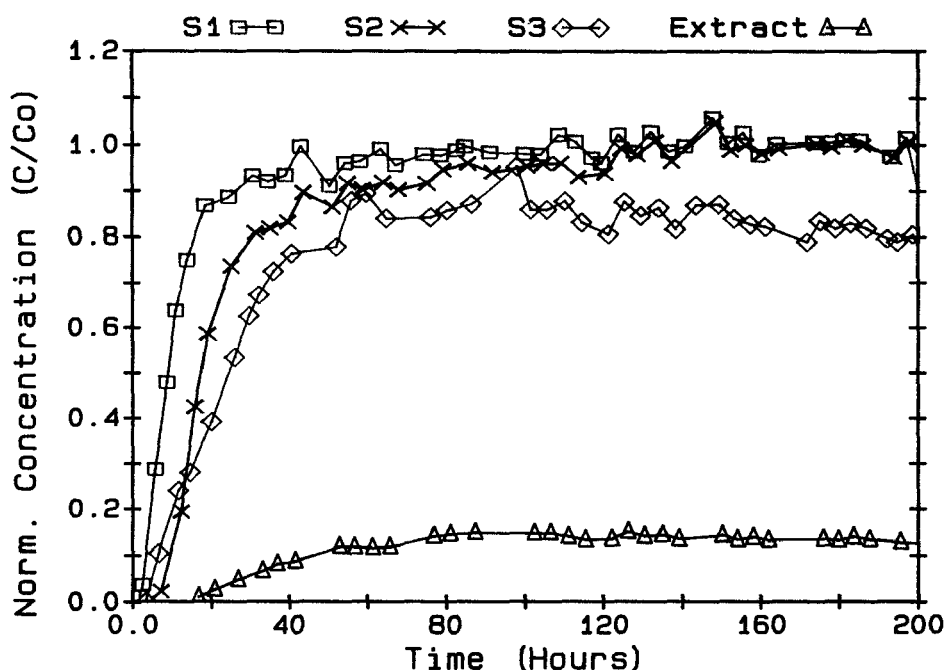


Figure 5.5. Initial breakthrough of bromide in the Tracer8 experiment.

Numerous bromide tracer tests were performed during the three years of field testing as part of organic solute transport experiments, and biostimulation-biotransformation experiments. The tests all showed very reproducible responses, similar in form to that shown in Figure 5.4. In all tests, the initial breakthrough at the S3 well always preceded that at the S2 well. Transport times were very reproducible from test to test, and similar degrees of fraction breakthrough at observation locations were obtained.

As summarized in Table 5.2, in the second and third seasons of testing, steady-state fractional breakthroughs at the S1 and S2 wells of 98% to 100% were always obtained, while some dilution was always observed at the S3 observation well. In the third season, the time to 50% breakthrough at the S2 and S3 observation wells increased, although injection and extraction rates were nearly unchanged. The third-season tests were performed during the second season of drought, which may have reduced the natural gradient component of the groundwater velocity. The biostimulation of the test zone in two successive seasons of field testing also may have resulted in some changes in flow characteristics of the test zone.

The degree of capture of the bromide tracer in the first season of testing ranged from 59% to 66%. In the second and third seasons, 94% to 105% of the injected bromide was captured by the extraction well. The mass balance of greater than 100% is within the experimental error. The increase in the tracer recovery most likely results from the higher extraction rates used in the later seasons. This ability to recover essentially all the bromide tracer reduced the error in mass balances used to estimate the degree of biotransformation of the chlorinated organics. It also enabled us to obtain regulatory support to evaluate the transformation of vinyl chloride in the test zone.

The DO transport experiments evaluated whether DO consumption occurred before the test zone was biostimulated, and if DO was transported at the same velocity as the bromide tracer. Since DO concentration of the native groundwater is very low, DO in the injected groundwater and its breakthrough at observation locations was monitored and compared to the bromide tracer.

Figure 5.6 shows the concentration breakthrough of DO observed in the Tracer4 experiment. The S1 observation well concentration was higher than the injection concentration. This results from diffusion of atmospheric oxygen through the Teflon tubing used to deliver the injected water to the test zone. The Teflon tubing was therefore replaced with stainless steel tubing for the subsequent experiments. Dissolved oxygen response was essentially the same as that of the bromide tracer (Figure 5.3). The results indicated little utilization or retardation of DO during transport. Thus, the ability to transport required DO through the aquifer was demonstrated.

DO concentrations were monitored as part of the Tracer8 experiment performed during the second season of field testing. This test preceded the biostimulation tests of the first season. The normalized concentration of DO compared to bromide at the S2 observation well is shown in Figure 5.7. The breakthrough of DO was delayed compared to bromide, and the fractional breakthrough of DO reached approximately 90% of the injected concentration, compared to the 100% achieved by bromide. Both observations indicated some DO consumption occurred during transport through the test zone. Based on the DO injection concentration of 15 mg/l and the fractional breakthrough being 10% lower than bromide, an estimated 1.5 mg/l of DO was consumed. Most of this consumption occurred within the first meter of transport, where most of the biomass was stimulated, as will be discussed in detail in Sections 6 and 13. The DO consumption probably results from the oxidation of organic matter that remains after the biostimulation of the test zone.

Induced flow tracer experiments with the chlorinated organics solutes were performed in all three seasons of field testing. Table 5.3 summarizes the organic solute tracer tests performed. In the first season both the breakthrough and elution of TCE was studied. In the second season, the transport of TCE, cis-DCE, and trans-DCE was studied, while in the third season the transport of vinyl chloride in addition to the prior year's solutes, was also studied. In the second and third seasons the biostimulation-biotransformation experiments immediately followed the tracer experiments. Thus, only data on the breakthroughs before biostimulation were obtained. The elution of these compounds from the test zone was monitored at the end of the biostimulation experiments.

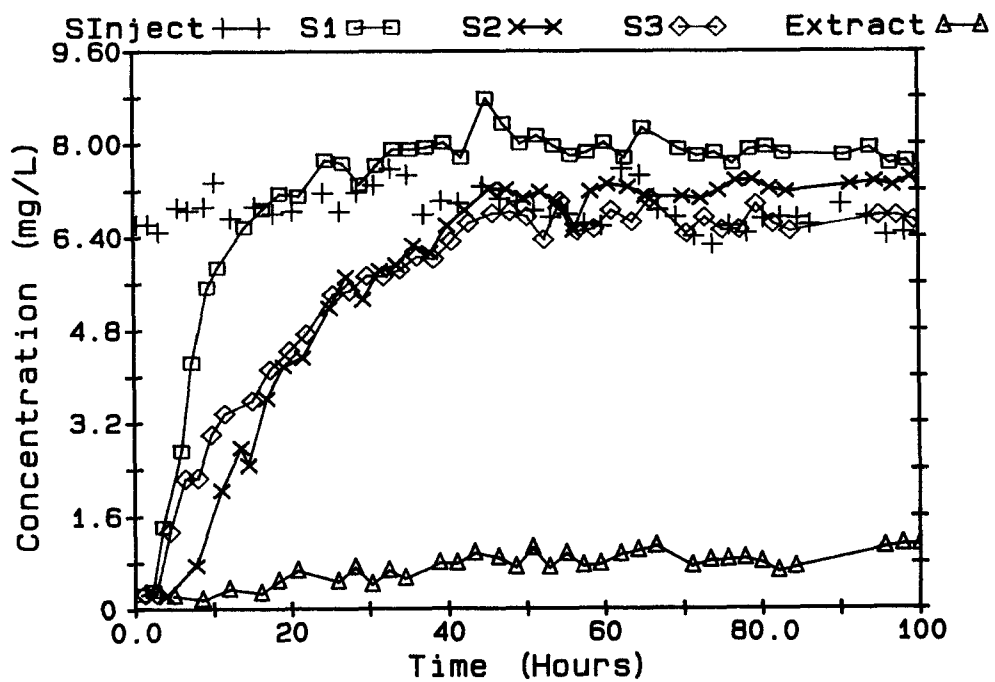


Figure 5.6. DO breakthrough in the Tracer4 experiment.

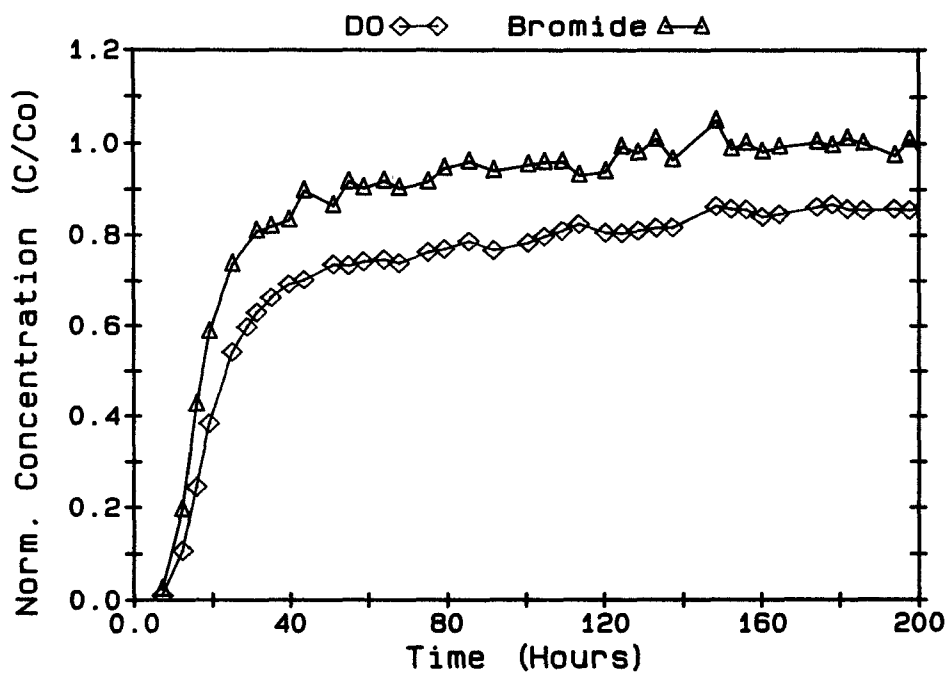


Figure 5.7. DO and bromide breakthroughs at the S2 well in the Tracer8 experiment.

TABLE 5.3. SUMMARY OF INDUCED ORGANIC TRACER TESTS PERFORMED

Experiment	Season	Chemicals Studied	Average Conc. ($\mu\text{g/l}$)	Processes Studied
Tracer5	1	TCE	165 \pm 30	Retardation Elution Mass Balance
Tracer8	2	TCE tran-DCE cis-DCE	48 \pm 10 112 \pm 39 110 \pm 36	Retardation Steady-State Breakthrough
Tracer11	3	TCE trans-DCE cis-DCE	47 \pm 6 50 \pm 7 85 \pm 13	Retardation Steady-State Breakthrough
Tracer12	3	VC	44 \pm 7	Retardation Steady-State Breakthrough

In the first season of field testing, the transport of TCE was studied in the Tracer5 experiment before the test zone was biostimulated. TCE was injected continuously for 240 hrs at an average concentration of 160 $\mu\text{g/l}$, after which its injection was terminated and its elution from the test zone was monitored.

Figure 5.8 shows the normalized breakthrough of both bromide and TCE at the S1 observation well. TCE is shown to be retarded with respect to bromide. The time to achieve 50% breakthrough for TCE (assuming TCE would achieve the same as that obtained by bromide) is 42 hrs. Comparing to the value of 8 hrs for bromide, indicates that TCE is retarded by a factor of approximately 5. Thus, due to the sorption onto the aquifer solids, the TCE takes a much longer time to achieve steady-state concentrations at the observation locations.

In order to complete system mass balances, the elution of TCE was monitored in the Tracer5 experiment. Based on the breakthrough response, extended tailing was expected during elution, thus prolonging the experiment. The injection of TCE was therefore stopped before steady-state breakthrough concentrations were achieved. Figure 5.9 shows both the breakthrough and elution of TCE from the test zone. The much slower increase at the S2 well due to the longer flow path is apparent. Very extended tailing in both the TCE breakthrough and elution from the test zone was observed at the observation wells and the extraction well.

The response of TCE to breakthrough and elution can be compared with the bromide tracer, using the Tracer8 test for comparison purposes (Figure 5.4; note the factor of two difference in the time scales). The TCE response does not conform to that expected for the processes of advection, dispersion, and retardation, assuming equilibrium sorption between the aquifer solids and the aqueous phase. Besides retardation, the TCE data show greater spreading (dispersion) compared to the bromide. Part of this spreading may be associated with recycle of the injected TCE. However, other factors probably contribute to the spreading, including (1) sorption, if the process is rate-limited, as will be discussed in Section 8; and (2) layers of differing hydraulic conductivity in the aquifer.

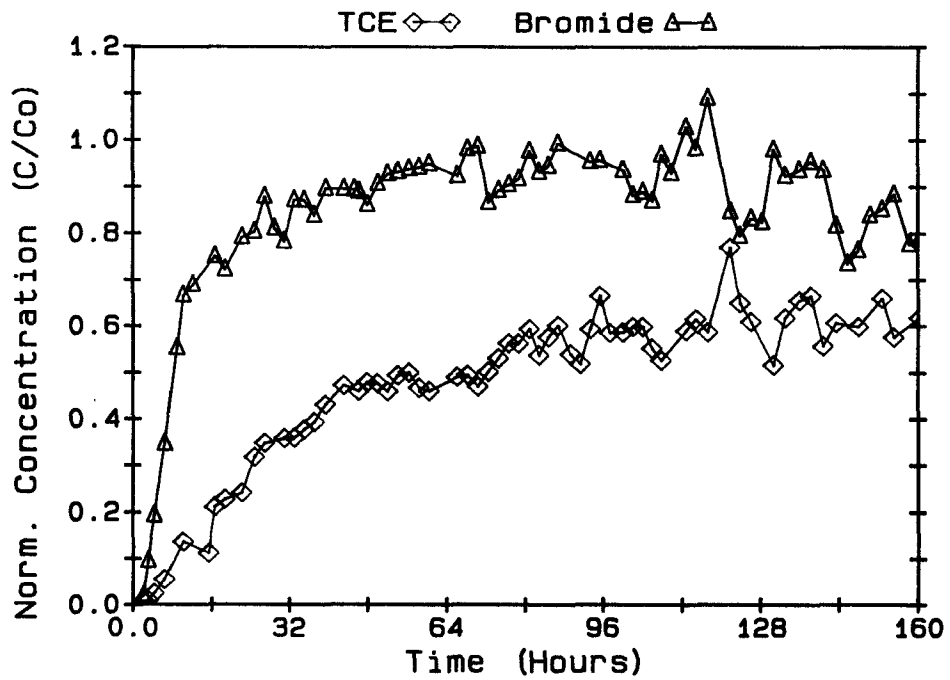


Figure 5.8. Normalized breakthrough of bromide and TCE at the S1 well in the Tracer5 experiment.

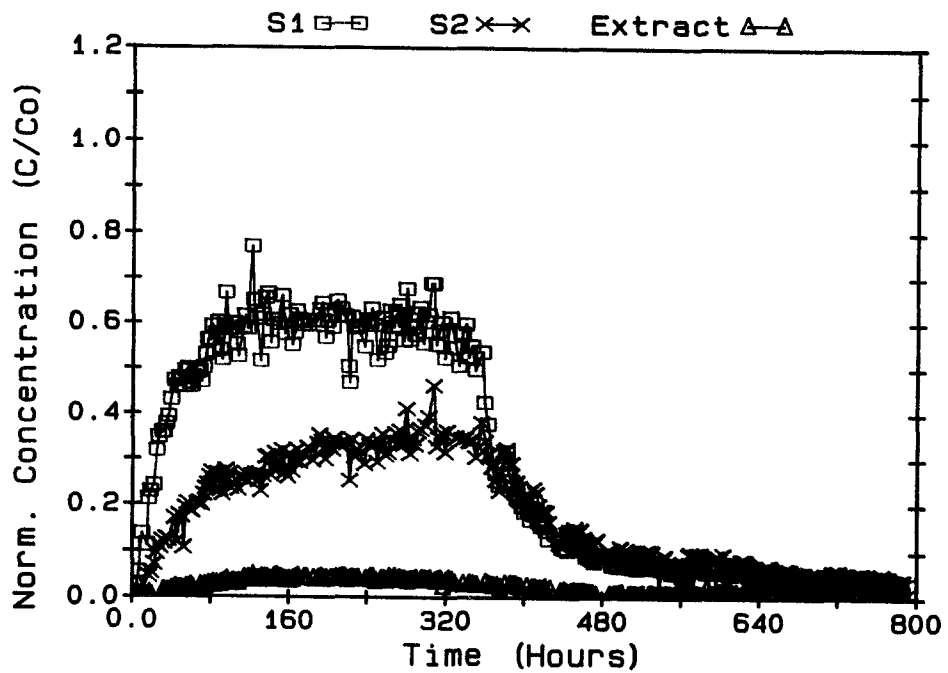


Figure 5.9. Breakthrough and elution of TCE in the Tracer5 experiment.

Extended tailing resulted in concentrations in the 1 µg/l range remaining at observation wells 600 hrs after the mass balance was completed. Since pumping was virtually continuous during that period, the TCE captured by the extraction well is estimated to be close to that of bromide. Thus, the results of this tracer test suggest little transformation of TCE before biostimulation.

In the Tracer8 and Tracer11 experiments, performed in the second and third seasons of field testing, trans-DCE and cis-DCE were added along with TCE. The experiments were also performed at higher injection and extraction rates, and at a lower TCE injection concentration (50 µg/l), compared to the Tracer5 experiment. One of the goals of these experiments was to achieve steady-state chlorinated organics concentrations at observation locations before the test zone was biostimulated. To accomplish this, the chlorinated organics were continuously injected for approximately 1000 hrs.

Figure 5.10 shows bromide, trans-DCE, cis-DCE, and TCE responses at the S1 well in the Tracer11 experiment. At early times, trans-DCE appears to be more strongly retarded than TCE, while at later times TCE appears to be more strongly retarded. Cis-DCE is clearly the least strongly retarded of the compounds tested. Based on the results of batch sorption studies (Section 8), TCE was anticipated to be the most retarded compound. One possible explanation for the delayed breakthrough of trans-DCE at early time is that trans-DCE was partially transformed during transport through the previously biostimulated test zone. However, we do not have independent evidence to confirm this transformation. The later time response, indicating greater retardation of TCE, is consistent with the results of batch laboratory studies, presented in Section 8.

The shape of the cis-DCE, trans-DCE, and TCE breakthrough responses in the Tracer8 and the Tracer11 experiments was observed to be similar in form. All responses showed a greater amount of spreading than observed with the bromide tracer.

Figure 5.11 shows the normalized TCE concentrations at observation locations in the Tracer8 experiment. The very gradual approach of TCE to the injection concentrations is apparent, especially at the S2 well and the extraction well, due to the longer distances traveled. With prolonged injection in both the Tracer8 and Tracer11 experiments, cis-DCE, trans-DCE, and TCE reached 90% to 95% of the injection concentrations at the S1 observation well. These results indicated little transformation of these compounds before the initiation of the biostimulation-biotransformation experiments.

Tracer12, the final organic tracer experiment, studied the transport of vinyl chloride. Results of the previous chlorinated organic transport experiments demonstrated that prolonged periods of addition were required in order to achieve steady-state breakthrough concentrations. To shorten this time, a two-step vinyl chloride addition method was used. In the first step, vinyl chloride was injected at 1.5 times the final desired concentration. After 50% fractional breakthrough was achieved at the S2 well, the injection concentration was reduced to the final operating concentration. Results of model simulations, presented in Section 14, indicated that a much faster approach to steady-state conditions would be achieved by the two-step approach, especially if the sorption-desorption process were rate-limited.

Results of the vinyl chloride addition experiment are presented in Figure 5.12. After injecting at a concentration of 69 µg/l for 48 hrs, the injection concentration was reduced to 44 µg/l. The concentrations at both the S1 and S2 wells approached steady-state levels rapidly. The results indicated that the two-step method of organic addition resulted in a rapid attainment of steady-state conditions. The results also showed vinyl chloride was not transformed before the test zone was biostimulated.

In this experiment, and in the later stages of the Tracer11 experiment, DO was not being injected into the test zone. Therefore background nitrate served as the electron acceptor. The results indicated little transformation under these anoxic conditions. However, unlike the Tracer8 experiment, where the cis-DCE, trans-DCE, and cis-DCE, were added along with DO, vinyl chloride was not added in the presence of DO. Thus, it is not known whether transformation of vinyl chloride would have been observed in the presence of DO.

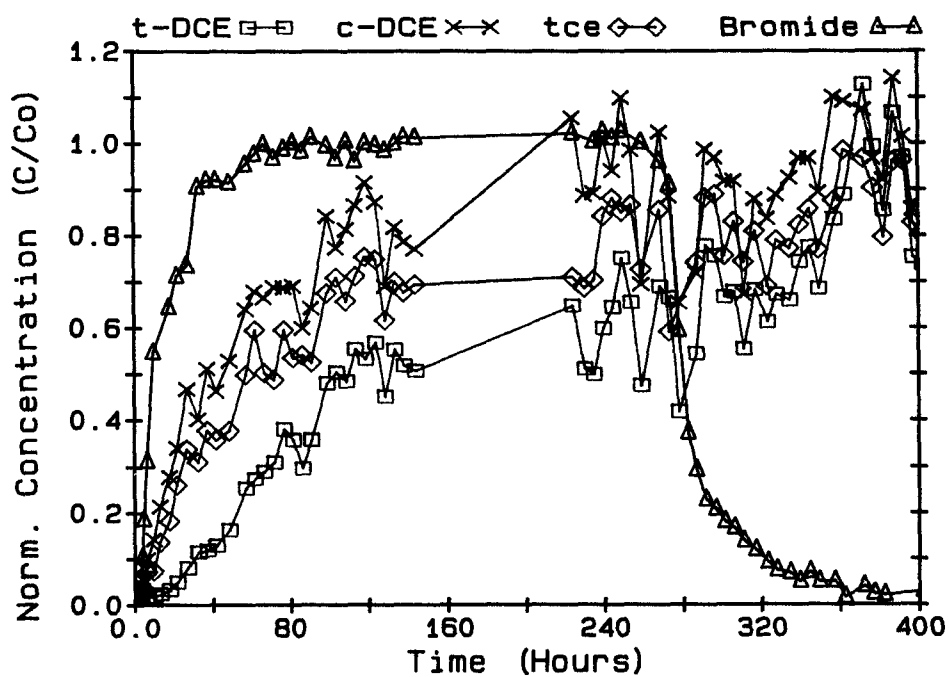


Figure 5.10. Normalized breakthrough of bromide, trans-DCE, cis-DCE, and TCE, achieved at the S1 well in the Tracer11 experiment.

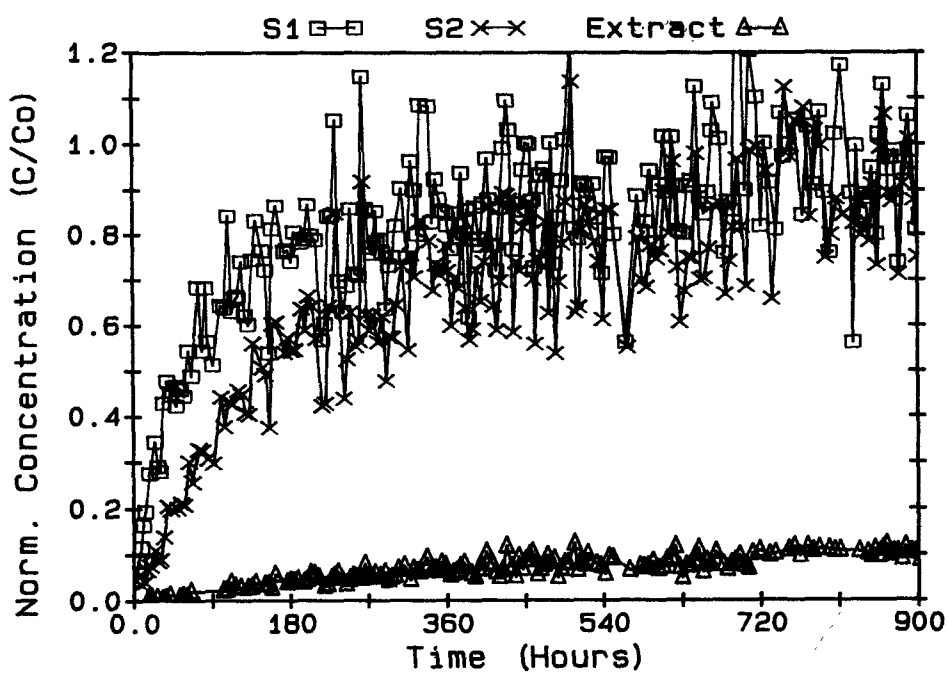


Figure 5.11. Normalized breakthrough of TCE during the Tracer8 experiment.

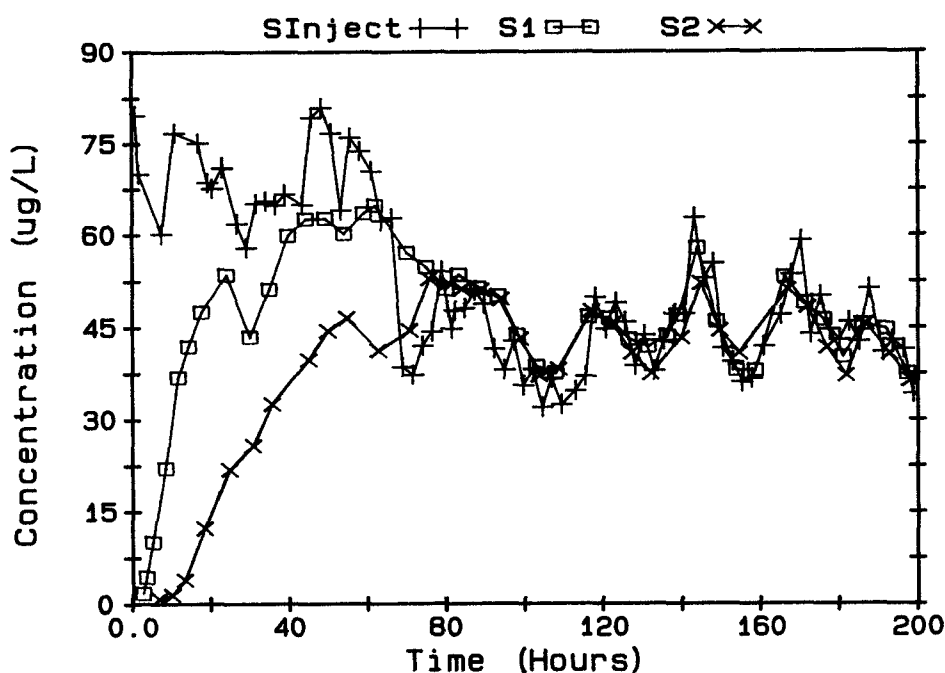


Figure 5.12. Response at the S1 and S2 wells to the two-step vinyl chloride addition.

Retardation Estimates

The retardation of the chlorinated organics with respect to bromide tracer was estimated using two methods: 1) the time required to achieve 50% of the steady-state fractional breakthrough, and 2) the center of mass of the breakthrough response, as described by Roberts et al. (1980). The second method is considered to be a better representation of the field response, since it takes into account the long tailing in the breakthrough response. However, maintaining constant conditions over the long experiment required for this estimate proves to be difficult in practice. Thus, both methods of estimating retardation factors will be evaluated and compared.

The 50% breakthrough method assumes that the chlorinated organics eventually achieved the same degree of fractional breakthrough as the bromide tracer. The retardation for TCE is given by the ratio of ($T_{50\% \text{ TCE}} : T_{50\% \text{ Br}}$). This method is expected to give a conservative estimate of the retardation factor due to the asymmetric shape of the observed breakthrough response.

Table 5.4 presents the estimates of 50% residence times, and estimated retardation for the organic addition experiments. Bromide residence times used in the retardation estimates were presented in Table 5.2. The residence time for 1,1,1-TCA, a background contaminant in the test zone, was based on its elution from the test zone during the Tracer4 experiment.

The estimated retardation factors for TCE were found to be fairly reproducible from test to test. No observable increase in retardation of TCE resulted from the biostimulation of the test zone in the previous year. Average retardation values of 6 and 8.3 were obtained for the S1 and S2 wells estimates, respectively. Vinyl chloride and 1,1,1-TCA were the least retarded, with an average retardation value of 1.8. The retardation of cis-DCE and trans-DCE differ by about a factor of 2, having respective values of 4 and 10. Results for cis-DCE were reproducible in the two tests performed as well. Trans-DCE estimates, however, differed by almost a factor of two in the different tests. The higher retardation estimate for trans-DCE in the Tracer11 test may have resulted from partial transformation at early time.

TABLE 5.4. RESIDENCE TIMES AND RETARDATION FACTORS FOR THE CHLORINATED ORGANIC COMPOUNDS BASED ON THE TIME REQUIRED TO ACHIEVE 50% FRACTIONAL BREAKTHROUGH

Experiment	Compound	Well S1 $t_{50\%}$ (hrs)	Well S2 $t_{50\%}$ (hrs)	R (S1)	R (S2)
Tracer4	1,1,1-TCA	10	30	1.3	2.0
Tracer5	TCE	40	160	5	9
Tracer8	TCE	60	150	7	8
	trans-DCE	50	150	6	8
	cis-DCE	30	70	3	4
Tracer11	TCE	50	175	6	8
	trans-DCE	120	280	13	12
	cis-DCE	45	90	5	4
Tracer12	Vinyl chloride	13	42	1.6	2.0

Table 5.5 presents estimates of mean residence times, \bar{t} , and retardation factors for the Tracer8 experiment using the center-of-mass method. The mean residence times are longer than those based on the 50% breakthroughs (Table 5.4). Bromide residence times are increased by almost a factor of 2, compared to those based on the 50% breakthrough. Part of this increase is related to recycle of the injected bromide, which caused some of the extended tailing. The residence times of the chlorinated organics were larger by factors of 2 to 5 compared to the 50% breakthrough results, due to the very asymmetric response observed. The retardation factors estimated using this method are as much as a factor of 2 greater than those achieved based on the 50% breakthrough. For this case, TCE was the most strongly sorbed compound, followed by trans-DCE and cis-DCE.

TABLE 5.5. RESIDENCE TIMES AND RETARDATION FACTORS FOR THE CHLORINATED COMPOUNDS BASED ON CENTER-OF-MASS ESTIMATES

Substance	\bar{t} Well S1 (hrs)	\bar{t} Well S2 (hrs)	\bar{t} Well S3 (hrs)	Mean R Factor
Bromide	14	27	23	1
TCE	160	300	300	12
cis-DCE	145	200	170	8
trans-DCE	155	250	225	10

The higher retardation factors based on the center-of-mass calculation are expected, since this method would better capture the long-term effects of rate-limited sorption, where the amount sorbed on the aquifer solids increases with exposure time. These results are in qualitative agreement with the results of batch laboratory studies reported in Section 8. There is some uncertainty in the estimates of retardation due to the difficulties in performing the long-term transport experiments. However, for the purposes of the field experiments and modeling exercises, the retardation effects were fairly well established.

The results of the field experiments are also in qualitative agreement with the results of the batch laboratory experiments. The rank order of retardation of TCE > trans-DCE and cis-DCE > vinyl chloride (Table 5.5), is consistent with K_d values given in Table 8.3, based on the headspace method.

Mathematical Simulation of the Tracer Test Results

Preliminary mathematical modeling of the results of the tracer experiments has been performed using 1-D and 2-D models. The semi-analytical model, RESSQ, developed by Lawrence Berkeley Laboratory and described by Javandel et al. (1984) was used to simulate 2-D advective transport under the injection, extraction and natural gradient conditions of the tracer experiments. 1-D analytical solutions were used to estimate dispersion coefficients and to determine if a 1-D modeling approach could be used in the development of a numerical model to simulate the biostimulation and biotransformation processes.

The RESSQ model was used to estimate (1) the areal extent of the injected fluid front that develops around the injection well and observation wells, (2) the fluid residence times from the injection well to the observation wells, and (3) the degree of recovery of the injected fluid at the extraction well.

Simulations were performed to illustrate the original design of the well field to permit simultaneous experiments along three experimental legs. The model input parameters were a fluid injection rate of 0.5 l/min at three wells, an extraction rate of 8 l/min, regional flow velocity of zero, a porosity of 0.35, and an aquifer thickness of 1.2 m. Figure 5.13 shows the results of the simulations. An injected fluid front of uniform size develops around each of the three experimental legs. The maximum width of the front is approximately 1.6 m in the vicinity of the S1 and S2 observation wells.

Figure 5.14 shows the fronts that develop when a regional groundwater velocity of 300 m/yr in a northerly direction is imposed on the simulation discussed above. The front around the east injection well is shifted northward due to the groundwater flow. The regional flow leads to a thinning of the front along the southern leg and a broadening along the northern leg. These results indicated that the southern leg (SI, S1, S2, S3) should be used in the experiments for the following reasons: 1) the injected fluid supplying the nutrients becomes less dispersed, and hence a more dense microbial population can be stimulated, and 2) the injected tracers and chlorinated hydrocarbons can be most effectively recovered at the extraction well by injecting upstream of the natural groundwater flow. The area dominated by the injected fluid does become smaller, however, which helps explain the dilution of the injected fluid by the native groundwater that was observed in the tracer experiments.

Simulations were performed with the RESSQ model to determine whether the predicted fluid residence times are in the range of values estimated by the tracer tests. The model predicted fluid residence times of 8 hrs and 21 hrs for wells S1 and S2, respectively. These results were in agreement with the tracer test values given in Table 5.2. The following aquifer properties were used in the simulation: a regional fluid velocity of 300 m/yr, a porosity of 0.35, and an aquifer thickness of 1.25 m. These values are in agreement with the measured and estimated values. The simulations indicate that the injected fluid should be totally captured by the extraction well under these conditions. The tracer tests, however, indicated that only 60 to 70% of the bromide was captured. The reason for this lower degree of capture is unknown, but heterogeneities in aquifer properties is a probable cause.

The simulations indicate that the region near the injection well does not conform to uniform flow, but that the flow is nearly uniform at distances of more than 0.5 m from the point of injection, and hence in the region of the observation wells. To determine the degree of dispersion required to fit the observed

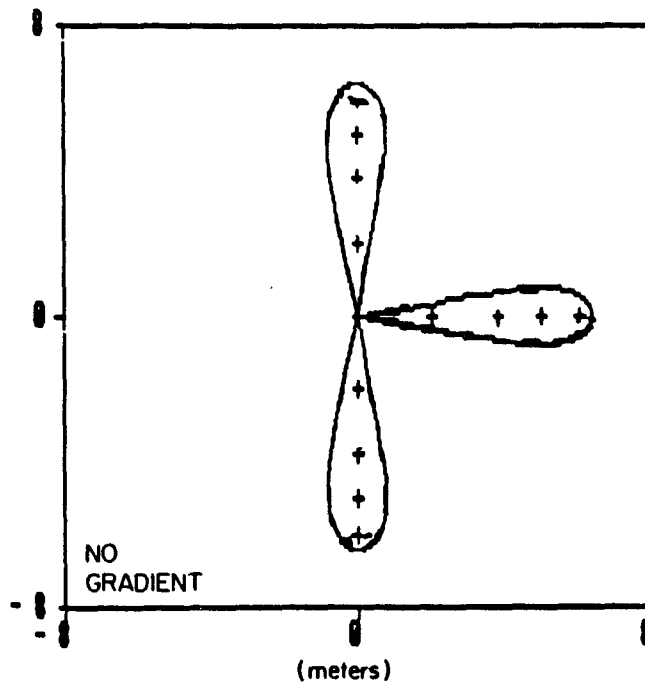


Figure 5.13. RESSQ simulations of the injected fluid fronts which develop under induced flow conditions of the tracer experiments with no regional flow.

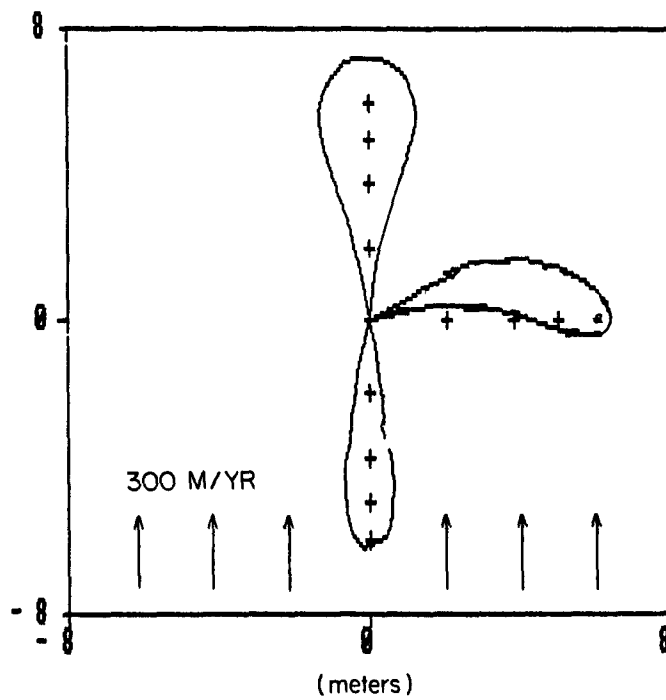


Figure 5.14. RESSQ simulations of the injected fluid fronts which develop under induced flow conditions of the tracer experiments with a regional flow of 300 m/yr.

breakthrough response at the S1 and S2 wells, 1-D simulations were performed. The nonlinear least-squares fitting program described by van Genuchten (1981) was used in fitting the data to the solution to the 1-D convective-dispersive transport equation.

Figure 5.15 shows the fit to the DO breakthrough response at the S-2 observation well in the Tracer4 experiment. A reasonably good fit is obtained with the 1-D model, with a resulting Peclet number (Pe) of 6.6, which corresponds to an aquifer dispersivity of 0.33 m (Length/Pe). Model fits of the data from the Br, DO, and methane experiments were performed for the S1 and S2 wells. The best-fit Peclet number based on the S1 well ranged from 2.7 to 4.0 with an average value of 3.1. The values based on data from the S2 well ranged from 3.4 to 6.6 with an average value of 4.4. The resulting average dispersivities were 0.32 and 0.45 m for the S1 and S2 wells, respectively. The 1-D analysis resulted in best-fit dispersivity values similar to those obtained from the analysis of the S1 and S2 data. The results indicate that 1-D transport modeling is of value in the initial stages of experimental design and data interpretation, when complex biostimulation and biotransformation processes must be taken into consideration. A more detailed analysis of the bromide tracer data is presented in Section 12.

PULSED INJECTION

To enhance the effectiveness of biostimulation, it was decided to introduce the methane (primary substrate) and oxygen (electron acceptor) as alternating, timed pulses. This decision was based upon two essential requirements: 1) the need to avoid clogging of the injection well and borehole interface, and 2) the need to achieve as uniform a distribution of microbial growth as possible throughout a substantial portion of the aquifer. Failure to fulfill the first requirement would cause loss of hydraulic capacity and premature termination of our experiments since the drastic chemical measures such as chlorination or

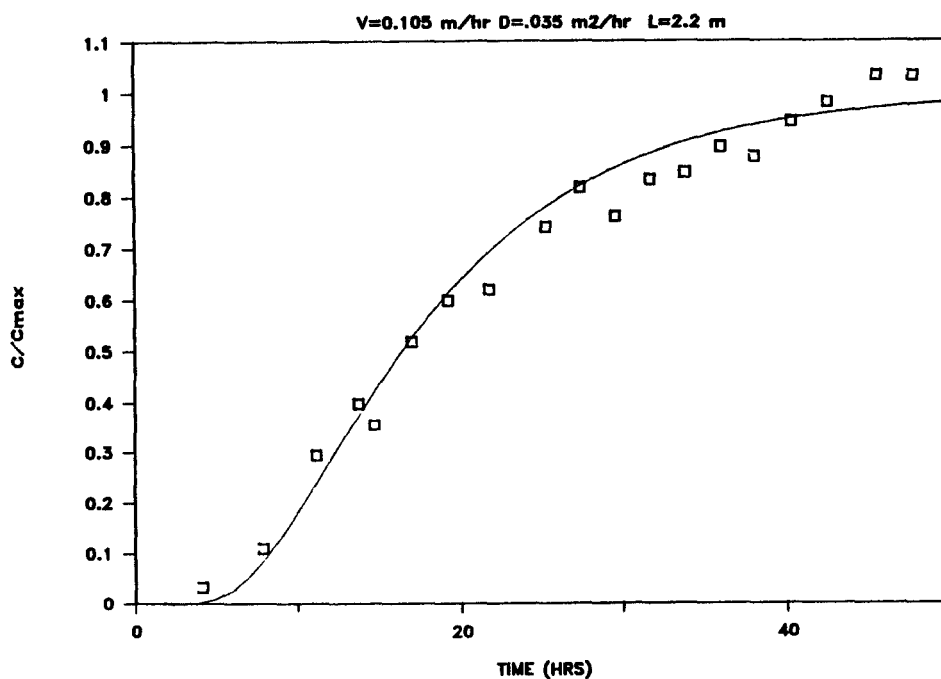


Figure 5.15. Fit of the 1-D advective-dispersion transport model to the breakthrough of DO at the S2 observation well during the Tracer4 test.

strong acid treatment, that are customarily employed to rejuvenate clogged wells, would interfere with biostimulation. Failure to satisfy the second requirement would lead to conditions of extremely high microbial densities near the injection point and low bacterial populations elsewhere. This would inhibit degradation of halogenated aliphatic compounds. It was anticipated that introduction of methane and oxygen as alternating timed pulses would assure their separation in the injection well and borehole, thus discouraging biological growth in that critical region. Subsequently, gradual mixing of the methane and oxygen would occur, owing to the action of hydrodynamic dispersion and associated mixing processes during transport through the aquifer. This would stimulate growth of methanotrophic bacteria over the mixing zone. In designing the pulsed injection system, two important variables had to be selected: 1) the ratio of the individual pulses of methane and oxygen, and 2) the overall pulse length.

The ratio of the individual pulses of methane and oxygen can be estimated approximately from knowledge of the stoichiometry of methane oxidation. The oxygen requirement for complete oxidation of methane is 2 moles oxygen per mole methane, which corresponds to a mass ratio of 4 g O₂ per gram methane. In choosing the pulse lengths, the concentrations achieved by the saturation columns for oxygen and methane also must be taken into account.

The overall pulse length was evaluated by employing a transport model that incorporates a periodic input (Valocchi and Roberts, 1983). The form of periodic input that corresponds most closely to the case of alternating inputs of methane and oxygen is the rectangular pulse, or saw-toothed wave. The model of Valocchi and Roberts (1983) takes into account the effects of advection, dispersion, and sorption on transport and mixing of rectangular pulses under conditions of uniform flow. Although the situation at the Moffett Field site certainly differs appreciably from the simple case of uniform flow in a homogeneous medium, the model computations based on the idealized case are instructive in exploring the effects of pulse length on mixing, and serve as a point of departure for experimental design.

In the absence of reaction, the normalized amplitude ratio is the most convenient measure of the degree to which the pulses remain separated during transport, or conversely the degree to which mixing has occurred. The amplitude ratio is the ratio of observed magnitude of concentration fluctuations measured at an observation a distance x removed from the injection point to the magnitude of the fluctuations measured at the injection point. The amplitude ratio varies from zero to unity: a value near zero means that concentration fluctuations are damped nearly completely, and signifies virtually complete mixing over the distance traversed, whereas a value near unity implies negligible mixing.

Model computations were conducted under conditions simulating those at the Moffett site. The important variables were the integral distance, x ; the pore water velocity, u ; and the Peclet Number for dispersion, Pe . The values for the simulation were chosen as $x = 1$ m, $u = 0.12$ m/h, and $Pe = 5$ (dimensionless), to correspond to the results at the nearest observation, S1, based on the results of the early tracer tests, i.e., the dissolved oxygen breakthrough in the initial stages of the Tracer4 set. The computation's results (Figure 5.16) indicated that substantial mixing over a transport distance of 1 m (the distance from SI to S1) would be attained using a pulse length on the order of several hours, and that pulse lengths on the order of several tens of hours would prevent adequate mixing prior to the first observation well.

To test the model, toward the end of the Tracer5 experiment the dissolved oxygen injection was switched to an on/off mode, with pulse lengths chosen to span the range of potential choices for experimental operation, i.e., less than one hour to 12 hrs. The observed values are shown in Figure 5.16 as open circles.

The observations show qualitatively the kind of trend predicted by the model: with short pulses (< 1 hr), the mixing is complete within the first meter, but, as the pulse period is increased to several hours, substantial concentration fluctuations begin to appear at the observation well, indicating that mixing is incomplete. The prediction does not agree quantitatively with the data, as the onset of substantial observed concentration fluctuations occurs at a lower critical value of the pulse period. Indeed, the value of the Peclet Number must be chosen as 100, rather than the observed value of 5, to simulate the pulsing

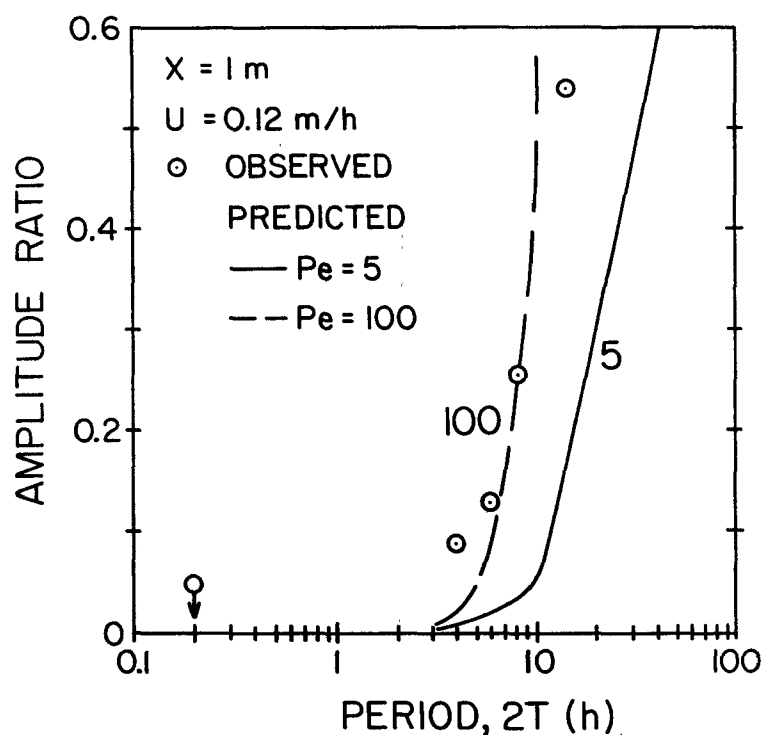


Figure 5.16. Comparison of predicted and observed effects of dissolved oxygen pulsing.

data satisfactorily. These deviations may well be caused by deviations from the model assumptions of uniform flow in a homogeneous medium. Nonetheless, the qualitative agreement between predicted and measured values for the effect of pulsing was deemed adequate as a framework for experimental design of the biostimulation phase.

SUMMARY

The tracer experiments provided the needed information on the transport characteristics of the test zone. The tests also demonstrated that controlled, reproducible experiments could be performed at the field site.

Natural gradient tracer tests indicated the presence of a strong regional component to fluid flow in a northern direction. The tests combined with RESSQ model simulations indicated that the induced flow experiments would be best performed by injecting into the upgradient S1 well and extracting from the P well downgradient.

Induced gradient bromide tracer tests established fluid residence times in the test zone. The tests also demonstrated that reproducible transport experiments could be performed at the test site. The tests showed that by increasing extraction rates, complete recovery of the injected bromide could be achieved. This ability to completely recover the injected fluid provided confidence in conducting subsequent biotransformation experiments with vinyl chloride.

The dissolved oxygen transport tests demonstrated that DO was not consumed and was transported like bromide. Due to the presence of organic matter after the test zone was biostimulated, a minor amount of DO consumption was observed.

The chlorinated organic transport experiments showed the retardation of these compounds compared to the bromide tracer. The rank order of retardation was as follows: TCE > trans-DCE and cis-DCE > vinyl chloride. Retardation estimates based on the center of mass of the breakthroughs curves were a factor of 1.5 to 2 greater than those based on the time to reach 50% breakthrough. The higher values are probably more representative of the actual retardation since they include the effects of long-term sorptive uptake onto the aquifer solids. Thus, the organic transport experiments provided required information on the sorption and retardation process of the organics in the test zone.

Modeling studies helped confirm the results of the tracer tests. Simulations using the model RESSQ indicated that the fluid residence times observed in the field are reasonable, when the fluid injection and extraction are superimposed on the strong regional flow field. The 2-D simulations indicated that uniform flow conditions in the direction of the monitoring wells were approached a short distance from the injection well.

Simulations assuming 1-D advection-dispersion transport, provide a good match to the observed DO breakthrough at observation wells. The match indicates that the transport to the observation wells can be reasonably approximated by the assumption of uniform flow.

Simulations of the response to pulsing of DO agreed with theoretical predictions. The requirement of lower dispersion coefficients (higher Peclet numbers) to match the pulse response, compared to those required to match the complete breakthrough suggests deviations from the assumption of uniform flow. Nonuniform flow was probably the result of aquifer heterogeneities.

SECTION 6

RESULTS OF BIOSTIMULATION AND BIOTRANSFORMATION EXPERIMENTS

Lewis Semprini, Gary Hopkins, and Paul Roberts

Biostimulation and biotransformation experiments were performed in three successive field seasons. Performing the experiments in this manner permitted the results of the previous field season, and information gained in laboratory studies to be incorporated into the next season's experimental design. Table 6.1 includes the series of experiments that were performed in each of the field seasons. In the latter years the number of chlorinated aliphatics studied increased, and the sequence of experiments was changed. These changes over the course of the experiments enabled the in-situ biotransformation process to be effectively demonstrated, and supplied detailed information on processes governing the rates of biotransformation.

The first season of testing focused on the ability to biostimulate a native population of methanotrophic bacteria, and on the biotransformation of TCE in the stimulated test zone. The biostimulation experiment was initiated by introducing methane and oxygen in the absence of TCE. After biostimulation was achieved, TCE was added, together with methane and oxygen, to assess TCE biotransformation.

TABLE 6.1. EXPERIMENTS AND PROCESSES STUDIED

Experiment	Duration	Chemicals Injected	Average ^a Conc. (mg/l)	Process Studied
<u>First Season</u>				
Bioestim1	9/05/86- 9/30/86	Methane DO Bromide	5.9±1.1 ^b 20.7±4.3 166±4.5	Biostimulation of native methane-utilizing bacteria. Alternating pulse injection of methane and DO.
Biotran1	9/30/86- 10/21/86	Methane DO TCE	5.7±1.2 22.2±1.7 0.097±0.024	Biotransformation of TCE with active biostimulation. Non-steady-state conditions.
Biotran4	12/10/86- 12/31/86	Methane DO Bromide TCE	5.2±0.9 23±1.5 159±16 0.051±0.010	Biotransformation of TCE with active biostimulation. Steady-state conditions.

TABLE 6.1 cont.

TABLE 6.1 (cont.)

<u>Second Season</u>				
Tracer8	7/06/87- 8/15/87	DO	14.3±1.3	Transport and breakthrough of bromide, TCE, cis-DCE, and trans-DCE before biostimulation.
		Bromide	78±6	
		TCE	0.048±0.010	
		cis-DCE	0.110±0.036	
		trans-DCE	0.112±0.039	
Biostim2	8/17/87- 10/26/87	Methane	5.3±0.9	Simultaneous biostimulation and biotransformation for TCE, cis-DCE, and trans-DCE.
		DO	23.4±2.0	
		Bromide	44±4	
		TCE	0.036±0.006	
		cis-DCE	0.091±0.025	
		trans-DCE	0.092±0.026	
Decmeth1	10/27/87- 11/08/87	DO	24.5±1.1	Test if biotransformation occurs without active methane utilization.
		TCE	0.045±0.005	
		cis-DCE	0.136±0.022	
		trans-DCE	0.095±0.013	
Peroxid2	11/30/87- 12/23/87	H ₂ O ₂	45	Test if increased biomass improves biotransformation by substituting hydrogen peroxide for oxygen.
		Methane	10.6±1.5	
		TCE	0.054±0.006	
		cis-DCE	0.143±0.026	
		trans-DCE	0.10±0.02	
<u>Third Season</u>				
Tracer11	8/10/88- 10/10/88	Bromide	72±5	Transport and breakthrough of bromide, TCE, cis-DCE, and trans-DCE before biostimulation.
		TCE	0.047±0.006	
		cis-DCE	0.085±0.013	
		trans-DCE	0.050±0.007	
Tracer12	10/20/88- 10/20/88	Bromide	44±3	Transport and breakthrough of bromide and vinyl chloride while continuing injection of TCE, cis-DCE,, and trans-DCE
		TCE	0.042±0.003	
		cis-DCE	0.100±0.011	
		trans-DCE	0.054±0.007	
		VC	0.044±0.007	
Biostim3	10/20/88- 11/23/88	Methane	6.6±0.7	Simultaneous biostimulation-bio-transformation of TCE, cis-DCE, trans-DCE, and vinyl chloride. Transient testing of formate and methanol as substitute for methane as electron donors.
		DO	21.3±0.7	
		Bromide	45±2	
		TCE	0.046±0.003	
		cis-DCE	0.100±0.015	
		trans-DCE	0.052±0.009	
		VC	0.034±0.007	
		Formate	73	
		Methanol	16.9	

^a Average values for methane, DO, H₂O₂, formate, and methanol are time-averaged due to pulsing.

^b Standard deviation of the injection concentrations.

In order to provide a more direct and convincing demonstration of the in-situ biotransformation process, the experimental sequence was changed, and additional compounds were studied during the second field season. This was accomplished by first adding TCE, cis-DCE, and trans-DCE before biostimulation, to achieve nearly complete breakthrough of these compounds at the observation wells. The test zone was then biostimulated, while continuing to add the halogenated organics. This sequence permitted the direct observation of the effect of biostimulation on biotransformation. In the second season, several supplementary transient experiments were also conducted: 1) hydrogen peroxide was introduced into the test zone as a source of oxygen to enhance a greater biomass of methane-utilizing bacteria, and 2) the methane concentration was varied stepwise to evaluate its effect on the biotransformation rates of the chlorinated aliphatics.

The sequence of field experiments in the third season was similar to that of the second, except that the biotransformation of vinyl chloride was also studied. Transient experiments included the substitution of formate and methanol for methane after biostimulation was achieved to investigate the influence of methane inhibition on the rates of biotransformation of the chlorinated aliphatics.

RESULTS OF THE FIRST SEASON OF FIELD TESTING

Biostimulation Experiment

The first biostimulation experiment (Biostim1) was conducted to determine (1) the ease of stimulating indigenous methane-oxidizing bacteria, (2) stoichiometric requirements for methane and oxygen, (3) information on the rate of growth, (4) the spatial extent over which biostimulation could be achieved, and (5) the effectiveness of the alternate pulsing of methane and DO for distributing microbial growth.

Groundwater containing either methane or oxygen was pulse-injected alternately at the SI injection well. The injection system used is described in detail in Section 4. The pulse cycle was varied during the course of the experiment, from less than 1 hr during start-up (to ensure that pulsing would not interfere with growth) to a 12-hr period during the latter stages of the experiment. This approach ensured that growth was distributed in the test zone. The pulse length ratio was 1:2 (methane:oxygen), resulting in time-averaged injected fluid concentrations of 5.4 and 19 mg/l for methane and oxygen, respectively. No additional nutrients (N or P) were added to the injected fluid.

Figure 6.1 shows the dissolved oxygen (DO) concentration as a function of time at the three observation locations: S1 (1 m), S2 (2.2 m), and S3 (4 m). During the first 140 hrs of the experiment there was little evidence of DO consumption. Within 50 hrs of injection, DO concentrations reached maximum steady-state values, which decreased slightly with distance from the injection well. During this period, the bromide tracer and methane achieved the same degree of fractional breakthrough as DO, indicating that this initial decrease in concentration with distance resulted primarily from dilution by the indigenous groundwater and not from microbial consumption. The maximum dilution occurred at the extraction well, due to the 1:8 ratio between the injection and extraction flow rates. This early response indicated that microbial activity in the test zone was sufficiently low so that no measurable DO utilization resulted.

The first signs of an onset of DO consumption were observed in the extraction well and the S3 observation well after approximately 200 hrs of injection. Owing to the increasing utilization removal by microorganisms with distance, the decrease in DO was greatest at the observation wells farthest from the injection well.

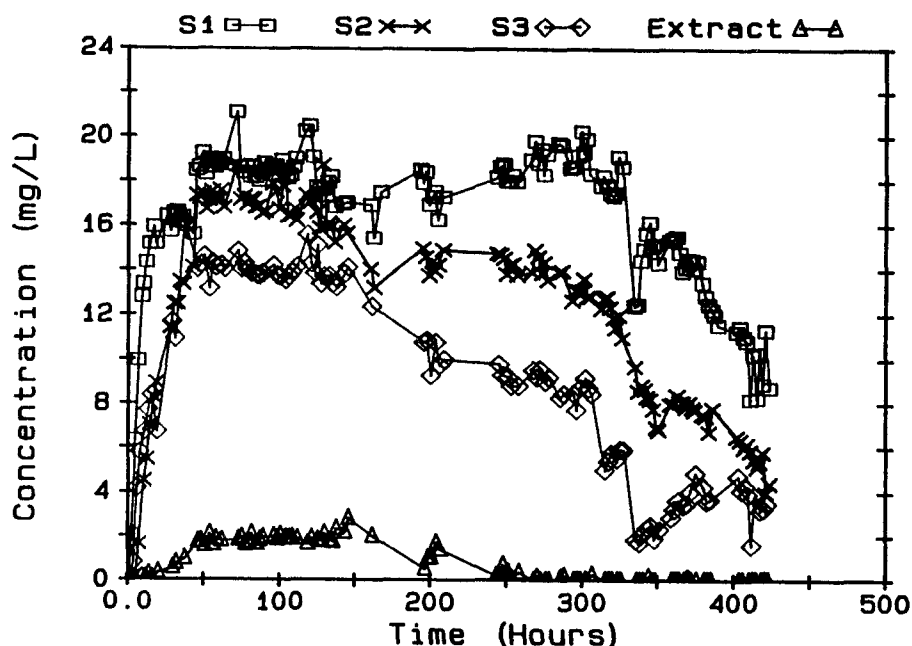


Figure 6.1. Dissolved oxygen (DO) concentration response at the observation wells and extraction well due to biostimulation of the test zone.

Figure 6.2 shows the similar response between methane and DO at the S2 observation well, decreasing as expected for methane oxidation by methanotrophs. At early time (0-50 hrs) methane and DO broke through similarly to the bromide tracer, indicating no retardation and minimal DO consumption. The relatively rapid decrease in the methane and oxygen concentrations over the period between 200 to 430 hrs indicates microbial growth. The methane concentrations at well S2 decreased below the detection limit (0.25 mg/l) after 430 hrs of injection, while a residual oxygen concentration of approximately 3.5 mg/l was maintained. Based on these values, the mass ratio of oxygen to methane consumed was approximately 2.5, which is significantly lower than the ratio of 4 that would be required for complete methane oxidation. The lower measured ratio was also expected, however, since some of the methane carbon utilized would be associated with biological growth.

The decrease of methane concentration below the detection limit at the S2 observation well after 430 hrs indicated that microbial growth was becoming concentrated near the injection well. The pulse cycle period was then lengthened to 12 hrs in order to prevent biofouling near the wellbore. The resulting response at the S2 well is shown in Figure 6.3. Peak methane values then increased from below detection to maximum values of approximately 1 mg/l. Peak methane concentrations occurred when minimum DO concentrations were observed, consistent with transport theory. The response to pulsing at the S1 well is shown in Figure 6.4. Peak methane and oxygen concentrations are less strongly attenuated than those at the S2 well. This was expected; since the S1 well is closer to the injection well than S2, less dispersive mixing occurs. Long pulse cycles were continued throughout the first year of experiments. Based on the low levels of methane that were observed consistently at the monitoring wells, the pulsing is believed to have promoted a spatially distributed microbial population in the test zone. Biofouling of the wellbore and sand pack was thus limited by the pulsing methodology.

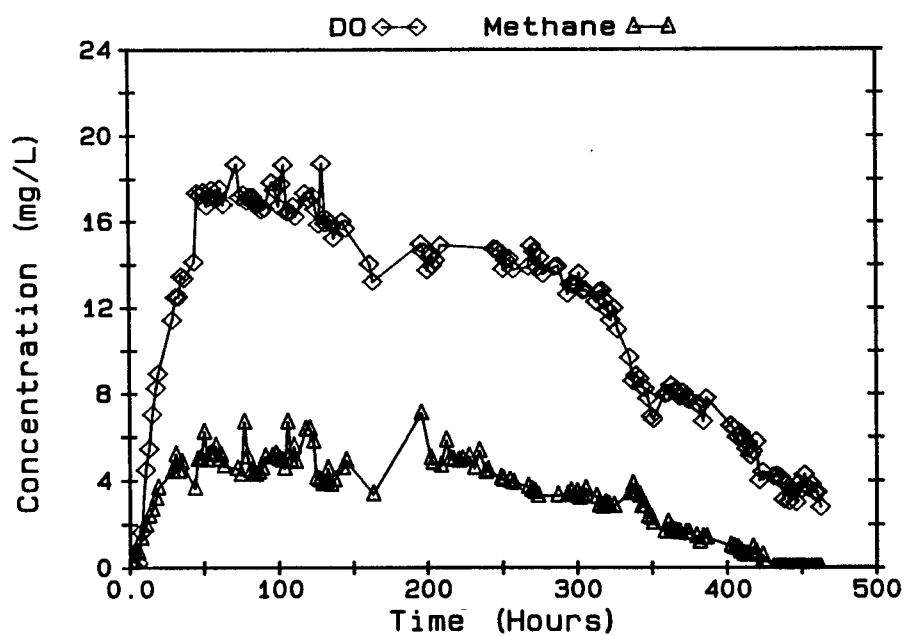


Figure 6.2. Methane and DO response at the S2 observation well due to the biostimulation of the test zone.

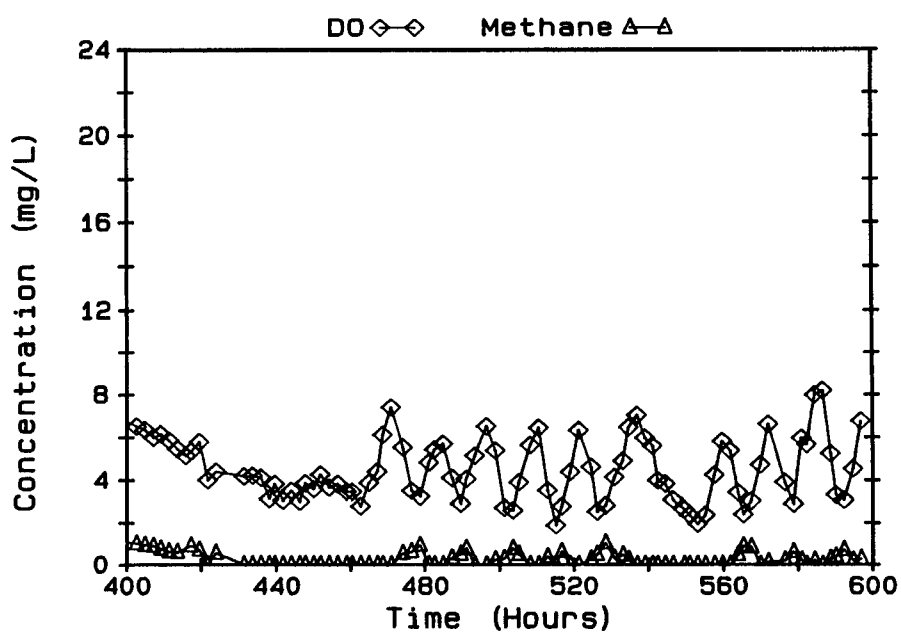


Figure 6.3. The response at the S2 observation well resulting from 8- and 4-hr alternate pulses of DO and methane.

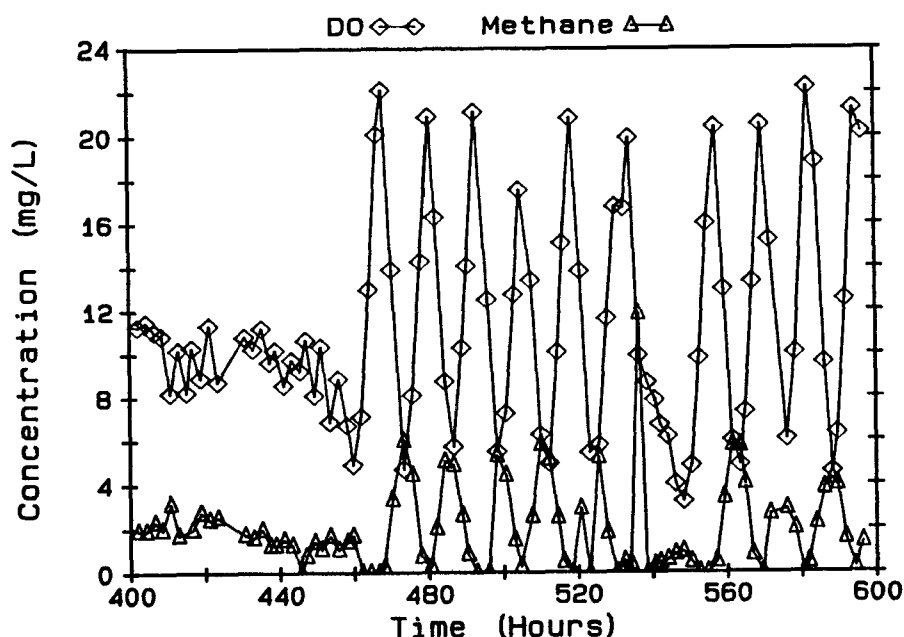


Figure 6.4. The response at the S1 observation well resulting from 8- and 4-hr alternate pulses of DO and methane.

Biotransformation Experiments

The initial biotransformation experiments were performed after the test zone was biostimulated. After biostimulation TCE was injected continuously over a three-month period. The initial concentration of TCE averaged 97 $\mu\text{g/l}$. Methane and oxygen were continuously pulse-injected during this period in order to maintain biostimulated conditions. The results of these initial TCE experiments are discussed in detail in a previous EPA report (Semprini et al., 1988), so they will be briefly summarized only.

In these experiments, estimates of biotransformation were assessed by: 1) comparing with TCE breakthrough in the pseudo-control experiment (Tracer5); 2) comparing the steady-state fractional breakthroughs of TCE to those of bromide as a conservative tracer; and 3) computing mass balances on the amount of TCE injected and extracted, and normalizing with respect to bromide mass balances. The three methods were found to agree closely, with all indicating that 20 to 30 percent of the TCE added to the system was biotransformed.

Comparisons with bromide as a conservative tracer are considered the most accurate estimate of the degree of transformation achieved. Before the extent of biotransformation was estimated by this method, the TCE injection concentration was lowered from 97 to 51 $\mu\text{g/l}$ to minimize sorptive loss due to slow uptake of TCE onto aquifer solids. The resulting steady-state fractional breakthrough of TCE is shown in Figure 6.5. Biotransformation is indicated by the lower breakthrough at the S2 well compared to the S1 well, with both wells having a fractional breakthrough significantly lower than a value of unity. The results of a bromide tracer test performed during this same time period are shown in Figure 6.6, for comparison. The steady-state fractional breakthroughs for bromide at each observation well (S3 not shown) are significantly higher than those of TCE, indicating transformation of TCE. Using equation (4-1) the degree of biotransformation of TCE was estimated based on the steady-state fractional breakthroughs of the two

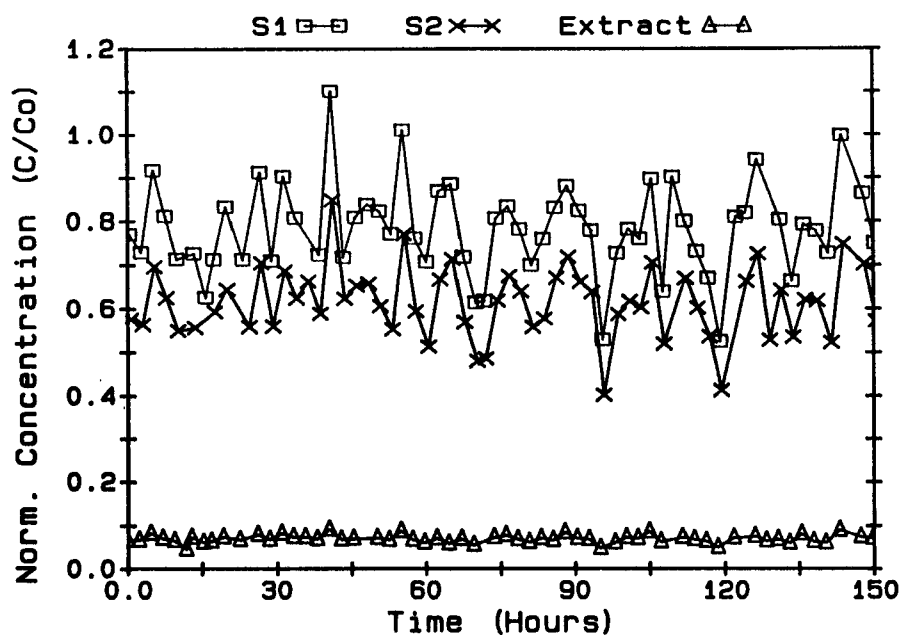


Figure 6.5. Steady-state normalized TCE fractional breakthroughs during the first season's biotransformation experiment, Biotrans4.

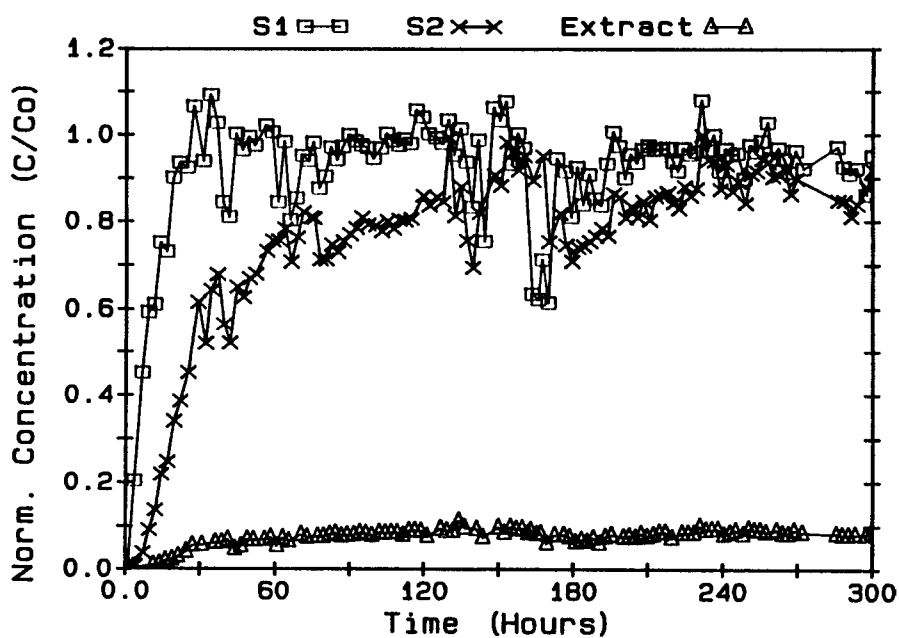


Figure 6.6. Normalized bromide tracer breakthrough for the steady-state period shown in Figure 6.5.

chemicals. The estimated transformation based on each observation location is as follows: S1, 17%; S2, 28%; S3, 23%; and extraction, 16%. Biotransformation was indicated only in the zone of active methane utilization. In the area between S2–S3 and the extraction well, no methane was present to support bacterial growth, and no additional degradation of TCE was observed.

The concentration of 1,1,1-trichloroethane (TCA), found as a background contaminant in the test zone, also was monitored during the biotransformation experiments. During the first season the average field concentration of TCA, based on extracted well samples, was 65 µg/l. The average concentration of TCA recycled in the injected fluid was 56 µg/l, due to partial stripping in the DO and methane sorption columns. During the same steady-state period, as presented in Figure 6.5 for TCE, the average TCA concentrations at monitoring wells S1 and S2 were 53 and 55 µg/l, respectively. These concentrations were essentially identical to the injected levels. This suggests that little biotransformation of TCA occurred during transport through the test zone. After normalizing for the degree of mixing of the injected fluid with the native fluid (based on bromide tracer test data shown in Figure 6.6), over 95% of the estimated TCA concentration was observed at the S1 and S2 observation wells. The estimate indicates minimal transformation of TCA. There is a large error associated with this estimate, however, due to the fluctuating concentration of TCA in the indigenous groundwater.

At the end of the first year's biostimulation experiment, TCE addition was stopped. Extraction and monitoring of the TCE elution continued for an additional 3 months. The observations indicate a slow release of TCE sorbed onto the aquifer solids. A TCE mass balance over the complete biotransformation experiment showed 10.1 g of TCE were injected and 4.5 g were extracted. This represents a recovery of 45%. During this same overall period, 65 to 70 percent of the bromide tracer was recovered. The lower recovery of TCE compared to bromide provides additional evidence that 25-30% of the injected TCE was biodegraded.

It could be argued that increases in the sorption capacity of the aquifer as a result of increased organic carbon due to biostimulation is responsible for these observations. We disagree on the following grounds. First, the amount of biomass produced by biostimulation was too small to account for the observed effect. Model estimates of the steady-state biomass stimulated are presented in Section 13. Based on these estimates the biostimulated organic carbon would increase the organic carbon content of the aquifer by only 1%, which is a very minor amount. Also the results of tracer experiments presented in Section 5 showed no significant increase in TCE retardation over the three years of testing, consistent with the above estimate.

The experimental approach taken also minimized the effects of sorption interactions. Injection concentrations of the chlorinated solutes were lowered before assessing the extent of biotransformation, so that desorption and not sorption was likely occurring. In making mass balances, the elution of the chlorinated solutes from the aquifer solids was monitored for several months in order to complete mass balances.

Summary of the First Season's Results

The first season of field testing demonstrated that indigenous methanotrophic bacteria could be easily biostimulated by the introduction of methane and oxygen to the test zone. Methane and DO were found not to be strongly sorbed and were transported like the bromide tracer. No additional nutrients (N, P) were required. Biostimulation of methanotrophs was demonstrated by the uptake of methane and DO after a lag period of approximately 2 weeks. The stoichiometric ratio of methane and DO consumption was consistent with expectations for an active methanotrophic community. Under the flow conditions prevailing in the test zone, complete methane utilization occurred over a flow path of 2 m, as long as the pulse cycle duration was short (< 1 hr). Alternate pulsing of methane and DO with long cycles (12 hr)

helped distribute methane, and presumably the microbial biomass, throughout the test zone, which minimized biofouling near the injection well.

TCE biotransformation experiments performed after the test zone was biostimulated indicated that 20 to 30% of the TCE was transformed during transport through the biostimulated zone. Different methods of estimating the degree of transformation yielded similar results. Measurements of TCA as a background contaminant indicated insignificant transformation of TCA.

Despite the fact that only partial TCE transformation was observed, the results of the first year of testing demonstrated that, if sufficient control and care are exercised in experimentation, quantitative evidence of degradation can be obtained in the field under conditions representative of real aquifer systems.

RESULTS OF THE SECOND SEASON OF FIELD TESTING

In the second season of field testing, the experimental design was modified to provide a more direct and convincing demonstration of biotransformation. The chlorinated organic solutes of interest were first added to the test zone to achieve steady-state fractional breakthroughs before biostimulation. The test zone was biostimulated subsequently through the addition of methane and oxygen, while continuing to add the chlorinated solutes. The resulting change in concentration of the chlorinated organic solutes due to biostimulation was observed directly. The number of contaminants studied was also increased. Cis-DCE and trans-DCE were added together with TCE. Laboratory studies of Henson et al. (1987, 1988) indicated methane-utilizing mixed cultures degraded cis-DCE and trans-DCE more rapidly than TCE while TCA was degraded more slowly. Fogel et al. (1986) presented similar results from mixed culture studies. It was desired to see if similar results would be obtained in the field demonstration.

Transient experiments were performed as well to study the effect of methane concentration on biotransformation and to determine whether continuous methane addition was required for transformation to occur. Finally, experiments were performed in which peroxide was substituted for oxygen in order to increase the amount of methane injected.

The Organic Addition Experiment

The objective of this experiment (Tracer8) was to establish steady-state concentrations of the organic contaminants in the test zone before restimulation. The experiment provided information on the transport of the three organics relative to bromide and the degree of capture of injected bromide at the extraction well. The results of these transport experiments are discussed in Section 5.

Before injecting the chemicals, a background contaminant was observed in the test zone's groundwater that co-eluted with trans-DCE during GC analysis. The peak area of this background contaminant was equivalent to 16 to 27 $\mu\text{g/l}$ of trans-DCE. GC-MS analyses identified this background contaminant as 1,1-dichloroethane (1,1-DCA). Later results showed that 1,1-DCA was not transformed to a significant extent in the test zone. Thus, the concentration of trans-DCE was corrected for the presence of this co-eluting compound by subtracting an average background concentration as measured in wells N1, N2, N3 outside the test zone during the second season's experiments.

The average concentrations injected were 112, 110, and 48 $\mu\text{g/l}$ for trans-DCE, cis-DCE, and TCE, respectively. Aerobic conditions were maintained by the addition of dissolved oxygen in the injected fluid at an average concentration of 14 mg/l. Gradual increases toward injected concentrations in TCE, cis-DCE, and trans-DCE were observed over the 40 day injection period. The rank order of retardation was as follows: TCE > trans-DCE > cis-DCE.

Table 6.2 summarizes the quasi-steady-state fractional breakthroughs achieved for bromide and the chlorinated organic solutes. Complete bromide breakthrough was observed at the S1 and S2 wells, indicating negligible dilution of the injected fluid by the indigenous groundwater. Mass balances, (Section 5), indicated 100 % recovery of the injected bromide by the extraction well. The organic solutes reached quasi-steady-state fractional breakthroughs of 90% to 95% at the S1 well, indicating negligible transformation by biotic or abiotic processes during this quasi-control stage before biostimulation.

Cis-DCE reached the highest fractional breakthrough, followed by trans-DCE, and TCE. This order is consistent with the degree of retardation, with TCE being the most strongly sorbed and having the lowest degree of fractional breakthrough. TCE concentrations at the S2 well and the extraction well increase very slowly due to advective, dispersive, and sorptive processes. Thus TCE, and to lesser extents cis- and trans-DCE, probably did not achieve a maximum steady-state breakthrough concentration at all locations before the start of the biotransformation experiment.

TABLE 6.2. TRACER8 EXPERIMENT – PERCENTAGE BREAKTHROUGH OF THE CHLORINATED SOLUTES AND BROMIDE AT THE OBSERVATION WELLS

Substance	Well S1 (%)	Well S2 (%)	Well S3 (%)	Extraction (%)
Bromide	100 ± 0.7 ^a	98 ± 3.0	83 ± 0.7	13.6 ± 0.1
TCE	94 ± 2	84 ± 2	68 ± 2	10.3 ± 0.2
cis-DCE	94 ± 3	94 ± 3	72 ± 3	12.4 ± 0.5
trans-DCE	94 ± 3	93 ± 3	72 ± 5	11.6 ± N.D.

^a Standard error of the mean.

The Biostimulation-Biodegradation Experiment

The combined biostimulation-biotransformation experiment (Biostim2) immediately followed the organic solute addition experiment. Operating conditions of this experiment are presented in Table 6.1. While injection of organic solutes continued, methane and oxygen were added in short pulses of 20 and 40 min, respectively. Average methane and DO injection concentrations were in the range of those used in the first season's tests. Methane and DO uptake occurred very rapidly, with essentially no lag observed. The response indicated that some of the methane utilizers stimulated in the first season were still present to immediately initiate methane utilization at the start of the second season.

Figure 6.7 shows the simultaneous response of methane, DO and trans-DCE at the S1 well. The decrease in all three components due to biological activity is apparent after about one day of injection. Methane decreased below the detection limit after 72 hrs of injection, while dissolved oxygen and trans-DCE showed a continued gradual decrease in concentration. The reduction in trans-DCE concentration, coincidental with the consumption of methane, provides direct evidence of its in-situ biotransformation in response to the biostimulation of the methane-oxidizing bacteria.

Figure 6.8 shows the S2 responses of all three organics resulting from biostimulation of the test zone. Bromide tracer results at S2 are also shown for comparison. A five-point running average is presented to clearly show the trends for each compound. The decreases in concentration from normalized values near unity are apparent, especially for cis-DCE and trans-DCE. During this period, the bromide tracer showed complete breakthrough to injected concentrations, demonstrating that decreases in the

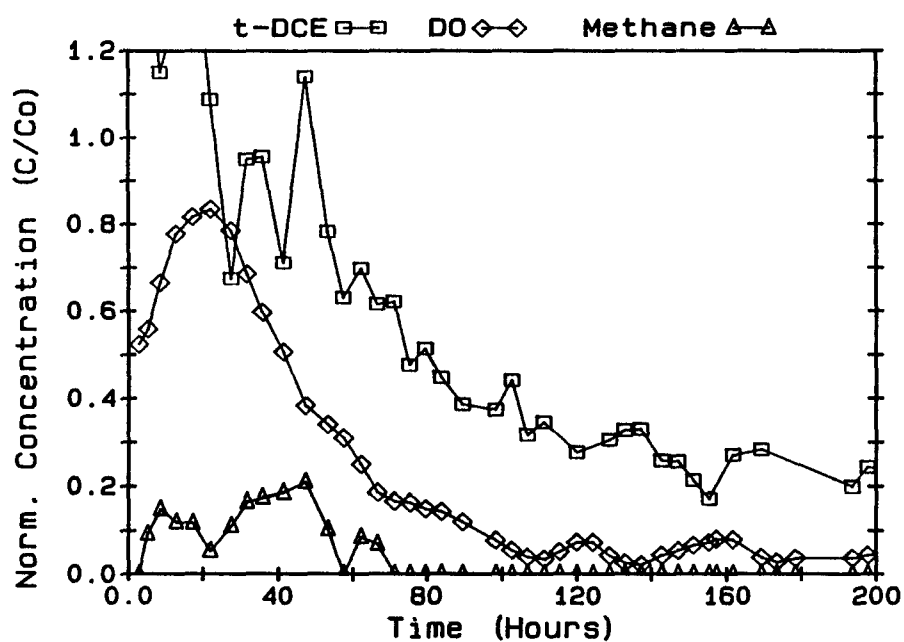


Figure 6.7. Response at the S1 well of methane, DO, and trans-DCE in the second season's biostimulation-biotransformation experiment, Biostim2.

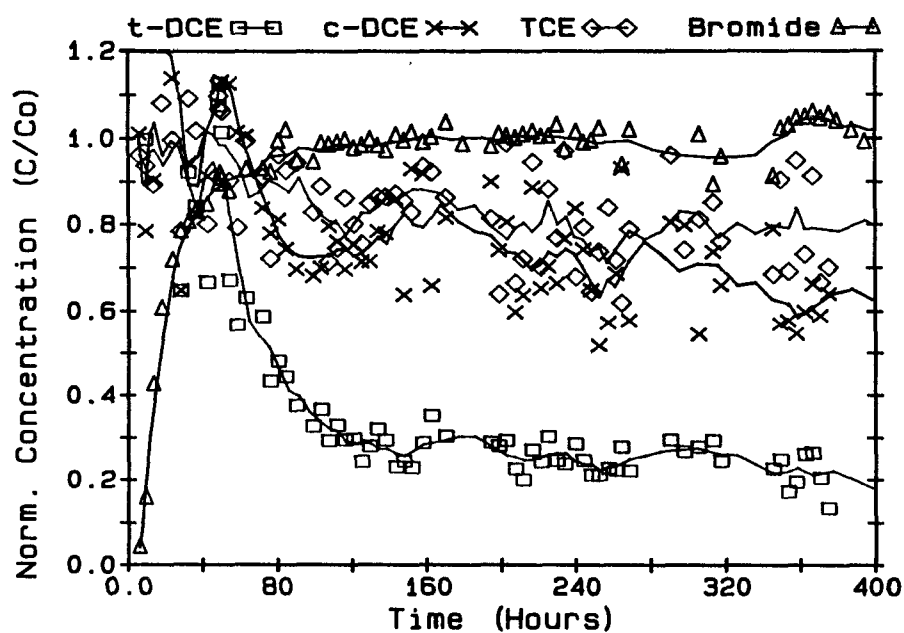


Figure 6.8. Response at the S2 well of trans-DCE, cis-DCE, and TCE in the second season's biostimulation-biotransformation experiment, Biostim2.

organic concentrations were not related to advective or dilution losses in the system, but were the result of biotransformation. Trans-DCE is shown to decrease in concentration most rapidly, followed by cis-DCE and TCE. The more rapid decrease in trans-DCE concentration, compared to cis-DCE and TCE, results primarily from its having a faster rate of transformation. Other processes affecting the transient response include sorption and microbial growth. These processes will be discussed in greater detail in the biotransformation modeling chapter.

In order to distribute the microbial growth population more evenly throughout the test zone, the pulse time was increased to the standard 12-hr cycle used in most experiments. Steady-state biotransformation conditions were achieved during this period of longer pulse cycle, as shown in Figure 6.9. Fractional breakthroughs of the chlorinated aliphatics at the S2 observation well indicate the following extents of transformation: TCE, 20%; cis-DCE, 50%; and trans-DCE, 80%.

Production of a Transformation Intermediate

At the onset of the second year's biotransformation experiment, an intermediate product was detected during the chlorinated organic's GC analysis. The sensitivity to electron capture detection indicated that this transformation product was halogenated. No peaks had appeared with a similar GC retention time during the previous year's study with TCE, indicating that the intermediate was associated with either trans-DCE and/or cis-DCE transformation. Janssen et al. (1987) reported the formation of a relatively stable trans-DCE oxide (epoxide) from the biodegradation of trans-DCE by a consortium of methanotrophic bacteria. It is plausible that such a compound might be formed as an intermediate product of trans-DCE degradation. Figure 6.10 shows the increase in the intermediate product's concentration that occurred simultaneously with the decrease in trans-DCE concentration. The production of the epoxide appears to be associated with the transformation of trans-DCE. Results of GC-MS analyses, discussed in Section 7, confirmed that this intermediate was indeed the trans-DCE oxide (epoxide).

Quantification of the epoxide concentration was made, using an epoxide standard synthesized in our laboratory. Stored peak areas were converted to concentrations based on the relative response of the epoxide and trans-DCE to ECD detection. There is some uncertainty in the epoxide concentration estimated, since the epoxide standard had to be synthesized and purified. Despite this uncertainty in the absolute concentration, the epoxide appears to represent only 5 to 10% of the trans-DCE degraded.

Transient Methane Addition Experiments

After steady-state biotransformation conditions were achieved, a series of transient methane addition experiments were performed to assess to what degree lower methane concentrations influence biotransformation rates. Moreover, results were used to determine if biotransformation continued after methane addition was temporarily ceased. Figure 6.11 shows the response of TCE, cis-DCE and methane at the S1 well due to these perturbations. During the period of 100-200 hrs, lower injected methane concentrations were produced by shortening the methane pulse length by a factor of two. Over this short study period no significant change in the degree of biotransformation resulted. Over the period of 275-475 hrs, methane addition was ceased, while input of the chlorinated solutes and DO continued. Gradual increases towards injected concentrations of cis-DCE, TCE, and trans-DCE (Figure 6.12), resulted. The increases indicated that transformation diminished in the absence of methane. The slow increase, due to sorptive retardation, makes it difficult to determine if biotransformation stopped immediately after methane was no longer available. After 475 hrs, methane addition was restarted to restimulate the test zone. A rapid decrease in concentration of the halogenated aliphatics to previous levels occurred as biotransformation commenced. These data demonstrate that the biostimulated population of methane-utilizing bacteria required active methane utilization for the biotransformation of halogenated aliphatics to occur.

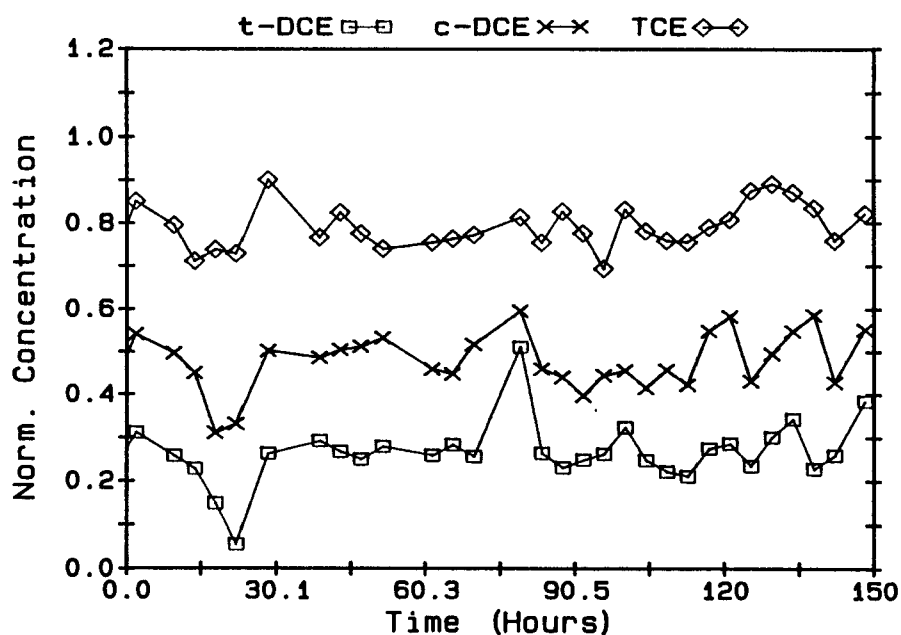


Figure 6.9. Fractional breakthrough at the S2 well of trans-DCE, cis-DCE, and TCE under steady-state biotransformation conditions at the end of Biostim2 experiment.

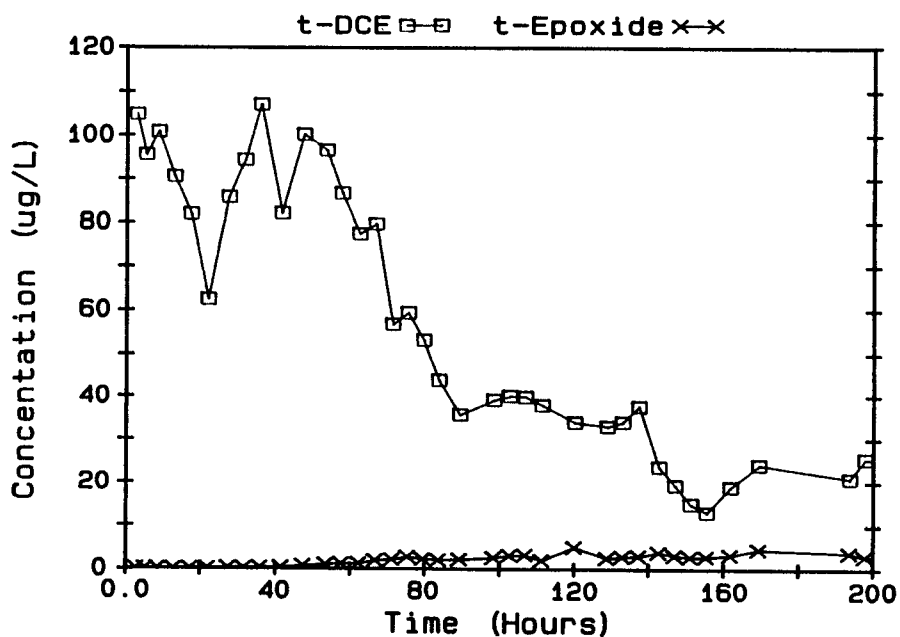


Figure 6.10. Production of trans-DCE oxide (epoxide), an intermediate of trans-DCE biotransformation in the Biostim2 experiment.

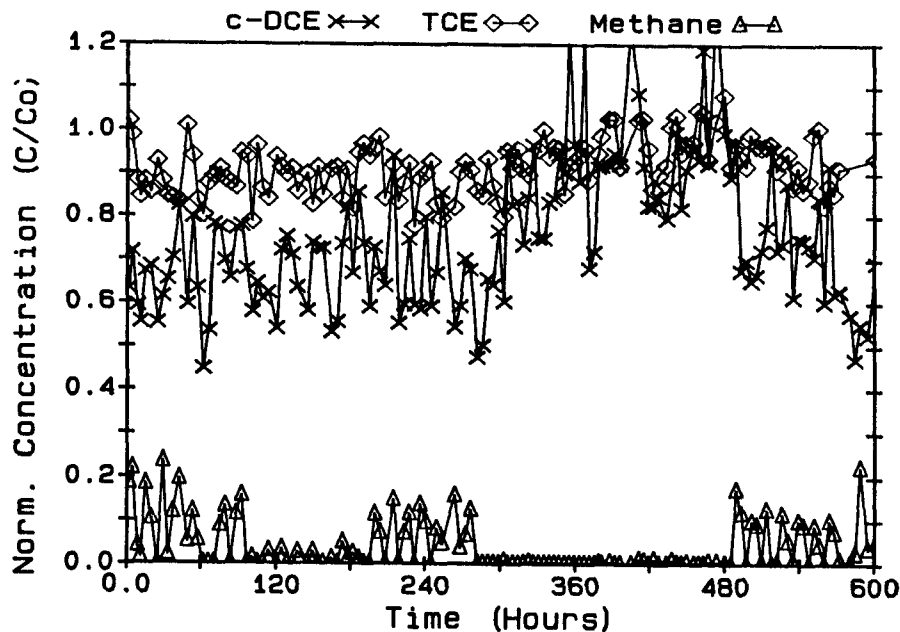


Figure 6.11. Response at the S1 well of TCE and cis-DCE to the reduction (100-200 hrs) and termination (275-475 hrs) of methane addition.

Figure 6.12 shows the response at the S1 well of the epoxide intermediate and trans-DCE during these transient experiments. A very rapid decrease in the epoxide concentration resulted after methane addition was stopped. The response, which was much faster than the increase in trans-DCE concentration, indicates that trans-DCE epoxide formation also ceased immediately after methane addition was stopped. This rapid decrease also suggests that the epoxide is much less strongly sorbed than trans-DCE, and/or that transformation of the epoxide continues after methane addition was stopped.

Peroxide Addition Experiment

A transient experiment was performed to determine if greater transformation rates could be achieved by increasing the methane-utilizing biomass through the addition of greater amounts of methane to the test zone. To achieve this, the methane pulse length had to be increased and the DO pulse length decreased. This was accomplished by injecting hydrogen peroxide (H_2O_2) as a source of dissolved oxygen under active biostimulation conditions.

Hydrogen peroxide was injected at a concentration of 272 mg/l, which upon complete breakdown would produce 128 mg/l of dissolved oxygen. This reduced the electron acceptor pulse time from 8 hrs (with oxygen) to 2 hrs with hydrogen peroxide, while the methane pulse was increased from 4 hrs to 10 hrs. Based on mass balances, the rate of methane addition was increased by a factor of 2, compared to the previous studies with oxygen. Theoretically, a corresponding increase in the methane-utilizing biomass should result.

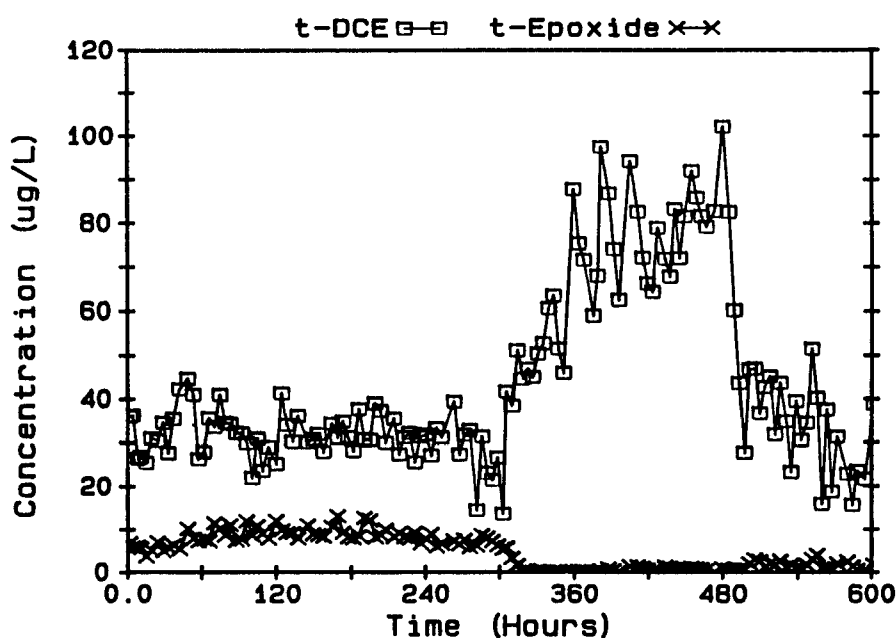


Figure 6.12. Response at the S1 well of trans-DCE and trans-DCE oxide (epoxide) to the reduction (100-200 hrs) and termination (275-475 hrs) of methane addition.

Analyses for hydrogen peroxide breakthrough at observation wells were performed on samples obtained manually. No breakthrough of hydrogen peroxide was observed, indicating that the H_2O_2 reacted rapidly to form oxygen within the first meter of travel in the test zone. Measurements at the S2 well indicated that methane was transformed completely during periods when oxygen was in sufficient excess. The stoichiometric ratio of methane to DO consumption appeared to be unchanged compared to earlier results. Hydrogen peroxide therefore did not appear to inhibit the activity of methane-utilizing bacteria.

Figure 6.13 shows the steady-state fractional breakthroughs of the chlorinated organics at the S2 well during the peroxide addition experiment, corresponding to the first 553 hrs of the graph. The breakthroughs, compared to those in Figure 6.9, indicate no significant enhancement in the degree of transformation was achieved with the increased methane addition made possible by switching to hydrogen peroxide as a concentrated oxygen source.

Upon completion of the peroxide addition experiment, the injection of oxygen and methane was resumed, using the standard 12-hr cycle. The time-averaged injection concentration of methane was reduced to 5.2 mg/l, a factor of 2 lower than the previous experiment with peroxide. These lower methane conditions correspond to the time interval of 553 to 750 hrs in Figure 6.13. The degree of transformation remained essentially the same as that achieved during the peroxide addition experiment.

The results of these transient experiments indicated that the addition of greater quantities of methane to increase methane-utilizing biomass did not result in greater extents of biotransformation. One possible explanation is that the higher methane concentrations inhibited the rates of transformation of the chlorinated aliphatics.

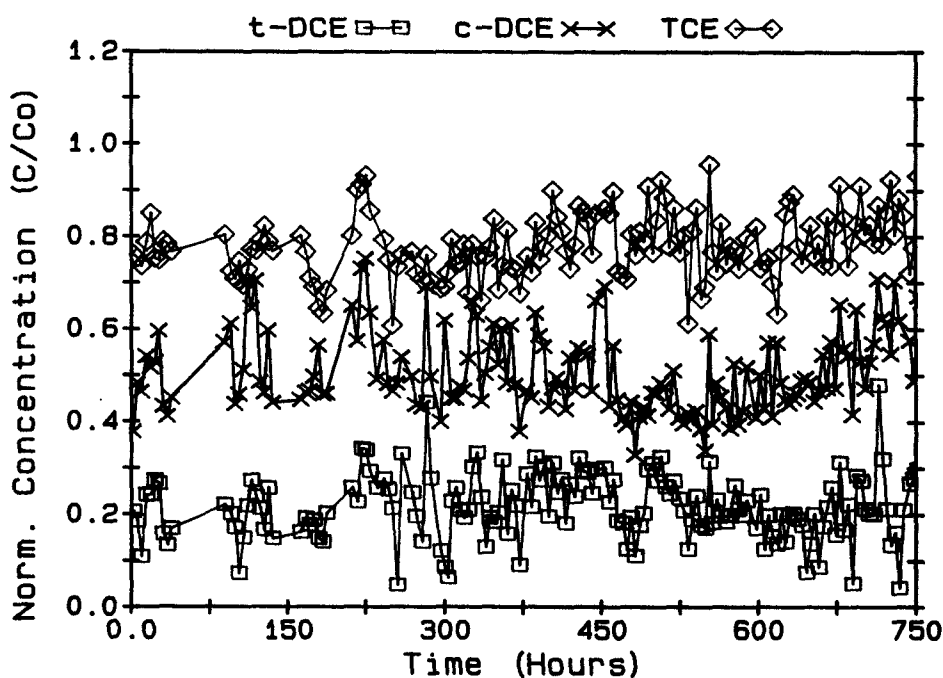


Figure 6.13. Fractional breakthroughs of the chlorinated organics during the peroxide addition (0-553 hrs) and methane reduction (553-750 hrs) experiments.

Degree of Biotransformation

The degree of biotransformation of the chlorinated solutes was estimated for periods when quasi-steady-state conditions were achieved. These biotransformation estimates were based on (1) comparisons with bromide as a conservative tracer, as given in equation (4.1), and (2) comparison with the fractional breakthroughs of the organic solutes before biostimulation. For the latter estimate, the fractional breakthrough of each chemical before biostimulation, as measured during the Tracer8 experiment (Table 6.2), was substituted for the bromide fractional breakthrough in equation (4.1). The steady-state fractional breakthroughs of bromide and the chlorinated organic compounds used in the estimates in Table 6.2 were based on as many as 40 measurements at each observation location. The great number of measurements reduced the mean standard error of the estimate.

The estimates of percentage biotransformation are presented in Table 6.3, with the range of the 95% confidence interval given for each location and chemical. The estimated range of minimum to maximum percentage biotransformation obtained by the two methods described above, based on the data from the farther observation wells (S2 and S3), were as follows: TCE, 4 to 30%; cis-DCE, 46 to 58%, and trans-DCE, 58 to 76%. With TCE, a significantly lower removal resulted from the comparison with the Tracer8 results, perhaps because TCE had not reached its true steady-state level in that experiment. It is believed that the higher removal estimated from the comparison with bromide provides the more accurate value.

TABLE 6.3. PERCENTAGE BIOTRANSFORMATION IN THE SECOND SEASON'S BIOSTIMULATION-BIOTRANSFORMATION EXPERIMENTS

	Halogenated Ethene	Well S1 (%)	Well S2 (%)	Well S3 (%)	Extract (%)
Comparison with Bromide Fractional Breakthroughs ^{a,b}	TCE	10–14	21–25	23–30	20–26
	cis-DCE	34–40	50–58	50–58	55–72
	trans-DCE	61–67	70–76	67–73	(N.D.)
Comparison with Fractional Breakthrough Before Biostimulation ^{b,c}	TCE	0–10	4–12	3–11	–6–1
	cis-DCE	29–37	46–54	40–48	51–69
	trans-DCE	55–64	62–72	58–66	(N.D.)

^a Percentage biotransformation estimates (95% confidence interval shown).

^b Values over a time interval of last 150 hrs of the experiment Biostim2 shown in Figure 6.9.

^c Fractional breakthrough before biostimulation given in Table 6.2.

Estimates at well S1 indicate that essentially all of the biotransformation of trans-DCE occurred within the first meter of travel in the zone between the injection and the S1 observation well. This corresponds to the zone of most active methane utilization. Cis-DCE and TCE appeared to have undergone additional transformation between the S1 and S2 wells. The extent of TCE transformation was consistent with the results from the first season of testing.

The extent of transformation of trans-DCE during the steady-state portion of the experiment, evaluated above, was lower than that achieved during the earlier stage, where greater than 80% transformation was achieved (Figure 6.8). Cis-DCE, however, shows the opposite result. It is not clear what caused these changes. The main difference in the experimental conditions was the change to longer methane-oxygen pulse lengths during the latter steady-state period.

The degree of biotransformation was also determined based on mass balances of TCE and cis-DCE injected over the course of the experiments, compared to the amount removed from the system by the extraction well. The concentrations of the extracted fluid were measured for a period of three months after organic addition was stopped in order to complete the mass balances. Biostimulation conditions were maintained throughout this period. Estimates are not presented for trans-DCE, since the presence of the co-eluting 1,1-DCA in the extracted groundwater resulted in a large error in the estimate.

Mass balances showed that 30% of the TCE and 54% of the cis-DCE injected were not recovered by the extraction well, while 100% of the bromide was recovered over the same period. This lower recovery of the organic solutes suggests biotransformation and not hydraulic losses from the system. The complete mass balance estimates of biotransformation are in good agreement with those based on the steady-state fractional breakthroughs given in Table 6.3. Thus, the estimates derived from the S2 and S3 data are believed to represent the degree of transformation that is occurring over the entire test zone, as determined using the extraction well data.

Summary of the Second Season's Results

Results of the second season of field testing directly demonstrated that biostimulation of methane-utilizing bacteria results in the biotransformation of trans-DCE, cis-DCE, and TCE. Trans-DCE was most rapidly degraded, followed by cis-DCE, and TCE. The maximum extent of transformation achieved in the

2-m biostimulated zone are as follows: trans-DCE, 80%; cis-DCE, 55%; and TCE, 20%. Similar estimates of the degrees of transformation were obtained from complete mass balances on the amount of chlorinated solute injected and extracted from the test zone.

Transient experiments demonstrated that the transformation of the chlorinated solutes rapidly ceased upon termination of methane addition in the test zone. Thus, biotransformation in the test zone required active utilization of the electron donor.

Transient experiments under active biostimulation conditions showed similar degrees of transformation, despite a two-fold variation in amount of methane injected. Methane-utilizers could be maintained with hydrogen peroxide used as a source of oxygen; however, higher degrees of transformation, as a result of stimulating a greater biomass, did not occur. These data suggest that the higher methane concentrations may have inhibited the rates of transformation of the chlorinated alkenes.

The formation of trans-DCE oxide resulted from the transformation of trans-DCE. The formation of the epoxide was found to be very sensitive to biostimulation conditions. A rapid decrease in the epoxide concentration occurred soon after methane addition was stopped, further confirming the close association of biotransformation with active methane utilization.

RESULTS OF THE THIRD SEASON OF FIELD TESTING

The biotransformation process was studied in greater detail in the third season of field testing. The experiments focused on the biotransformation of vinyl chloride along with TCE, trans-DCE, and cis-DCE. Based on the mixed culture studies of Fogel et al. (1986) and our soil column studies (Section 10), we anticipated that vinyl chloride would be nearly completely transformed. The incorporation of a Hall detector in the automated data acquisition system permitted more accurate quantification of the concentrations of the less chlorinated organics and eliminated the problem of the interference of the trans-DCE measurement, due to the co-elution of 1,1-DCA. Thus, a repeat of the second year's experiments with a more accurate detector permitted confirmation of those results.

Along with the initial biotransformation experiment, several key transient experiments were performed to determine whether methane was inhibiting the transformation of the chlorinated ethenes. In the previous year's tests, increased methane addition failed to enhance transformation. These results, and our laboratory results, indicated that high methane concentration inhibits transformation rates of the chlorinated ethenes as secondary substrates.

The third year's transient experiments were designed to determine if transformation was enhanced by the absence of methane. To accomplish this, formate and methanol, which are intermediates in methane utilization (Anthony, 1982), were substituted for methane once the test zone was biostimulated. Anthony (1982) in reviewing the oxidation of hydrocarbons by whole cells of methanotrophs discussed the requirement of a reductant (usually NADH) for the initial oxidation of the hydrocarbon. He indicated that NADH in methanotrophs is generated by further metabolism of the hydroxylation product, or by metabolism of a second oxidizable substrate (e.g., methanol or formaldehyde), or by oxidation of internal storage polymers. Stirling and Dalton (1979) also observed more rapid oxidation of several hydrocarbons in the presence of formaldehyde. The slower oxidation of these compounds in the absence of formaldehyde was believed to result from poor generation of NADH. Since formaldehyde is a hazardous substance, formate was chosen for use in our experiments. It was assumed that these electron donors (formate, methanol) would not inhibit transformation and would keep the MMO enzyme system active. Thus, if methane did inhibit transformation, then enhanced transformation should be observed when these electron donors were introduced.

The sequence of field experiments was similar to that used in the second season of field testing. The chlorinated organics were first added to the system to achieve steady-state breakthroughs before biostimulation. Methane and DO were then added to biostimulate the test zone while continuing to add the organics. After steady-state biotransformation conditions were attained, the transient experiments, including the addition of formate and methanol, were performed.

The chlorinated organics were added in experiments Tracer11 and Tracer12, as discussed in Section 5. Table 6.4 presents quasi-steady-state fractional breakthroughs of bromide and the chlorinated aliphatics at the end of the Tracer12 test. The chlorinated solutes reached 90% to 95% of their respective injection concentrations at the observation wells, after adjusting for dilution by indigenous groundwater. The results indicate minimal transformation of the chlorinated organics during this period when neither methane or oxygen was being added. As was the case in the second year's organic addition experiment, TCE, the most strongly sorbed compound, had the lowest fractional breakthrough before the start of the biotransformation experiment. The fractional breakthroughs were lowest at the extraction well, indicating that steady-state conditions had not been achieved in all areas of the test zone before the biostimulation experiment was initiated.

TABLE 6.4. TRACER12 EXPERIMENT PERCENTAGE BREAKTHROUGH OF CHLORINATED SOLUTES AND BROMIDE AT THE OBSERVATION WELLS

Well	Bromide (%)	VC ^a (%)	t-DCE (%)	c-DCE (%)	TCE (%)
S1	100±0.6 ^b	95±1.8	100±1.2	100±1.2	95±0.9
S2	99±0.8	92±2.0	96±1.6	99±1.5	88±1.3
S3	100±0.5	100±1.8	97±1.6	98±1.3	86±1.2
Ext	15±0.5	92±2	97±3	91±2	70±2

^a Chlorinated organics adjusted for dilution by native groundwater based on the bromide fractional breakthrough present in column 1.

^b Standard error of the mean.

Results of the Biostimulation-Biotransformation Experiment (Biostim3)

The operating initial conditions of the Biostim3 experiment were similar to that of the second season of testing, as indicated in Table 6.1. Methane and DO addition was initiated using a 3-hr pulse cycle, slightly longer than the previous year. Methane was utilized immediately upon addition. After methane-saturated water had been injected for one day, concentrations remained below 0.5 mg/l at the S1 well and below detection at the farther observation wells, S2 and S3. The limited breakthrough indicated that a significant numbers of methanotrophs from the prior field season had survived and were immediately able to consume essentially all the methane within the first meter of transport. After injection of methane and DO for one day, the pulse cycle length was increased to the standard 12-hr period to distribute methane in the test zone.

Figure 6.14 shows the corresponding decrease in concentrations of vinyl chloride, trans-DCE and cis-DCE at the S2 well, in response to biostimulation. Biotransformation started immediately upon methane addition, demonstrating that active methane utilization was required to initiate the transformation of the chlorinated organics. As in previous tests, the bromide tracer breakthrough reached unity, demonstrating that decreases in organic solute concentrations result from biotransformation. Vinyl

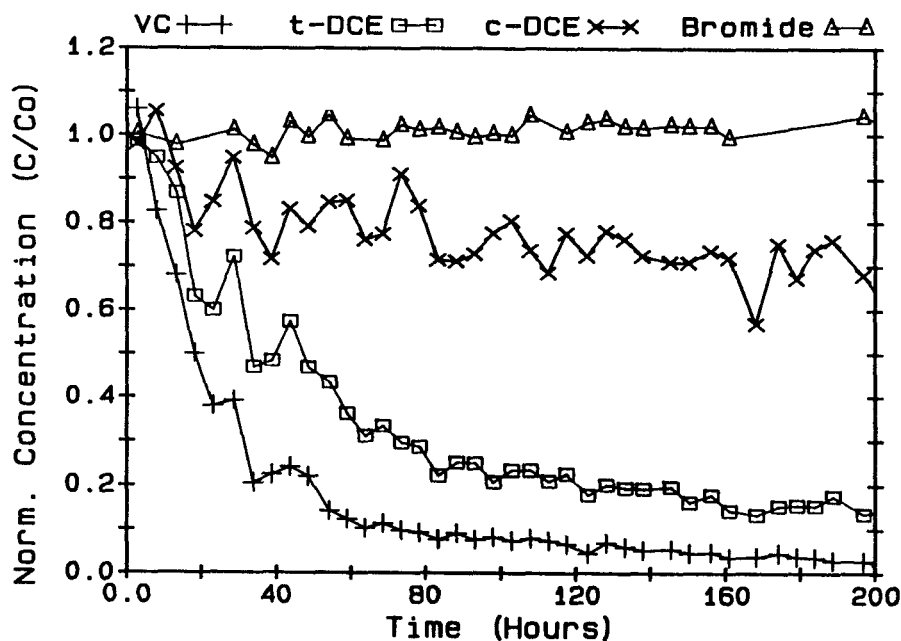


Figure 6.14. Decreases in normalized concentration of vinyl chloride, trans-DCE, and cis-DCE at the S2 well in response to biostimulation in the third season.

chloride was the most rapidly transformed, followed by trans-DCE, and cis-DCE. TCE (not shown) was the most slowly transformed. The concentrations of both vinyl chloride and trans-DCE were observed to decrease most rapidly within the first 50 to 80 hrs, followed by a more gradual decline. Cis-DCE decreased more gradually with time. The rank order of rates of biotransformation, trans-DCE > cis-DCE > TCE, is consistent with the second season's results. The decrease in trans-DCE concentration was more rapid than observed in the second-season tests (Figure 6.8), which is also consistent with the more rapid methane uptake. This result indicated that more methane-utilizing bacteria were initially present in the test zone, resulting in faster removal rates.

System Response to Methane Pulsing

Direct evidence of methane inhibition was obtained when the pulse cycle time was increased from 1 to 12 hrs. The transient response of methane, trans-DCE and vinyl chloride at the S1 well is shown in Figure 6.15. During the first day, using short pulses of methane, an 80% reduction in vinyl chloride and a 60% reduction in trans-DCE occurred with minimal methane breakthrough. Upon initiation of the longer methane pulses, distinct cyclic oscillations in vinyl chloride and trans-DCE concentrations were observed, which correlated with methane pulses. The degree of attenuation of the pulses in chlorinated organics were related also to methane pulse heights. At the S2 well, shown in Figure 6.14, the amplitudes of the vinyl chloride and trans-DCE concentration cycles were damped, as methane concentrations remained near the detection limit. The response at the S3 well, presented in Figure 6.16, shows definite oscillations of all three components, which are reduced in amplitude compared to those observed at the S1 well. Based on the response at the three observation wells, the degree of attenuation in aqueous-phase concentration of the chlorinated organics is shown to be directly related to the attenuation in the methane pulse heights. Oscillations in concentrations observed in the region near the injection well were strongly attenuated during transport, by the processes of dispersion, sorption, and transformation.

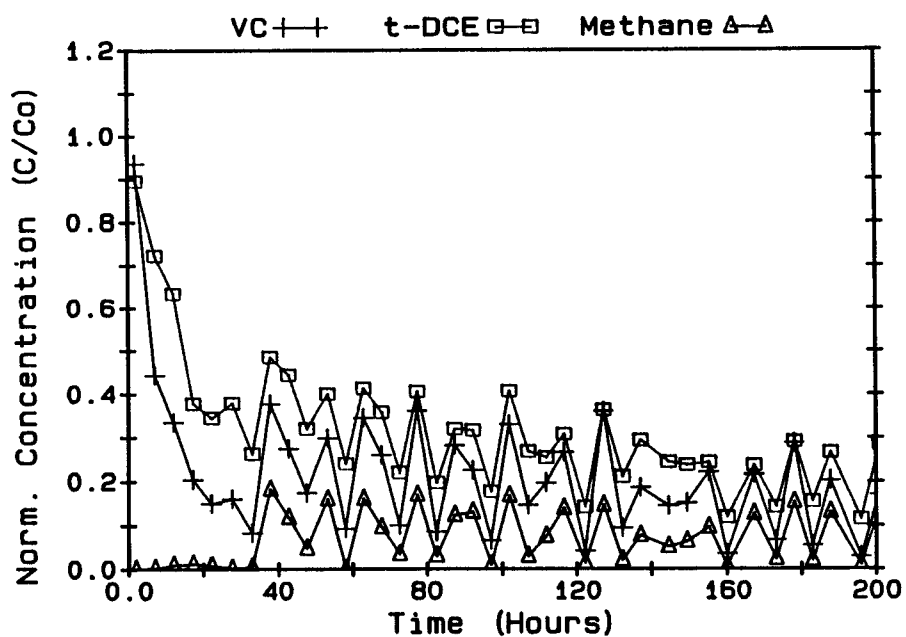


Figure 6.15. Transient responses of vinyl chloride and trans-DCE at the S1 well due to methane pulsing.

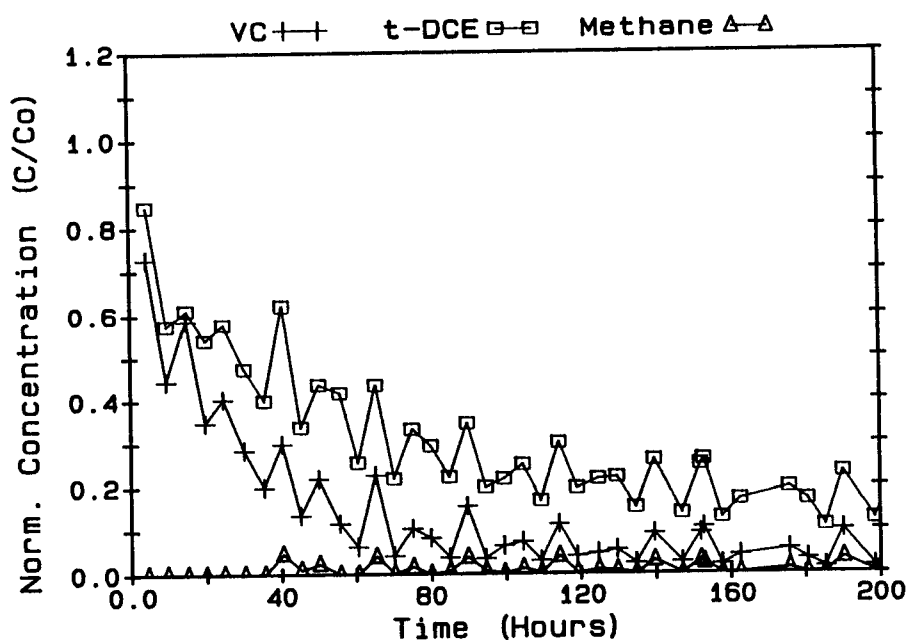


Figure 6.16. Transient responses of vinyl chloride and trans-DCE at the S3 well due to methane pulsing.

Methane inhibition is the most likely explanation for this behavior. Higher methane concentrations reduce the rates of transformation of the chlorinated aliphatic compounds, and hence the aqueous-phase concentrations of the chlorinated organics increase during periods of high methane concentration as the reaction rates decrease. The reverse would be true for periods of low methane concentration. The rapid changes indicate that the methane-utilizers respond very quickly to changes in methane concentration. Model simulations discussed in Section 13 will discuss the interactions of inhibition and rate-limited sorption on this observed behavior.

Figure 6.17 shows the gradual decrease in concentration of cis-DCE and trans-DCE at the S2 well that occurred over the first 400 hrs of the experiment. Vinyl chloride injection was stopped at 200 hrs. The gradual decrease results from increase in the microbial mass with time, as well as from the slow desorption of these compounds from the aquifer solids. Model simulations presented in Section 13 will discuss these processes in greater detail.

Transient Experiments With Formate and Methanol

In order to study the competitive inhibition phenomenon in greater detail, a series of transient experiments were performed in which different electron donors were substituted for methane. The series of experiments included the following measures: 1) the substitution of formate for methane; 2) the reintroduction of methane; 3) the substitution of methanol for methane; and 4) the termination of injection of methanol, i.e., no electron donor injection.

In the first phase of the transient experiments, formate addition was initiated after quasi-steady-state biotransformation of trans-DCE was achieved after 350 hrs of methane addition. Formate (NaCOOH) was injected at a concentration of 218 mg/l, using a pulse duration of 4 hrs, the same as that used for methane addition. This resulted in a time-weighted concentration of 73 mg/l. These conditions were chosen in order to maintain the same DO consumption in the test zone, assuming complete oxidation of formate. During the test, formate concentrations were not measured, but DO consumption was used as an indicator of formate utilization. Upon adding formate, a slight increase in DO concentration was observed, confirming that the stoichiometric model was appropriate and that complete formate utilization was attained in the test zone.

Figure 6.18 shows methane and trans-DCE concentrations at the S1 well for the periods of methane and formate addition. During the period of methane addition, oscillations in concentration are superimposed on a gradual trend of decrease in concentrations, to quasi-steady-state values. A clear response of trans-DCE to formate addition was observed. Trans-DCE concentrations decreased rapidly, while the oscillations in concentration essentially disappeared. Both responses indicated that inhibition had ceased. During the early stages of the formate addition, concentrations decreased to levels slightly lower than the minimum achieved when no methane was present with pulsed methane additions. These results indicate that, during early stages of formate addition, trans-DCE transformation proceeded at an enhanced rate that was not inhibited due to the presence of methane. The results also indicate that, during pulsed methane addition, the microbes responded quickly to changes in methane concentration, attaining near-maximum rates of secondary substrate transformation as the methane concentration temporarily receded below the detection limit.

As the formate addition experiment progressed, trans-DCE concentrations at the S1 well gradually began to increase. Apparently, the ability to keep the system stimulated with formate was gradually lost. This decrease may result from the following possible causes: 1) the loss in microbial mass, with microbial decay proceeding at a faster rate than microbial growth, 2) the inability of formate to keep the MMO enzyme system activated, or 3) competition of other heterotrophs for formate.

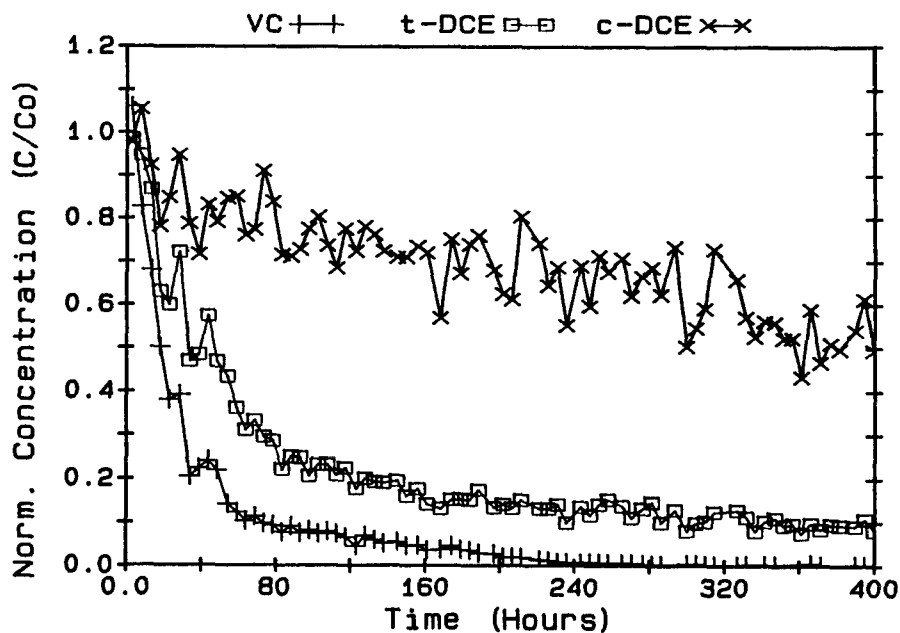


Figure 6.17. Decreases in cis-DCE and trans-DCE concentration during the first 380 hrs of biostimulation in the third season.

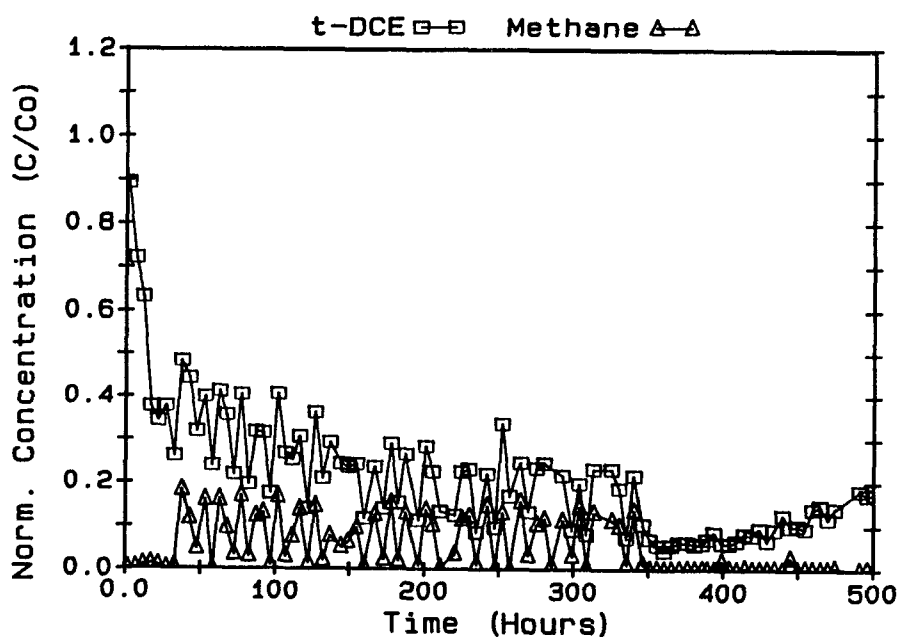


Figure 6.18. Methane and trans-DCE concentrations at the S1 well for periods of methane (0-350 hrs) and formate (350-500 hrs) addition.

The subsequent three transient experiments included the following phases: 1) reintroduction of methane; 2) methanol addition; and 3) no electron acceptor addition. The responses of trans-DCE and cis-DCE at the S1 observation well for all four phases of transient experiments are shown in Figure 6.19. During the preceding period of methane addition, cis-DCE concentration variations were not strongly correlated with the pulses in methane concentration. With the addition of formate, the cis-DCE response was similar to that of trans-DCE; the concentrations decreased for a short period of time, and then increased. Variations in cis-DCE concentrations, however, did not decrease with formate addition; thus, methane inhibition was not clearly demonstrated. However, the decrease in cis-DCE concentration for the initial period of formate addition suggests that cis-DCE transformation rates may be inhibited by the methane. Like trans-DCE, concentrations of cis-DCE increased with prolonged formate addition, indicating a decrease in transformation rate with time.

Upon reintroducing methane (520-660 hrs), decreases in both trans-DCE and cis-DCE concentrations resulted, demonstrating restimulation of the test zone. Oscillations in the trans-DCE concentration appeared, indicating a resumption of competitive inhibition by methane. The restimulation with methane indicates that methanotrophs were not growing on formate, and formate may not have kept the MMO enzyme activated.

Methanol was cut off and methanol addition was started at 660 hrs (Figure 6.19). Like formate, methanol was injected at a concentration of 51 mg/l, to maintain a DO consumption equivalent to the complete oxidation of 20 mg/l of methane. Following the switch to methanol, trans-DCE concentrations decreased during formate addition and the oscillations in concentration were greatly reduced. Cis-DCE showed an initial reduction in concentration, similar to that achieved with formate. The methanol experiment was conducted for only 100 hrs, not long enough to determine if trans- or cis-DCE concentrations would increase with prolonged addition. The limited data suggest that cis-DCE concentrations were increasing at the end of the methanol addition.

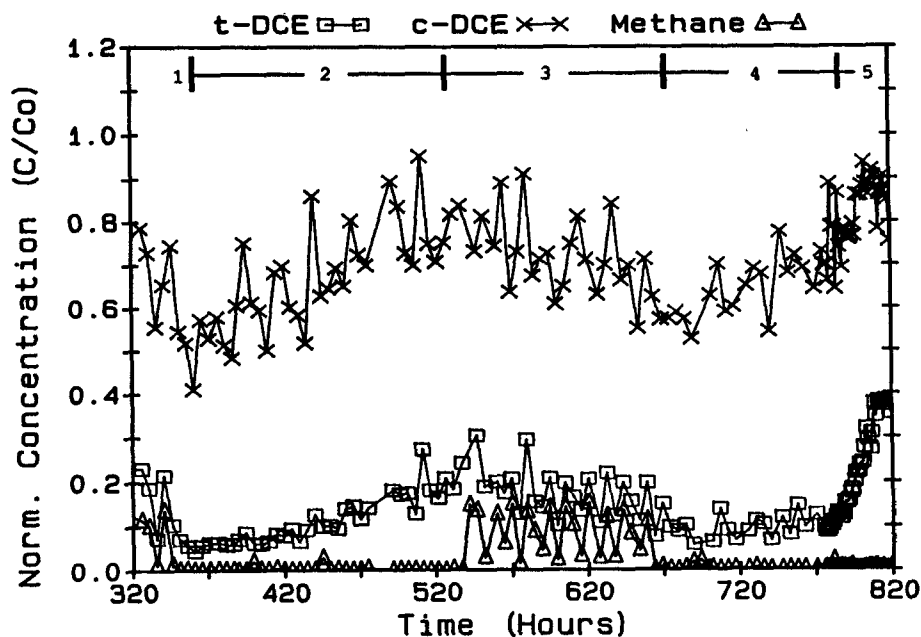


Figure 6.19. Response of trans-DCE and cis-DCE to injection of: 1) methane, 2) formate, 3) methane, 4) methanol, and 5) no electron donor.

The final transient test performed was termination of electron donor addition. Methanol addition was terminated at 774 hrs, while the addition of DO and the chlorinated organics continued. As illustrated in Figure 6.19, an abrupt increase in trans-DCE concentration was observed, indicating that transformation ceased soon after methanol addition was stopped. The increase is shown to be much more rapid than the increase observed during formate addition. The results are consistent with those observed in the second field season (Figures 6.11 and 6.12), and clearly demonstrate that the biotransformation of the chlorinated organics in the test zone required the utilization of an appropriate electron acceptor for MMO enzyme activity. Along with methane, both formate and methanol appear suitable for this purpose.

Degree of Transformation

The degree of biotransformation was determined based on 1) comparisons with bromide as a conservative tracer, and 2) comparisons with the fractional breakthrough of the chlorinated organics before the test zone was biostimulated (Table 6.4). The degrees of transformation estimated by both methods are presented in Table 6.5 for the various compounds.

Vinyl chloride was biotransformed more than 95% within 2 m of travel in the test zone. The lower degree of biotransformation of vinyl chloride, based on the extraction well estimates, probably results from not having achieved steady-state concentrations at that location in the 200 hr evaluation period. Transformation greater than 95% might have been achieved if vinyl chloride addition had been continued for a longer period. Vinyl chloride concentrations were reduced to approximately 1 µg/l, demonstrating that drinking water standards could be satisfied by this process.

Ninety percent of the trans-DCE was biotransformed during transport through the biostimulated zone. Greater than a 90% reduction would have been achieved with prolonged treatment of the test zone. The degree of biotransformation was greater than the 80% estimated in the second season of testing. The difference probably resulted from the larger error associated with the second year's estimate due to the presence of a 1,1-DCA peak that co-eluted with trans-DCE in the GC analysis and the lower sensitivity of the ECD detector.

TABLE 6.5. PERCENTAGE BIOTRANSFORMATION – THIRD FIELD SEASON

	Halogenated Ethene	Well S1 (%)	Well S2 (%)	Well S3 (%)	Extract (%)
Comparison with Bromide Fractional Breakthroughs ^a	TCE	7-13	15-19	16-22	24-30
	cis-DCE	28-34	38-44	41-45	46-52
	trans-DCE	83-87	89-91	89-91	68-72
	vinyl chloride	81-90	94-98	93-97	85-91
Comparison with Fractional Breakthrough Before Biostimulation	TCE	2-10	1-9	6-14	-9-9
	cis-DCE	25-37	36-44	38-46	33-53
	trans-DCE	81-89	86-94	86-94	64-76
	vinyl chloride	78-90	92-98	91-99	84-91

^a Percentage biotransformation estimates (95% confidence interval shown).

As shown in Figure 6.17, the cis-DCE concentration gradually decreased with time. Steady-state conditions required for cis-DCE transformation estimate were probably not achieved during the 400 hr time period of these experiments. The 45% reduction in cis-DCE concentration is in the range of values determined in the second year's tests. If steady-state conditions had been achieved, a higher degree of transformation might have been achieved.

The TCE transformation estimates based on the bromide comparison are in agreement with values from earlier field seasons. Lower estimates result from comparisons with the fractional breakthrough of TCE before the test zone was biostimulated, consistent with the second year's study. As previously discussed, the bromide estimates are probably more correct, since TCE is the most strongly retarded compound and steady-state fractional breakthroughs were probably not achieved before the start of the biostimulation experiment.

Most of the transformation occurs within the first meter of travel in the test zone. Slight additional decreases are observed in the second meter of travel, as indicated by the greater degrees of transformation at the S2 well, especially for cis-DCE and TCE, the least degraded compounds.

Summary of Third Season Results

The third season of field testing demonstrated that nearly complete transformation of vinyl chloride could be achieved in the test zone. Upon introducing methane and oxygen, a 95% reduction in vinyl chloride concentration was observed within 200 hrs. Over 90% of the trans-DCE was transformed within 350 hrs. The extents of transformation of cis-DCE and TCE, approximately 50% and 20% respectively, were similar to those achieved in the first and second seasons of testing.

Oscillations in vinyl chloride and trans-DCE concentrations were correlated with pulses in methane, providing evidence that methane inhibits the transformation of the chlorinated organics. The effect of methane inhibition also was observed in transient experiments, when formate and methanol were substituted for methane. Maximum transformation rates resulted when methane concentrations were low, or when a suitable electron donor is substituted for methane. When no electron donor was added, the transformation ceased rapidly, consistent with the results of previous experiments.

SUMMARY

The biostimulation and biotransformation experiments conducted at the Moffett field site demonstrated conclusively the feasibility of the in-situ biostimulation of an indigenous methanotrophic community and the cometabolic biotransformation of the target organic compounds. Methane utilization commenced rapidly, and the resulting methanotrophic community was easily restimulated following long periods of starvation. Cometabolic transformation of the target compounds ensued immediately after the onset of methane utilization, and was clearly linked to the presence of an active methanotrophic community. The extents of transformation of the target compounds were consistent from year to year. The rate and extent of transformation was greater for compounds that are less chlorinated: VC > DCE > TCE. The cometabolic transformations appeared to be inhibited by high methane concentration. Substitution of an alternative electron donor, e.g. formate or methanol, temporarily enhanced the biotransformation of the target compounds but could not sustain it in the long term. Transformation of the target compounds ceased soon after the addition of the electron donor was terminated. The region of cometabolic transformation extended over the entire spatial domain occupied by methane-oxidizing bacteria.

SECTION 7

FORMATION AND FATE OF trans-DICHLOROEOXIDE

Martin Reinhard, Franziska Haag, and Gary Hopkins

Laboratory studies using methanotrophic consortia have indicated that trans-1,2-dichloroethene (trans-1,2-DCE) is transformed via epoxidation to trans-1,2-DCE epoxide (also referred to as trans-1,2-dichlorooxirane) (trans-DCO) (Janssen et al., 1987). High concentrations of trans-DCE were found to inhibit both growth of methanotrophs and co-metabolic transformation of trans-1,2-DCE. Thus, formation of trans-DCO may be a complicating factor in bioremediation schemes using methanotrophs. Moreover, formation of epoxides constitutes a public health concern. Ethylene epoxide, for instance, is a carcinogen and a reproductive toxicant. The formation and fate of such compounds must be understood before biostimulation of methanotrophs can be confidently applied for aquifer restoration.

In this section we report a procedure for the chemical preparation of trans-DCO at the milligram scale. A trans-DCO standard was needed for compound verification, calibration and for laboratory transformation studies. We also report data on the hydrolytic transformation rate of trans-DCO at different pH values and discuss the observed formation of trans-DCO in the biostimulated aquifer.

CHEMICAL SYNTHESIS OF trans-DCO

We synthesized trans-DCO by adapting the procedure used by Liebler and Guengerich (1983) for the epoxidation of vinylidene chloride. An aliquot of 2 ml trans-1,2-DCE was added to 7 g m-chloroperbenzoic acid (Aldrich) in 50 g p-dichlorobenzene (Aldrich). The mixture was reacted at 55°C for 24 h. The reaction mixture was distilled under vacuum and the distillate (approximately 1 to 1.5 ml) was collected in a condenser cooled with dry ice.

GC/MS analysis of the distillate indicated the presence of trans-1,2-DCO and impurities such as trans-DCE, cis-DCE, cis-DCO, dichloroacetaldehyde and p-dichlorobenzene. Both cis-DCE and cis-DCO are suspected rearrangement products formed during the epoxidation reaction (Griesbaum et al., 1975). The structure of trans-DCO was verified using ¹H-NMR (Varian EM360, 60 MHz) and GC/MS (Model 5070, Hewlett-Packard, Palo Alto, CA). Both NMR and MS spectra agreed with those reported by Griesbaum et al. (1975).

The product trans-DCO was separated from the impurities on a GC (Packard Model 437A) equipped with a 3 ft x 1/4 in packed column (3 % SP-1500, 80/120 Carbopack B, mR54966, Supelco). The outlet of the column was connected to a programmable Valco gas switching valve (Valco, Houston, TX). The fraction containing trans-DCO was trapped at the column outlet using a cold finger condenser submerged in liquid N₂. Five 100-μl portions of the distillate were injected. After warming the trapped trans-DCO to room temperature, the concentrated trans-DCO was weighed (5.4 ± 1.1 mg) and dissolved into 1 ml pentane. The purity of the solution was checked using GC/MS.

Initial experiments indicated that dichloroacetaldehyde coeluted with trans-1,2-DCO on the Carbowax column. To circumvent this problem, a procedure was developed to chemically remove dichloroacetaldehyde from the mixture. This was accomplished using p-dichlorophenylhydrazine to form the hydrazone derivative (March, 1985). However, in samples stored for periods of six to nine months, dichloroacetaldehyde decomposed and p-dichlorophenylhydrazine treatment was unnecessary. The procedure was tested as follows: To 10- μ l distillate in 1 ml pentane were added 0.5 g dichlorophenylhydrazine. The reaction mixture was reacted for one hour at ambient temperature. After one hour, aldehyde was removed. The epoxide was relatively nonreactive toward this agent. After 3-1/2 hrs in the presence of excess dichlorophenylhydrazine, only a small fraction reacted.

Analytical Procedures

Using the purified standard and an electron capture detector (ECD), the response factor of trans-DCO was determined to be 150 times greater than that of trans-DCE, permitting us to detect very low concentrations. This ratio was used to calculate the trans-DCO concentrations in the field. In the automated field system, trans-DCO was separated from all other known peaks and was apparently detected as a single peak. However, the field system was not calibrated using the trans-DCO standard. The reported field data thus assumes the same recovery for trans-DCE and trans-DCO, and similar response factors for the field and laboratory ECD detection. The relative response factors were determined on the GC/MS system also using total ion current (TIC) detection. The TIC response for the trans-DCO was stronger than cis-DCE by a factor of 1.7. Estimates using GC/MS data agreed with the field data.

Laboratory Hydrolysis Study

Hydrolysis of trans-DCO was measured at 25°C at pH 5.0, 7.9 and 10.6. Trans-DCO in pentane was added to 40 ml of 0.03 M phosphate buffer in a 60 ml volumetric flask to give an initial concentration in the range of 310 to 315 mg/l.. After vigorously shaking the flask, a 1-ml aliquot was added to glass ampoules containing 12 ml buffer solution. The ampoules were then flame-sealed with less than 1 ml of headspace (Burlinson et al., 1982), placed into a 25°C water bath, and analyzed at regular intervals over a period of 240 hrs.

RESULTS

Confirmation of trans-DCO in Field Samples

The formation of a biotransformation intermediate was observed during the field biotransformation experiment Biostim2. Initially, only the peak area of the unknown was recorded, but the peak could not be identified on the basis of retention time alone.

To confirm the suspected presence of trans-DCO in field samples, 100-ml samples from the stimulated zone were analyzed using closed-loop-stripping/desorption analysis (Graydon et al., 1983). A GC/MS equipped with a 60 m thick-film capillary column (DB5, 0.32 mm i.d., 1- μ m film thickness; J & W Scientific, Rancho Cordova, CA) was used. Both trans-DCO and 1,1,1-TCA (which was present in the formation water) coeluted on this column. The trans-DCO was present at much lower concentration than TCA, but positive identification of trans-DCO was possible using chemically prepared trans-DCO standard.

Hydrolysis Kinetics

The rate data of trans-DCO transformation obtained at 25°C is shown in Figure 7.1. The observed first order rate constants and the 95% CI for pH 5, 7.9, 10.6 are $0.0135 \pm 0.0003 \text{ h}^{-1}$, $0.0145 \pm 0.0002 \text{ h}^{-1}$,

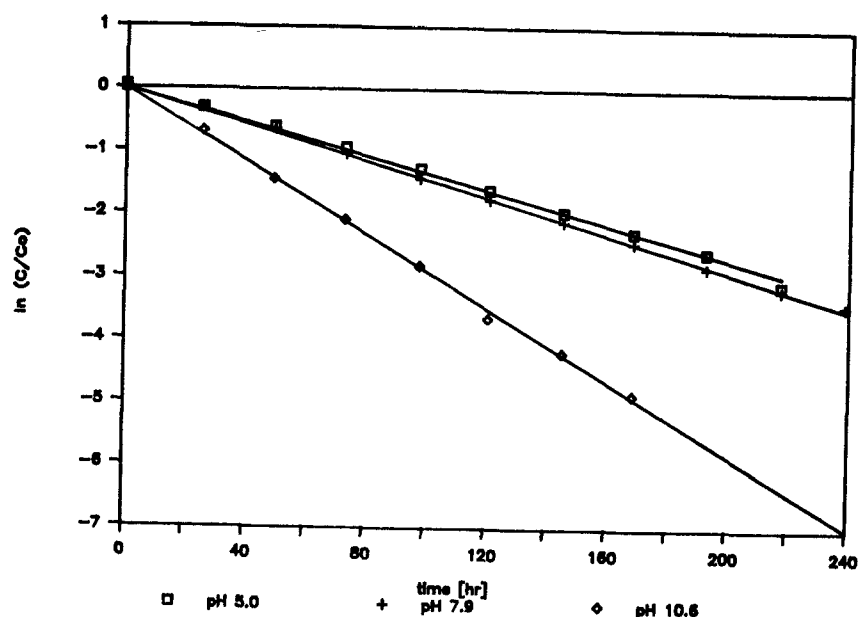


Figure 7.1. Pseudo-first-order plots for trans-1,2-DCE epoxide hydrolysis at pH values of 5.0, 7.9, and 10.6.

and $0.0291 \pm 0.0006 \text{ h}^{-1}$, and the corresponding half-lives are 51.3 hr, 47.8 hr, and 23.8 hr, respectively. The rate at pH 10.6 was approximately twice that determined at pH 5.0 and at 7.9, indicating that hydrolysis at pH 5.0 and 7.9 is due to reaction with water. The average of the pseudo-first order rate constants for the neutral (water) reaction is 0.0140 h^{-1} , with a half-life of 49.5 hr at 25°C .

The increase in transformation rate at pH 10.6 by a factor of 2.1 indicates some reaction with the hydroxide ion. By invoking the following relationship,

$$[\text{OH}^-] = K_w/10^{-\text{pH}} \quad (7-1)$$

we obtain a value of 37.9 mol/l-sec for the second-order reaction constant of the base (OH^-) promoted process. This rate is too small to be significant in the environmentally relevant pH range 6 to 9; and hence, the pH is not a significant variable under field conditions. The pH profile of DCO hydrolysis derived from our data is shown in Figure 7.2.

Janssen et al. (1987) have reported a half-life of 30 h at 30°C , corresponding to a reaction rate of 0.023 h^{-1} . From these data and our rate constant of 0.014 h^{-1} at 25°C , an activation energy (E_a) of 17.8 kcal/mol may be estimated. The typical ground water temperature at the Moffett field is 18°C . Using the estimated E_a , we estimate a pseudo-first-order rate constant and a half-life of 0.0068 h^{-1} , and 114 hrs (4.3 days), respectively, at 18°C .

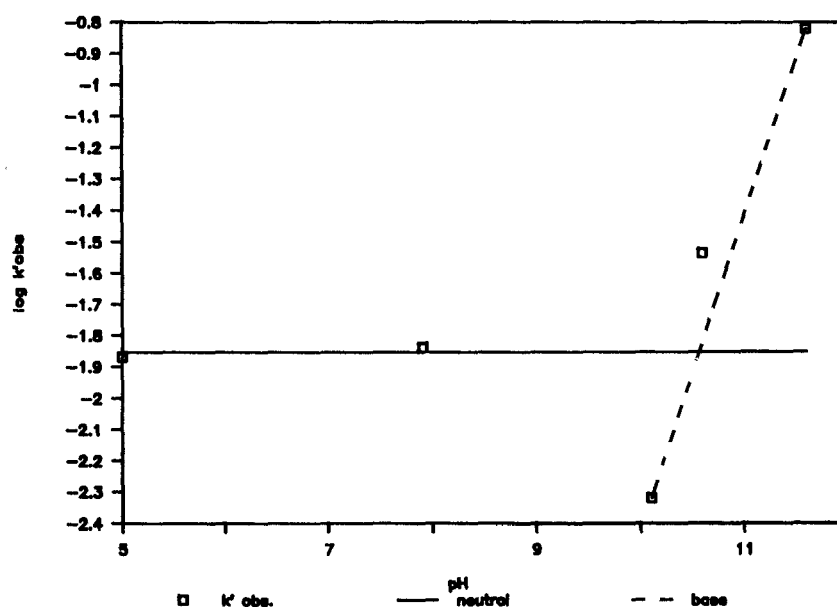


Figure 7.2. k_{obs} as a function of pH. Open symbols are measured data, full symbols are calculated values. The lines indicate the neutral (full line) and the base-promoted component (dashed line) of the measured overall pseudo-first-order hydrolysis constant, k'_{obs} .

trans-DCO Formation During Biostimulated Transformation of trans-DCE

Formation of trans-DCO was observed during Biostim2 when trans-DCE was one of the secondary substrates. Figure 7.3 shows the concentration of trans-DCO at S1, S2 observation wells and at the extraction well during the 600 h experiment. Formation of trans-DCO was believed to occur in the immediate vicinity of the injection well, where growth of methanotrophs and consumption of methane was occurring. After an initial lag phase of approximately 20 to 30 hrs, the trans-DCO concentration began to increase rapidly at S1 and S2 to a range of three to five $\mu\text{g/l}$. This rise was observed at the extraction well also, although the trans-DCE concentration remained lower due to dilution by indigenous groundwater. The absence of a measurable delay in the appearance of trans-DCO indicates that this compound was not sorbed significantly. The concentrations measured at S1 and S2 for the most part followed the same time profile.

In the extraction well, the expected attenuation factor due to dilution was 7.35. This estimate is based on an injection rate of 1.36 l/min, an extraction rate of 10 l/min, and the assumption of complete recovery of the injected water. The average trans-DCO concentration and the 95 % confidence interval at S1 were $4.99 (\pm 0.38) \mu\text{g/l}$. At S2 and at the extraction well, the trans-DCO concentrations (and 95% CI) were $4.54 (\pm 0.31)$ and $0.56 \mu\text{g/l} (\pm 0.03)$, respectively. Thus, the average trans-DCO concentrations at S2 and the extraction well were lower by 9.0 and 89 %, respectively. The expected concentration at the extraction well based on the dilution ratio was $0.68 \mu\text{g/l}$. Comparison with the observed value of $0.56 \mu\text{g/l}$ indicates that 18 % may have transformed during transport between S1 and the extraction well.

Based on an average residence time of approximately 10 hrs between S1 and S2 and 24 hrs between S1 and the extraction well, and using the measured hydrolysis rates, we would expect hydrolysis of 7% and 15 % of the trans-DCO, respectively. Hence, predicted and observed transformation rates are consistent with the observed concentration decreases in the field, although the relatively close agreement may be fortuitous. In any case, there does not seem to be a transformation pathway other than hydrolysis for trans-DCO outside the biostimulated zone.

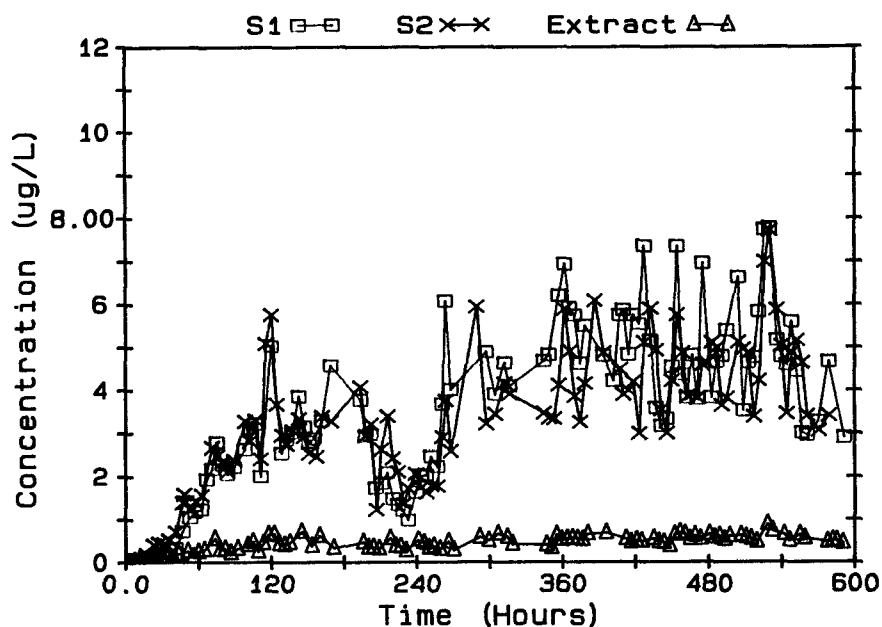


Figure 7.3. Concentrations of trans-DCO at observation wells S1, S2, S3, and the extraction well in the Biostim2 experiment. The data range of 300-600 hours was used for estimating hydrolysis rates.

Within the biostimulated zone, where the concentration of microorganisms is greater, other and more effective transformation pathways seem to exist. The data shown in Figure 9.12 indicate rapid decrease (within approximately 8 hrs) after the methane injection was terminated. Part of this decrease results from advective transport from the test zone. Another component of this decrease may be reaction with nucleophiles present in the biomass of the test zone. Trans-DCO, which is an electrophile, may react with nucleophiles, such as sulfur and nitrogen compounds, and covalently bind to enzymes and other cell material. This questions merits further investigation.

Summary and Conclusions

Formation of trans-DCO, which was previously detected in laboratory experiments, was confirmed in field biostimulation experiments using GC/MS and a standard compound. On a mass basis, approximately 5 to 10% of the trans-DCE was converted into trans-DCO. Laboratory studies have indicated a reaction rate and half-life of 0.014 h^{-1} and 49.5 hrs, respectively, at 25°C , and the reaction rate was found to be independent of pH in the pH range 5 to 10. Using literature data, the E_a was estimated as 17.8 kcal and the half-life extrapolated to 18°C was estimated as 4.2 d.

Although the hydrolysis rate of trans-DCO is relatively fast, formation of this potentially harmful by-product may have to be considered in remediation schemes using methane, particularly in cases where the treated water is recycled rapidly into the water supply. Assuming a $t_{1/2}$ of six days (15°C), a decrease from 100 µg/l to 2 µg/l (the USEPA standard for vinyl chloride in drinking water) will take approximately 1 month.

SECTION 8

SORPTION

Thomas Harmon and Paul Roberts

INTRODUCTION

The ultimate goal in solute transport modeling in groundwater is the independent estimation of the relevant parameters. The Moffett field site has provided an outstanding opportunity for advancement towards this goal. With the monitoring capabilities in the field, laboratory techniques for parameter estimations can be rigorously evaluated, and employed subsequently in cases where the field characteristics are less fully known.

The focus of the Moffett solids sorption studies was to increase the understanding of the interrelationship between a complex natural aquifer environment and a greatly simplified laboratory experiment. More specifically, experiments have included the estimation of laboratory-scale equilibrium parameters (partitioning coefficients) for comparison with observed field parameters. Field observations (Section 5) have indicated that the time scale of sorption processes is large enough, relative to that of groundwater flow, to cause significant deviations from local equilibrium. Thus, laboratory scale studies have included an investigation of nonequilibrium modeling parameters (apparent diffusivities for transport within solid grains, and equivalent first-order rate constants).

MOFFETT SOLIDS

Solid samples were obtained from cores taken near the test zone. Figure 8.1 provides a plan view of the field site, and the exact location of the cores used for the sorption studies. One core (B2) held together sufficiently to yield a sample from what appeared to be loose material composing the aquifer of the test zone. The remaining cores provided material from above or below the high conductivity zone, or a mixture of solids from different layers (drilling slough).

A description of the solids characterization and sorption studies is facilitated by a clarification of nomenclature. The few samples obtained from the aquifer zone in core B2 were used in one set of sorption experiments involving 'bulk' solids. Because no portion of the majority of the cores appeared to be representative of the aquifer zone, the remaining solids were sieved into fractions. Table 8.1 provides a list of the U.S. standard sieve sizes used, and the mass fraction of each particle size from the aquifer zone sample of cores SU-39-4 and 6 (see Figure 8.1). The particle size distribution from which these mass fractions were derived is shown in Figure 8.2, for the aquifer zone sample of SU-39-6. The particle size distribution for SU-39-4 is similar. The fractions combined according to this particle size distribution were used in a second set of sorption experiments involving 'synthesized bulk' solids.

Solids Preparation

Each of the cores was extruded carefully to separate the interior core solids from those near the walls, where oxidation of the steel core barrels appeared to have altered the solids. The high fraction of silts and clays in the nonrepresentative samples necessitated the wet sieving of slurries prepared in a ratio



TABLE 8.1. MASS FRACTION OF PARTICLE SIZES USED TO PREPARE SYNTHESIZED BULK SAMPLES
(Determined Using Distribution in Figure 8.2)

U.S. Standard Sieve No.	Particle Diameter (mm)	Mass Fraction (-)
+4-10	4.75-2.00	0.45
10-20	2.00-0.85	0.24
20-40	0.85-0.425	0.10
40-60	0.425-0.25	0.057
60-80	0.25-0.18	0.025
80-120	0.18-0.125	0.032
120-200	0.125-0.075	0.026
< 200	< 0.075	0.07

of about two liters of Moffett groundwater to one kilogram of solids. To avoid dissolution of calcium carbonate (CaCO_3), groundwater was equilibrated with reagent grade CaCO_3 prior to slurry preparation. Solids retained on the No. 4 mesh sieve (> 4.75 mm) were discarded. Solids retained on each subsequent sieve were then re-sieved in amounts no greater than about 100 g. Portions of the fractions designated for surface area and pore analyses were rinsed with a solution of calgon (sodium hexameta-phosphate) to disperse persistent clays that might affect the results.

Bulk and fractionated solids were oven-dried at 50-60°C. To avoid biasing samples towards particular particle sizes, solids were riffle-split down to sample size, as described by Ball et al. (1989).

Particle Characterization

Methods of particle surface area and pore size characterization have been refined recently in our laboratory for the analysis of sandy aquifer material of relatively low specific surface area ($< 3 \text{ m}^2/\text{g}$) (Ball et al., 1989). Surface area methods used include low-temperature nitrogen adsorption, low-temperature krypton adsorption, and ethylene glycol monoethyl ether (EGME) adsorption. Particle porosity was characterized using low-temperature nitrogen desorption and mercury porosimetry.

Low-temperature adsorption was interpreted by the BET approach, as developed by Brunauer et al. (1938). The krypton method was used to surmount the possible limitations of the nitrogen-BET method for low-surface solids and has been applied successfully to well-characterized solids such as glass and quartz (Beebe et al., 1945; Gaines and Cannon, 1960; Sing and Swallow, 1960). However, the krypton-BET method shares a known limitation of the nitrogen-BET method: interlayer surfaces of expanding clay minerals are not measured. The EGME method of Carter et al. (1965) utilizes a polar adsorbate to measure both the external and internal surfaces of soils and clays.

Mercury porosimetry measures a wide range of pore sizes, but is limited at the lower end by the high pressures required. Nitrogen desorption is capable of measuring smaller pore sizes, but is limited at the upper end by very large errors in measurement at high partial pressures of N_2 . The range of pore radii accessible by a combination of the two methods is approximately 1.5 to 10,000 nm.

Specific Surface Area--

Figure 8.3 contains BET plots for the results of krypton and nitrogen surface area determinations of a silica standard (No. 2008, $5.29 \pm 0.08 \text{ m}^2/\text{g}$, Quantachrome Corporation) by Ball et al. (1989). For

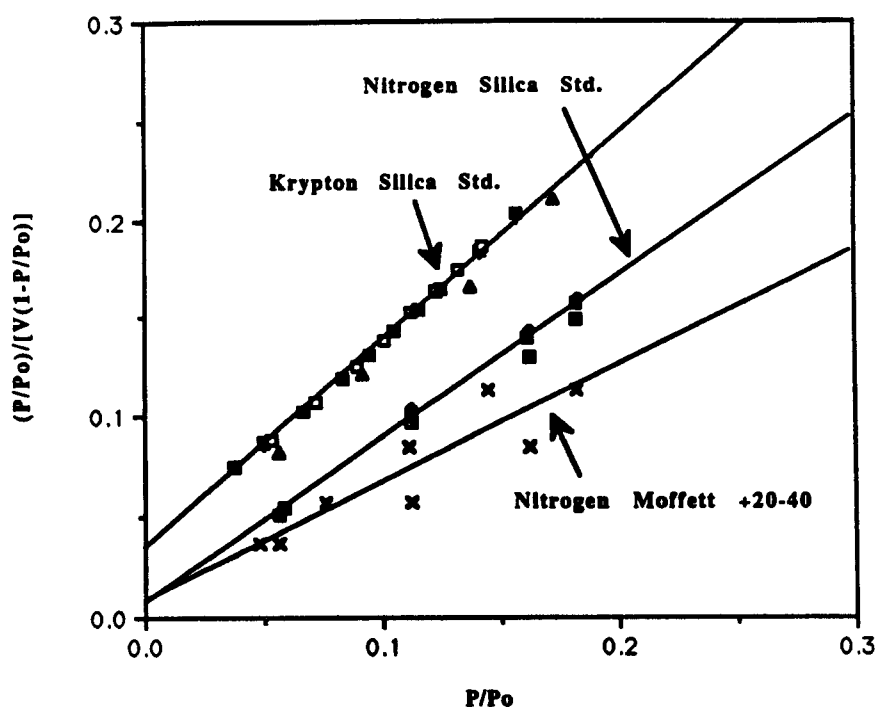


Figure 8.3. BET plots for nitrogen and krypton adsorption by silica standard, and nitrogen adsorption by Moffett 20-40 fraction.

triplicate analyses, the figure shows the nitrogen approach is accurate and precise: results of a linear regression based on the data yield a reasonably precise surface area estimate of $5.20 \pm 0.23 \text{ m}^2/\text{g}$. Triplicate krypton analyses were also accurate, and yielded a more precise surface area estimate of $5.26 \pm 0.11 \text{ m}^2/\text{g}$.

The BET plot in Figure 8.3 for the +20-40 mesh Moffett solids shows that the nitrogen method is less accurate for these natural materials, but still provides reasonable accuracy. The specific surface area estimate for each of the Moffett size fractions is provided in Table 8.2. The results show relatively high surface areas--3.6 to $7.0 \text{ m}^2/\text{g}$ -- even though the internal surface areas of expanding clays were excluded. The krypton method, accurate for total sample surface areas ranging from about 0.1 to 5.0 m^2 , failed for what was considered a representative sample mass of the Moffett solids ($> 1 \text{ g}$).

The EGME method applied to the same silica standard yielded a specific surface area estimate of $3.92 \text{ m}^2/\text{g}$. Only one sample was analyzed because of the substantial amount of standard required (approximately 5 g) by the method. Results from analyses of the Moffett fractions are shown in Table 8.2. The EGME surface areas range from 18 to $45 \text{ m}^2/\text{g}$, and in all cases are at least three times higher than the N_2 BET value for the respective size fraction, indicating the presence of a substantial fraction of expanding clay minerals. Surprisingly, the EGME surface area is nearly as large for the coarsest fraction as for the finest fraction, and twice as large as for the intermediate fractions. This suggests that the large particles consist in part of agglomerates of clay-sized particles.

The mass fraction of clay-sized particles which may exist in the Moffett fractions was estimated using the BET and EGME surface areas. The estimates indicate that if the surface area of the clays is on the order of $800 \text{ m}^2/\text{g}$, then this mass fraction is in the range of 2 to 4% . Surface areas of this magnitude

TABLE 8.2. SPECIFIC SURFACE AREA AND INTERNAL POROSITY FOR MOFFETT SIZE FRACTIONS

Fraction	Specific Surface Area (m ² /g)		Intra-Particle Porosity
	N ₂ BET	EGME	
4-10	5.9	38	ND
10-20	6.0, 4.1	28, 36, 36	0.029
20-40	6.8, 5.6	22	0.022
40-60	3.6	19	0.015
60-80	5.0	18	
80-120	4.8	26	0.014 (60-100)
120-200	7.1	21	0.017, 0.015 (100-200)
< 200	7.1	45	

have been measured in smectites, which are common at the site. The possibility of contamination of the fractions with clays from the confining layers seems unlikely. The mass fraction of even the upper clay (157 m²/g) would have to be at least 30% to explain the EGME surface areas for some of the fractions.

Intra-Particle Porosity--

The nitrogen adsorption/desorption isotherm for the +20-40 mesh fraction is shown in Figure 8.4. This type of isotherm, with its characteristic hysteresis loop, has been well-documented in the physical adsorption literature (e.g., Gregg and Sing, 1982). Its shape is attributed to differences in capillary condensation in constricted pores along the adsorption and desorption branches of the isotherm. Using the Kelvin equation to relate adsorbate gas pressure to meniscus radius, and assuming a pore geometry, the pore volume and the pore size distribution can be determined from the isotherm. The simplest and most commonly applied model of pore geometry is that of cylindrical, open-ended, non-intersecting pores. For the pressures associated with the nitrogen method, the pore radii sampled correspond to the lower third of the mesopore range (2-15 nm) and the upper portion of the micropore range (1.5-2 nm), as categorized by Gregg and Sing (1982).

Figure 8.5 combines the pore size distributions derived from mercury intrusion and nitrogen desorption. The two methods have been discussed in detail elsewhere (Gregg and Sing, 1982; Ball et al., 1989). Here and in general, the mercury data describes a much larger range of pore sizes than does the nitrogen data. The distribution derived from nitrogen does, however, include pores smaller than 3 nm in radius (the lower limit of the mercury method) which are approaching the molecular size of the solutes of this study.

The intra-particle porosity of the Moffett solids was relatively higher for the larger size fractions than for the smaller ones. The results of mercury intrusion studies, included in Table 8.2, show the internal porosity ranges from 0.029 and 0.022 cm³/g for the +10-20 and +20-40 fractions, respectively, to an average of about 0.015 cm³/g for all of the smaller fractions. Particles larger than 2 mm (No. 10 mesh) were too large for the analysis.

Discussion of Solids Characterization

Discussion of the characteristics of the Moffett solids is facilitated by comparison to a more homogeneous aquifer solid. The Borden aquifer solids, which have been studied in great detail (Curtis, 1984; Ball and Roberts, 1985, 1987; Ball et al., 1989), consist of a relatively clean, sandy material, with a size

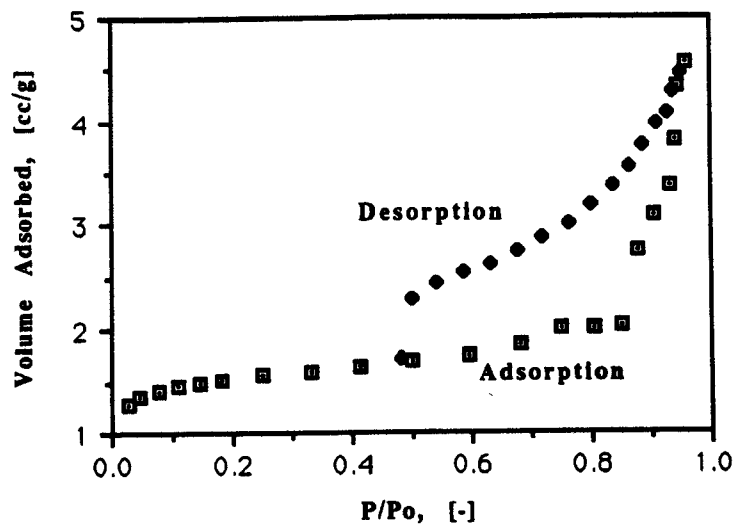


Figure 8.4. Nitrogen adsorption/desorption isotherm for Moffett 20-40 fraction.

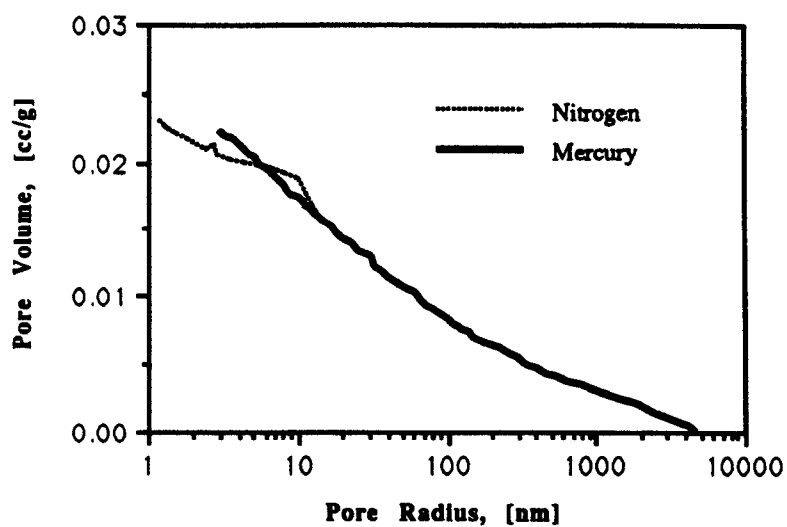


Figure 8.5. Combined nitrogen adsorption and mercury intrusion cumulative pore size distribution for Moffett 20-40 fraction.

distribution dominated by medium to coarse sizes (0.42-2 mm), and a bulk value of organic carbon content of about 0.0002. The Moffett material is much more heterogeneous mineralogically, and composed of a greater fraction of coarse sands and gravels (> 2 mm) and silts and clays. The organic carbon content of the Moffett solids (approximately 0.001) indicates a higher organic partitioning potential. The BET surface area for the Moffett fractions ranges from about two times greater than that of the Borden sand, for the largest fraction, to about an order of magnitude greater for the fine fractions. However, the two materials exhibit very similar values of intra-particle porosity, providing two indications: 1) the Moffett solids are characterized by a much rougher, more weathered surface than the Borden sands (electron microscopy has confirmed this suspicion), and 2) the Moffett solids have a potential for the diffusion-limited uptake of solute similar to that observed in sorption experiments with Borden sand. The results from the EGME surface area analyses suggest that a fraction of expanding clay minerals, probably weathering products, are present in the Moffett fractions. Because the samples for surface analysis were rinsed with a dispersant, it may be that these clays are present deep within the internal pores of the particles. Electron microscopy seems to support this hypothesis by indicating the presence of tiny particles along the internal pore walls of the Moffett particles. The effects of such clays are uncertain, but their presence must be taken into account in understanding sorption processes.

MOFFETT SOLIDS SORPTION STUDIES

Background

The procedure for the batch sorption studies using radio-labeled (^{14}C) compounds has been used previously in this laboratory (Curtis, 1984; Ball and Roberts, 1985). The method, outlined schematically in Figure 8.6, entails adding known quantities of aquifer solids and water to glass ampules, spiking the resultant samples with a known quantity of radio-labeled contaminant, flame-sealing the ampules, and incubating the samples for a given period of time. At the end of the incubation period, the samples are centrifuged, and a portion of the supernatant is collected in liquid scintillation cocktail for counting. Using control samples (containing no aquifer solids) to account for volatilization losses, the concentration of sorbed contaminant is taken as the difference between the mass added and the mass in the aqueous phase. The method was adapted for headspace analyses with non-labeled compounds by equilibrating a portion of the sample supernatant in headspace vials, and analyzing the vapor phase with the Hall electroconductivity detector.

The procedure employing radio-labeled compounds has the advantage of accuracy (> 95% recovery on controls). Such accuracy is necessary for an investigation of sorption rate limitations. The disadvantages of the method are primarily associated with the expense of the compounds. While the headspace modification of the method is less accurate, and probably not suitable for detailed investigations, it offers the advantage of enabling the simultaneous analysis of several compounds.

Solids Sorption Studies

The batch sorption studies were undertaken to characterize the equilibrium behavior of the contaminants of interest with the Moffett solids. More specifically, the studies were used to investigate the linearity of the equilibrium behavior, and to quantify the distribution coefficients (K_d) and the rate at which equilibrium is achieved.

Partitioning of ^{14}C -Labeled TCE--

Early studies were aimed at measuring the apparent equilibrium isotherm of TCE for equilibration times corresponding to the contact time of the contaminants in the field. Figure 8.7 shows such an isotherm for TCE equilibrated with Moffett bulk material for 10 days. The data exhibit a slightly nonlinear behavior, and are best fitted by a Freundlich isotherm model. However, as shown by the regression line in the plot, a linear approximation agrees reasonably well; the resulting value for K_d using the data obtained with 10 days equilibration is 2.0 ml/g.

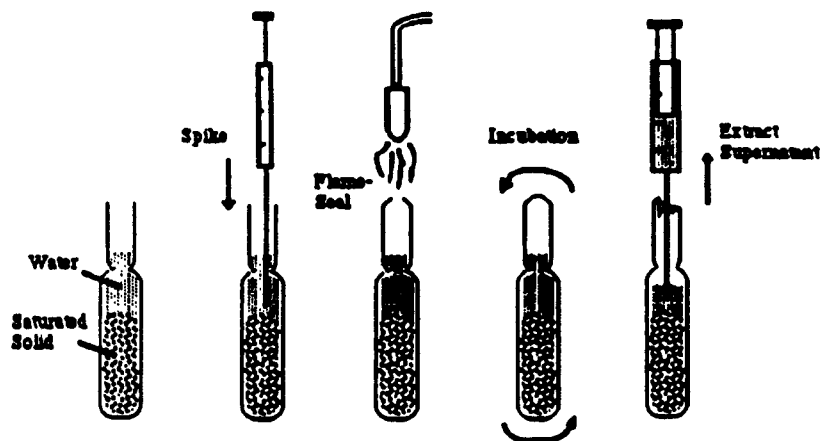


Figure 8.6. Flame-sealed ampule method for batch sorption studies (Curtis, 1984; Ball and Roberts, 1985, 1987).

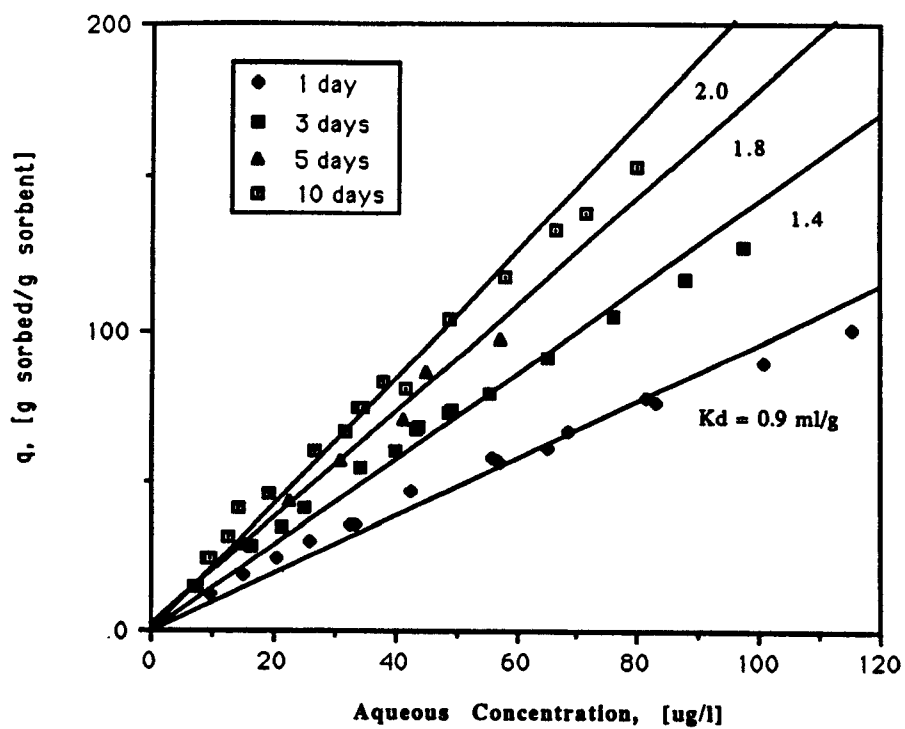


Figure 8.7. Sorption isotherm at increasing times for Moffett bulk solids and TCE.

Similar studies of TCE sorption by bulk Moffett solids for 1, 3, and 5 days resulted in similar behavior, with apparent K_d values increasing with incubation time. A second series of experiments was arranged to include 30 day equilibration. Due to a lack of bulk solids, this second series employed synthesized bulk samples, and repeated 1, 3, 5, and 10 day equilibration times for comparison with the bulk sample results. Figure 8.8 shows the results of the synthesized bulk runs along with the earlier bulk runs. The plot provides the apparent K_d as a function of time, in an attempt to characterize the approach to equilibrium. Results for the synthesized bulk suggest that batch systems require at least 30 days to approach true equilibrium.

Figure 8.8 also shows a discrepancy between the apparent K_d values observed with the bulk and synthesized bulk materials. A possible explanation is simply the difference in the samples used. The bulk samples, as discussed previously, were representative of the aquifer zone, while synthesized bulk samples were composed of materials mainly from above and below the zone. Estimates of the organic carbon content of the upper and lower confining materials were about 4 times greater than the estimates for the fine fraction of the aquifer material. Substitution of these confining materials for the fine fraction in the synthesized bulk would account for a portion of the discrepancy observed among the apparent K_d values. Also, it may be speculated that the larger fractions obtained from the confining layers possess higher f_{oc} values, or perhaps were contaminated by the confining clays to the extent that they also contribute to the higher partitioning.

Experiments with the Moffett fractions were used to separate the effects of particle size on the sorption process. The results of 1 and 30 day studies with the size fractions are shown in Figure 8.9. For the one day results, the value of the apparent K_d shows a definite increase with decreasing particle size. This observation is consistent with our hypothesis that sorption is rate-limited by slow diffusion at a time scale of days to tens of days. At 30 days, however, the effect of particle size is much less distinct, as the K_d values seem more or less randomly distributed between 7 and 9 ml/g. The lack of particle size dependency at approximately 30 days also seems plausible, if true equilibrium is indeed achieved within this time.

Sorption Studies of Vinyl Chloride, c-DCE, and t-DCE--

The headspace variant of the sorption experiment methodology offers the advantage of allowing for the simultaneous measurement of several solutes. However, inadequate control of volatile organics losses, particularly vinyl chloride, may result in large errors in the mass balance calculations used to estimate distribution coefficients. For this reason, the headspace analyses were employed solely for the purpose of estimating values of K_d for the three compounds. The resolution required for quantitative interpretation of the rate of solute uptake would have been unattainable using headspace analysis.

Figure 8.10 shows the results of the 10-day studies of vinyl chloride, cis- and trans- DCE with synthesized bulk Moffett solids. Although, as the correlations indicate, the error is substantial among the individual samples, a linear relationship can be established. The estimates of the 10-day K_d values for the three compounds are included in Table 8.3.

^{14}C -Labeled Sorption Studies with PCE and 1,1,1-TCA--

A limited number of experiments conducted using radio-labeled tetrachloroethylene (PCE) and 1,1,1-trichloroethane (1,1,1-TCA) with bulk Moffett solids demonstrated the effect of solute on sorption behavior. Table 8.3 contains the estimated K_d values for all of the solutes tested in this study.

Discussion

Discrepancies in Bulk and Synthesized Bulk Behavior--

The discrepancy shown in Figure 8.8 demonstrates the difference in solid samples used in the respective experiments. The bulk samples, as discussed previously, were representative of the aquifer zone, while synthesized bulk samples were composed of materials mainly from above and below the

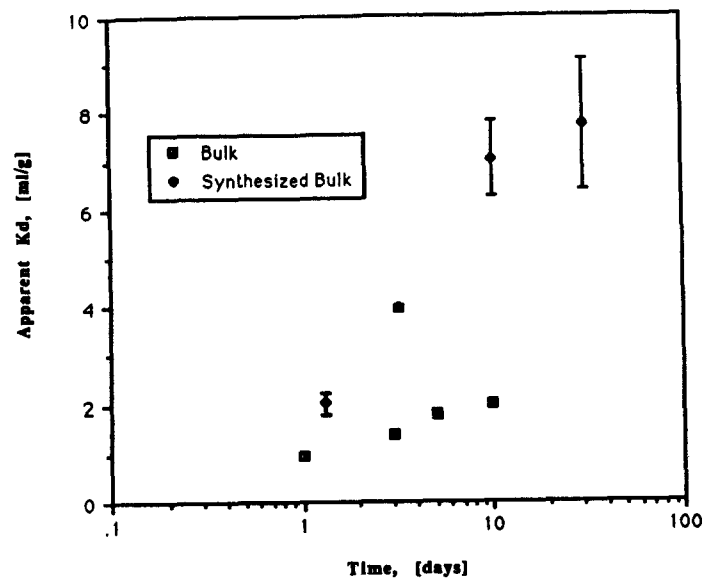


Figure 8.8. Increase of apparent K_d with time for sorption of TCE on bulk and synthesized bulk solids.

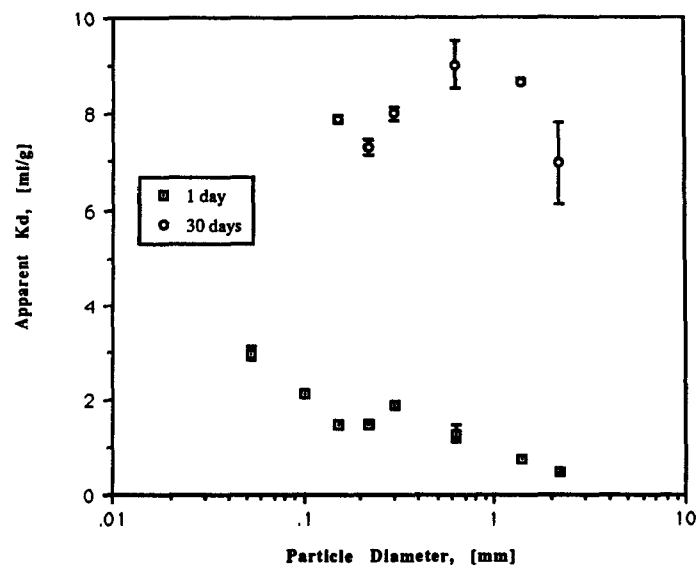


Figure 8.9. One-day and thirty-day apparent K_d values for Moffett size fractions and TCE.

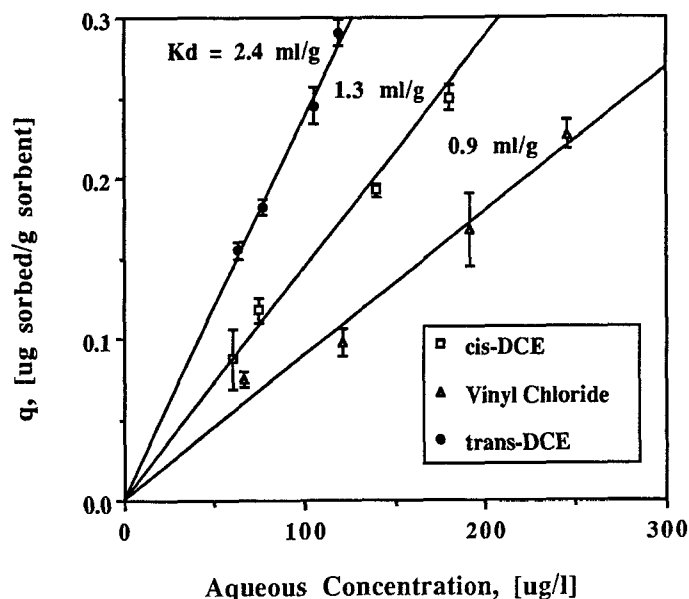


Figure 8.10. Sorption isotherms and K_d values for vinyl chloride, cis-, and trans-DCE and Moffett synthesized bulk; determined by headspace variation of flame-sealed ampule method.

TABLE 8.3. PARTITIONING COEFFICIENTS OF THE SOLUTES STUDIED WITH MOFFETT BULK AND SYNTHESIZED BULK SOLIDS

Compound	Apparent K_d (ml/g)	Equilibration Time (d)	Method	Material
1,1,1-TCA	0.4 ± 0.05	3	radiolabeled	bulk
TCE	1.4 ± 0.06	3	"	"
PCE	4.0 ± 0.3	3	"	"
Vinyl chloride	0.9 ± 0.2	10	headspace	syn. bulk
cis-DCE	1.3 ± 0.4	10	"	"
trans-DCE	2.4 ± 0.6	10	"	"
TCE	7.0 ± 0.4	10	radiolabeled	"
TCE	1.9 ± 0.1	10	"	bulk
TCE	7.8 ± 0.6	30	"	syn. bulk

zone. Estimates of the organic carbon content of the upper and lower confining materials were about 4 times greater than the estimates for the fine fraction of the aquifer material. Substitution of these confining materials for the fine fraction in the synthesized bulk would account for a portion of the discrepancy observed among the apparent K_d values. Also, it may be speculated that the larger fractions obtained from the confining layers possess higher f_{OC} values, or perhaps were contaminated by the confining clays to the extent that they also contribute to the higher partitioning. These results emphasize the importance of conducting organic carbon content measurements in conjunction with sorption studies.

Diffusion Rate--

The dependency of sorption on particle size has been observed previously (Ball and Roberts, 1985; Wu and Gschwend, 1986; Ball and Roberts, 1987), and has been attributed to mass transfer (diffusional) limitations. Ball and Roberts (1985,1987) employed a model based on diffusion of solute through intra-particle pores that is retarded by equilibrium partitioning. For the case of linear sorption isotherms, Fick's Second Law becomes

$$\frac{\delta C_r}{\delta t} = D_a \frac{\delta}{\delta r} \left[\frac{1}{\delta} \right] \frac{\delta C_r}{\delta r} \quad (8-1)$$

where C_r = the solute concentration at a point within the pore space of a particle, $[M/L^3]$; r = a point along the radius of the particle, $[L]$; and D_a = the apparent diffusivity of the solute within the particle pores, $[L^2/T]$.

The apparent diffusivity is defined as follows:

$$D_a = \frac{D_e}{\left(1 + \frac{\rho K_d}{\epsilon} \right)} \quad (8-2)$$

where D_e = the effective pore diffusivity, that is, the bulk diffusivity adjusted for the tortuosity of the pores, $[L^2/T]$; ρ = the grain density, $[mass\ solid/volume\ particle]$; and ϵ = the intra-particle porosity, $[volume\ pore/volume\ particle]$.

By assuming that the ultimate uptake of solute has been reached within 30 days, the TCE sorption data of the synthesized bulk in Figure 8.8 were transformed to provide the plot of fractional uptake with time in Figure 8.11. The fit shown is for the analytical solution of the problem of diffusion from a well-stirred solution of limited volume by Crank (1975). The fit provides a rough estimate of the apparent diffusivity, averaged over a wide range of particle sizes.

For comparison with field scale behavior, the best estimate of the apparent diffusivity ($5 \times 10^{-12} m^2/s$) was converted to an equivalent first-order rate parameter, or mass transfer coefficient, for one-dimensional transport. This approximation greatly simplifies the mathematics by enabling the substitution of a first-order differential equation for equation (8-1).

Wu and Gschwend (1988) studied the effects of particle size distribution on the first-order approximation of the diffusion model in batch systems. They concluded that the approximation was appropriate only for a relatively narrow range of particle sizes (within an one order of magnitude). With the intent of estimating the field scale behavior, we applied the approximation over a relatively wide range of particles. An empirical method provided by van Genuchten (1985) uses the following conversion:

$$\alpha = \frac{22.7 D_a}{a^2} \quad (8-3)$$

where α is an equivalent first-order mass transfer coefficient, $[d^{-1}]$, and a is the particle radius. A variation used by Goltz (1986) employs the method of moments to derive a slightly different conversion:

$$\alpha = \frac{15 D_a}{a^2} \quad (8-4)$$

Using equations (8-3) and (8-4), the estimates of α range from 0.4 to 0.6 d^{-1} .

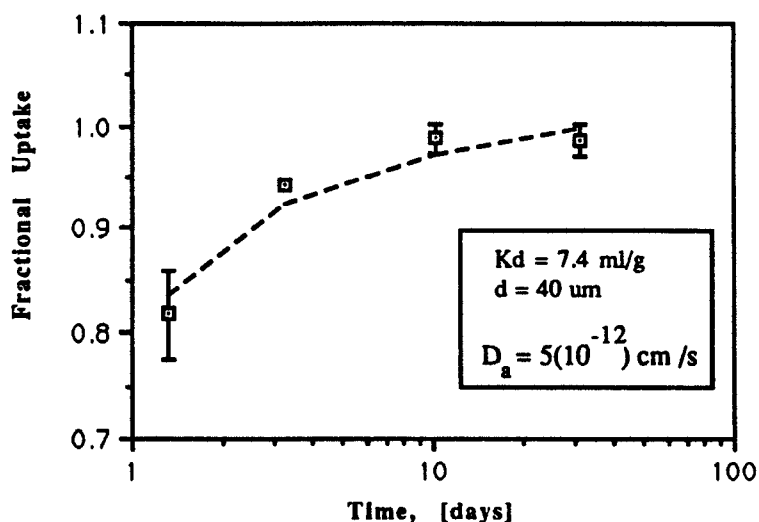


Figure 8.11. Sorption rate of TCE by synthesized bulk, showing diffusion model fit.

SUMMARY

Laboratory studies using solids from Moffett cores have focused on quantifying sorption equilibrium and rate parameters at the particle scale. Results of solids characterization studies indicate that the Moffett particles provide a complex system for sorption processes. The particles seem to be extremely weathered aggregations of grains, possibly containing clay-sized particles. The relatively high organic carbon content of the solids within, and adjacent to, the test zone seems to vary by as much as a factor of four. Applying the methods developed in our laboratory for a relatively clean, homogeneous sand, we observed a fast fraction of contaminant uptake by the solids, followed by a fraction of uptake governed by a rate that is orders of magnitude slower. This indicated that, although the solids are quite complex, the suspected sorption mechanism--organic partitioning limited by mass transfer--adequately explains the rate behavior.

The transport parameters derived from laboratory scale studies provide a basis for independently estimating field-scale transport parameters. The results presented in this section will be used in Section 13 to interpret field observations of transport behavior.

SECTION 9

TCE TRANSFORMATION BY MIXED AND PURE GROUNDWATER CULTURES

Susan Henry and Dunja Grbić-Galić

INTRODUCTION

Although TCE transformation by methanotrophic mixed cultures (consortia) and pure cultures has been well-documented, research on this topic is still in its nascent stages, and it may be premature to generalize. What appears to be emerging, however, is that different methanotrophs possess different TCE-transformation capabilities, and respond differently to different conditions.

In order to develop and optimize methanotrophic bioremediation methodologies, and to develop predictive capabilities, we must achieve a fundamental understanding of the transformation process. This includes defining the effects of operational parameters on TCE transformation, and defining the physiological bases for given responses. Since it is evident that not all methanotrophs possess the same capabilities, the greatest value lies in evaluating many methanotrophic cultures. In that manner, it should be possible to define the characteristics of a methanotrophic culture that is most suitable for a given application.

In our research, we have obtained TCE-degrading bacterial cultures from the Moffett Field groundwater aquifer. These cultures have been evaluated for their TCE transformation capabilities by radiolabeling experiments and by gas chromatography, and have been examined by scanning and transmission electron microscopy. One of the objectives of our work is to characterize the behavior of these cultures under conditions that may be considered operational parameters in either in situ bioremediation or waste treatment applications. We have evaluated the effects of methane concentration, availability of reducing power, oxygen concentration, TCE concentration, and mineral medium formulation on TCE transformation by these cultures; the physiological bases for some TCE transformation phenomena; and the intermediates and products resulting from the methanotrophic transformation of TCE.

METHODS

Aquifer Cultures

Enrichment of Cultures--

Mixed cultures were enriched from aquifer material or groundwater collected from the Moffett field test site, or from effluent from a soil column. The aquifer material used was gravelly, silty sand from the core SU-39-2 (B series) aseptically collected on August 27, 1985, before the test site had been enriched with methane (Section 4). The groundwater was withdrawn from the test site July 1987, after the site had been enriched with methane. The soil column had been packed with aquifer material from core SU-39-2, and had been enriched on methane and transformed TCE (Section 10).

Continuously-stirred reactors containing one liter of a phosphate-buffered nitrate salts mineral medium formulation, here termed "regular mineral medium" (per liter: 1 g NaNO₃, 0.5 g K₂HPO₄, 0.5 g

KH₂PO₄, 0.2 g MgSO₄·7H₂O, 0.02 g CaCl₂·2H₂O, 0.005 g FeSO₄·7H₂O; trace metals: 70 µg ZnSO₄·7H₂O, 17 µg MnSO₄·H₂O, 20 µg H₃BO₃, 100 µg CoCl₂·6H₂O, 10 µg CuCl₂·2H₂O, 20 µg NiCl₂·6H₂O, 30 µg Na₂MoO₄·2H₂O) were inoculated with approximately one gram aquifer material or approximately 20 ml groundwater or column effluent, and incubated under a continuous flow of approximately 25% gaseous substrate (methane, ethylene, or propane) in air. When turbidity was observed, 10 ml of the culture was transferred to a new reactor and incubated as before. This process was repeated 5 to 10 times, depending upon the culture, over the period of several months, until culture stability, as determined by light microscopy and consistent colony morphology, appeared to have been achieved.

Isolation of Pure Cultures--

Pure cultures were isolated on agarose plates made with regular mineral medium. Plates were incubated in dessicators filled with approximately 25% substrate (methane or ethylene) in air. Purity was confirmed on the basis of repeated colony isolation; constant, homogeneous colony morphology; and constant, homogeneous cell morphology.

The methane-oxidizing isolate was tested for growth on multicarbon substrates in liquid and on solid media, including blanks (no substrate); blanks + vitamins; glucose; glucose + casamino acids; fructose; fructose + casamino acids; succinate; succinate + casamino acids; casamino acids; formate; glyoxylate; and dichloroacetate. Lack of growth on any of these substrates in liquid culture was a confirmation of purity. Background growth on solid media, regardless of substrate, was not an indication of lack of purity. The isolate, after seven sequential transfers on blank, glucose, glucose + casamino acids, casamino acids, and methanol plates, would still grow on methane when transferred back to liquid or solid media, and maintained consistent colony morphology throughout. It is assumed that the growth on solid media is due to C-1 contaminants in the solid media.

Enzyme Assays--

The methane-oxidizing pure culture was tested for enzymes characteristic of type I and type II methanotrophs. The hydroxypyruvate reductase assay (Large and Quayle, 1963) tested for the serine pathway of carbon assimilation. The hexulose phosphate synthase assay (Mary Lidstrom, pers. comm.) tested for the ribulose monophosphate (RMP) pathway of carbon assimilation.

Microscopy--

The cultures were evaluated by light microscopy and by scanning and transmission electron microscopy. The cultures were examined by phase contrast for motility and morphology, and by differential staining, including the Gram stain and staining with sudan black B for poly-β-hydroxybutyrate (PHB) granules (Norris and Swain, 1971).

For electron microscopy, the cultures were fixed with glutaraldehyde and stained with osmium tetroxide and uranyl acetate, and dehydrated in increasing strengths of ethanol (Hayat, 1981). For scanning electron microscopy the samples were then dried with hexamethyldisilazane (HMDS, Polysciences, Inc.) (Nation, 1983). For transmission electron microscopy the samples were imbedded in VCD-HXSA, a low viscosity imbedding medium (Oliveira et al., 1983) with 0.5% silicone added for ease of sectioning (Fran Thomas, pers. comm.). Thin sections were stained with lead citrate. Scanning electron micrographs (SEMs) were taken on a Philips 505 scanning electron microscope, and transmission electron micrographs (TEMs) were taken with a Philips 410 transmission electron microscope.

TCE DEGRADATION EXPERIMENTS

Cultures were raised to mid-log phase of growth in continuously-stirred reactors under a continuous stream of methane in air, then transferred to 100 ml serum bottles or 250 ml screw cap bottles for degradation studies. In early experiments cultures were raised under a stream of 20-25% methane in air, which was later changed to 35-45% methane to enhance the growth rate. Cultures were raised in "regular" mineral medium unless otherwise specified. Cultures were raised on a formulation here termed "Whittenbury" mineral medium (Whittenbury et al., 1970) for some experiments. The pure culture

received vitamins (20 µg/l biotin, 20 µg/l folic acid, 50 µg/l thiamine.HCl, 50 µg/l calcium pantothenate, 1 µg/l B12, 50 µg/l riboflavin, 50 µg/l nicotinamide) (Mary Lidstrom, pers. comm.) when grown in liquid culture. All degradation experiments were conducted in shake flasks, which were incubated upside-down on a rotary shaker in a 21°C environmental chamber.

Radiotracer Experiments

Degradation experiments with ^{14}C -labeled TCE were conducted to positively confirm that TCE was being biologically transformed, and to determine the percentage of the TCE carbon in the cell, the CO_2 , and the aqueous intermediate fractions. The shake flasks were sacrificed for analysis using a liquid scintillation counting (LSC) assay. Three types of controls, autoclaved cultures, gamma irradiated cultures, and sterile mineral medium blanks were evaluated. Gamma irradiation kills the cultures but does not rupture the cells as autoclaving does. Gamma-irradiated cultures were used to evaluate sorption of TCE to the cells. Less than 3% of the ^{14}C was associated with the gamma irradiated cultures after a one-week incubation. It was therefore concluded that sorbed TCE represents a negligible fraction of the ^{14}C that is associated with TCE-transforming cultures. No significant differences were observed for the three different kinds of controls. Autoclaved cultures were used for most experiments, and mineral medium blanks were used for some.

LSC Assay--

A modification of a liquid scintillation counting assay, described in Section 10, was used to evaluate the amount of ^{14}C carbon in the TCE, CO_2 , nonvolatile aqueous, and cell fractions. The method entails nitrogen stripping 1 ml fractions to which base or acid has been added. In order to pull into solution the CO_2 in the headspace of the shake flask, base was added to the flasks before samples were withdrawn for stripping (Figure 9.1). The method was modified because it was observed that raising the pH of the shake flasks to pH 9.5–10 resulted in an artificially high aqueous intermediate radioactivity and an artificially low cell radioactivity, most likely because the high pH was causing cell lysis. The modification involved adding base to one set of replicate bottles to determine the TCE and CO_2 radioactivity, and separating the cells and the aqueous fraction in another set of replicate bottles by centrifugation, and acidifying the supernatant after the cells had been removed.

Fractions were combined with 10 ml Insta-gel (Packard) liquid scintillation cocktail and evaluated by liquid scintillation counting.

Preparation of Stock Solution--

It was discovered that the TCE arrives from the manufacturer with an approximately 6% nonvolatile contaminant fraction. Therefore, it was necessary to prepare aqueous stock solutions in such a manner that the nonvolatile contaminant fraction was not transferred to the stock solution. The radiolabeled TCE stock solutions were prepared by diffusing the ^{14}C -TCE (Sigma/Pathfinder) into sterile Milli-Q water. The break-seal ampule containing the gaseous TCE was first dipped into liquid nitrogen to freeze the TCE into the bottom of the sealed ampule. The break-seal was then broken with a sterile glass rod, and the ampule tube was quickly inverted and attached with a Teflon/stainless steel swagelok fitting onto a flask containing 100 ml sterile Milli-Q water and a stir rod. The flask was secured to a stir plate in a 4°C chamber and stirred for two days, permitting the TCE to diffuse into the water, while the nonvolatile contaminant fraction remained behind in the break-seal ampule. A ^{14}C -TCE stock solution of 99.3% purity was thereby achieved, and the recovery of the TCE was approximately 90%.

Time-Series Experiments for Rate Determinations

Time-series analyses of TCE concentrations were conducted to generate rate coefficients. Cultures were incubated with unlabeled TCE and the headspace concentration was analyzed according to a method developed by Criddle et al. (1989) on a Tracor gas chromatograph equipped with an electron capture detector. Sorption of TCE to cells was found to be insignificant and mineral medium blanks were found to behave identically to autoclaved controls, so mineral medium blanks were used as controls. TCE calibration standards were made up by weight in methanol and stored in a freezer.

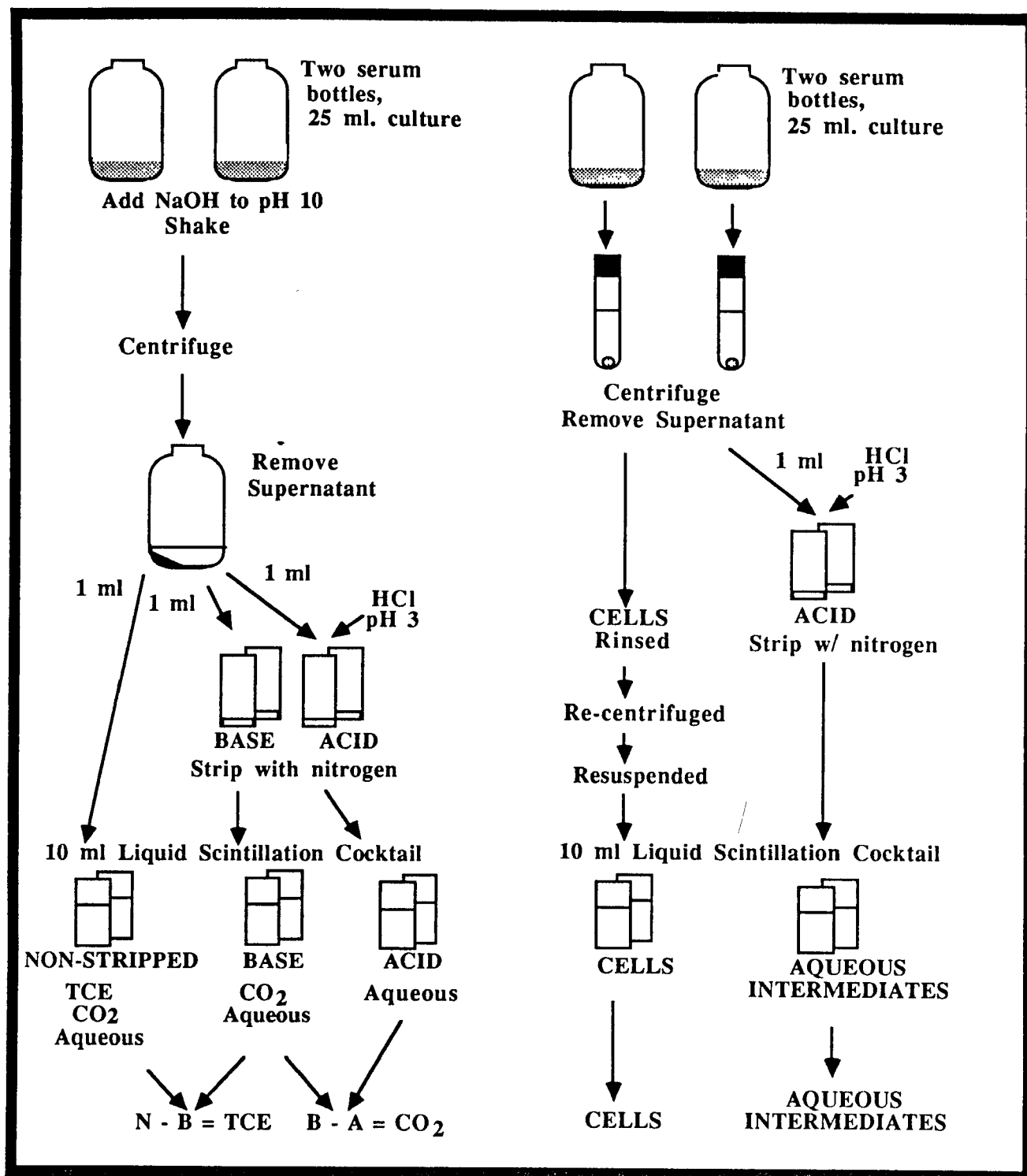


Figure 9.1. Diagram of LSC assay.

Cultures were diluted as necessary with either phosphate buffer or the same mineral medium formulation in which they had been cultured, so that the rate of change of the TCE concentration in the shake flasks did not exceed mass transfer rates. Cultures grown in Whittenbury mineral medium were diluted approximately 1:20, and those grown in the Whittenbury without EDTA or FeNaEDTA, approximately 1:2. Cell biomass was determined on a dry weight basis using pre-weighed rinsed and dried 0.2 μm Supor (Gelman) filters. Filters were dried overnight at 105°C and cooled in a desiccator over phosphorous pentoxide.

The data generated by these experiments were modeled on a mass basis using the Monod equation of substrate utilization kinetics, $-dS/dt = kXS/(K_s + S)$. Mass was converted to aqueous concentration on the basis of the headspace and aqueous volumes, using a Henry's constant of 0.33 (dimensionless ratio of mass concentrations). To generate the second-order rate coefficient, k/K_s , degradation experiments were conducted at initial TCE concentrations of 35 to 60 $\mu\text{g/l}$, and it was assumed that $K_s \gg S$, yielding an equation of the form $-dS/dt = kXS/K_s$. The maximum utilization rate k was determined at 3 mg/l TCE, at which concentration it was assumed that $S \gg K_s$, yielding $-dS/dt = kX$. Given k/K_s and k , K_s was then generated. The correlation coefficient R^2 that describes the fit of the data to the model was greater than 0.95 for all data reported here. Biomass was assumed to be constant throughout, which proved to be a reliable assumption. Most rate experiments were conducted with no methane added. When methane was added, it was at less than 0.4 mg/l, and given the low methane concentration and the slow growth rate of the organisms, no significant increase in the biomass was detected during the duration of the transformation experiments.

Analysis for TCE Transformation Products

Products of the oxidation of TCE by the pure culture *Methylobacter* MM2 were evaluated in the nonvolatile aqueous fraction and in the headspace. To obtain an aqueous fraction with a high concentration of products, but with a low anion concentration (NO_3^- , PO_4^{3-} , SO_4^{2-} , Cl^- : resulting from the mineral medium), cells were centrifuged and resuspended in a 1/8th dilution of regular mineral medium. Dense cultures were incubated with 3 to 10 mg/l TCE, followed by centrifugation. The supernatant was then filter-sterilized. Acidic break-down products in the supernatant were evaluated by ion chromatography on a Dionex Ionalyzer using 5 millimolar borate buffer. Volatile chlorinated products were evaluated by gas chromatography. Carbon monoxide was evaluated by headspace analysis on a Trace Analytical RGD2 reduction gas detector (hydrogen analyzer).

RESULTS

Cultures

Propane-Oxidizers--

Two propane-utilizing mixed cultures were enriched from aquifer material. The cultures did not transform TCE and were not studied further.

Ethylene-Oxidizers--

Mixed culture--An ethylene-degrading mixed culture, EM1, was enriched from aquifer material. The culture contained Gram variable bacilli as well as Gram negative bacilli and coccobacilli (Plate 9.1a).

Pure culture--A pure culture, "Ethyl", was isolated from the ethylene-oxidizing mixed culture. This pure culture was a Gram variable bacillus approximately $0.5 \times 2 \mu\text{m}$ in size (Plate 9.1b). It formed slow-growing bright yellow slimy colonies on solid media. Ethyl grows best on ethylene, and grows less well on fructose, succinate, and tryptone-glucose. Fructose and succinate inhibit growth on ethylene. No growth was observed on methane, methanol, or ethanol. When incubated under a 5% oxygen and 95% nitrogen headspace with succinate in mineral medium lacking nitrate or ammonia, no growth was observed,

indicating that Ethyl is not a *Xanthobacter* sp. Ethyl appears to fit the description of *Mycobacterium* sp., but this has not been confirmed.

Methane-Oxidizers--

Mixed cultures--Three different methane-oxidizing mixed cultures were obtained by enrichment. The cultures are different, on the basis of macroscopic and microscopic appearance. MM1, enriched from aquifer material, consisted of various Gram negative bacilli, coccobacilli, cocci, and prosthecae (Plate 9.2a). MM1 contains a type II methanotroph, an irregular sphere that is less than 1 μm in diameter (Plate 9.3a). MM2, enriched from column effluent, contained predominantly Gram negative motile bacilli and Gram negative coccobacilli, as well as some yeasts (Plate 9.2b). Two different methanotrophs, a type I (Plate 9.3b) and Type II (Plate 9.3c) were observed in this culture. MM3, enriched from groundwater, contained primarily Gram negative bacilli and coccobacilli (Plate 9.2c). MM3 contained a type II methanotroph, an irregular sphere even smaller than the one in MM1 (Plate 9.3d).

Pure culture--A pure culture, *Methylomonas* MM2 ("NAL") was isolated from mixed culture MM2 (Plate 9.2d). This pure culture contains the stacked internal membranes characteristic of type I methanotrophs (Plate 9.4a). *Methylomonas* MM2 is pigmented pink on liquid and solid media, turning yellow with age. It is a Gram negative motile bacillus. *Methylomonas* MM2 assimilates carbon by the ribulose monophosphate pathway, and does not test positive for enzymes of the serine pathway. It is microaerophilic and grows well on methane and methanol. It exhibits background growth on solid media, but exhibits no growth on multicarbon substrate in liquid media.

An unusual pattern of lysis, uncharacteristic of old age or nutrient deprivation, was sometimes observed. Transmission electron micrographs of the lysed cells revealed electron-dense, regularly-shaped hexagonal spots approximately 60 nm in diameter, within the perimeter of lysed cells (Plates 9.4b and 9.4c) as well as attached to the surface of some live cells (Plate 9.4d). The spots, on the basis of the fixing and staining protocol, could only be nucleic acids. All of this strongly suggests that the culture had a phage associated with it. Attempts to obtain plaques on *Methylomonas* MM2 were unsuccessful. This cannot be taken as an indication the phage are not present, however. It is likely that the culture was already lysogenized by the phage, rendering it immune to infection and subsequent lysis.

TCE Transformation--

Table 9.1 summarizes a range of TCE transformation rates observed for the cultures when grown in regular mineral medium and incubated with and without methane under various conditions. The TCE concentrations used in these experiments were 40 to 60 $\mu\text{g/l}$.

Propane-oxidizers--The propane oxidizers did not transform TCE.

Ethylene-oxidizers--Both the ethylene-oxidizing mixed culture EM1 and the pure culture Ethyl transformed 100% of the TCE. Transformation occurred with and without ethylene present, and high ethylene concentrations (tested at 13 mg/l) inhibited transformation. The mixed culture transformed most of the TCE to CO_2 and cell fractions, with about 10% remaining in the nonvolatile aqueous fraction. The pure culture transformed the TCE to CO_2 , cell, and nonvolatile aqueous fractions. The pure culture was tested for growth on TCE, cis-DCE, and trans-DCE. No growth was observed. The rate of TCE transformation by the ethylene-oxidizers was approximately two orders of magnitude less than the rates exhibited by the methane-oxidizers (Table 9.1).

Methane-oxidizers--All the methane-oxidizing cultures transformed TCE. Rates were variable, depending upon growth conditions and incubation conditions. All exhibited what has been termed "stationary transformation", that is, they transformed TCE in the absence of methane. Unless impaired by incubation conditions, 100% of the TCE was transformed. In mixed cultures, the TCE was transformed primarily to CO_2 and cells, with about 5-10% remaining in the nonvolatile aqueous fraction after extended incubation. In pure cultures, approximately 5-10% was transformed to CO_2 , 10-20% to cells, with 70-80% remaining in the nonvolatile aqueous fraction. Acetylene inhibited methane oxidation and TCE transformation, indicating that the methane monooxygenase enzyme catalyzed the oxidation.

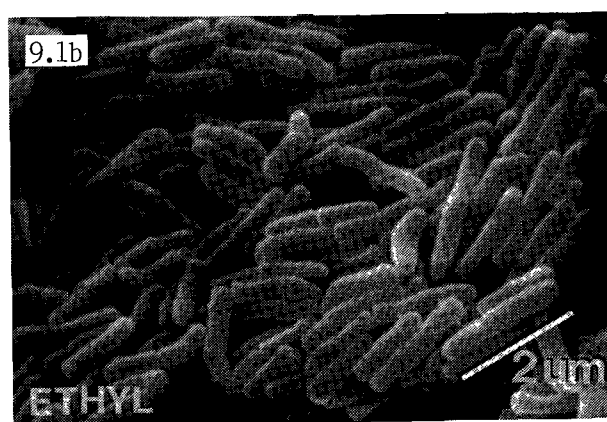
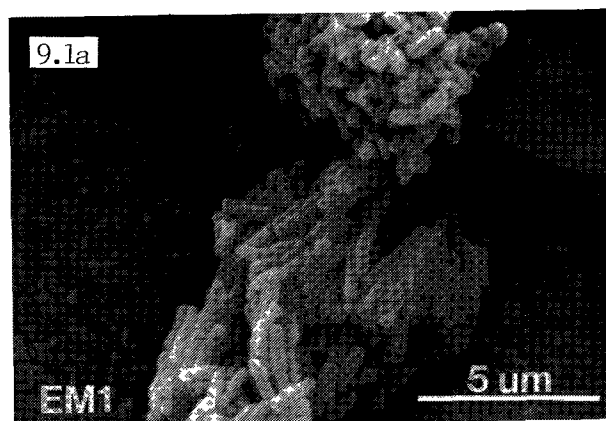


Plate 9.1. Scanning electron micrographs of ethylene-oxidizing cultures. Mixed culture EM1 (9.1a) and pure culture 'ethyl' (9.1b).

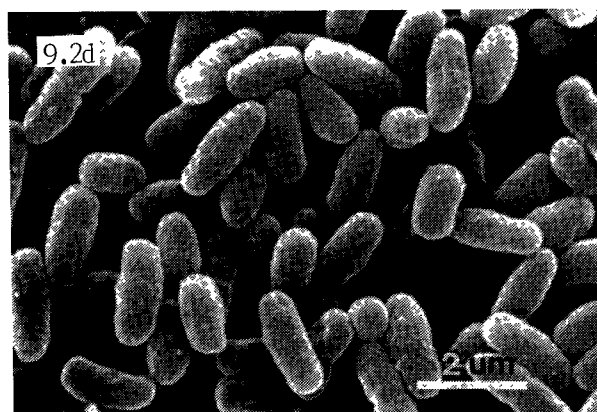
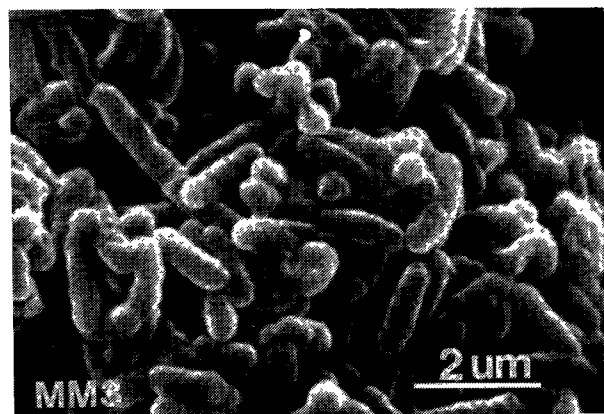
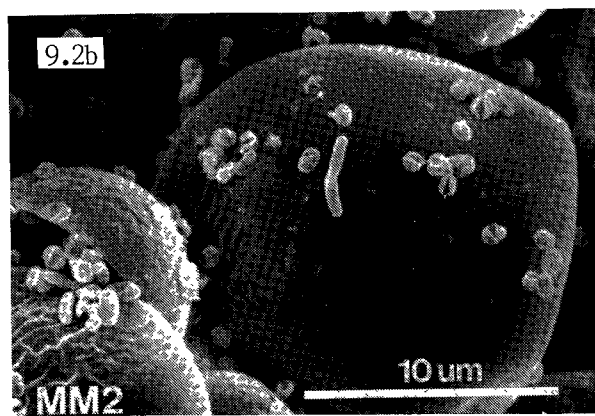
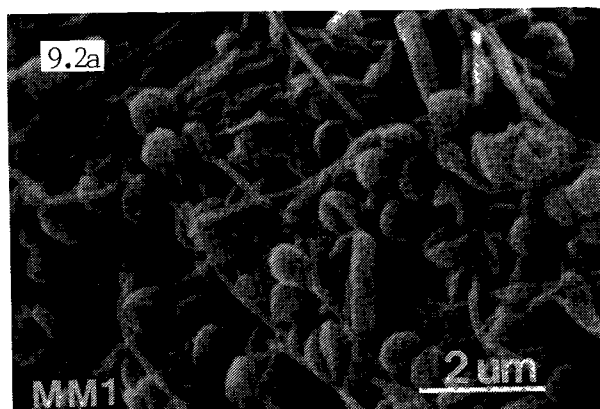


Plate 9.2. Scanning electron micrographs of methane-oxidizing cultures. Mixed cultures MM1 (9.2a), MM2 (9.2b), MM3 (9.2c), and pure culture *Methylobionas* MM2 (9.2d).

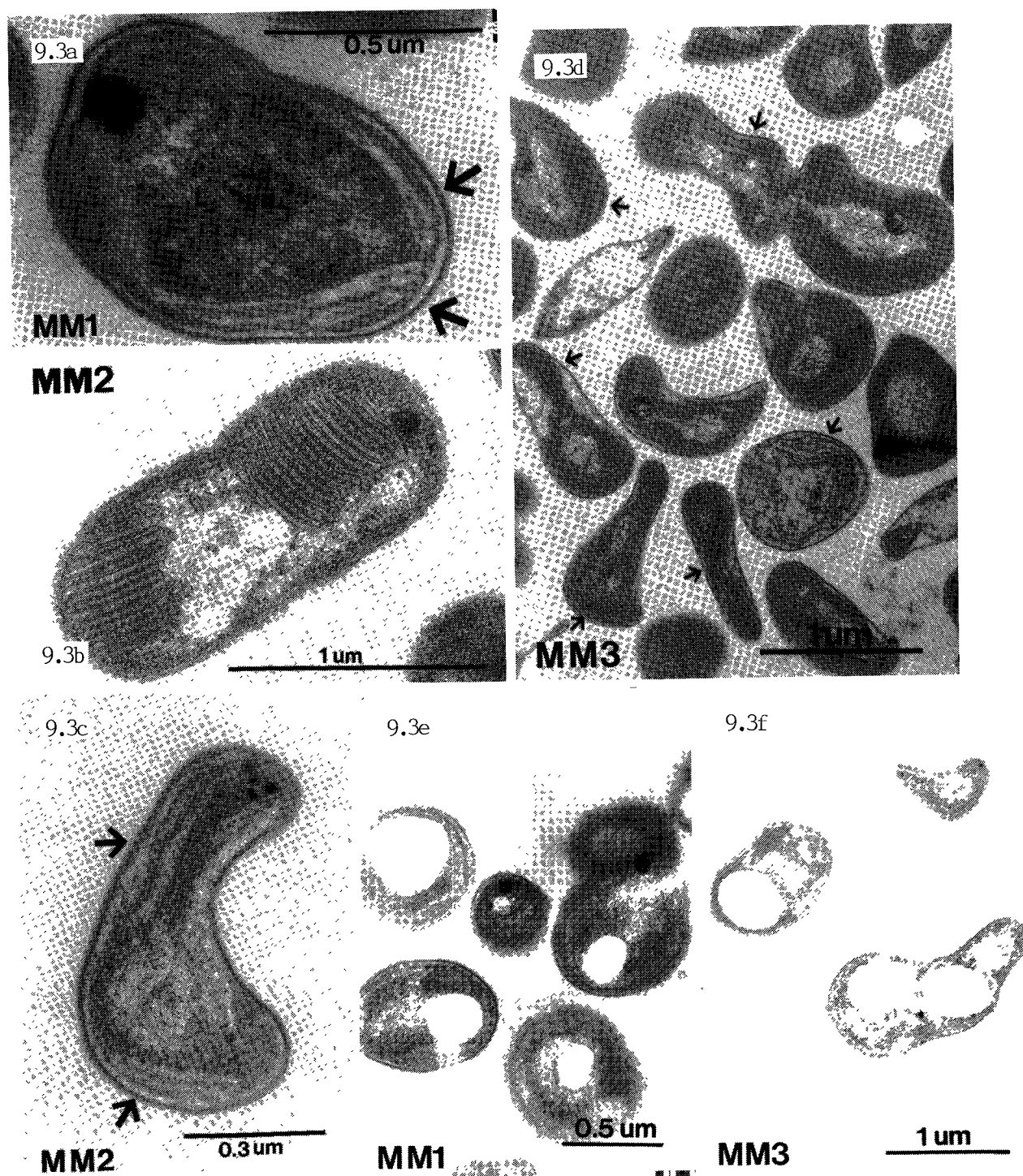


Plate 9.3. Transmission electron micrographs of the methane-oxidizing mixed cultures. (9.3a) Type II methanotroph in MM1. (9.3b) Type I and (9.3c) type II of MM2. (9.3d) Type II of MM3. Methanotrophs of MM1 (9.3e), and MM3 (9.3f) containing PHB granules.

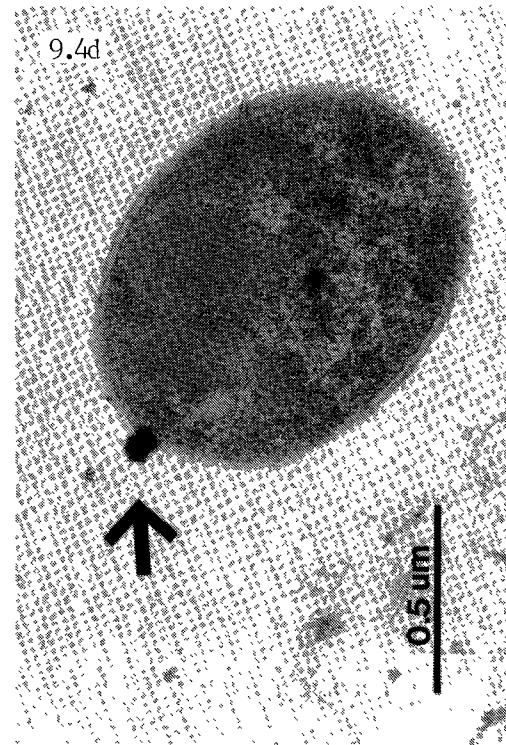
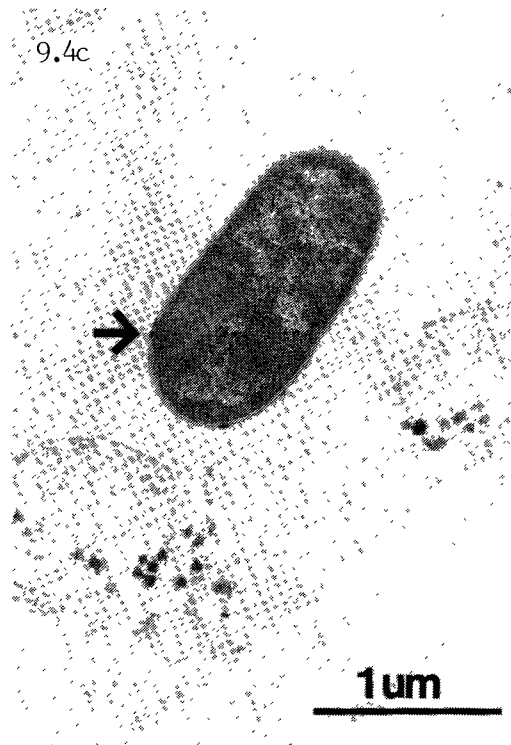
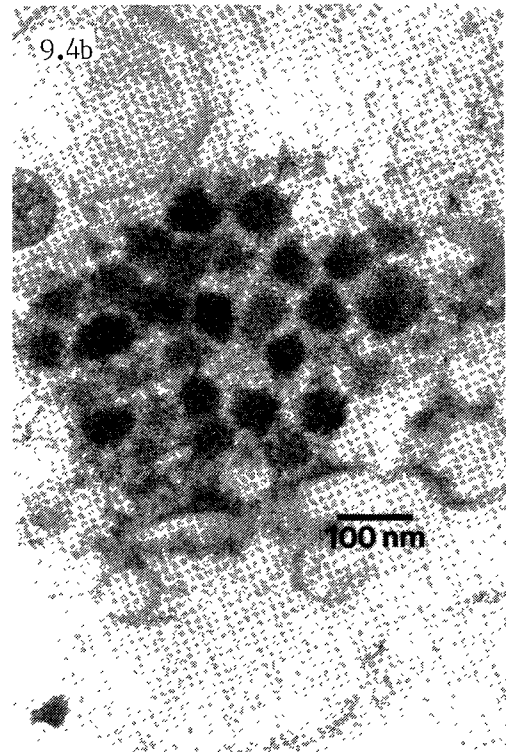
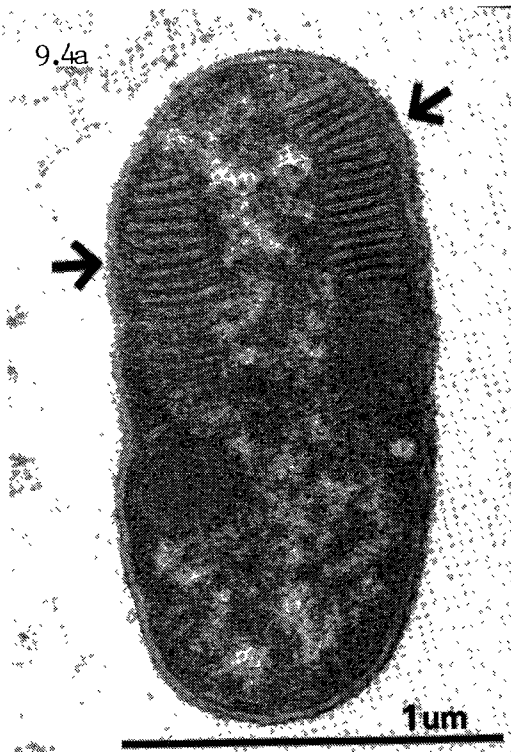


Plate 9.4. Transmission electron micrographs of pure culture *Methylobacterium* MM2 showing Type I membranes (9.4a), and cells infected with phage (9.4b, 4c, 4d).

TABLE 9.1 TCE TRANSFORMATION RATES

	k/K _s (l/mg-day)
<u>Methane-oxidizers</u>	
mixed culture MM1	0.039–0.047
mixed culture MM2	0.000–0.010
mixed culture MM3	0.043–0.048
<i>Methylomonas</i> MM2	0.000–0.17
<u>Ethylene-oxidizers</u>	
mixed culture EM1	0.0002–0.0006
pure culture ("Ethyl")	0.0008–0.0009

Rate coefficients were determined for the three mixed cultures. Using the first and second-order coefficients generated from degradation studies conducted at 3 mg/l and 60 µg/l respectively, the half-saturation coefficient K_s was calculated (Table 9.2). The fit of the data to the model is described by the R² value, an R² value of 100 describing a perfect fit.

TABLE 9.2 RATE COEFFICIENTS FOR METHANE-OXIDIZING MIXED CULTURES

		3 mg/l TCE		0.07 mg/l TCE		K _s (mg/l)
		k (d ⁻¹)	R ²	k/K _s (l/mg-day)	R ²	
<u>Mixed Culture</u>						
	MM1	0.0060	0.97	0.041	0.99	0.15
	MM2	0.0088	0.99	0.01	— ^a	0.9
	MM3	0.0097	0.90	0.046	0.99	0.21

^a The k/K_s value used for this calculation is the average of several experiments.

Effects of Variables on TCE Transformation by Methane-Oxidizers --

Methane concentration--Mixed cultures MM1 and MM2 and pure culture *Methylomonas* MM2 were tested for the effects of 3 different methane concentrations--no methane; 2% of headspace (1.3 mg total, 0.45 mg/l aqueous); 20% of headspace (13 mg total, 4.5 mg/l aqueous)--on TCE transformation.

The LSC assay method was used to evaluate the fraction of the TCE transformed into the nonvolatile aqueous, CO₂, and cell fractions by determining the ¹⁴C in those fractions. Results are presented in Figures 9.2, 9.3, and 9.4. The percent of the TCE transformed at the given time in hours is represented by bar graphs. The percent of methane and oxygen in the headspace, representing a mean of four bottles, is also given. Determinations were done in replicate as described in the methods section.

All three cultures transformed TCE when no methane was present. However, mixed culture MM1 was the only one in this experiment to transform TCE significantly faster when no methane was present. Rates of transformation for MM2 and the pure culture when no methane was present were significantly slower than when methane was provided.

The enzyme system that oxidizes TCE, methane monooxygenase (MMO), is the same enzyme that oxidizes methane. Since the TCE and methane compete for the same enzyme, methane will competitively inhibit TCE transformation. In all cultures tested, high methane concentrations had an inhibitory effect. This effect was particularly pronounced in mixed culture MM1: at 1/2 hour, 70% and 60% of the TCE had been transformed under 'no' and 'low methane' respectively, and only 10% had been transformed under 'high methane'. In other experiments with the pure culture, *Methylobacter* MM2, 2 mg/l methane resulted in a 25% reduction in the initial TCE oxidation rate.

Availability of reducing power--All of the cultures transformed TCE in the absence of methane, a desirable capability in light of the competitive inhibition. However, the response to methane deprivation was variable. Depending upon the duration of deprivation, TCE transformation capability was lost. This effect relates to the availability of reducing power. The MMO requires a source of reducing power to carry out its oxidative function. When methanotrophs are cometabolizing TCE in the absence of a substrate, depletion of the source of a source of reducing power can halt the cometabolic transformation.

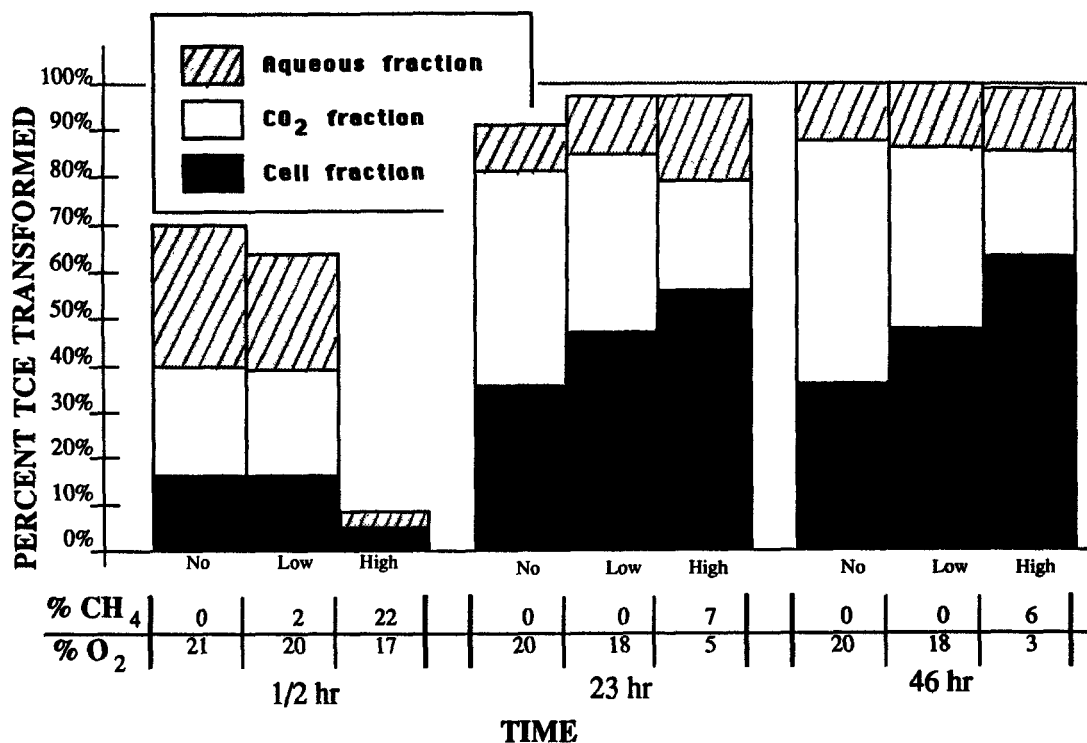


Figure 9.2. Effects of methane concentration on percent TCE transformed into the nonvolatile aqueous, CO₂, and cell fractions by mixed culture MM1 (dry weight = 0.40 mg/ml).

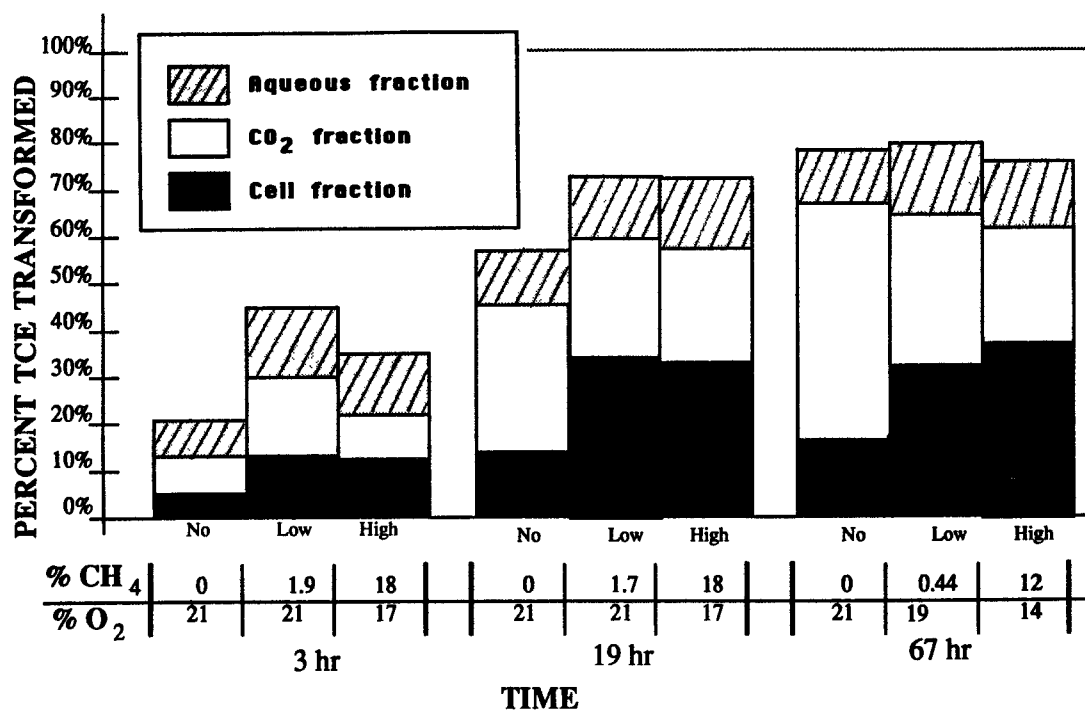


Figure 9.3. Effects of methane concentration on percent TCE transformed into the nonvolatile aqueous, CO₂, and cell fractions by mixed culture MM2 (dry weight = 0.33 mg/ml).

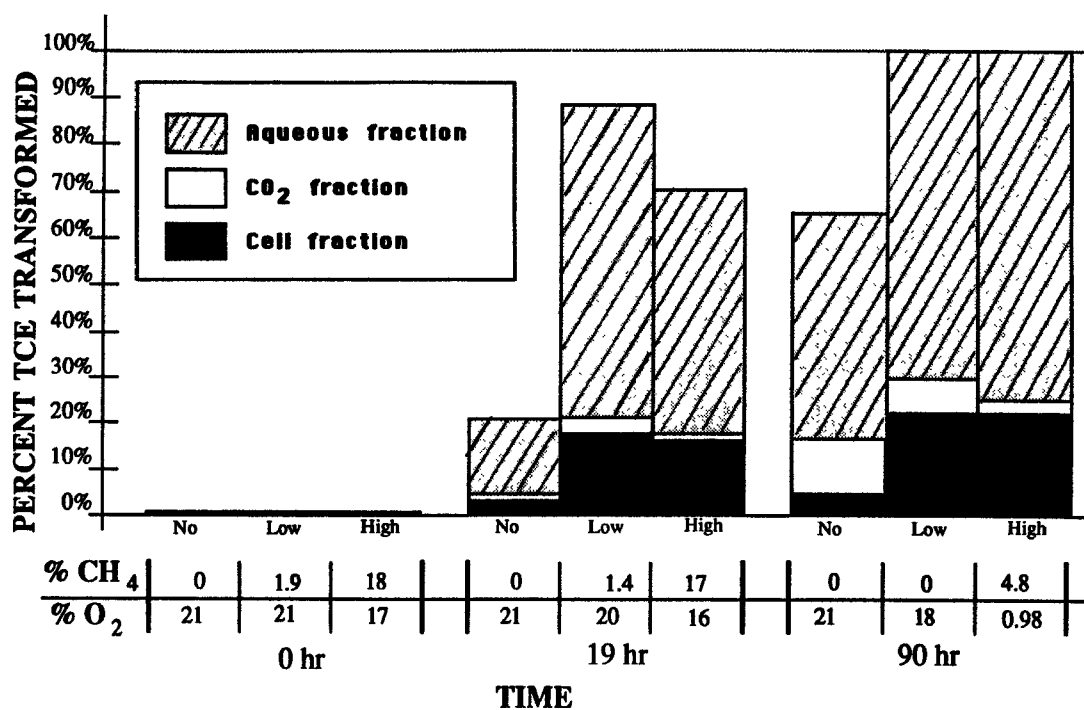


Figure 9.4. Effects of methane concentration on percent TCE transformed into the nonvolatile aqueous, CO₂, and cell fractions by *Methylomonas* MM2 (dry weight = 0.12 mg/ml).

Mixed cultures MM1 and MM3 were found to transform TCE as rapidly in the absence of methane as in the presence of low concentrations of methane. Mixed culture MM2, and pure culture *Methylobacter* MM2 transformed TCE less well in the absence than in the presence of millimolar concentrations of methane. In one experiment, when *Methylobacter* MM2 was incubated without methane for 24 hours and then tested for TCE oxidation, it had completely lost its ability to transform TCE. We had hypothesized that the PHB granules may act as a source of reducing power for the oxidation of non-metabolizable compounds by the methane monooxygenase enzyme, and that the methanotrophs of mixed and pure cultures MM2 and *Methylobacter* MM2 lacked such storage granules. Transmission electron micrographs revealed that the methanotrophs of mixed cultures MM1 and MM3 contain PHB granules (Plates 9.3e and 9.3f), whereas *Methylobacter* MM2 and the methanotrophs of mixed culture MM2 do not contain PHB granules.

Table 9.3 presents the results of an experiment evaluating the effects of starvation on TCE transformation. The mixed cultures MM1, MM2, and MM3 were incubated for 15 hours in the absence of methane, and then evaluated for TCE transformation capability in the presence and absence of methane. The change in the TCE concentration was evaluated in duplicate bottles. MM1 and MM3, the two cultures with methanotrophs containing PHB granules, transformed TCE as well, whether or not methane had then been added to the shake flasks. Mixed culture MM2, however, could no longer transform TCE unless methane was added, and even when methane was added the culture did not recover its full capabilities.

TABLE 9.3. MIXED CULTURE TCE TRANSFORMATION RATES

		k/K _s (l/mg, day)	
		No Methane Mean ± Std. Dev.	0.4 mg/l Methane Mean ± Std. Dev.
<u>Mixed Culture</u>			
	MM1	0.041±0.003	0.046±0.001
	MM2	0	0.004±0.001
	MM3	0.046±0.001	0.046±0.004

Oxygen concentration--Oxygen is required by methanotrophs both for respiration and for the oxidative function of the MMO. Many methanotrophs, however, have been described as microaerophilic, and grow best at oxygen tensions below atmospheric. High oxygen concentrations at 50% of headspace were inhibitory, reducing TCE transformation by approximately 20%, in all cultures tested. Oxygen at 35% was not inhibitory. When cultures were incubated under near-anoxic conditions (< 1% O₂), very little methane or TCE was oxidized. When oxygen was depleted, TCE transformation stopped.

TCE concentration--TCE and its oxidation product, the TCE epoxide, are cytotoxic. Toxic inhibition of TCE transformation can be anticipated at some concentration in the mg/l range. The mixed cultures MM1, MM2, and MM3 were evaluated for TCE transformation and methane consumption at 5, 10, 44, and 87 mg/l TCE using radiolabeled TCE. All of the TCE was transformed and all of the methane was consumed at 5 and 10 mg/l TCE. At 44 and 87 mg/l TCE, very little or none of the methane was consumed and 20%

or less of the TCE was transformed, depending upon the culture. Rate studies with *Methylomonas* MM2 suggest that TCE or some of the oxidation intermediates may exert a subtle inhibitory effect on TCE transformation by the pure culture at concentrations as low as 3–5 mg/l. Such an effect could complicate the determination of the rate constant k and the half-saturation constant K_s using Monod kinetics, and may require the inclusion of a term to describe the inhibitory effect.

Biomass concentration/mass transfer limitations--In early experiments with radiolabeled TCE, mass transfer may have limited transformation rates. To test for this, a degradation study with mixed culture MM1 was conducted at four different cell densities using radiolabeled TCE. Mixed culture MM1 was raised to a cell density of 0.41 mg/ml dry weight and diluted, achieving the following cell densities: 0.014 mg/ml, 0.078 mg/ml, 0.24 mg/ml, and 0.41 mg/ml. After dilution, cultures were transferred to bottles for degradation studies. Each bottle received 1.3 mg methane, achieving an initial aqueous concentration of 0.45 mg/l, as well as 6 μ g TCE, achieving an initial aqueous concentration of 105 μ g/l TCE. In Figure 9.5, the natural log of the percent TCE remaining is plotted against time. If no other factor were affecting TCE transformation, then the amount of TCE transformed would have increased proportionately with increasing biomass. However, at 2 hrs and again at 8 hrs, the amount of TCE transformed was not significantly different for 0.24 and 0.41 mg/ml dry weight cells. Mass transfer of oxygen, or more likely TCE, must have been inhibiting transformation rates.

In subsequent studies, care was taken to ensure that TCE transformation rates did not exceed TCE mass transfer rates. The shaker table speed was doubled to greater than 250 rpm and cultures were diluted, as described in the Methods subsection.

Mineral medium formulation--Pure culture *Methylomonas* MM2 and mixed culture MM1 were evaluated for the effects of growth in different mineral media on TCE transformation rates. Tables 9.4 and 9.5 summarize the rates of TCE transformation in the absence of methane at a TCE concentration of approximately 40 μ g/l. Each value represents the mean of two to four bottles. Whittenbury mineral medium is different from regular medium in that it lacks copper, but contains nickel, EDTA and FeNaEDTA.

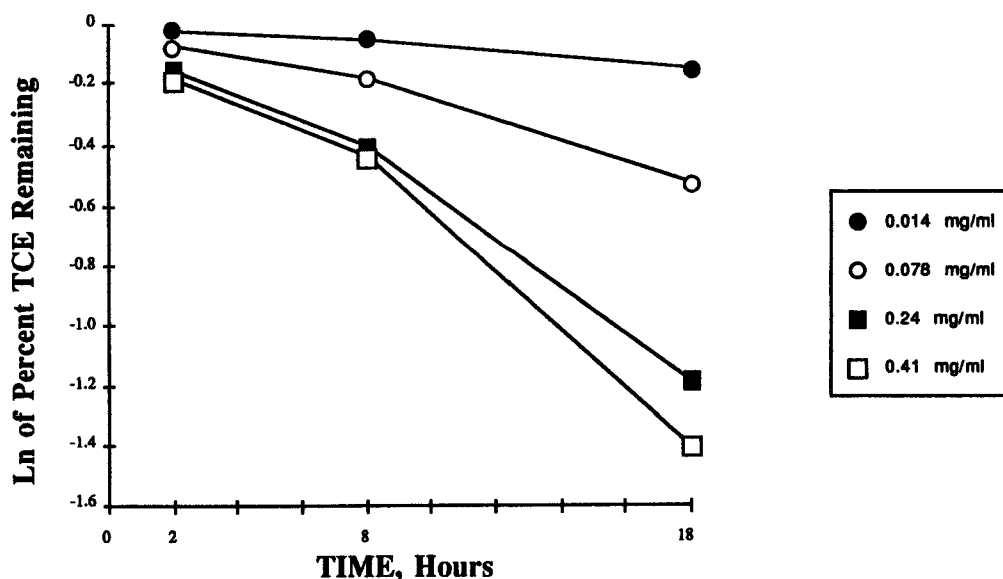


Figure 9.5. Biomass concentration/mass transfer limitation study.

TABLE 9.4 *METHYLOMONAS* MM2 TCE DEGRADATION RATES

		k/K _S (l/mg, day)
		Mean ± Standard Deviation
<u>Mineral Medium Formulation</u>		
	Regular	0.17 ± 0.03
	Whittenbury	0.50 ± 0.03
	Whittenbury + copper	0.57 ± 0.03
	Whittenbury, no EDTA or FeNaEDTA	0.01 ± 0.002
	Whittenbury, no EDTA	0.01 ± 0.002

TABLE 9.5. MIXED CULTURE MM1 TCE DEGRADATION RATES

		k/K _S (l/mg, day)
		Mean ± Standard Deviation
<u>Mineral Medium Formulation</u>		
	Regular	0.041 ± 0.003
	Whittenbury	0.61 ± 0.02

For both cultures, when EDTA was included in the growth medium, there was a significant increase in the TCE degradation rates. *Methylomonas* MM2 grown in Whittenbury mineral medium degraded TCE three times faster than when it was grown in regular mineral medium, and fifty times faster than when it was grown in Whittenbury without EDTA. Mixed culture MM1 grown in Whittenbury mineral medium degraded TCE fifteen times faster than when it was grown in regular mineral medium. The presence of copper was not responsible for the lower rates observed for the culture grown in regular mineral medium: addition of copper to the Whittenbury formulation did not decrease the rate. Neither is increased iron availability responsible for the increased rates observed when the culture is grown in the Whittenbury formulation: omitting EDTA but including FeNaEDTA in the formulation does not increase the rates.

The literature reports (summarized by Hou, 1984a) that the soluble methane monooxygenase enzyme (MMO), of the three described methanotrophs that do express a soluble MMO, has a broader specificity, and it has been proposed that the soluble MMO may have a greater affinity for TCE than the particulate MMO (R. S. Hanson, pers. comm.). The soluble MMO in these three strains is expressed under conditions of high density and copper limitation. Copper is thought to control the expression of the soluble MMO at the level of transcription (Mary Lidstrom, pers. comm.), and when copper is available, the methanotroph expresses the membrane-bound "particulate" MMO that is thought to have a lower affinity for TCE. Since addition of copper to the Whittenbury medium does not decrease the TCE transformation

rate, however, and in fact may increase it, it is unlikely that such a mechanism of control is operative in *Methylobacter* MM2. Moreover, transmission electron micrographs reveal that *Methylobacter* MM2 produces intracellular membranes regardless of growth conditions, which further indicates that the organism is not expressing a soluble form of the MMO.

TCE Transformation Intermediates--

Based on studies of the products resulting from the breakdown of TCE epoxide under aqueous conditions (Henschler et al., 1979; McKinney et al., 1955; Miller and Guengerich, 1982), carbon monoxide, formate, glyoxylate, and dichloroacetate have been proposed as the principal products resulting from the methanotrophic oxidation of TCE and the subsequent abiotic rearrangement of the epoxide (Henry and Grbić-Galić 1986, Little et al., 1988). Using ion chromatography to evaluate the nonvolatile aqueous intermediate fraction produced by his pure cultures, Little trapped radiolabeled fractions eluting from the ion chromatograph that had the same retention time as glyoxylate and dichloroacetate standards (Little et al., 1988, C. D. Little, pers. comm.).

Methylobacter MM2 does produce acids from the oxidation of TCE. Either glyoxylate or formate or both were present in the supernatant (the glyoxylate and formate peaks overlapped so it was not possible to quantify these acids), but no mono-, di-, or tri-chloroacetate were present. There were, however, three large peaks that could represent di-acids, and/or chlorinated di-acids, and/or chlorinated acids or di-acids with more than two carbons. The culture supernatant will have to be derivatized and evaluated by gas chromatography/ mass spectrometry to distinguish between formate and glyoxylate and to identify the unknown acid peaks. No volatile chlorinated products were detected.

No carbon monoxide was detected in the headspace while *Methylobacter* MM2 was oxidizing TCE. However, this does not confirm that carbon monoxide is not a transformation intermediate. *Methylobacter* MM2 oxidized carbon monoxide, and it is possible that the carbon monoxide was oxidized before the bottles were evaluated. The effect of carbon monoxide as a competitive inhibitor of TCE oxidation is being investigated.

CONCLUSIONS

These findings contribute to the emerging definition of the range of capabilities that can be anticipated in a methanotrophic treatment application, and help delineate some of the desirable characteristics of a methanotrophic community suitable for treatment applications. A suitable methanotrophic community should be able to transform TCE in the absence of methane, and should contain storage granules as a source for regenerating reducing power in the absence of substrate, such as the type II methanotrophs in mixed cultures MM1 or MM3. It should be able to tolerate variations in oxygen concentration, as well as high TCE concentrations, without significant cytotoxicity or impact on TCE transformation rates. Especially promising is the discovery that a given mineral medium formulation can increase rates by one to two orders of magnitude. The ideal methanotroph would be one capable of the rapid TCE transformation rates exhibited by pure culture *Methylobacter* MM2 and by mixed culture MM1 when grown on Whittenbury mineral medium.

SECTION 10

BATCH EXCHANGE SOIL COLUMN STUDIES OF BIOTRANSFORMATION BY METHANOTROPHIC BACTERIA

Nancy Lanzarone, Kevin Mayer, Mark Dolan, Dunja Grbić-Galić, and Perry McCarty

INTRODUCTION

Laboratory-scale columns containing aquifer material were found effective for studying the potential of aquifer and soil organisms to biotransform halogenated compounds (Wilson and Wilson, 1985; Siegrist and McCarty, 1987). However, the strong sorption of halogenated organics by aquifer material (Mackay et al., 1986) complicates the interpretation of laboratory studies (Wilson and Wilson, 1985; Siegrist and McCarty, 1987). Sorption retards the transport of pollutants in groundwater and may affect their transformation as well.

The objective of this study was to evaluate the use of laboratory-scale soil columns for estimating the important factors in the development of in-situ treatment processes. The significant questions to be answered when considering in-situ bioremediation include: 1) are native bacteria present in the aquifer that are capable of growing on an added primary substrate, 2) what is the period of time required to increase the population of such bacteria to an adequate level, and 3) following the population increase of such bacteria, are they capable of transforming the contaminants of concern? The contaminants of interest in the batch exchange soil columns were TCE, 1,2-DCA, and VC; the primary substrates (electron donors) were propane and methane. Electron acceptors included dissolved oxygen and hydrogen peroxide as a substitute for dissolved oxygen. Assuming that contaminant transformation could be achieved, it was desired to investigate the effects of the primary substrate concentration and nutrient supplements ($\text{NH}_3\text{-N}$ and $\text{PO}_4\text{-P}$) on the rate and/or extent of aerobic TCE degradation. The extent of degradation of TCE that had been sorbed to the aquifer solids also was studied.

MATERIALS AND METHODS

Column Preparation

The aquifer solids were obtained in July 1986 from the Moffett Naval Air Station, Santa Clara Valley, California, using a hollow-stem auger drilling rig. A 6" pitcher barrel that had been flamed with ethanol to reduce contamination of the cores was driven ahead of the drill bit. The material, which was recovered from a depth of 14.5-19.5 ft, consisted primarily of fine through coarse sand, gravel, and minor clay. To remove the inner core material without contamination, a 4"-diameter pipe that had been flamed with ethanol was hammered into the aquifer material inside the pitcher barrel. All tools that might come in contact with the aquifer material were either autoclaved or flamed with ethanol. The material obtained was wet sieved with an autoclaved number 10 sieve (openings < 2 mm) and stored in sterile mason jars until used.

The laboratory columns (Figure 10.1) (Siegrist and McCarty, 1987), were autoclaved prior to being filled with the aquifer material. A Bunsen burner was operated during the packing to maintain the airflow in an upward direction and thus help prevent airborne contamination. Aquifer material was added with a scoop while the columns were lightly tapped with a plastic rod to help the material settle evenly.

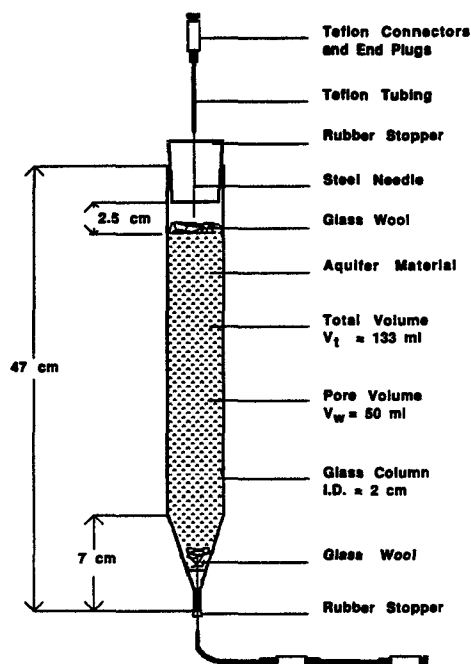


Figure 10.1. Column design.

Groundwater from the field site that had been air-stripped and autoclaved was pumped in an upflow direction at approximately 8-10 ml/min to help eliminate fines that otherwise might cause clogging. The columns were visually inspected for uniformity of packing, covered with aluminum foil to prevent the growth of photosynthetic organisms, and kept fully water-saturated and at room temperature (22°C) for the duration of the experiment.

Chemicals and Stock Solutions

The ^{14}C -trichloroethylene (^{14}TCE) used (Pathfinder Laboratories Inc., St. Louis, Mo.) had a specific activity of 4.11×10^4 dpm/ μg . Radiolabelled ^{14}C -1,2-dichloroethane ($^{14}\text{1,2-DCA}$) in methanol (Amersham Corp., Grover Heights, IL) was diluted with unlabeled reagent grade 1,2-DCA (J. T. Baker Chemical Co., Phillipsburg, N. J.), yielding a specific activity of 1.38×10^4 dpm/ μg . A nutrient stock solution was prepared in Milli-Q water with $(\text{NH}_3)_2\text{HPO}_4$ (0.170 g/l) and NH_4Cl (0.244 g/l) (J. T. Baker Chemical Co., Phillipsburg, N. J.). The vinyl chloride (VC) used (Alltech Associates Inc., Deerfield, IL) was a 1027 ppm VC in nitrogen gas 2-component NBS traceable Scott specialty gas equilibrated under pressure in Milli-Q water.

Column Operation

The column fluids were exchanged approximately once each week with 126 ml (st. dev = 2 ml; $n = 187$) of new feed solution. A syringe pump (Sage Instruments; Division of Orion Research Inc., Cambridge, Mass) with two 100-ml gas-tight syringes with adjustable plungers (Spectrum, Houston, Tx.) was used to exchange the liquid in an upflow direction at a flow rate of 5 ml/min. Dissolved oxygen breakthrough curves were similar for all of the columns (data not shown). These indicated that the first 18-20 ml of liquid removed from a column during an exchange would not be significantly contaminated by short-circuiting of influent fluid.

Three different samples, collected and analyzed during each exchange, were termed as follows: influent, initial effluent, and final effluent (Figure 10.2). The influent sample was obtained from the feed syringes before any contact with the column occurred. The initial effluent sample represented the first 18

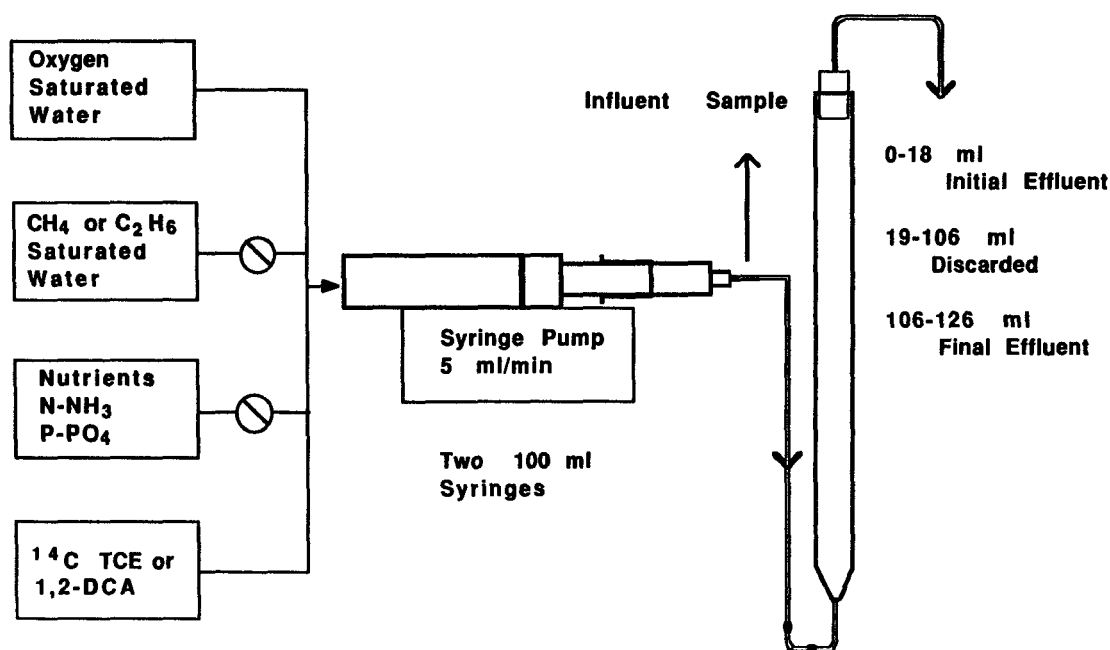


Figure 10.2. Experimental design for sample mixing and column feeding.

ml of liquid removed from the column during an exchange. The initial effluent was assumed to represent the composition of the pore fluid within the column just prior to an exchange, and was compared with the influent from the previous exchange to determine oxygen demand, primary substrate consumption, TCE, 1,2-DCA, or VC degradation, and mass balances. The final effluent sample represented the last 18-20 ml removed from the column during an exchange.

Feed Solution Preparation

Groundwater from the field site that had been air-stripped was used to exchange the columns and was stored in the dark at room temperature (22°C) until used. Prior to exchange, the water was filter-sterilized using 0.2- μ m sterile cellulose nitrate filters (Micro Filtration Systems, Dublin, Ca.) and placed in autoclaved glass bottles that were connected to gas cylinders. The volume of the bottle attached to an oxygen cylinder was 4.0 l, that to a methane cylinder was 2.0 l, and that to a propane cylinder was 1.0 l. Some of the filtered water also was placed in an autoclaved 2-l glass jar. The appropriate gas was bubbled through each bottle of water using a gas diffuser for one hour prior to exchange.

An appropriate amount of methanated or propanated water and 2 ml of nutrient supplement solution were drawn into one 100-ml syringe and mixed back and forth through Teflon tubing to another 100-ml syringe. If a column received a low concentration of methane (1.5 mg/l) rather than a high concentration (4.5 mg/l), water from the 2-l glass jar was added for dilution to give the same total volume (50 ml).

The 50-ml solution was then divided evenly between the two syringes, and both were filled to 100 ml with oxygenated water. The syringe fluids were mixed again through connecting tubing to create a single uniform feed. Influent samples for dissolved gas analyses were taken with a 20-ml glass syringe attached to the connecting tubing, and analyzed immediately. The syringes then were separated and emptied to 75 ml, and either 0.5 ml of the 14 C TCE stock solution, 0.10 ml of the 14 C 1,2-DCA stock solution, or 5 ml of the VC stock solution was added. The syringes were reconnected, and the solutions mixed.

Next the syringes were reconnected with Teflon tubing and placed on the syringe pump. After the influent samples for gas chromatographic analysis and scintillation counting were taken with a 20-ml glass syringe, the 100-ml syringes were attached to the column, and the column fluid was exchanged in an upflow direction at a flow rate of 5 ml/min.

Microcosm Batch Experiments

A set of microcosm batch experiments was designed to supplement the aquifer column studies of trichloroethylene degradation by a mixed culture of methanotrophic bacteria. The 35-ml microcosms were sacrificed at various time intervals to measure the growth rate and to examine the relationship between the growth stage of the methanotrophic community and the degradation of TCE.

Initial experiments were conducted using sets of 35-ml vials inoculated with 1.5 g of well-mixed aquifer solids (sand) from columns that had been operated as draw-and-fill sequential batch reactors. In the second of the two initial experiments, additional inoculum was added in the form of 2 ml of effluent that had been collected while operating the draw-and-fill aquifer material columns. A mineral solution containing 4.5 mg/l of dissolved methane, 24 mg/l of dissolved oxygen and 50 µg/l of TCE was added to each vial. An equal number of vials were established as controls by omitting the dissolved methane from the solution. The microcosms were sealed to exclude any headspace, then placed in a rotary shaker in the dark at room temperature (22°C). Triplicate microcosms were sacrificed at various time intervals, as often as every 4 hours during periods of rapid growth.

Each vial was analyzed for methane, dissolved oxygen, and ¹⁴C-labeled TCE and CO₂ activity. Acridine orange direct counts (Ghiorse and Balkwill, 1983) and total protein determination (Kennedy and Fewson, 1968) were used to estimate microbial population.

Analytical Methods

Dissolved Oxygen--

Dissolved oxygen (DO) concentrations were measured with a Model 54A oxygen meter (Yellow Springs Instruments, Yellow Springs, OH) that had been calibrated in air-saturated water. The coefficient of variation for DO less than 20 mg/l was 4% (n = 8), and for higher DO was 1.3% (n = 10).

Dissolved Methane and Propane Analyses--

Dissolved methane and propane concentrations were determined by headspace analysis. Bottles of known volume (approximately 13 ml) and weight were sealed with rubber stoppers, and 10 ml of air was withdrawn twice with a 10-ml glass syringe to create a vacuum. From the 20-ml sample syringe, 5 ml of sample was placed in an evacuated bottle. The bottles were shaken vigorously by hand for 30 sec, equilibrated with air to atmospheric pressure using a syringe, and 0.5 ml of the gas phase was removed with a 1-ml gas-tight syringe for analysis on a Hewlett Packard 5730A gas chromatograph (Hewlett Packard, Avondale, Pa.) equipped with an FID detector and a 60/80 Carbosieve column (5 ft×1/8"; Supelco Inc., Bellefonte, Pa.). Quantification was achieved by injecting 0.5 ml of calibration gas (1000 ppm) of either methane or propane (Alltech Associates, Deerfield, IL) and comparing the relative area with a Spectra-Physics 4020 calculating integrator (Spectra-Physics, Sunnyvale, Ca.). The coefficient of variation for methane based on three sets of data was 9%.

TCE, 1,2-DCA, and VC Analyses--

Concentrations were determined by gas chromatography. Samples collected in 20-ml syringes were transferred immediately to 14-ml bottles, sealed without headspace with Teflon-faced septa and aluminum crimp tops, and extracted with 1 ml of degassed iso-octane (after Henderson et al., 1976) using bromochloropropane as an internal standard. A 5 µl sample of the extract was injected into a packed column (10% squalene on Chromosorb W/AW, at 60°C) on a GC equipped with a linearized Ni-63 electron capture detector. Quantification was achieved by injecting 10, 50, and 100 µg/l standards that had been treated like samples and comparing the relative areas with a Spectra-Physics 4020 calculating integrator. The influent was analyzed for each exchange, but the initial effluent was analyzed only periodically. The analytical coefficients of variation for TCE and 1,2-DCA were ± 5% and ± 6%, respectively.

Vinyl chloride concentrations were determined by headspace analysis using gas chromatography. Approximately 5 ml of the collected samples were transferred immediately into 15-ml glass vials and sealed with Teflon-faced septa and screw top closures. The vials were inverted, placed on a shaker table, and allowed to equilibrate for 30 min. A 300- μ l sample of the headspace gas was injected into a capillary column (J&W fused silica megabore DB 624) on a Finnigan 9610 GC fitted with a Hall electrolytic conductivity detector. Quantification was achieved using standard curves created by injecting NBS traceable vinyl chloride in nitrogen gas standards with peak areas integrated using the Nelson Analytical 3000 Series chromatography data system. The influent, initial effluent, and final effluent were analyzed for each exchange.

Radioactivity Analyses--

Carbon-14 activity was assayed using a Tricarb Model 4530 scintillation spectrometer (Packard Instrument Co., Downers Grove, IL) which made counting efficiency corrections with the external standard channels ratio method (Harrocks, 1974). For each sample, three separate aliquots were counted. A 1.0-ml sample was injected into a glass counting vial containing 3 drops of 1N HCl, another 1.0 ml into a vial containing 6 drops 1N NaOH, and a third 1.0 ml into a vial containing 10 ml of liquid scintillation cocktail (Instagel; Packard Instrument Co., Downers Grove, IL). The first two vials were stripped with nitrogen gas (100 ml/min for 15 min), and then 10 ml of liquid scintillation cocktail was added. This procedure allowed making a presumptive test for the production of $^{14}\text{CO}_2$, which would not be stripped at high pH but would be at low pH. The volatile ^{14}C -activity, which was air-stripped at any pH, was assumed to represent nontransformed TCE or 1,2-DCA, or VC.

Hydrogen Peroxide Determination--

The presence of hydrogen peroxide, in the experiments where hydrogen peroxide was used as an alternate source of dissolved oxygen, was detected by peroxide test strips (EM Science). The concentration of hydrogen peroxide was measured by diluting 10-ml samples with deionized water, adding 5 ml of 10% sulfuric acid, and three drops of ferroin indicator, and titrating the solution with 0.1N ceric sulfate to a blue endpoint. Two moles of cerium are reduced in an acidic solution by each mole of hydrogen peroxide present. A series of standard solutions and deionized water blanks were analyzed along with the samples.

Evaluation of Transformation and Degradation--

The term biotransformation generally represents a change in the chemical structure of a compound, while degradation represents the combination of mineralization to inorganic end products and conversion to cellular products. In this study, no volatile transformation products were found. Moreover, since GC analyses for TCE and 1,2-DCA corresponded closely with the concentration of ^{14}C measured volatile compounds, no measurable quantities of volatile transformation products were formed. Thus, the measured transformation products were in the form of either nonvolatile organics or CO_2 .

Measurement of compound degradation presented some difficulties. The ^{14}TCE was contaminated such that about 8% of the activity was nonvolatile organics or CO_2 , with about 90% being the former. The uncharacterized nonvolatile fraction was completely biodegradable and could be transformed to $^{14}\text{CO}_2$ while in the column. To reduce errors in interpretation, degradation is defined here to be the change in the ^{14}C activity of the nonvolatile plus CO_2 fractions between the initial effluent from the current exchange and the influent from the previous exchange ($\text{NaOH sample activity}_{\text{initial effluent}} - \text{NaOH sample activity}_{\text{influent}}$). Degradation thus represents the change in the nonvolatile plus CO_2 fractions rather than just the production of CO_2 . This procedure may underestimate the extent of mineralization that may have actually occurred since the TCE that was incorporated into biomass could not be determined for the columns, because it would have required their destruction.

RESULTS

Initial Column Studies on TCE, 1,2-DCA, and VC Decomposition

Approach--

Seven columns were initially operated as described in Table 10.1, and the subsequent modifications that were made are described below. The columns were exchanged 6 times before TCE was added, and 7 times before 1,2-DCA was added. Day 0 on all graphs represents the first day that the chlorinated compound was added.

TABLE 10.1. THE ORIGINAL EXPERIMENTAL DESIGN

Column Number	Original Operating Conditions ^a
1	Dissolved oxygen and TCE (Control)
2	Dissolved oxygen, dissolved propane, nutrient supplements, and TCE.
3	Dissolved oxygen, 4.5 mg/l dissolved methane, nutrient supplements, and TCE
4	Same as 3
5	Dissolved oxygen, 4.5 mg/l dissolved methane, and TCE
6	Dissolved oxygen, 1.5 mg/l dissolved methane, nutrient supplements, and TCE
7	Dissolved oxygen, 1.5 mg/l dissolved methane, nutrient supplements, and 1,2-DCA

^aInfluent concentrations were: DO - 25 to 35 mg/l; TCE - 25 µg/l; 1,2-DCA - 80 µg/l.

Electron Donor and Acceptor Utilization--

Dissolved oxygen (DO) was consumed in the control column (Figure 10.3) and in all of the columns fed methane and propane (data not shown). The oxygen demand was greater than expected from the stoichiometry for complete oxidation of methane and propane, and averaged 17 mg/l (st. dev. = 7 mg/l). It may have been associated with reduced aquifer solid components, but the actual source was not found.

An active methane-utilizing population was present within the aquifer solids, as evidenced by the decrease in the initial effluent methane concentration within 7 days (data not shown). This corresponded closely with the two-week period required for methane utilization to begin in the field studies (Figure 6.2). Propane did not stimulate the growth of an active biomass capable of its own oxidation, even after several months of operation (data not shown). Thus, a propane-utilizing population did not appear to be present in the aquifer material. No TCE degradation occurred in this column.

The Effect of Methane on TCE Degradation--

Two methane concentrations were evaluated: 4.5 mg/l (high) and 1.5 mg/l (low). A pulsing strategy also was investigated in which one column was fed an alternating pulse of methane and oxygen one week followed by oxygen alone in the next. Profiles of influent and effluent methane concentrations before and after pulsing are illustrated in Figure 10.4.

The influent TCE concentration for all columns was approximately 25 µg/l. Negative values sometimes calculated for TCE degradation probably reflect errors due to the initial sorption of the ¹⁴C-labeled nonvolatile fraction prior to the initiation of its biodegradation, or analytical errors as indicated by the slight fluctuation around zero for the control column (Figure 10.5). Degradation is believed not to have occurred in the control column and certainly was so small as to be insignificant.

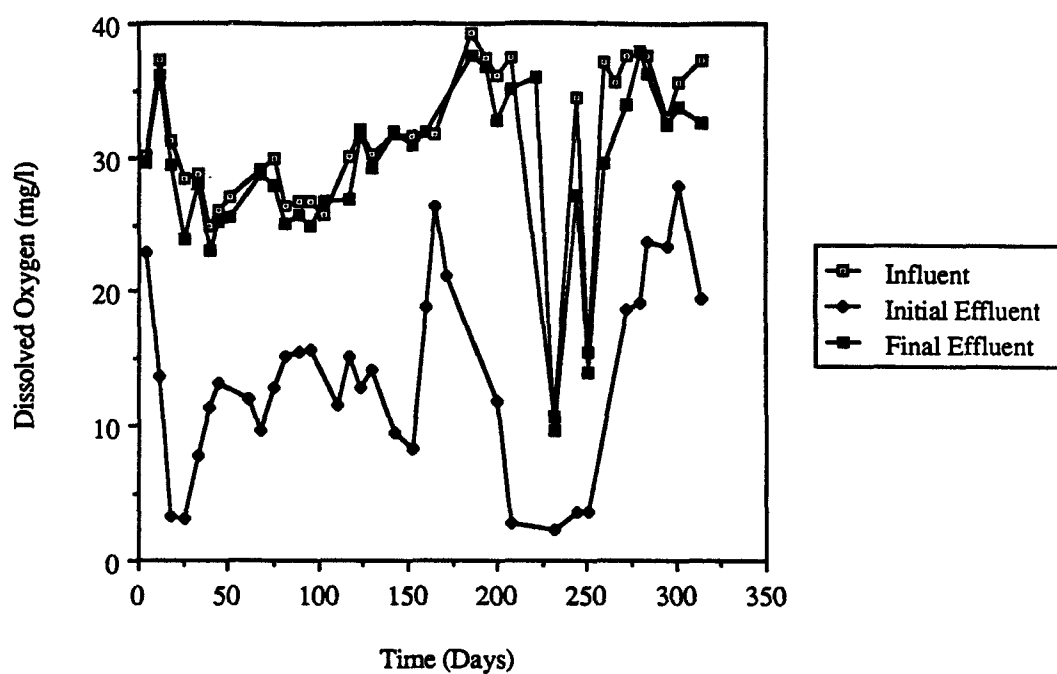


Figure 10.3. Dissolved oxygen concentration versus time for the control column (oxygen and TCE).

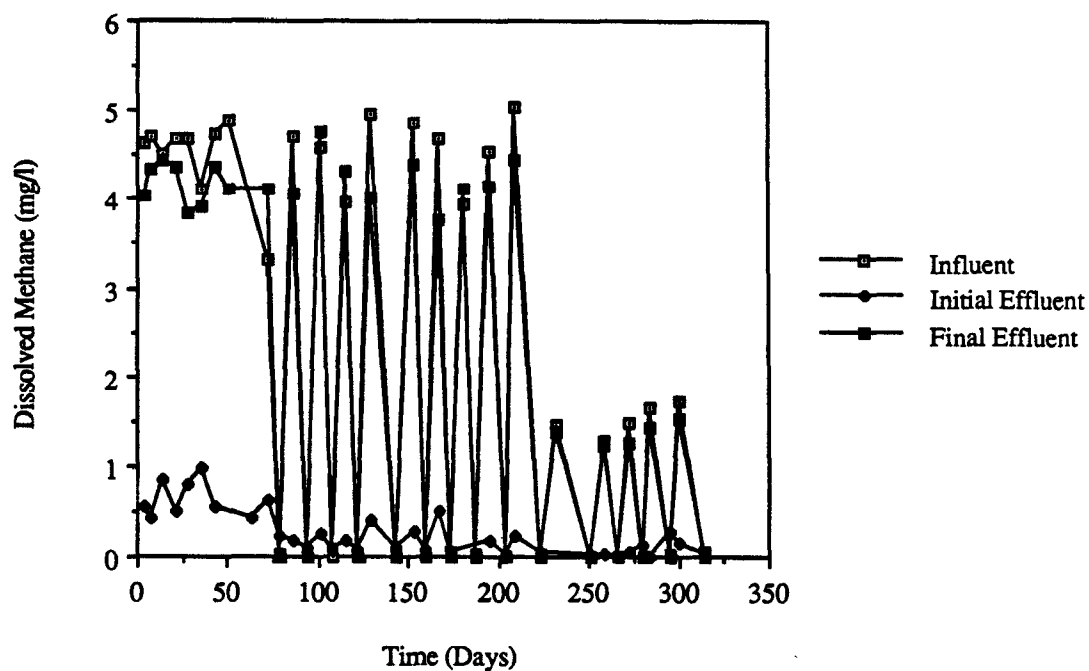


Figure 10.4. Methane concentration versus time for column 4.

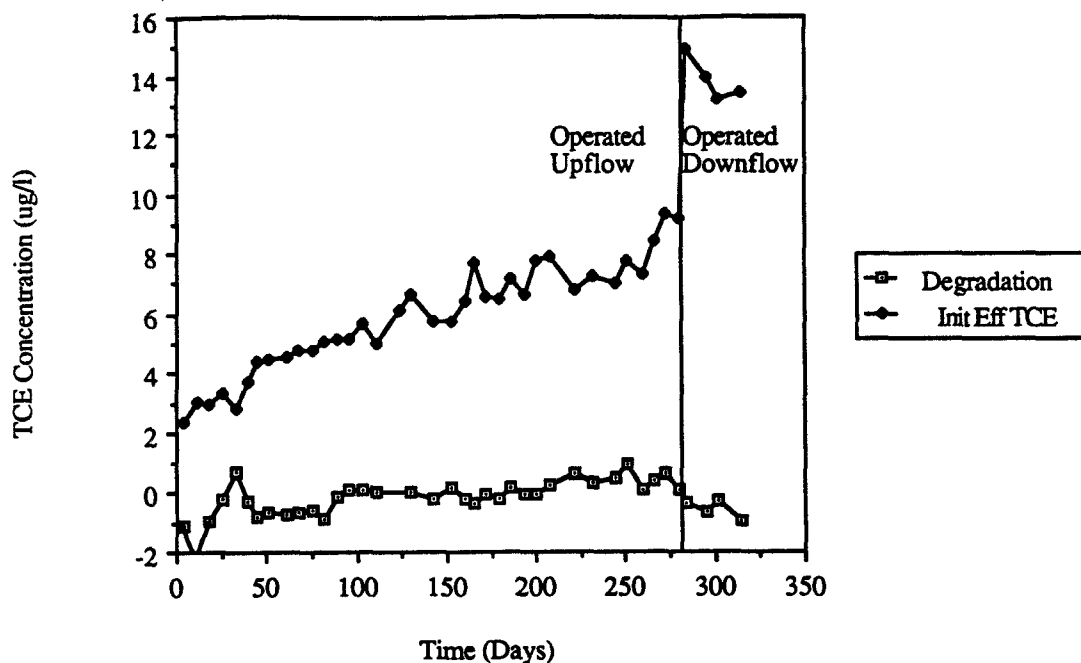


Figure 10.5. TCE degradation and concentration in the initial effluent from the control column (oxygen and TCE).

Column 6, with 1.5 mg/l methane and nutrients, was the first to show TCE degradation, which became measurable after about 80 days (Figure 10.6). The extent of TCE degradation there shown, as well as the pore water TCE concentration based upon the volatile ^{14}C activity (Figure 10.7), rose throughout the experiment.

Little or no TCE degradation occurred in columns 3 and 5 when operated initially with 4.5 mg/l methane. Subsequently, when the methane was reduced to 1.5 mg/l, degradation began in both columns (Figures 10.8 and 10.9).

The high methane feed to column 4 was pulsed after 79 days, and TCE degradation began (Figure 10.10). When the pulsed methane concentration was 4.5 mg/l, the extent of degradation clearly was related to the pulsing, and more degradation occurred during the weeks in which no methane was fed to the column. Later, when the methane concentration was reduced to 1.5 mg/l and pulsed, the difference in the extent of TCE degradation between one week and the next was less evident. Furthermore, the extent of degradation here was the highest achieved (about 4 $\mu\text{g/l}$).

The Effect of Nutrient Supplements on TCE Degradation--

Columns 3 and 5 were operated identically throughout the entire experiment, except that nutrients were added only to the former column (Figures 10.8 and 10.9). A permutation test (Bowker and Lieberman, 1972) indicated that the TCE degradation was statistically higher in column 3 than in column 5 (99%, one-tailed test). However, this test was insufficient to prove that the nutrient addition was responsible. It is possible that other factors, such as differences in the nature of the aquifer materials or microbial cultures in the columns, was the cause.

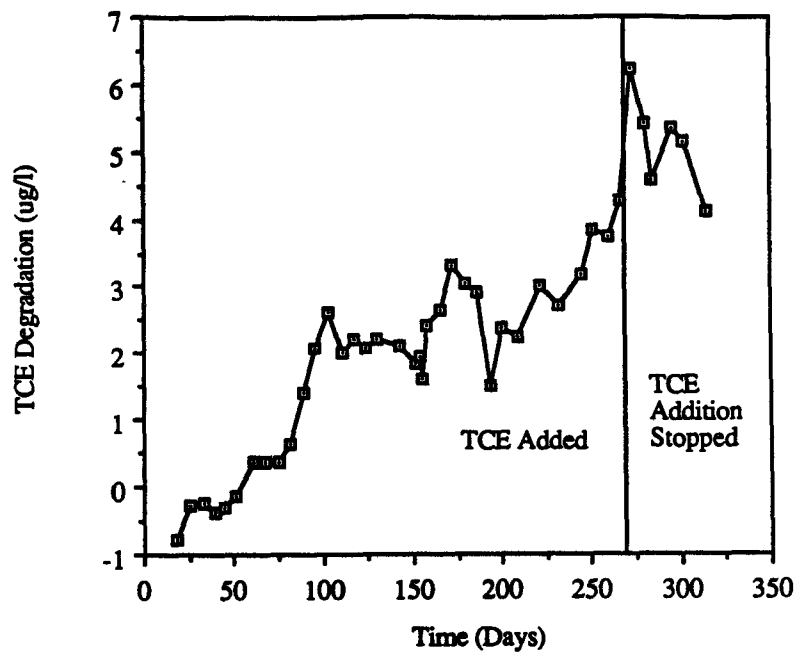


Figure 10.6. TCE degradation in column 6 (low methane plus nutrients).

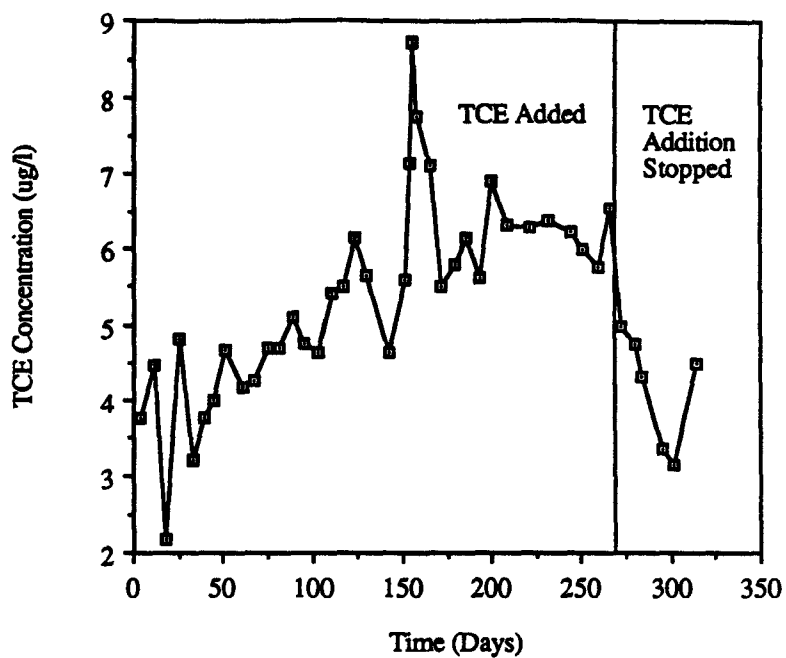


Figure 10.7. TCE concentration in the initial effluent from column 6 (low methane plus nutrients).

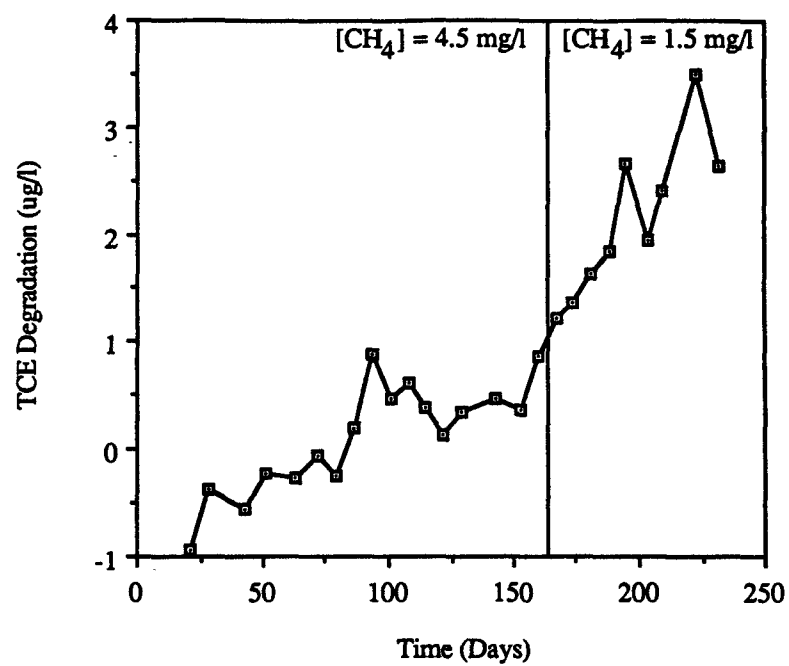


Figure 10.8. TCE degradation in column 3 (high/low methane plus nutrients).

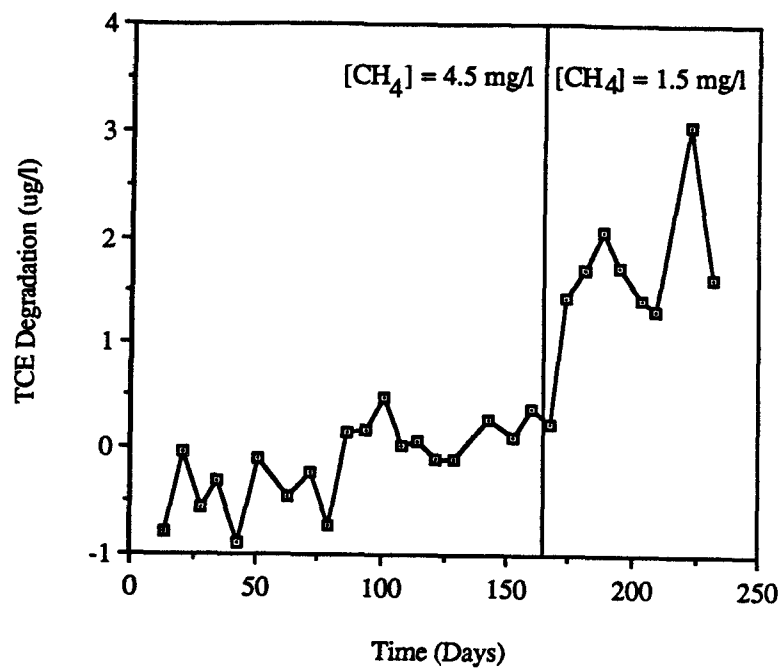


Figure 10.9. TCE degradation in column 5 (high/low methane no nutrients).

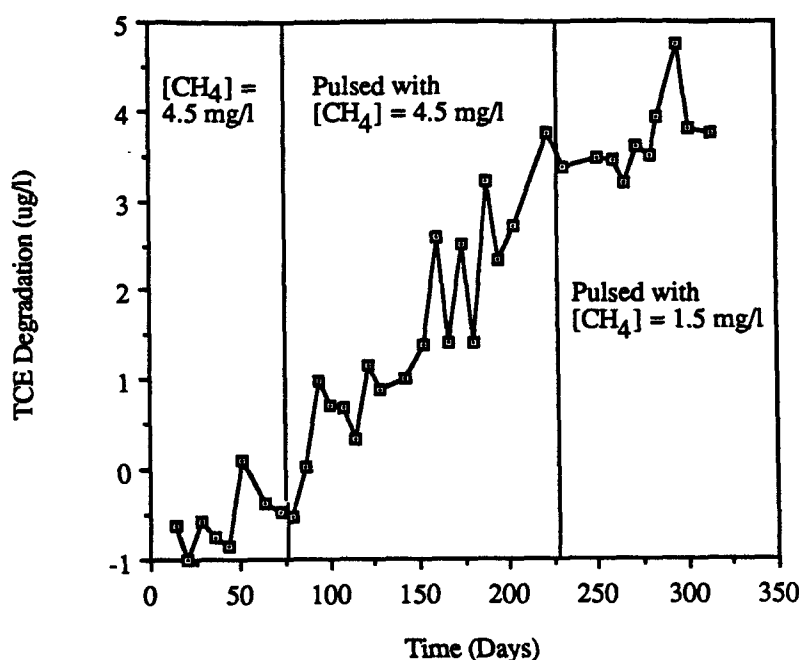


Figure 10.10. TCE degradation in column 4 (pulse high/low methane plus nutrients).

Time Studies--

Experiments were conducted with column 6 to determine the approximate rates of oxygen consumption, methane utilization, and TCE degradation. One-, two-, and three-day exchange intervals were used. Utilization of DO, methane, and TCE appeared complete within the first one to two days after an exchange and was similar to that at the end of a seven-day exchange period. It would appear from these results that when methane was completely consumed, TCE utilization terminated. However, in the pulsing studies, TCE degradation occurred following an exchange with only dissolved oxygen in the feed solution. Other factors which are not yet understood appear to be involved.

1,2-DCA Degradation--

The 1,2-DCA degradation (Figure 10.11) began sooner than TCE degradation, and the extent of degradation was higher. However, the influent 1,2-DCA concentration (80 $\mu\text{g/l}$) was also significantly higher than that of TCE (25 $\mu\text{g/l}$). The percentage degradations based upon the influent concentration for TCE and 1,2-DCA are shown in Figure 10.12.

VC Degradation--

After completion of the 1,2-DCA and TCE experiments, columns 5 and 7 were used to study VC degradation. Weekly feeding of the columns with methane (1.5 mg/l) and oxygen continued while VC was introduced at influent concentrations of approximately 125 $\mu\text{g/l}$. An additional column, prepared similar to the other columns, was employed as a control column by feeding it only oxygen and vinyl chloride.

In columns 5 and 7 only trace levels of VC (< 5 $\mu\text{g/l}$) remained after the one-week exchange period, while approximately 25 $\mu\text{g/l}$ VC remained in the control column (Figure 10.13). The presence of VC in the initial effluent of the control column and its absence from the initial effluents in columns 5 and 7 indicate biodegradation of the VC by the enriched methanotrophic cultures.

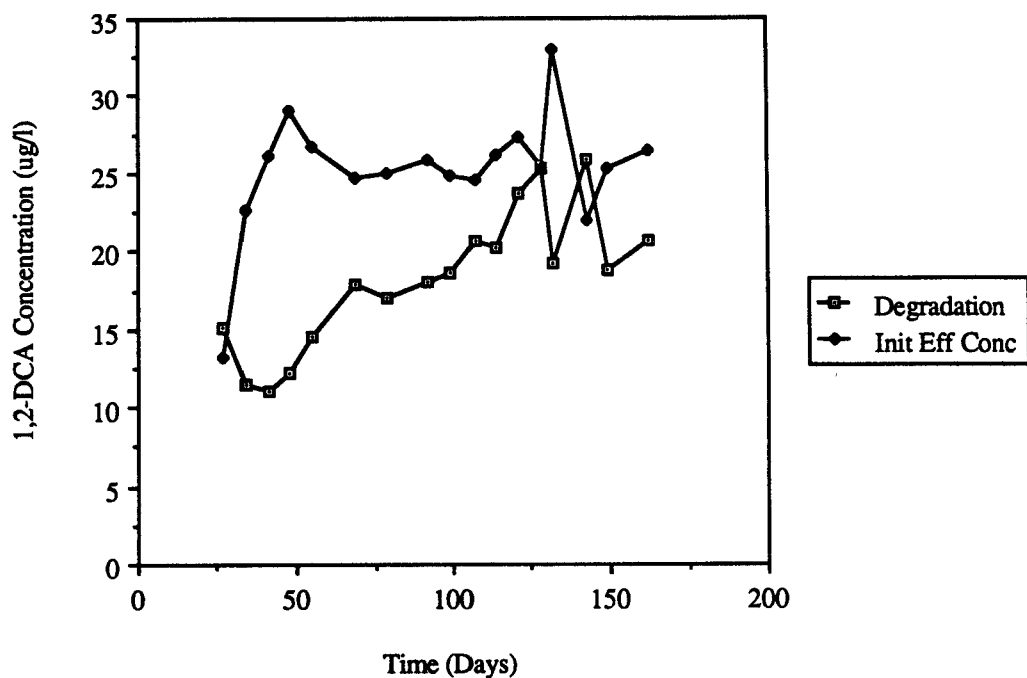


Figure 10.11. The 1,2-DCA degradation and concentration in the initial effluent from column 7 (1,2-DCA: low methane plus nutrients).

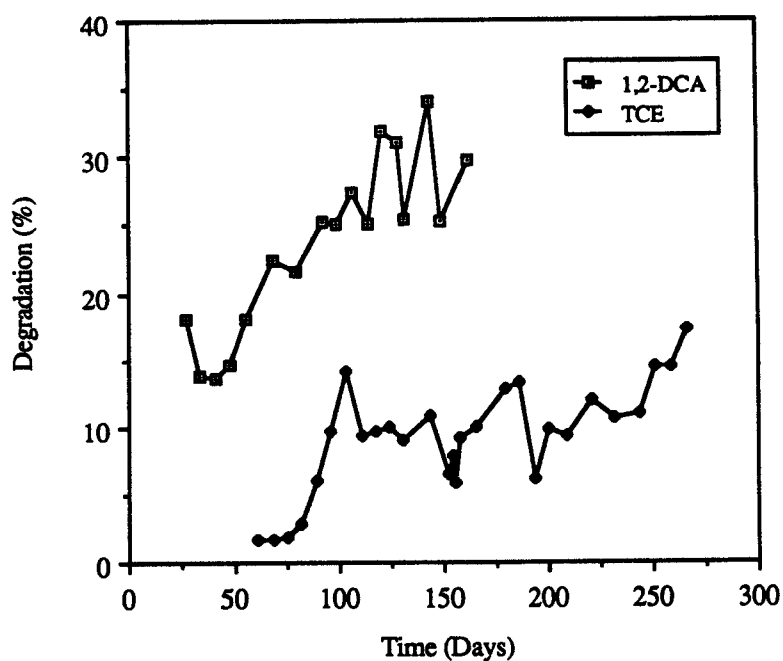


Figure 10.12. Percent degradation for TCE and 1,2-DCA in columns 6 and 7, respectively (low methane plus nutrients for both TCE and 1,2-DCA).

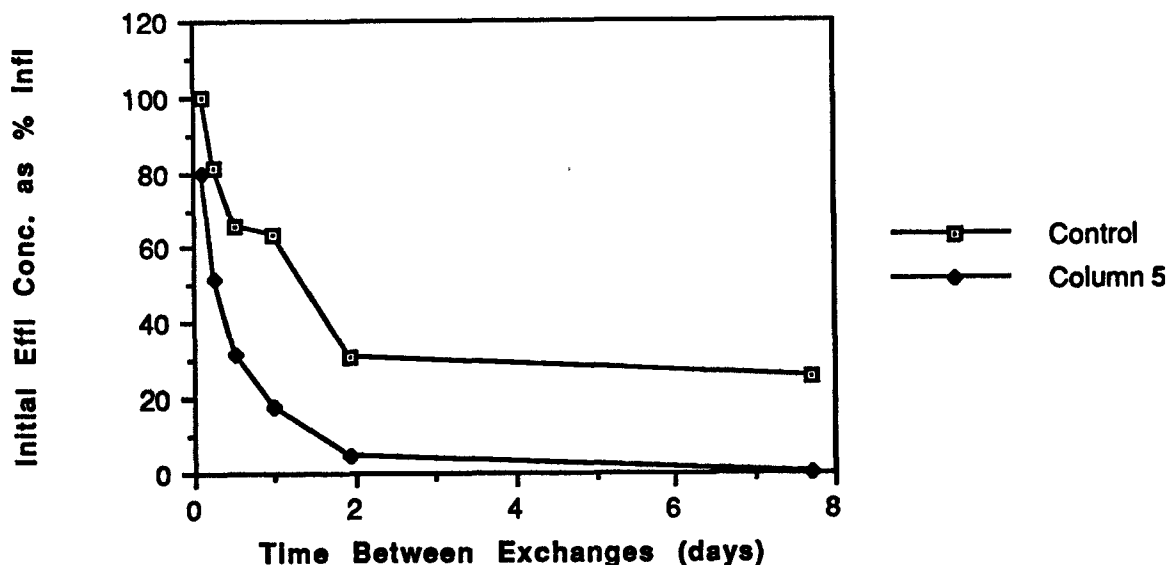


Figure 10.13. Vinyl chloride removal efficiency in biostimulated column versus control column.

The time between exchanges was varied from 3 hrs to 1 week to determine the minimum time necessary for complete VC removal from columns 5 and 7. VC was removed at about one-half the rate of methane utilization. The methane in columns 5 and 7 was utilized within 1 day of feeding, while VC was found to remain for approximately 2 days (Figure 10.14). The presence of methane did not seem to inhibit VC transformation, as most of the VC was removed in the first day when methane concentrations were highest.

Mass Balances of TCE and 1,2-DCA--

The pore water concentrations of TCE and 1,2-DCA (Figures 10.7 and 10.12) always were lower than the influent concentrations. Conversion to CO_2 accounts for some of the net loss of TCE and 1,2-DCA from the pore water, but other processes, such as sorption and incorporation into biomass, probably were involved as well.

An approximate ^{14}C mass balance for TCE and 1,2-DCA was made by dividing the total ^{14}C activity in the initial effluent by the total ^{14}C in the influent. Even after nearly one year of operation with TCE, less than 50% of the influent ^{14}C was present in the initial effluent. A better mass balance was achieved with 1,2-DCA (70%). It is apparent from this and other studies that 1,2-DCA did not sorb as strongly to the aquifer solids as the TCE. In order to make better quantitative mass balances, the extents of sorption to the solids and incorporation into the biomass need to be evaluated.

Degradation of TCE That Had Been Sorbed--

The degradation of TCE that had been previously sorbed to the aquifer material was investigated in column 6 by discontinuing the addition of TCE, but continuing the exchange of the column fluid. Here, ^{14}C activity detected in either the initial or the final effluent sample resulted from ^{14}C -labeled TCE or intermediate products that had desorbed from the solids or from biological solids decomposition. The results, assuming that all of the ^{14}C -nonvolatile compounds and $^{14}\text{CO}_2$ in the initial effluent resulted from TCE degradation between exchanges, are shown in Figure 10.6.

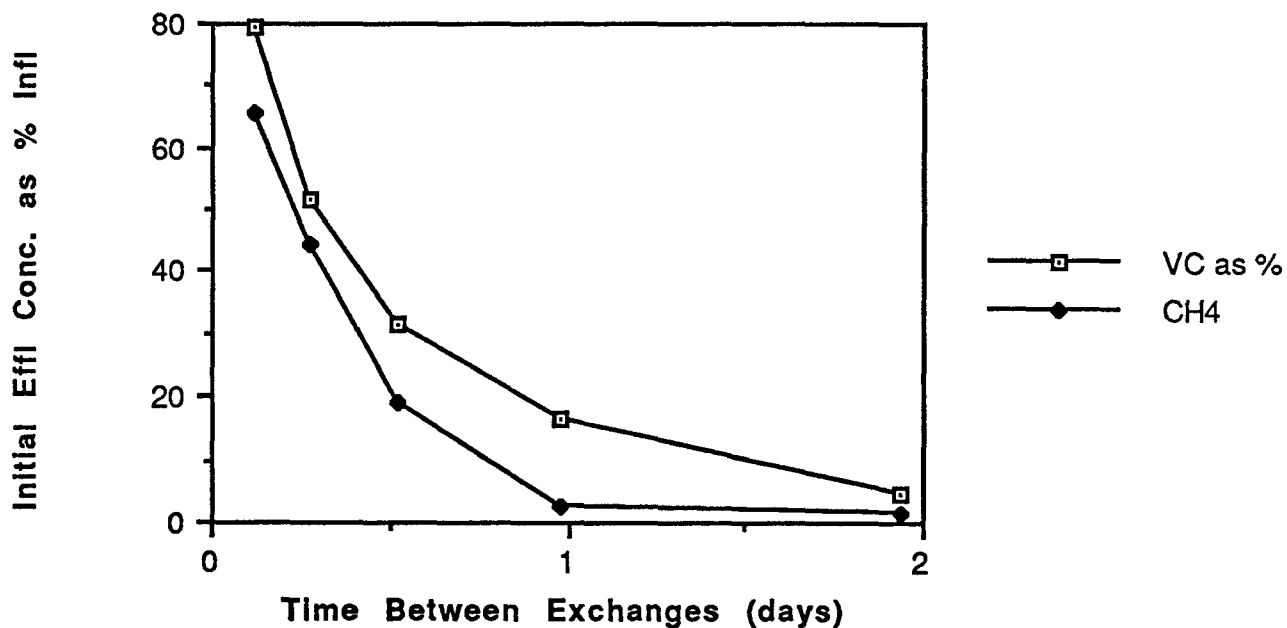


Figure 10.14. Methane utilization versus VC removal in a methanotroph enriched column.

About 55% of the initial effluent ^{14}C was in the form of nonvolatile compounds plus CO_2 and the remainder was TCE (Table 10.2). Interestingly, the initial effluent concentration of the ^{14}C nonvolatile plus CO_2 fractions was about the same after the ^{14}C addition was stopped as when it was added, but the TCE concentration was lower (Figure 10.7).TCE

TABLE 10.2. THE DISTRIBUTION OF ^{14}C IN THE INITIAL EFFLUENT REMOVED FROM COLUMN 6 AFTER ^{14}TCE ADDITION TO THE INFLUENT WAS STOPPED^a

Number of Exchange Without TCE Addition	CO_2 ($\mu\text{g/l}$)	Nonvolatile Products ($\mu\text{g/l}$)	CO_2 + Nonvolatile Products ($\mu\text{g/l}$)	TCE ($\mu\text{g/l}$)	Total Removed as CO_2 + Nonvolatile Products + TCE ($\mu\text{g/l}$)
1	5.52	0.708	6.22	4.98	11.2
2	5.01	0.430	5.44	4.76	10.2
3	4.05	0.557	4.61	4.3	8.90
4	4.76	0.607	5.37	3.36	8.72
5	4.63	0.531	5.16	3.14	8.30
6	3.69	0.430	4.12	4.48	8.60
Average	4.61	0.544	5.15	4.17	9.32

^aThe results are expressed as $\mu\text{g/l-TCE}$.

Distribution in the Columns--

The lower portion of the columns, which was nearer the influent port, was exposed to a higher TCE concentration during the column fluid exchange than the upper portion because some sorption occurred during the exchange. To illustrate this, the control column was operated for the last four exchanges in a downflow direction. The TCE concentration in the pore water near the lower port, as measured by the first 18 ml of effluent was significantly higher (Figure 10.5), but the other parameters, such as dissolved oxygen, did not change appreciably. This uneven TCE distribution perhaps affected to some degree the mass balances and the measured extent of degradation. This is a difficult problem to overcome in column studies of this type.

Additional Column Studies on TCE Degradation and Peroxide Addition

Approach--

Six glass columns were packed with completely mixed aquifer material for this study. Each of the columns received 50 µg/l of ¹⁴C-labeled TCE. Four of the columns were fed dissolved methane and a source of oxygen. Two of these columns were operated with filtered groundwater containing 5 mg/l dissolved methane and 22 mg/l dissolved oxygen - sufficient to maintain aerobic conditions following oxidation of all the methane. An additional two columns received hydrogen peroxide as a source of dissolved oxygen to permit a higher concentration of dissolved methane in the feed solution. The concentration of this mixture was set at 10 mg/l methane and 85 mg/l peroxide (equivalent to 40 mg/l dissolved oxygen). A gas phase formed in the columns when a greater concentration of hydrogen peroxide was added. One of the control columns received a solution of dissolved oxygen and TCE but no methane. The other control column was established as a control for the methane/peroxide treatment by omitting the methane from the influent solution. The feed conditions are summarized in Table 10.3.

The laboratory columns were operated as sequential batch reactors, as previously discussed. To test the effect of the feeding schedule on the bacteria population and TCE degradation, exchanges were performed at intervals of 3 days, one week, or two weeks.

Breakthrough curves using bromide, dissolved oxygen and dissolved methane as tracers showed that the first 25 ml of effluent were unmixed with the fresh influent solution and could be considered a representative effluent sample. The effluent sample was analyzed for methane concentration (gas chromatography), dissolved oxygen (dissolved oxygen probe), number of bacteria [acridine orange direct count (Ghiorse and Balkwill, 1983)], TCE and other ¹⁴C-labeled compounds (scintillation counting and gas chromatography).

TABLE 10.3. FEED CONDITIONS FOR PEROXIDE STUDY

Column Number	Concentration in Batch Feed (mg/l)			
	CH ₄	O ₂	H ₂ O ₂	TCE
P1	5	22	—	0.05
P2	5	22	—	0.05
P3	10	—	85	0.05
P4	10	—	85	0.05
P5	—	22	—	0.05
P6	—	—	85	0.05

Methane and Dissolved Oxygen Utilization--

The presence of methanotrophs in the aquifer material was demonstrated within several weeks of the commencement of methane and dissolved oxygen treatment. Operating with a 3-day residence time, the methane concentration decreased after each exchange. After the third 3-day treatment period, the methane concentration had fallen by two orders of magnitude, from 5 mg/l to 0.05 mg/l. Complete methane consumption (below the 0.01 mg/l detection limit) occurred within three days for all subsequent conditions, except for the experiments using hydrogen peroxide as the oxygen source.

Dissolved oxygen concentration declined in stoichiometric ratios with the methane utilization. The minimum dissolved oxygen concentration approached the sensitivity limit of the measurement system, but remained in the 0.5 to 1 mg/l range. The control column, with no methane added, exhibited an oxygen demand as well. When the time between pore solution exchanges was lengthened to two weeks, dissolved oxygen dropped from 30 mg/l to 20 mg/l, which was still above the concentration at equilibrium with the atmosphere (approximately 8 mg/l) (Figure 10.15).

The addition of hydrogen peroxide as the source of oxygen partially inhibited methane utilization. At least 40 mg/l of hydrogen peroxide reached the effluent port of the columns during each solution exchange, exposing all portions of the system to this strong oxidant. Although the peroxide had completely degraded to oxygen within several hours, the high level of oxidant may have disrupted the activity of the methanotrophic bacteria. More than 1 mg/l of methane remained after the treatment period. Since the dissolved oxygen concentration had dropped to between 1 and 2 mg/l and no measurable peroxide remained, it was thought that the non-methanotrophs could be out-competing the methanotrophs for oxygen (Figure 10.15). Decreasing the methane concentration in the influent from 10 mg/l to 7 mg/l should have had the effect of increasing the oxygen available to the methanotrophs, but the residual methane remained in the 1 to 2 mg/l range. It seems likely that competition for oxygen with heterotrophic bacteria may be combined with some toxic effect of hydrogen peroxide to limit methanotrophic activity.

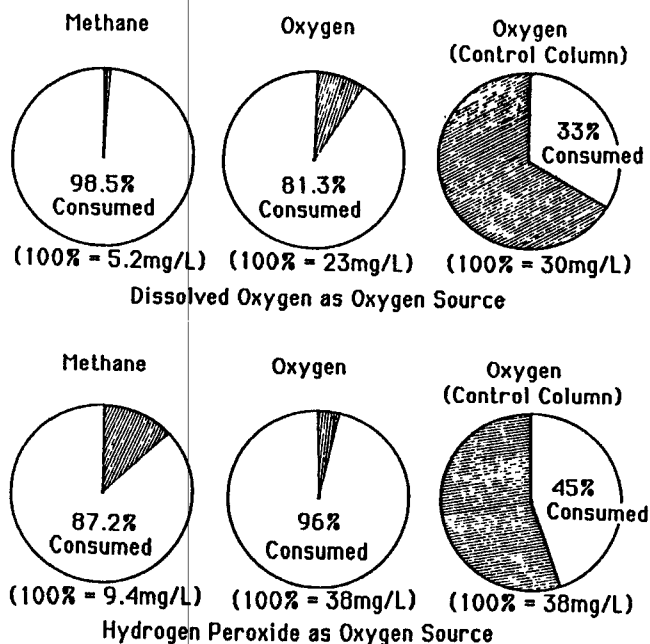


Figure 10.15. Effect of hydrogen peroxide on methane and oxygen consumption in batch exchange soil columns.

TCE Transformation--

After three months of operating the methane/dissolved oxygen columns, unequivocal evidence of TCE transformation was established. The added TCE was strongly sorbed to the aquifer solids so that only half of the labeled TCE could be recovered in the effluent after the treatment period. From the first exchange period, ^{14}C -labeled CO_2 was detected in the effluent of both the methane-fed columns and the control columns. However, only in the methane-fed columns did the activity of the labeled CO_2 in the effluent surpass the activity added in the form of the non-volatile contaminant in the TCE solution (Figure 10.16). After nearly one year of operation at two-week exchange intervals, the methanotrophic bacteria transformed 15 to 20% of the ^{14}C -labeled TCE to ^{14}C -labeled CO_2 , while there was no evidence of TCE transformation in the control column. Labeled carbon that had been incorporated into biomass could conceivably double the measured transformation, but confirmation of the rate of incorporation awaits destructive sampling of the columns.

No transformation products other than CO_2 could be detected. The only ^{14}C -labeled components in the effluent were TCE, CO_2 species and a negligibly small amount of non-volatile compounds.

The columns using hydrogen peroxide, rather than oxygenated water, as a source of oxygen received ^{14}C -TCE for over three months. Degradation of TCE remained less than 5% under these conditions, so the addition of hydrogen peroxide was discontinued.

Reaction Time--

By decreasing the time between exchanges, more primary substrate (methane) is made available to the methanotrophs and theoretically a greater population could be maintained. The three-day reaction period was sufficient for complete methane utilization, but ^{14}C -labeled CO_2 production remained at 15 to 20%. For each of the reaction periods tested, the experiments were continued for at least twelve exchanges to allow sufficient time for a new equilibrium to be established.

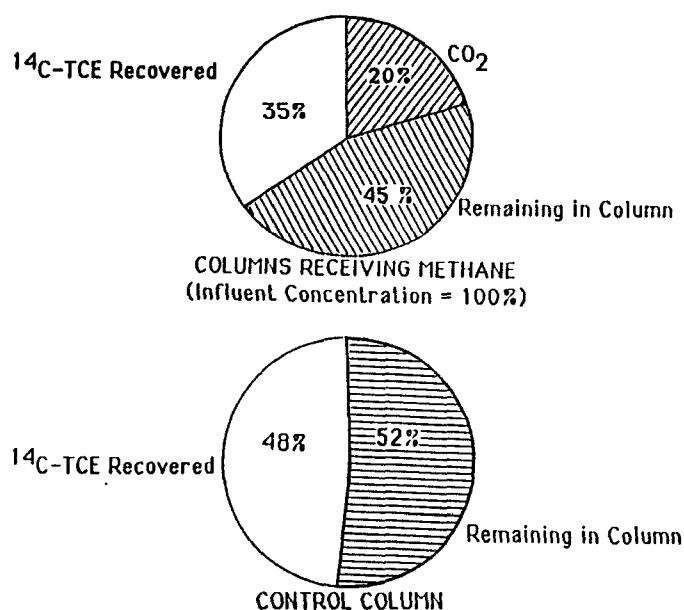


Figure 10.16. Mass balance of ^{14}C -labeled TCE in batch exchange soil columns with fourteen days between exchanges of pore liquid.

Bacterial Population--

Bacterial population in the effluent samples has been examined by direct microscopic counting, using epifluorescence of acridine orange-stained samples under blue light. This method does not distinguish methanotrophic from heterotrophic bacteria, nor does it provide direct information on the bacteria attached to aquifer solids.

Bacteria in the effluent from the methane-fed columns averaged approximately 8×10^5 bacteria per milliliter, with substantial variability even in replicate samples. The control column tended to have slightly fewer bacteria in the effluent but the difference was not statistically significant. The shorter time between exchanges did not noticeably affect the numbers of bacteria in the effluent. Populations in effluent from the hydrogen peroxide columns fell in the same range as populations from the columns using oxygenated water.

Batch Microcosm Results

In the first batch microcosm experiment, methane was slowly consumed for the first five days, followed by a relatively rapid and complete utilization by the sixth day. No TCE degradation was observed until after all methane had been depleted. However, TCE degradation (as measured by labeled carbon dioxide production) continued for approximately 5 days, until 6% of the initial TCE had been degraded to carbon dioxide.

The mean direct count of the final bacterial population in the methane-fed microcosms was approximately 10^6 organisms per ml, about twice the average counted in the initial samples. Although triplicate samples were analyzed for bacteria using acridine orange direct counting and protein measurements, the variability remained too high to statistically distinguish the final population numbers from either the initial population or the population in the control microcosms which received no methane. The bacterial population estimated in sequential batch aquifer material columns (the source of inoculum for the microcosms) was approximately twice the number of the final microcosm populations. This seems to provide a likely explanation for the diminished TCE degradation.

In the second experiment using 35-ml vials, slow methane utilization continued for only two days before a 24-hour period of rapid consumption. After all the methane had been consumed, a 5-day period of TCE degradation began. Only 3% of the initial TCE had been recovered as carbon dioxide by the end of the experiment. Results of bacterial population observations were nearly identical to those of the first microcosm experiment.

The temporal separation of methane utilization and TCE degradation was one of the more intriguing results of these experiments. This may be due to insufficient biomass for measurable TCE degradation until the period of rapid growth and increase of the population. Another likely explanation is the effect of competition between methane and TCE for the active sites on the monooxygenase enzyme.

Another important observation was the continuation of TCE degradation for several days after the primary substrate had been consumed. One conclusion would be that the methane monooxygenase enzyme remains active for some time after methane is depleted, utilizing some stored reducing power (Henry et al., 1988). A potential method for enhancing TCE degradation, besides increasing the population of methanotrophic bacteria, is to support the activity of the bacteria during the period immediately following methane depletion. Building on the results of recent field experiments at Moffett Field (Section 6), it may be possible to supply additional reducing power to the methanotrophic bacteria without competing for the methane monooxygenase enzyme.

DISCUSSION

Environmental factors that contribute to the persistence of a pollutant include the lack of a degrading population and substrate concentrations so low that sufficient energy for microbial growth cannot be obtained. Halogenated aliphatic compounds, such as TCE, 1,2-DCA, and VC, often are present at

very low concentrations in groundwater and therefore may not be able themselves to support the growth of an active transforming population. Furthermore, no organism has been identified yet that can obtain energy for growth from TCE degradation. Transformations observed to occur are generally considered to result from co-metabolism. In this manner, trace concentrations of TCE, 1,2-DCA, and VC were aerobically biodegraded in the studies reported here when methane was used as a primary substrate.

If indigenous groundwater microorganisms cannot utilize a primary substrate which is supplied, then population growth and organic decomposition cannot occur. The same holds true if the primary substrate does not encourage the production of organisms with the necessary enzymes for co-metabolism. The Moffett-site aquifer material did not appear to contain a propane-using microbial population, but did contain a methane-using population with the capability to degrade TCE and 1,2-DCA. The latter has been confirmed in the Moffett Field demonstration (Section 6), where the extent of TCE degradation was similar to that found in this laboratory evaluation. This illustrates the value of column studies for evaluating the potential for in-situ biodegradation.

The laboratory column studies were also useful for evaluating several important factors. In this research the dissolved methane concentration had the greatest effect on the extent of TCE degradation. Some methane was necessary to stimulate the growth of a TCE-degrading culture, but the methane did not have to be added continuously, and TCE degradation occurred during pulsing intervals when only oxygen was added. Methane monooxygenase (MMO) is probably responsible for the initial oxidation of TCE (Little et al., 1988). However, in previous studies (Hou et al., 1979a; and Patel et al., 1982) methane was shown to compete with other possible substrates for MMO activity. In this study, little or no TCE degradation occurred when the added methane concentration was 4.5 mg/l, but did occur with 1.5 mg/l, and this might have been due to the competition between methane and TCE for MMO. Even so, in the columns with high methane concentration, it would have been expected that methane might have only initially inhibited TCE degradation. Once methane was consumed, and the concentration became low enough to no longer be inhibitory, not enough dissolved oxygen perhaps remained for TCE degradation to occur. Therefore, both the dissolved methane and dissolved oxygen concentrations might have had an effect on the extent of TCE degradation.

Column 6, which was fed low methane (1.5 mg/l) and nutrients throughout the experiment, was the most successful in degrading TCE. Pulsing methane with oxygen followed by oxygen only was also an effective treatment for stimulating TCE degradation. When the high methane (4.5 mg/l) was pulsed, more degradation occurred during the weeks when no methane was added, perhaps because substrate competition for MMO was reduced. When the pulsed methane concentration here was reduced (1.5 mg/l), the difference in the extent of degradation between exchanges was less apparent, and was also the highest observed. Perhaps the larger population resulting from the higher initial methane concentration additions was a factor in the subsequent higher rates.

Time studies with column 6 showed that the methane was consumed within one day and most of the TCE degradation occurred within two days after an exchange. In the column that received pulsing, the methane probably also was gone after one or two days. However, when only dissolved oxygen was added to the feed solution the following week, the methanotrophic bacteria again initiated TCE degradation. Why TCE degradation stopped within one or two days after an exchange and began again when only oxygen was supplied needs to be clarified. One possibility is that the oxygen concentration after two days was insufficient for continued TCE utilization. More study is needed here.

The effect of the methane concentration on the extent of TCE degradation has important implications for in-situ treatment systems. These results suggest that the methane should not be present at too high a concentration. In addition, methane does not have to be added continuously for degradation to occur. Pulsing should help reduce the operating costs because less methane would be used. These results, however, need to be confirmed with other cultures, as well as in actual field experiments where operating conditions would necessarily be somewhat different than in this laboratory evaluation.

The three contaminants studied in this research behaved differently. VC was completely degraded, whereas 1,2-DCA and TCE were partially degraded. The 1,2-DCA degradation began sooner and was more complete than TCE degradation. The 1,2-DCA appeared to sorb less strongly to the aquifer solids,

and more of the 1,2-DCA could be accounted for in a crude mass balance. In both the 1,2-DCA column and the TCE columns, the ratio of the compound concentration remaining after degradation to the concentration of the halogenated organic in the pore water was approximately the same. This was not the case with VC degradation, where pore water concentrations fell below the detection limit (2 µg/l).

A limitation of this research is that better quantitative mass balances on TCE and 1,2-DCA were not obtained. The concentrations of TCE and 1,2-DCA in the pore fluids always were significantly lower than in the influent feed. Two possible sinks for the halogenated compounds are sorption and incorporation into biomass. To the extent that degraded TCE and 1,2-DCA were incorporated into biomass, the degradation reported in these studies has been underestimated. Furthermore, if the extent of degradation is proportional to the concentration of the contaminant, more degradation might have occurred in the bottom portion of the columns, where a higher concentration of the halogenated organics appears to have been present due to sorption. Another limitation, due to the lack of radiolabeled VC, was the inability to determine the ultimate fate of the removed VC. It was uncertain how much of the removal of VC from the control column could be attributed to biodegradation and how much was due to non-destructive fates, such as sorption and volatile losses.

The study in which the degradation of TCE that had been sorbed to the aquifer material was investigated was the most realistic in terms of simulating an in-situ treatment of a contaminated aquifer. Based on the results of this limited study, twice as much TCE was removed from the column through the combination of biodegradation and desorption as would have been removed by desorption alone during passage of water through the column. These results suggest that the addition of methane and oxygen to water circulated through a groundwater system to remove TCE for above ground removal could result in at least a doubling of the rate of removal, and at the same time accomplish degradation of about one half of the TCE removed. This encouraging observation should be pursued further.

Use of sealed microcosms permitted an accurate accounting of the total mass of methane, oxygen and TCE in the systems. The precision of bacterial population measurements proved less satisfactory. No TCE was degraded while detectable methane remained in the microcosms. While it is possible that this was an effect of low population during the initial growth stages of the batch systems, the complete absence of TCE degradation in the late stages of growth (when more than 50% of the methane had been consumed) suggests that the presence of methane inhibits degradation. Population density does seem to have an effect on the efficiency of TCE degradation, since the percentage of degradation was less during the microcosm experiments than during sequential batch experiments which apparently support higher populations. It was not possible to quantify the relationship between bacterial numbers and TCE degradation in this study.

Temporal separation between methane consumption and TCE degradation was well documented in the batch microcosm study. The methanotrophic community transformed TCE for several days after the primary source of energy had been exhausted, implying the utilization of a stored energy source and the continued viability of the monooxygenase. This suggests the potential for a sequence of bacterial activation with a methane solution followed by support of the TCE-degradation activity by an alternative energy source which does not compete for the methane monooxygenase enzyme. The effect of adding single-carbon compounds (methanol, formate, and/or formaldehyde) to the microcosms immediately after methane has been consumed should be investigated further to assess whether the rate or the duration of TCE degradation can be increased by supplying an alternative source of reducing power to an active methanotrophic community.

CONCLUSIONS

The 20% transformation of TCE to CO₂ under aerobic saturated conditions, with methane as the primary substrate, offers encouragement for in-situ treatment of TCE-contaminated aquifers. Microorganisms enriched from Moffett core material were able to degrade TCE, although they had been enriched from an aquifer previously unexposed to halogenated alkenes. Laboratory studies performed on carefully prepared columns of aquifer material permit evaluation of the potential of the indigenous microbial population for biotransformation of the contaminant.

The results suggest that approximately half of the TCE added to the columns may be sorbed to the aquifer solids during the treatment period. In the methane-fed columns, incorporation of labeled carbon into biomass may account for a portion of the missing TCE.

A greater efficiency of TCE degradation was not obtained by increasing the rate of methane addition from once every 14 days to once every 3 days, a fourfold increase. Further studies are needed in order to explain this phenomenon.

Inhibition of methanotrophic activity resulted from the use of hydrogen peroxide as an oxygen source in the feed solution. Less TCE was degraded under these conditions even though the dissolved methane concentration of the influent could be doubled.

Sealed microcosm studies and some of the column studies indicated temporal separation of CH₄ utilization and TCE transformation, which suggests competition between CH₄ and TCE for the MMO active site, and greater affinity of the enzyme for CH₄, resulting in competitive inhibition of TCE transformation in the presence of detectable quantities of CH₄.

SECTION 11

CONTINUOUS FLOW COLUMN STUDIES

Robert Roat, Lewis Sempri, and Paul Roberts

INTRODUCTION

Experiments with a continuous flow column were undertaken to model the conditions of the field tests. As a working hypothesis for these experiments, we aimed to prove that a continuous flow column, filled with screened aquifer solids, may be used to simulate transient and steady-state biodegradation field results for trichloroethylene(TCE) and trans-1,2-dichloroethylene (trans-DCE). The objectives of the study were to determine:

- 1) the lag time required for biostimulation of methanotrophs as indicated by uptake of methane;
- 2) the ratio of methane to oxygen use in the biostimulated column;
- 3) the degree of biodegradation of TCE and trans-DCE in a continuous flow laboratory column;
- 4) the amount of TCE converted to CO₂ using radiolabeled carbon (¹⁴C-TCE, ¹⁴C-CO₂);
- 5) the relationship between methane uptake, TCE degradation, and CO₂ production;
- 6) the transient response of the TCE and ¹⁴C-CO₂ concentrations following stimulation of a methanotrophic bacterial population;
- 7) the concentrations of any degradation intermediates and the relation between the appearance of these intermediates and the onset of biotransformation of trans-DCE;
- 8) the effect of varying methane concentrations on degradation rates; and
- 9) the long-term effect of the shutdown of methane on concentration responses of TCE, trans-DCE and their intermediates and degradation products following termination of methane feed.

The use of a continuous flow column in the laboratory combines several advantages: 1) the continuous flow system has transport characteristics similar to those at the field site, allowing observation of transient responses; 2) the continuous flow columns asymptotically approach steady-state effluent conditions; and 3) the laboratory setting permits the detection of degradation products such as CO₂ using radiolabeled compounds. The first of these advantages is not shared by the semi-batch columns (Section 10). The last advantage could not be realized in the field work (Section 6) since radiolabeled compounds could not be used.

METHODS

Column Description

A glass column packed with aquifer solids was used in the experiments. The column, shown in Figure 11.1, was 40 cm long and 2.5 cm ID, with a ground-glass stopper at the top and a taper at the bottom. Side sampling ports were affixed to the column to allow sample collection at intermediate locations. The inflow and outflow ports, along with the side ports, were plugged with Teflon-coated butyl rubber stoppers to minimize chemical losses.

The column was packed with aquifer material from the test zone at Moffett Field. Aseptic procedures (Section 10) were used in obtaining the core samples. To eliminate particles larger than 4 mm, the aquifer material was passed through a number 8 Tyler sieve. The column was packed using procedures described in Section 10. This procedure elutriated any silt or clay which might clog the column. After obtaining a clear effluent, a glass wool filter was placed at the level of the inflow port to evenly distribute the influent solution over the top of the column. The ground-glass plug was then clamped in place to prevent losses from the top of the column.

Setup

The column was configured for downward flow. A syringe pump (Orion Research, Cambridge, MA) drove two 100-ml gas-tight syringes (Spectrum, Houston, TX) containing aquifer water amended with chemicals of interest. In order to minimize release of radio-labeled TCE into the lab, the excess effluent was collected in a Teflon gas collection bag (Alltech) mounted at the same height as the inflow syringe. This physical arrangement also minimized the risk of inadvertent draining of the column during syringe changes. To prevent chemical losses, 1/16" OD stainless steel tubing was used at the inflow, outflow and sample port manifolds. For physical flexibility, inch-long 1/16" OD Teflon lines connected the syringes to the stainless steel lines at the top of the column.

Analytical Techniques

The concentrations of dissolved oxygen, methane, TCE, trans-DCE, CO₂, and trans-DCE epoxide (DCO, Section 7) were measured. The analytic techniques used for each of these data sets are mentioned here: a complete discussion of each of these methods may be found in Section 10. Sample collection techniques are discussed below in detail, since they differ from those described in Section 10.

Dissolved oxygen (DO) was measured using an oxygen electrode (Yellowsprings Instruments, model 54A). After meter calibration, 3 ml of water collected from the column were exposed to the probe and allowed to reach equilibrium. Concentrations in the range of 0.5–29 mg/l were measured, although the probe appeared to underestimate concentrations above 25 mg/l.

Methane concentrations were measured using head space analysis on a Hewlett-Packard 5730A gas chromatograph with an FID detector and 60/80 Carbosieve column. Samples of approximately 2 ml of column liquid were collected, stored and measured as described in Section 10.

TCE concentrations were determined by two techniques. Scintillation counting on a scintillation spectrometer (Tricarb model 4530, Packard Instrument Co., Downers Grove, IL) was used for influent and effluent column measurements of carbon-14 (¹⁴C) labeled TCE (see Section 10). In order to obtain normalized TCE and CO₂ concentrations from the activity data of the scintillation counter, three 1-ml samples of column influent or effluent were required. One sample, designated "neutral", was placed directly in 10 ml of scintillation cocktail. The second, designated "acid", was injected into a vial containing 5 drops of 1N HCl, while the third, called "base" was injected into 5 drops of 1N NaOH. The acid and base samples were purged with nitrogen for 10 minutes. 10 ml of scintillation cocktail were then added to each and the scintillation count performed.

Continuous Flow Column

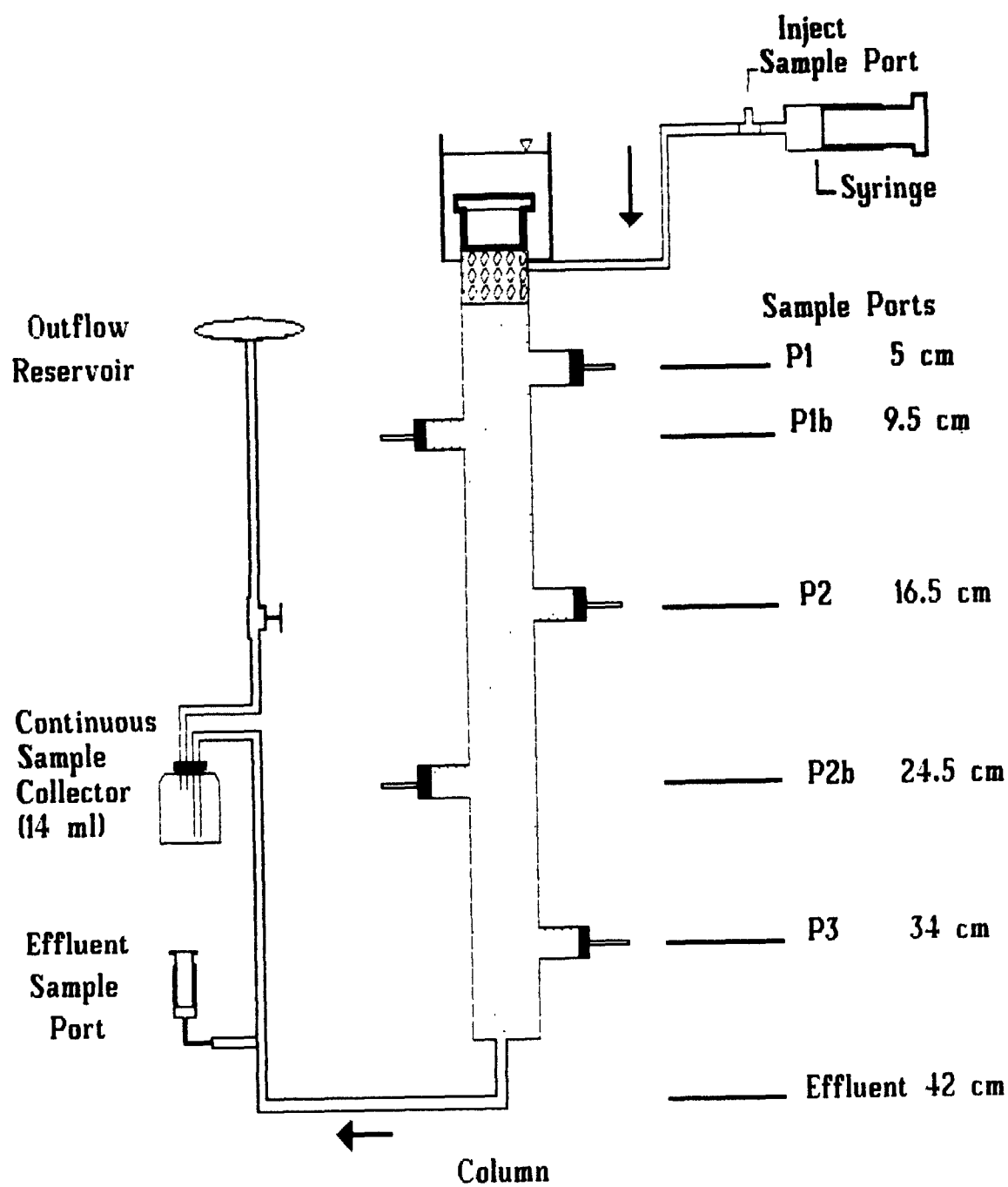


Figure 11.1. Design of the continuous flow column.

Pentane extraction and analysis on a Tracor GC with a packed column and electron capture detector (ECD) permitted correlation of scintillation counts with concentration in the source syringe and the influent. The extraction and chromatography techniques are described more completely in Section 10. Scintillation counting required 3 ml of sample, whereas pentane extraction required 14 ml.

Concentrations of ^{14}C - CO_2 also were determined using the scintillation spectrometer. Radiolabeled carbon dioxide was assumed to be the product of TCE degradation, since TCE was the only significant source of carbon-14. These samples were generated simultaneously with the TCE scintillation counts.

Concentrations of trans-DCE were determined using a headspace analysis technique with the Tracor ECD-GC and packed column. This technique, described in Section 10, required 2 ml of solution from the column. Standard solutions of trans-DCE in water were prepared and analyzed to determine both the residence time and a calibration curve for concentration versus peak area.

Sample Collection

As Figure 11.1 shows, samples could be collected at the influent, sideports, or effluent of the column. The influent sampling protocol comprised three steps. First, the effluent valve near the Teflon collection bag was closed. Next the influent sample port was opened and a 10-ml glass syringe was attached to the port using swagelok fittings and a 2 cm, 1/16" OD Teflon line. After the syringe and Teflon line were purged of trapped air, the pump speed was increased to quickly fill the syringe with liquid, after which the speed was returned to normal. The syringe was then disconnected. To prevent the trapping of air in the influent lines, the effluent valve was then reopened and the collection bag was squeezed to force a few drops of column water and any entrained air bubbles out of the influent collection port. The port was then recapped and normal flow continued.

Effluent samples were collected from the column in much the same manner. The effluent valve was closed and a syringe attached to the effluent sample port. Following the purging of any air bubbles, the syringe was allowed to fill at the normal 66 ml/day flow rate.

The solution collected in the glass syringe was used for three separate analyses. Aliquots of 1 ml each were placed in three flasks containing either scintillation cocktail, 1N HCL, or 1N NaOH, for use in the detection of TCE and CO_2 . If methane stimulation was underway, 2 ml were placed in a 14-ml preweighed vial for use in methane analysis. Finally, a 3-ml sample was placed in the DO sampler and tested. If trans-DCE samples were required, a second syringe was allowed to fill, then 2-ml samples were added to a Teflon-capped 14-ml vial.

In order to obtain effluent samples for the pentane extraction ECD-GC analysis discussed above, a flow-through collection loop was used. The sample collection method was adapted from that described in Roberts and Mackay (1986). To collect a sample, the effluent valve was closed and an empty 14-ml sample bottle clamped in line. The effluent sample port was then opened, the effluent valve reopened, and the bottle was allowed to fill from the effluent collection bag. After the bottle had filled, the effluent port was closed, and at least 2 volumes of column effluent were allowed to flow through the bottle. The sample was then removed, capped and refrigerated. A new sample bottle was placed in line. This collection method allowed the relatively large sample sizes needed for the pentane analysis to be collected without losses due to leakage of the glass collection syringe. It also allowed unattended overnight sample collection.

Stock Solution Preparation

^{14}C -trichloroethylene (^{14}C -TCE) was obtained from the same source as Section 10. The original stock solution of ^{14}C -TCE had a specific activity of 4.11×10^4 dpm/ μg . The continuous flow studies required the addition of unlabeled TCE, so as to increase the inflow concentration of TCE to field concentrations of about 40 $\mu\text{g/l}$, while maintaining an ideal influent scintillation count of 1000 dpm/ml. This unlabeled TCE spike reduced the specific activity of the stock solution to 2.55×10^4 dpm/ μg .

In addition, experiments involving the use of unlabeled (trans-DCE) (Aldrich Chemical Co.) at an inflow concentration of 800 µg/l required that trans-DCE also be added to the stock solution after final adjustment of the TCE concentration.

This spiked stock solution was stored in a refrigerated gas-tight syringe and used as a source for the inflow syringes for the column. The stock solution allowed the maintenance of consistent inflow TCE activity and trans-DCE concentration over time.

Column Operation

The column was operated at a continuous flow rate of 66 ml/day with a continuous feed of TCE and oxygen. This flow rate equals one pore volume (PV) per day through the column: it approximates the residence time of tracer between the injection well and well S2 in the field study. In both the TCE and trans-DCE experiments, the halogenated solvents were fed continuously to the column. Biostimulation experiments were not started until the effluent and influent concentrations of the organic compounds had reached equilibrium.

The inflow syringes held a total of 200 ml of Moffett site water amended with oxygen, TCE, and at times methane and trans-DCE. The inflow was changed every third day. Proper concentrations of methane and oxygen were added by the method described in Section 10, while TCE and later trans-DCE were added by spiking the inflow syringes with small amounts of the concentrated stock solution. The chemically-amended water was carefully mixed between the two inflow syringes to obtain equal concentrations in both syringes. The activity, DO concentration and methane concentration of the resulting mixture were then sampled and analyzed. The use of two sets of inflow syringes allowed the new solution to be prepared with minimum disruption of the column flow.

Column effluent was sampled on a regular basis, ranging from once every several hours during periods of major transformation activity to once every other day.

RESULTS

Operation History

Table 11.1 is a chronological summary of the experiments performed with the continuous flow system. The gap between the TCE addition and Biostim experiments represents a 4-month period during which the stock solution and inflow concentration procedures were refined to improve the precision of inflow concentration measurements. The period also represents the time required for the TCE effluent and influent concentrations to reach equilibrium.

In general, the column was operated non-stop for the duration of the experiments. Two major exceptions to this generality should be mentioned. The column was shut down for 25 days during the methane variation experiment from 1/1/88 to 1/26/88. The column was also shut down for 28 days between 7/20/88 and 8/17/88. In addition, several minor shutdowns of several hours to a day occurred during occasional pump failures.

Column Transport Experiments: Tracer and TCE Addition

It was desired to operate the column with fluid residence times similar to those observed in the field. The initial experiments, therefore, focussed on the determination of critical transport properties. These experiments were performed prior to biostimulating the column. Tritium was assumed to be a conservative tracer, while lissamine, an organic dye, also was tested to determine if it could serve as a non-sorbing conservative tracer, in conjunction with radiolabeled TCE. After initial results were obtained with tritium and lissamine, radiolabeled TCE addition was started.

TABLE 11.1 EXPERIMENTS AND PROCESSES STUDIED

Experiment	Duration	Pore Volume	Chemicals Injected	Average Conc. (mg/l) (95% Conf. Int.)	Process Studied
Tracer	2/19/87- 2/23/87	1-4	tritium lissamine (dye)		Transport, dispersion.
TCE Addition	2/23/87- 3/1/87	4-11	^{14}C -TCE O_2	0.040 ± 0.003 27.0 ± 1.3	Retardation, tailing.
Biostim.- Biotrans	7/23/87- 11/17/87	120-190	^{14}C -TCE O_2 CH_4	0.040 ± 0.003 25.9 ± 1.1 4.5 ± 0.2	Biostimulation of native methanotrophs, Biotransformation of TCE and production of CO_2 .
Methane Variation	11/17/87- 3/2/88	243-346	^{14}C -TCE O_2 CH_4	0.040 ± 0.003 17.9 ± 1.8 6.5 ± 0.3	Effect of methane con- centration variation on the degree of degradation and production of CO_2 .
Methane Shutdown	3/3/88- 6/28/88	346-466	^{14}C -TCE O_2 CH_4	0.040 ± 0.003 17.9 ± 1.3 0.0	Effect of removal of methane as a primary substrate on the degradation of TCE.
trans-DCE Addition	6/28/88- 11/2/88	466-593	^{14}C -TCE O_2 CH_4 trans-DCE	0.040 ± 0.003 17.9 ± 1.3 0.0 0.796 ± 0.057	trans-DCE uptake by column with no biostimulation.
trans-DCE Biostim and Biotrans.	11/2/88- 12/10/88	593-631	^{14}C -TCE O_2 CH_4 trans-DCE	0.040 ± 0.003 22.5 ± 1.0 4.5 ± 0.3 0.796 ± 0.057	Biostimulation of methanotrophs and biotransformation of trans-DCE.
Methane Shutdown2	12/10/88- 12/27/88	631-648	^{14}C -TCE O_2 CH_4 trans-DCE	0.040 ± 0.003 17.9 ± 1.3 0.0 0.796 ± 0.057	Effect of methane shutdown on trans- DCE degradation and epoxide production.

Figure 11.2 shows the tracer experiment data, expressed as normalized concentration as a function of the number of pore volumes eluted. Note that, although the TCE results are presented in the same graph as those of the tritium and lissamine experiment, TCE addition actually occurred at a later time in order to avoid confounding of tritium and TCE scintillation counts.

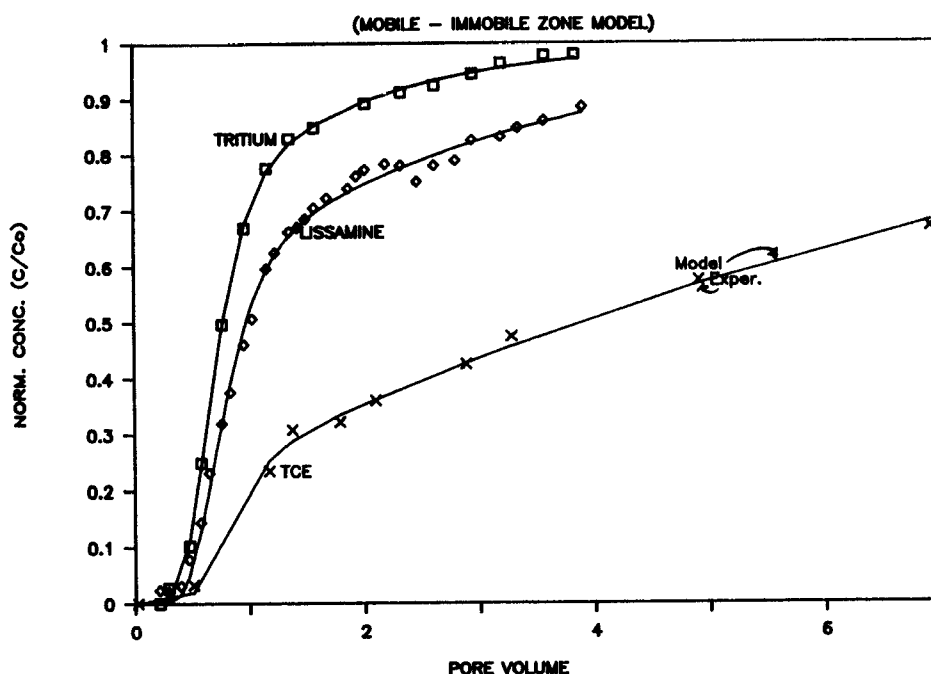


Figure 11.2. Results of column transport experiments and model simulations.

As expected of a conservative tracer, tritium broke through most quickly, followed by lissamine and TCE. However, the tritium data show exhibited substantial tailing, since the influent concentration was not reached for four PV, although 80% of influent concentration was reached in only 1.2 PV. Lissamine showed more severe tailing, as it reached only 62% of the inflow concentration in 1.2 PV. TCE shows a high degree of tailing. In fact, the TCE data reached only 28% of inflow concentration in 1.2 PV before the rate of increase in concentration slowed dramatically.

The tailing evident in Figure 11.2 is not consistent with the usual advection-dispersion model. The large amount of tailing may result from immobile (or slow flow) zones in the column due to non-uniform packing. The results were therefore compared to the mobile-immobile zone model of van Genuchten (1981). Results of this modelling exercise are shown in Table 11.2. The results are plotted in Figure 11.2 as solid lines. The mobile-immobile zone model appears to describe the experimental data quite well.

TABLE 11.2. MODEL RESULTS: MOBILE-IMMOBILE ZONE MODEL

Peclet Number:	16
Mobile Zone:	70% of pore volume
Pore Volume:	66 ml
Mass Transfer Coeff.:	$1-5d^{-1}$
Retardation Factor:	
Tritium:	1
Lissamine:	1.8
TCE:	6

The most important result of this experiment from an operational standpoint was the determination of the pore volume. The mobile-immobile zone modeling, fitted to the tritium data, provided an estimate of the pore volume. This finding allowed the flow rate to be set at 66 ml/day, or 1 pore volume per day, in order to simulate flow conditions at the Moffett field site, which exhibited hydraulic residence times between the injection and observation points that were on the order of one day (Section 5). Thus, in all of the following graphs, units of pore volume and days may be used interchangeably.

Biostimulation Experiments (Biostim-Biotrans)

The first set of biostimulation experiments was performed to characterize the ability of indigenous methanotrophic populations to transform TCE as a secondary substrate, with methane as the primary substrate, under continuous flow conditions.

The objectives of the Biostim-Biotrans sequence of experiments were to 1) determine the lag time between methane breakthrough and the onset of methane utilization; 2) measure the ratio of dissolved oxygen to methane consumed; 3) observe the transient transformation of TCE and production of labeled CO₂ in response to biostimulation; and 4) estimate the degree of TCE degradation after steady state conditions were achieved.

Prior to the stimulation of the indigenous bacterial community, an extended period was allowed for equilibration of the TCE concentration and stabilization of the column operation procedure. During this 120-day period, the column was operated at a flow rate of 66 ml/day, an influent TCE concentration of 40 µg/l, and a dissolved oxygen concentration of 28-30 mg/l.

The biostimulation of methanotrophs was undertaken by introducing 4.5 mg/l of methane into the influent syringes. Since this concentration was achieved by mixing ratios of methane- and oxygen-saturated water, the influent concentration of dissolved oxygen was reduced to 22.5 mg/l. Inflow TCE concentration remained steady at 40 µg/l.

Figure 11.3 shows normalized column effluent concentrations for methane, as well as the amounts of TCE transformed and radio-labeled CO₂ produced. Methane concentrations were found directly using an externally calibrated headspace technique for the HP Gas Chromatograph described in Section 10.

The TCE and CO₂ data were obtained from the scintillation counting of carbon-14 activity described above. This activity (in units of disintegrations per minute (DPM)) has three components: ¹⁴C associated with TCE; ¹⁴C associated with CO₂; and ¹⁴C associated with a non-volatile contaminant in the TCE source. As mentioned in the methods section, the three samples measured were designated neutral, base and acid. The neutral fraction corresponds to the total carbon-14 activity in the 1-ml fluid sample. The base fraction provided the activity of the labeled CO₂ and the non-volatile contaminant, while the acid fraction contributed scintillation counts for the non-volatile component alone. The ¹⁴C-TCE activity was defined, therefore, as the difference between neutral and base counts; ¹⁴C-CO₂ activity was calculated as the difference between base and acid counts.

Figure 11.3 presents data termed "TCE Transformed", "Net CO₂ Produced" and "Effluent CH₄". The normalized "TCE Transformed" values represent the difference between the average inflow ¹⁴C-TCE activity and the effluent ¹⁴TCE activity, all divided by the average inflow TCE activity: $(\langle TCE_{in} \rangle - TCE_{out}) / \langle TCE_{in} \rangle$. The normalized "Net CO₂ Produced" data are defined by the difference between the effluent ¹⁴CO₂ activity and the average background effluent ¹⁴CO₂ activity, all divided by the average ¹⁴TCE inflow activity: $(CO_{2out} - \langle CO_{2out, bkgnd} \rangle) / \langle TCE_{in} \rangle$. Background effluent ¹⁴CO₂ is defined as the quantity of radiolabeled CO₂ produced prior to biostimulation. This CO₂ production, which averages 8% of the inflow concentration, is attributed to the mineralization of the non-volatile fraction in the stock TCE. The background ¹⁴CO₂ production is factored out of the data in Figure 11.3 by the preceding equation.

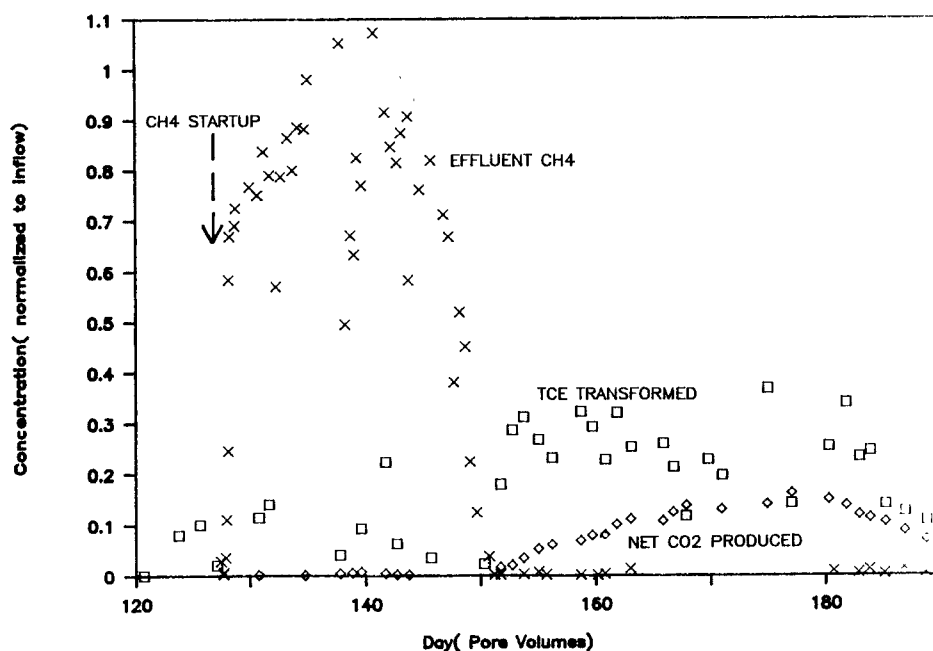


Figure 11.3. The results of the first biostimulation-biotransformation experiment.

Methane addition began at PV 127, i.e. on day 127 of column operation. As the first 6 data points of Figure 11.3 show, neither TCE transformation nor net CO₂ production was observed between the time at which TCE saturation was attained and the time at which methane utilization commenced. Methane breakthrough to the extent of 80% of the inflow concentration occurred within 2 PV. Following breakthrough, the normalized methane concentration fluctuated within the range of 0.7 to 1.1, showing essentially no uptake in the column for 20 days. After PV 147, methane utilization was observed. Effluent concentrations rapidly declined below a normalized value of 0.7 and were below detection levels (0.1 mg/l) within 5 days (PV 152).

Prior to PV 152, virtually no TCE was degraded between column inflow and effluent. Over the same period, no net radiolabeled CO₂ was produced. Not until all of the methane had been consumed did degradation of TCE and production of CO₂ in excess of the contaminant fraction begin. TCE transformation began immediately following the complete consumption of methane. Carbon dioxide production lagged behind TCE transformation, suggesting that some carbon from the TCE may have been incorporated into cell mass or intermediates before complete mineralization was attained.

Between PV 152 and 184, the average TCE transformation shown in Figure 11.3 reached 25.5%. CO₂ gradually climbed to a high of 15% (average 12%, PV 160-184), then dropped below 10% after PV 184. The discrepancy between TCE disappearance and CO₂ production suggests that approximately one-half the labelled carbon was not accounted for, at least in the short term. It is conceivable that some of the missing ¹⁴C was stored in the column in the form of carbonate, possibly as a result of precipitation or isotope exchange with pre-existing carbonate. It was not feasible to test this hypothesis by analyzing for ¹⁴C in the solids, since the column would have to be destroyed.

Figure 11.4 demonstrates the relationship observed between the consumption of methane and oxygen as the biostimulation commenced and reached steady state. The steady state is defined here as a prolonged period in which influent conditions were maintained constant and the effluent methane

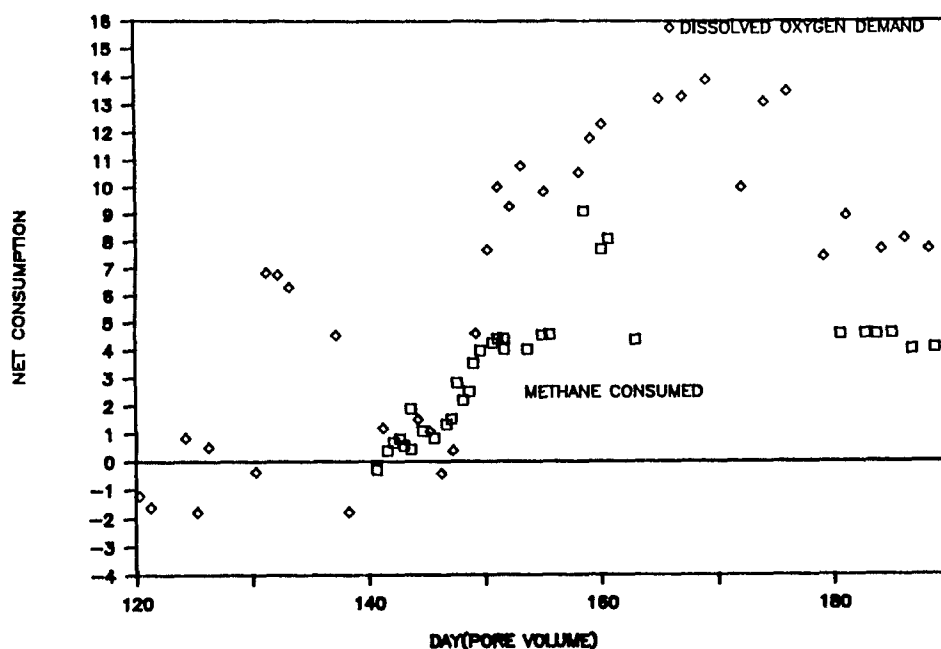


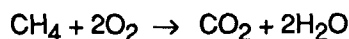
Figure 11.4. The net methane and DO consumption in the biostimulation experiment.

concentration did not change appreciably over time, e.g., beginning at PV 150, in Figure 11.4. Data were collected for inflow and effluent samples over the course of the experiment. Figure 11.4 presents these data for CH_4 consumption, as the difference between inflow and effluent concentrations (CH_4 Consumption = CH_4 inflow - CH_4 effluent) and for biological DO demand, calculated as the difference between the average background effluent DO concentration prior to biostimulation and the individual effluent DO values ($\text{DO Demand} = \langle \text{DO}_{\text{effluent, background}} \rangle - \text{DO}_{\text{effluent}}$). Note that although the same methane data are portrayed in Figures 11.3 and 11.4, the presentation of those data differs. The methane information in Figure 11.3 is presented as the difference between inflow and effluent concentrations rather than as the ratio of effluent to inflow concentrations. This alternative presentation method allows direct visual comparison of the ratio of methane consumption to oxygen demand.

The DO values prior to methane addition (before PV 127) indicate a 12 mg/l oxygen demand in the column, independent of the biostimulation of methanotrophs. Abiotic oxidation reactions may explain this demand.

Coincident with the uptake of methane between day PV and 152, the DO demand in the column increased. Figure 11.4 shows a rapid increase in biological oxygen demand at PV 148, from 0 mg/l to 9.0 mg/l, followed by a more gradual increase between PV 152 and 167 to 12.7 mg/l. The demand then decreased slowly to 6.0 mg/l at PV 178. The change from rapid to gradual increase in oxygen demand coincided approximately with the complete utilization of methane at PV 152. This behavior seems consistent with a rapid uptake due to methane utilization by a growing population of methane utilizing bacteria, followed by a slow increase in demand due to cell biomass decay.

Recalling that the inflow methane concentration averaged 4.5 mg/l, the biostimulated column required about 12.7 mg/l O_2 (Figure 11.4). As the stoichiometry of the balanced equation for complete methane mineralization



implies, 2 moles (64 g) of O_2 are theoretically required to completely convert 1 mole (16 g) of CH_4 to CO_2 . On a mass basis this implies an ideal ratio of 4:1 $O_2:CH_4$. The $O_2:CH_4$ consumption ratio inferred from the experimental data is 12.7:4.5 or 2.82:1. The lower DO demand compared to the stoichiometric ratio for complete oxidation, probably is explained by cell growth and incorporation of methane into cell mass as a carbon source. It also was observed that the DO probe underestimated values of oxygen concentration when the concentration exceeded 20 mg/l, causing a negative bias in the DO demand.

Methane Variation/ Methane Shutdown Experiments

The objectives of the transient methane variation experiments were to: 1) determine the effect of methane variations on the steady state percent of degradation of TCE and production of CO_2 ; and 2) observe the transient effects of the methane variation on the TCE degradation and CO_2 production.

After allowing the transformation to equilibrate for 90 PV after the onset of methane utilization, the inflow methane was first increased from 4.5 to 6.5 mg/l (PV 242, Figures 11.5 and 11.6). The increased methane feed was continued until PV 272, when the column flow was shut down completely for 44 days. Subsequently, flow was restarted with a methane feed concentration of 6.5 mg/l and continued through PV 299. At that time the inflow methane concentration was reduced to 0 mg/l. The cessation of the methane feed continued to the end of the experiment at PV 346 and for an additional 120 days. The 120 day operation without methane feed allowed the TCE transformation in the column to stop completely.

Figures 11.5 and 11.6 show the normalized effluent TCE concentrations and CO_2 concentration history, respectively. The data are presented as the ratio of the instantaneous value of the respective parameters to the average TCE inflow concentration. The CO_2 data were adjusted to remove the contribution of the degraded non-volatile contaminant fraction.

No trace of the increased inflow methane concentration was ever detected in the effluent methane analysis. DO demand decreased from 16.7 to 11.9 mg/l. As Figure 11.5 shows, the increase had virtually no effect on the effluent TCE concentration. TCE transformation remained at about 23%, and, as Figure 11.6 indicates, CO_2 production stayed relatively constant.

The 44-day column shutdown, which is represented as the break at PV 272 in Figures 11.5 and 11.6, caused a temporarily high TCE transformation and CO_2 production. These values quickly returned to the averages seen before shutdown. The reduced TCE concentrations might have also resulted from slow sorptive uptake during the 44-day shutdown.

Elimination of inflow methane caused a more pronounced change. With no methane present in the inflow, TCE transformation increased slightly to a maximum of 34.8% during the subsequent 20 days (days 303-323, Figure 11.5). Following that time, the amount of degradation began to decrease. Within 70 days after methane shutdown, the TCE degradation ceased and the effluent TCE concentration again equaled the inflow concentration. CO_2 production changed more substantially (Figure 11.6). Immediately following the cessation of methane, the production of radiolabeled CO_2 doubled, reaching 14% of the influent radiolabeled TCE (average, PV 303-313). This increase lasted for 10 days, then decreased over the next 30 days to background levels.

Biostimulation Experiments with trans-DCE

The objectives of the trans-DCE Biostim/Biotrans experiments were to 1) determine the time required to restimulate the methanotrophic population; 2) quantify the steady-state transformation of trans-DCE in the column; 3) observe the production of degradation intermediates; and 4) assess the effect of methane shutdown on the degradation of trans-DCE.

In view of the field experiment results for the second season, presented in Section 6, a higher degree of degradation was expected for trans-DCE than for TCE. In addition, formation of an epoxide intermediate was anticipated. Field results also raised the expectation of rapid restimulation of bacteria and rapid shutdown of trans-DCE degradation following shutdown of methane.

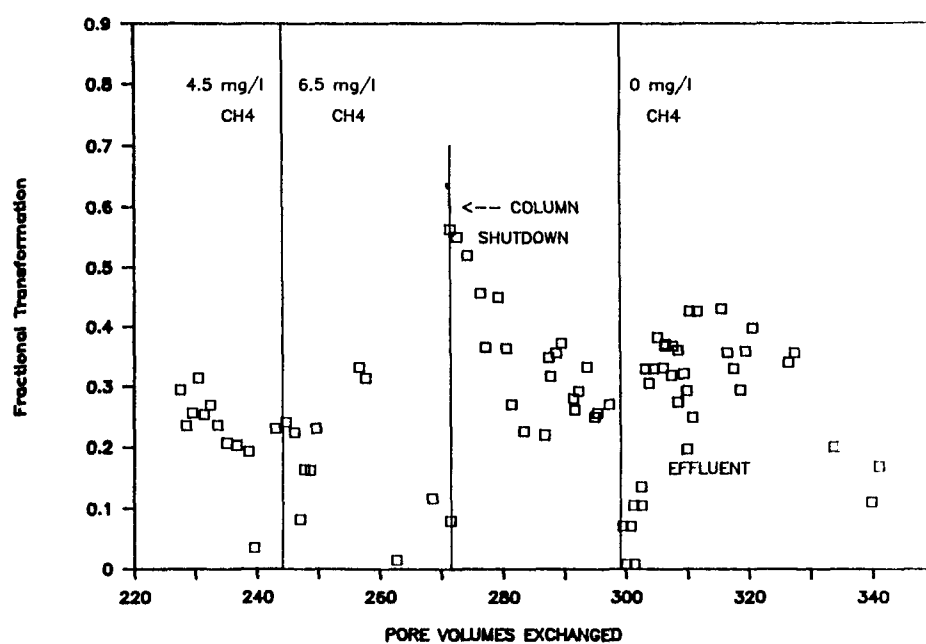


Figure 11.5. Fractional transformation of TCE during methane variation experiments.

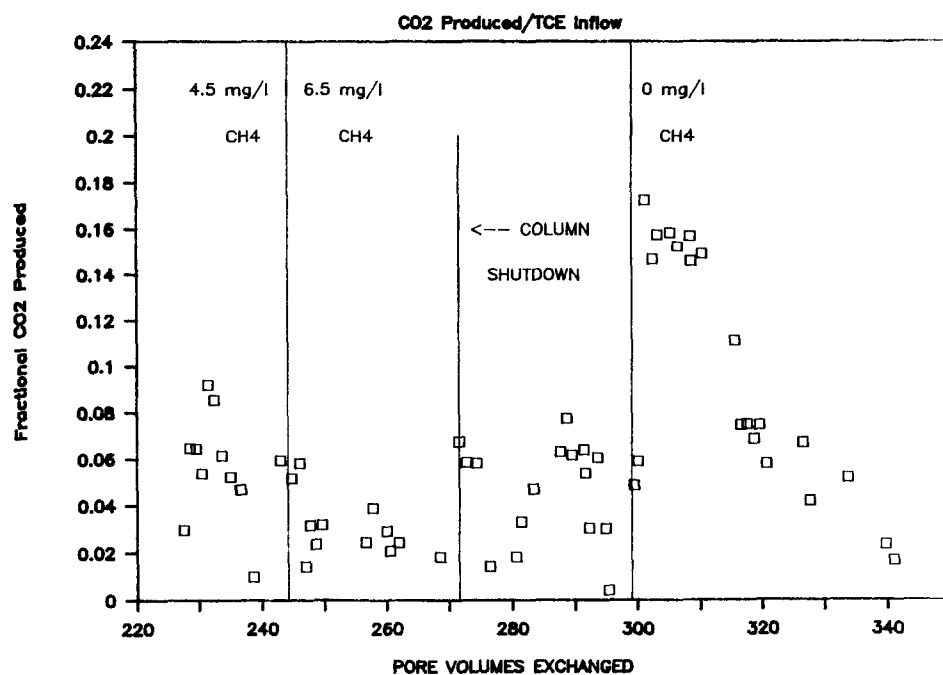


Figure 11.6. Labeled CO₂ produced during methane variation experiments.

For this final experiment, unlabeled trans-DCE was added to the column inflow in addition to labeled TCE. The trans-DCE addition began following the cessation of TCE degradation in the methane shutdown experiments. During the start-up and stabilization of trans-DCE concentration in the column, the operating conditions were as follows: trans-DCE, 796 ± 57 $\mu\text{g/l}$; TCE, 40 ± 0.3 $\mu\text{g/l}$; and dissolved oxygen, 17.9 ± 1.3 mg/l . After a 120-day stabilization period, methane addition was restarted.

Field results had indicated immediate degradation of trans-DCE upon reintroduction of methane. Instead, degradation did not become observable for 7 days (Figure 11.7). After 18 days of stimulation (Day 18), 85% of the influent trans-DCE was being degraded. At day 20, the methane was once again shut down; despite the absence of primary substrate, the degradation of trans-DCE continued unaffected, remaining in the 80-90% range, for 30 days. Only after day 50 did the degradation of trans-DCE decrease.

Degradation of trans-DCE coincided with the production of an intermediate suspected to be trans-DCE epoxide (Figure 11.8). The identification of the unknown intermediate resulted from the sudden appearance of a new peak in the gas chromatograms for the effluent, beginning at approximately 10 pore volumes. The peak residence time was 3.9 minutes, or 1.4 minutes after the trans-DCE peak and 4.2 minutes before the TCE peak. This finding corresponded to the residence time observed in other laboratory work (Section 7).

Figure 11.8 shows the epoxide concentration history: the data have been converted from peak areas to concentrations using a sensitivity of 150 times that of trans-DCE based on response factors given in Section 7. Results show a maximum epoxide concentration of 40 $\mu\text{g/l}$ during the period of methane consumption (day 7 through 20), and a maximum concentration of 69 $\mu\text{g/l}$ during the 30 days (days 20 to 50) before trans-DCE degradation shut down. The epoxide concentration represents approximately 10% of the trans-DCE degraded.

SUMMARY

The experiments permitted a direct comparison with the field results, unlike the batch column experiments (Section 10). Tables 11.3 and 11.4 summarize the major findings of the continuous-flow experiments. The steady-state differences in concentrations (influent -effluent) of TCE and trans-DCE following biostimulation agreed well with field results. The extent of biotransformation of TCE and trans-DCE estimated from the continuous column experiments was 25.5% and 85%, respectively. Both field and column work with trans-DCE showed the appearance of an intermediate thought to be trans-DCE epoxide coincident with the disappearance of trans-DCE. Major differences between field and continuous flow laboratory experiments were observed regarding the time required to restimulate the bacterial population needed to degrade the trans-DCE. The column required a much longer restimulation time, probably as a result of decay due to prolonged DO addition during the period between the biostimulation experiments. In addition, the column experiment continued to show trans-DCE transformation for several weeks after the cessation of methane addition, whereas in the field experiment transformation began to decrease within a few days.

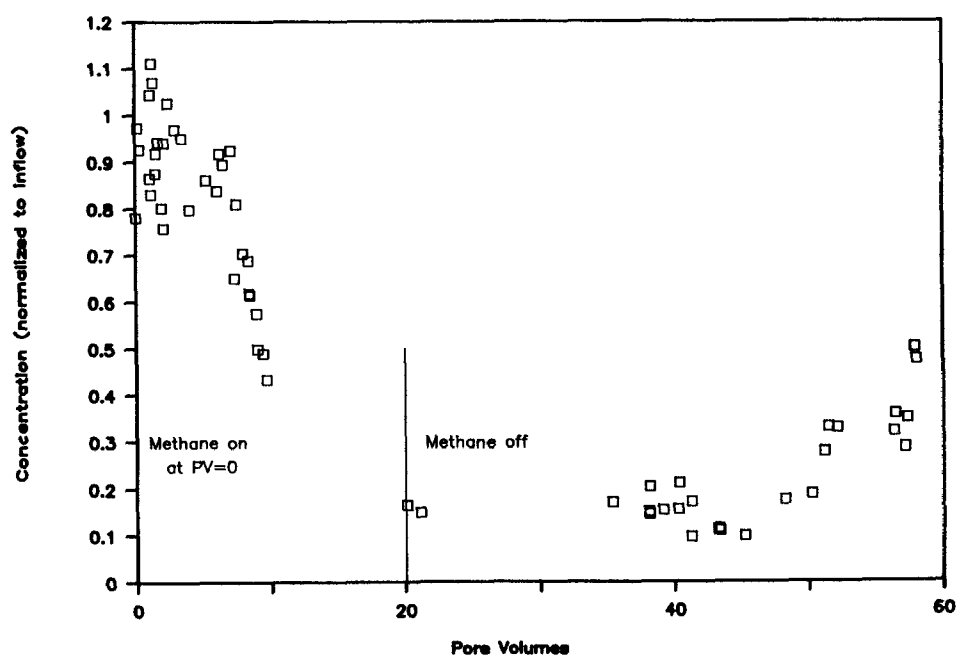


Figure 11.7. Methane stimulation experiment with trans-DCE.

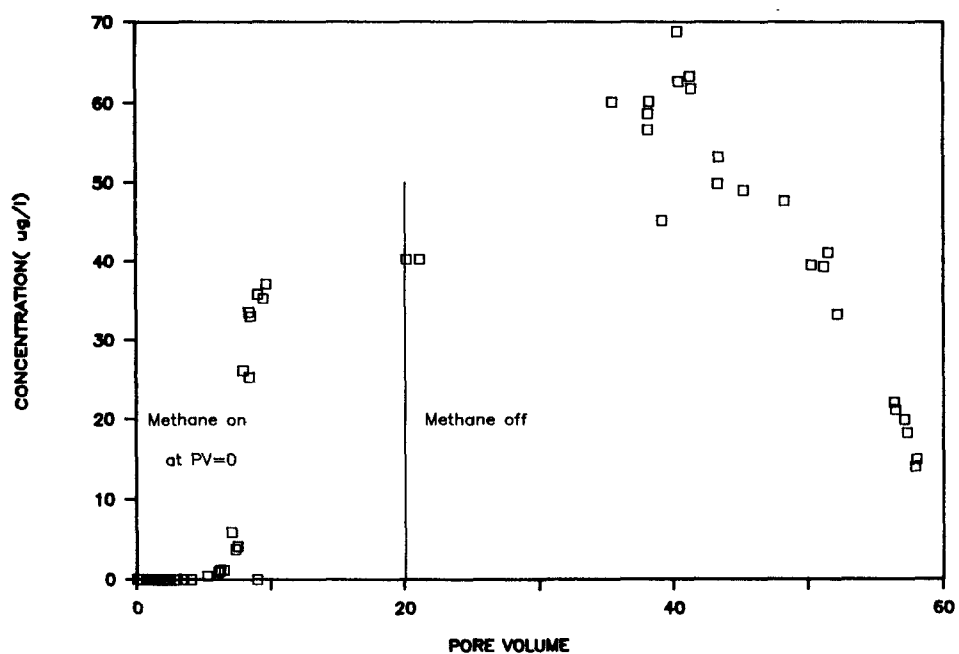


Figure 11.8. trans-DCE epoxide concentration history.

TABLE 11.3. TCE BIOSTIMULATION RESULTS

Methane Conc.	TCE Loss ^a (%)	Net DO Consumed ^{a,b} (mg/l)	Net CO ₂ Produced ^{a,b} (%)	Time Period ^c
4.5	25.5±6.8	11.3±1.3	12±3	152-184
4.5	29.2±5.1	7.5±0.3	7.1±0.9	184-240
6.5	23.1±5.3	11.5±0.3	3.3±1.4	240-299
0.0	34.8±7.4	7.6±0.6	14.2±1.3	303-323

^a Mean ± 95% confidence limit.

^b Adjusted by subtracting values measured before biostimulation.

^c Expressed as an interval of days, or pore volumes.

TABLE 11.4. trans-DCE BIOSTIMULATION RESULTS

Methane Conc.	trans-DCE Loss ^a (%)	Maximum trans-DCE Epoxide Produced (µg/l)	Time Period ^b
4.5	84.0±9.0	40	0-23
0.0	85.4±3.4	69	23-50

^a Mean ± 95% confidence limit.

^b Expressed as an interval of days, or pore volumes.

SECTION 12

ONE-DIMENSIONAL SOLUTE TRANSPORT IN POROUS MEDIA WITH WELL-TO-WELL RECIRCULATION

Constantinos V. Chrysikopoulos and Paul Roberts

This section summarizes the development, testing, and application of a mathematical model adapted to account for the recycling of solute between an injection well and an extraction well. This kind of coupling through recycle from the extraction well to the injection well is inherent to the experiments conducted at the Moffett site, as described in Section 4.

BACKGROUND

The transport of nonreactive solutes through homogeneous porous media consisting of impermeable particles commonly has been characterized by the classical advection-dispersion equation, which is based on the empirical relation of Fick's diffusion law (Fried and Combarnous, 1971; Bear, 1972). For sorbing solutes, the advection-dispersion equation has been modified to incorporate the effects of adsorption (Hashimoto et al., 1964; Lindstrom et al., 1967) and hysteresis (van Genuchten et al., 1974). However, in order to simulate the asymmetry and tailing of breakthrough curves observed in several experimental studies of solute transport, first-order rate models have been developed to account for solute exchange between zones of mobile and completely mixed immobile water (Coats and Smith, 1964; van Genuchten and Wierenga, 1976; Rao et al., 1980), while physical nonequilibrium models incorporate solute transfer into immobile regions of various geometries using the second law of diffusion (Rasmuson and Neretnieks, 1980; Goltz and Roberts, 1986a). Most mathematical models in current use for simulating the transport of sorbing solutes are based on chemical equilibrium isotherms rather than on kinetic sorption relationships, because of their computational simplicity. However, the validity of the local chemical equilibrium assumption has been questioned in studies of sorbing solute transport through laboratory columns (Nkedi-Kizza et al., 1983; Hutzler et al., 1986; Miller and Weber, 1986) and through aquifers (Goltz and Roberts, 1986b; Roberts et al., 1986).

There are certain cases where direct application of the existing solute transport models is not adequate. For example, the conditions of the transport experiments at the Moffett site, where a flow field is induced between an injection-extraction well-pair and chemicals of interest are introduced into a fraction of the extracted fluid which is reinjected, cannot be simulated accurately without taking into account the feedback due to recirculation.

In order to represent realistically the field conditions, a semi-analytical solution and an approximate analytical solution are derived for a model describing one-dimensional solute transport through porous media under local equilibrium conditions and solute recirculation between the extraction-injection well-pair. The solutions are developed for a flux-type inlet boundary condition in a semi-infinite medium. Although one-dimensional models may not be adequate for every field situation, this particular model provides a starting point for investigating the effects of well-to-well recirculation. Furthermore, for one-dimensional models, analytical or semi-analytical solutions are more likely obtainable, leading to more efficient and accurate computations than the purely numerical solutions of multi-dimensional models. The model is applied to the field-data of experiments Tracer8 and Tracer11 (Section 5).

MODEL FORMULATION AND SOLUTION

The transport of a sorbing solute through one-dimensional porous media under steady-state flow conditions is governed by the following partial differential equation (Lapidus and Amundson, 1952):

$$\frac{\partial C(t,x)}{\partial t} + \frac{\rho}{\theta} \frac{\partial C^*(t,x)}{\partial t} = D \frac{\partial^2 C(t,x)}{\partial x^2} - V \frac{\partial C(t,x)}{\partial x} \quad (12-1)$$

where C is the liquid-phase solute concentration (M/L^3), C^* is the solid-phase concentration of the adsorbed solute (M/M), D is the hydrodynamic dispersion coefficient (L^2/t), V is the average interstitial fluid velocity (L/t), x is the spatial coordinate in the direction of flow (L), t is the time (t), ρ is the bulk density of the solid matrix (M/L^3), and θ is the porosity (L^3/L^3). For linear, reversible, instantaneous sorption, the equilibrium relationship between the solute substance in the aqueous and solid phases is given by

$$C^*(t,x) = K_d C(t,x) \quad (12-2)$$

where K_d is the partition or distribution coefficient (L^3/M). The distribution coefficient is a measure of solute retention by the solid, and is expressed as the ratio of solute concentration on the adsorbent to solute concentration in solution. Combining equations (12-1) and (12-2) leads to

$$R \frac{\partial C(t,x)}{\partial t} = D \frac{\partial^2 C(t,x)}{\partial x^2} - V \frac{\partial C(t,x)}{\partial x} \quad (12-3)$$

where the dimensionless variable R is the retardation factor defined as

$$R = 1 + \frac{\rho}{\theta} K_d \quad (12-4)$$

For a semi-infinite system and pulse input conditions that take into account the effect of solute recirculation, the appropriate initial and boundary conditions are

$$C(0,x) = 0 \quad (12-5a)$$

$$-D \frac{\partial C(t,0)}{\partial x} + VC(t,0) = \begin{cases} V[C_p + qC(t,L)] & 0 < t \leq t_p \\ qVC(t,L) & t > t_p \end{cases} \quad (12-5b)$$

$$\frac{\partial C(t,\infty)}{\partial x} = 0 \quad (12-5c)$$

where C_p is the pulse-type injection concentration (M/L^3), and t_p is the duration of the solute pulse (t). The condition (12-5a) corresponds to the situation in which the solute is initially absent from the one-dimensional porous medium. The third- or flux-type boundary condition (12-5b) for pulse injection implies concentration discontinuity at the inlet and leads to material balance conservation (Brigham, 1974; Kreft and Zuber, 1978). The upstream boundary condition (12-5b) includes on the right hand side the term $qC(t,L)$, where $C(t,L)$ is the solute concentration at the extraction location L , and q is the fraction of the recirculating solute mass, $0 \leq q \leq 1$. This term accounts for solute recirculation between the extraction-injection locations by adjusting instantaneously the inlet concentration in proportion to the

solute concentration at the exit. The downstream boundary condition (12-5c) preserves concentration continuity for a semi-infinite system.

The solution to (12-3), subject to initial and boundary conditions described by equations (12-5a, b and c) is obtained by taking the Laplace transforms of these equations with respect to the time variable t and the space variable x . The details of the mathematical derivations have been reported by Chrysikopoulos et al. (1989). Here, only the solution to the well-to-well recirculation model is presented.

The semi-analytical solution in the Laplace domain is given by

$$C(t,x) = \begin{cases} \Omega(t,x) & 0 < t \leq t_p \\ \Omega(t,x) - \Omega(t - t_p, x) & t > t_p \end{cases} \quad (12-6a)$$

where

$$\Omega(t,x) = L^{-1} \{ \bar{C}(s,x) \} \quad (12-6b)$$

$$\bar{C}(s,x) = -\frac{VC_p e^{-(M+N)x}}{sD(M-N)} \left[\frac{1}{1 - \frac{qV e^{-(M+N)L}}{D(N-M)}} \right] \quad (12-6c)$$

$$M = -\frac{V}{2D} \quad (12-6d)$$

$$N = \left(\frac{Rs}{D} + \frac{V^2}{4D^2} \right)^{1/2} \quad (12-6e)$$

s is the Laplace domain time variable and L^{-1} is the Laplace inverse operator. Numerical inversion of the Laplace transform can be obtained by techniques such as the Stehfest algorithm (Stehfest, 1970).

The approximate analytical solution is obtained by employing Maclaurin's approximation to simplify equation (12-6c) so that its analytical inversion from Laplace time variable s to real time t is achievable, and it is given by

$$C(t,x) = \begin{cases} \Phi(t,x) & 0 < t \leq t_p \\ \Phi(t,x) - \Phi(t - t_p, x) & t > t_p \end{cases} \quad (12-7a)$$

where

$$\Phi(t,x) = A(t,x) + \sum_{m=1}^{\infty} \alpha_m(t,x) * G(t,L) \quad (12-7b)$$

$$\alpha_1(t,x) = A(t,x) \quad (12-7c)$$

$$\alpha_m(t,x) = \alpha_{m-1}(t,x) * G(t,L) \quad m \geq 2 \quad (12-7d)$$

$$A(t,x) = \frac{C_p}{2} \operatorname{Erfc} \left[\frac{Rx - Vt}{2(D Rt)^{1/2}} \right] + C_p \left(\frac{V^2 t}{\pi D R} \right)^{1/2} \exp \left[-\frac{(Rx - Vt)^2}{4D Rt} \right] - \frac{C_p}{2} \left(1 + \frac{Vx}{D} + \frac{V^2 t}{D R} \right) \exp \left[\frac{Vx}{D} \right] \operatorname{Erfc} \left[\frac{Rx + Vt}{2(D Rt)^{1/2}} \right] \quad (12-7e)$$

$$G(t,L) = q \left(\frac{V^2}{\pi D Rt} \right)^{1/2} \exp \left[-\frac{(RL - Vt)^2}{4D Rt} \right] - \left(\frac{qV^2}{2D R} \right) \exp \left[\frac{VL}{D} \right] \operatorname{Erfc} \left[\frac{RL + Vt}{2(D Rt)^{1/2}} \right] \quad (12-7f)$$

The "*" signifies convolution, and the nested convolution integrals are easily determined by numerical integration techniques.

Figure 12.1 shows plots of dimensionless concentration versus time for the approximate analytical solution (12-6), the semi-analytical solution (12-7), and the case of no recirculation ($q = 0$). The semi-analytical solution was obtained by numerical inversion of the Laplace transform utilizing the Stehfest algorithm (Stehfest, 1970), while the convolution integrals of the approximate analytical solution were evaluated by Simpson's rule. For this illustrative comparison only the first three terms of the infinite series (12-7b) were taken into account. The predictions of the analytical and semi-analytical solutions are indistinguishable. The model without recirculation predicts a steady-state breakthrough concentration C_p , while the recirculation model doesn't approach a steady state, but rather the predicted concentration increases with injection time. For $q \ll 1$, the approximate analytical solution can be utilized efficiently with just a few terms of the infinite series, because at late stages of a broad pulse injection the breakthrough concentration increases only very slowly. However, for $q \sim 1$ the number of the required summation terms in the infinite series is determined by the number of injected fluid recirculations, or equivalently the number of pore volumes passing through the system during the experimental period. For example, if $q = 1$, the breakthrough concentration at the end of k fluid recirculations is approximately kC_p .

PARAMETER ESTIMATION METHODOLOGY

The model developed above contains four parameters, namely the retardation factor, the dispersion coefficient, the fluid velocity, and the fraction of the recirculating solute mass. In applying the model to laboratory or field data, it is necessary to best estimate these parameters and to quantify their uncertainty. There are several approaches available for parameter determination. Here, the nonlinear least-squares regression method has been adopted.

In general, the objective of the nonlinear least-squares method is to obtain estimates of the model parameters which minimize the residual sum of squares between simulated and observed data. For this work, the Standards Times Series and Regression Package (STARPAC) (Donaldson and Tryon, 1983) was used for parameter estimation. STARPAC includes an adaptive nonlinear least-squares algorithm developed by Dennis et al. (1981). This algorithm adaptively decides when to use the computationally expensive second-order part of the least-squares Hessian, which accounts for its reliability and efficiency when the residuals are large or the model is highly nonlinear.

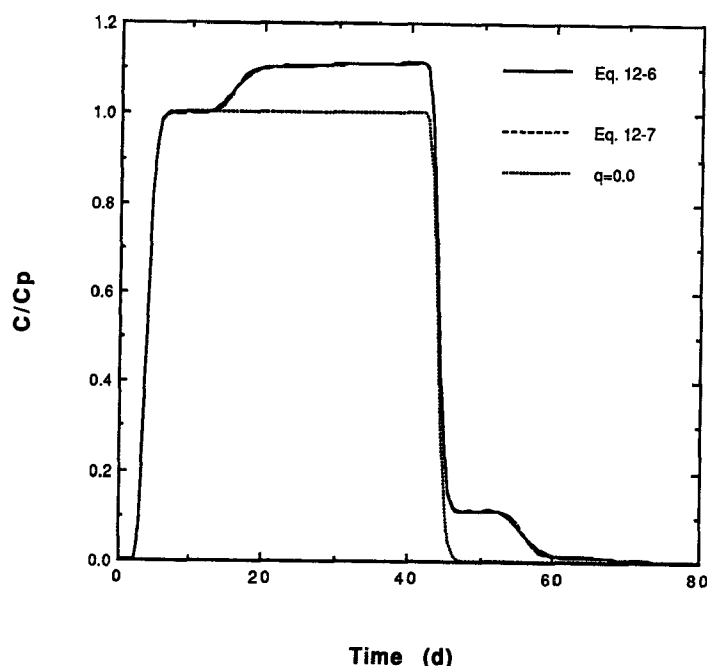


Figure 12.1. Comparison of the approximate analytical, semi-analytical, and case of no recirculation solutions: $V = 0.5$ m/d, $D = 0.02$ m²/d, $R = 1$, $C_p = 1.0$ mg/l, $x = 2.0$ m, $l = 6.0$ m, $t_p = 40.0$ days, and $q = 0.1$.

The uncertainty of the estimated nonlinear parameters is quantified by approximate 95% confidence intervals, which are based on the single-variate Student's t distribution, assuming normally distributed parameter estimates. This may be criticized because these limits do not yield joint confidence regions. However, although the concept of confidence region construction is intuitively simple, it can lead to considerable difficulties. The results of a Monte Carlo study on approximate confidence region evaluations for nonlinear least-squares parameter estimates conducted by Donaldson and Schnabel (1987) have shown that the simple and most frequently used linearization methods often grossly underestimate confidence regions. On the other hand, the likelihood and lack-of-fit methods are considered reliable. Since the utilization of such methods is a computationally demanding task, only the approximate 95% confidence intervals are presented in the following example.

APPLICATION TO FIELD EXPERIMENTS

The bromide breakthrough data observed at monitoring wells S1 and S2 from the experiments Tracer8 and Tracer11 were used to validate the well-to-well recirculation solute transport model. For each data set, the best estimates of the three unknown parameters V , D , and q were obtained by the estimation methodology previously described. The fourth parameter of the model, R , was set equal to unity, because bromide was considered as a conservative tracer. Since the estimation of the model parameters depends critically on the early and late parts of the observed breakthrough responses, to improve convergence only these portions of the breakthrough histories were employed. The parameter estimates, together with relevant statistics, are given in Table 12.1. The relatively narrow 95% confidence limits of the estimated parameters, as well as the close agreement of the parameter estimates obtained for the two observed tracer concentration profiles, indicate that the model can simulate adequately the bromide transport and the solute recirculation effects, at least within the experimental sub-zone.

TABLE 12.1 ESTIMATED TRANSPORT PARAMETERS FOR THE BROMIDE BREAKTHROUGH DATA OF EXPERIMENTS TRACER8 AND TRACER11

	Parameter	Estimate	Standard Deviation	Approximate 95% Confidence Limits	
				Lower	Upper
<u>Tracer8: Monitoring Well S1</u>					
	V (m/h)	0.119	0.003	0.113	0.125
	D (m ² /h)	0.032	0.004	0.024	0.040
	q (—)	0.138	0.005	0.127	0.149
<u>Tracer8: Monitoring Well S2</u>					
	V (m/h)	0.123	0.002	0.120	0.127
	D (m ² /h)	0.032	0.002	0.027	0.037
	q (—)	0.154	0.005	0.145	0.164
<u>Tracer11: Monitoring Well S1</u>					
	V (m/h)	0.113	0.003	0.107	0.119
	D (m ² /h)	0.032	0.004	0.024	0.040
	q (—)	0.135	0.009	0.116	0.154
<u>Tracer11: Monitoring Well S2</u>					
	V (m/h)	0.094	0.001	0.091	0.096
	D (m ² /h)	0.021	0.002	0.018	0.025
	q (—)	0.181	0.008	0.165	0.197

The actual bromide breakthrough responses of experiment Tracer8 observed at sampling locations S1 and S2, together with the model simulated profiles, are shown in Figures 12.2 and 12.3, respectively. Similarly, the breakthrough responses of experiment Tracer11 observed at sampling locations S1 and S2, together with the model simulated profiles, are shown in Figures 12.4 and 12.5, respectively. Good agreement between the experimental data and the simulated concentration history is shown for both cases. Clearly, the observed data incorporate some experimental error caused mainly by slight inconsistencies in daily calibrations of the analytical apparatus. Such variations in the observed data cannot be simulated. Furthermore, the one-dimensional, well-to-well recirculation solute transport model cannot account for the inhomogeneities and the three-dimensional nature of the real environment. Nonetheless, for experiment Tracer8 there is remarkably good agreement between the parameter estimates for V and D at the two different monitoring wells, S1 and S2, as seen in Table 12.1. Good agreement is also observed between the model parameter estimates for experiments Tracer8 and Tracer11 at monitoring well S1. However, the parameter estimates for the two different experiments at monitoring well S2, as well as the parameter estimates for the two different monitoring wells, S1 and S2, of experiment Tracer11 differ by 20 to 50 percent. For Tracer11 the experimental data at monitoring well S2 indicate a reduction in both V and D, and an apparent increase in q. This might be attributed to the changes in the permeability of the aquifer caused possibly by the biostimulation experiments conducted during the one-year time lag between the two tracer experiments.

To demonstrate the advantage of the well-to-well recirculation model, the classical advection-dispersion model is employed to fit the bromide breakthrough responses of experiment Tracer8. The simulated concentration histories at sampling locations S1 and S2 for the case of fixed injection concentration of bromide are shown in Figures 12.6a and 12.6b, respectively. For the case where the injection concentration is considered as an additional fitting parameter, the simulated profiles at sampling locations S1 and S2 are shown in Figures 12.6c and 12.6d, respectively. For both cases, the fitted values for V at S1 and S2 are reasonable (see Table 12.2), but the estimated 95% confidence limits are broader than

those obtained by the well-to-well recirculation model. However, the values of the dispersion coefficients are approximately double the values estimated when recirculation is properly taken into account. It should be mentioned that, for the second case, the fitted injection concentration is approximately 30% higher than its true value. Figures 12.6c and 12.6d show visually-good curve matches to the experimental data; however, the estimated parameter values are unrealistic since the classical advection-dispersion model does not fully represent the physical system.

SUMMARY

A semi-analytical and an approximate analytical solution to the one-dimensional advection-dispersion transport model accounting for well-to-well recirculation have been presented. Solutions are given for a flux-type inlet boundary condition and a semi-infinite medium. Sorption is assumed to be governed by a linear equilibrium isotherm.

Bromide breakthrough concentration profiles obtained from the transport studies at the Moffett site (Section 5), were used to validate the model. Parameter estimates for the velocity, dispersion coefficient, recirculation rate, and the associated 95% confidence intervals were determined by nonlinear least-squares regression. Good agreement was shown between the observed tracer breakthrough responses and the simulated concentration history.

TABLE 12.2 ESTIMATED TRANSPORT PARAMETERS OBTAINED BY THE CLASSICAL A-D MODEL FOR THE BROMIDE BREAKTHROUGH DATA OF EXPERIMENT TRACER8

Parameter	Estimate ^a	Standard Deviation	Approximate 95% Confidence Limits		
			Lower	Upper	
<u>Monitoring Well S1</u>					
V (m/h)	0.123 (0.112)	0.019 (0.007)	0.086 (0.097)	0.161 (0.126)	
D (m ² /h)	0.062 (0.114)	0.034 (0.022)	0.005 (0.069)	0.129 (0.158)	
<u>Monitoring Well S2</u>					
V (m/h)	0.128 (0.115)	0.013 (0.006)	0.103 (0.103)	0.155 (0.127)	
D (m ² /h)	0.083 (0.130)	0.034 (0.023)	0.016 (0.084)	0.150 (0.176)	

^a Estimates in parentheses are obtained with injection concentration as an additional fitting parameter.

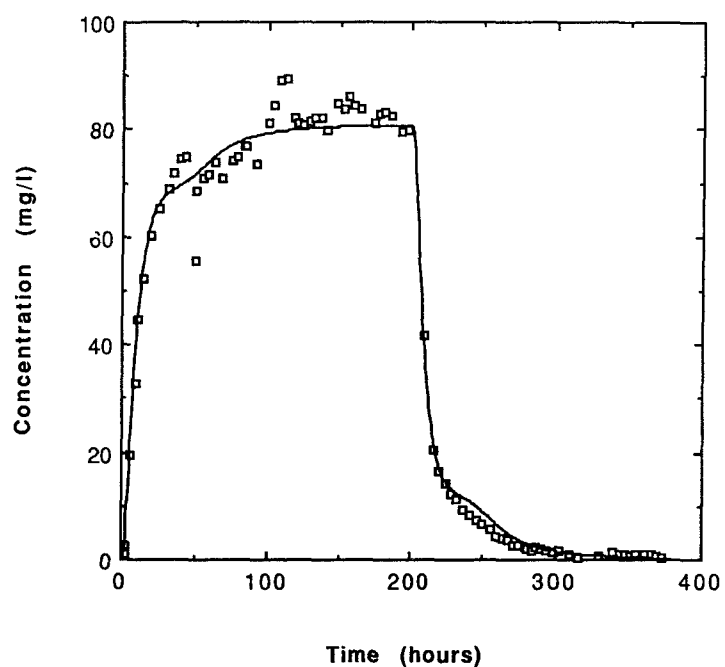


Figure 12.2. Bromide concentration breakthrough data of experiment Tracer8 observed at S1 (squares), and simulated concentration history (solid curve).

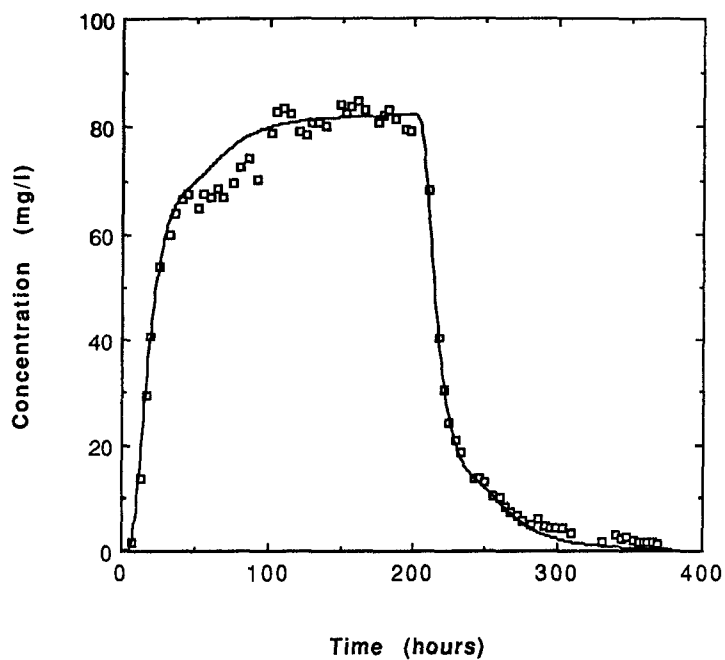


Figure 12.3. Bromide concentration breakthrough data of experiment Tracer8 observed at S2 (squares), and simulated concentration history (solid curve).

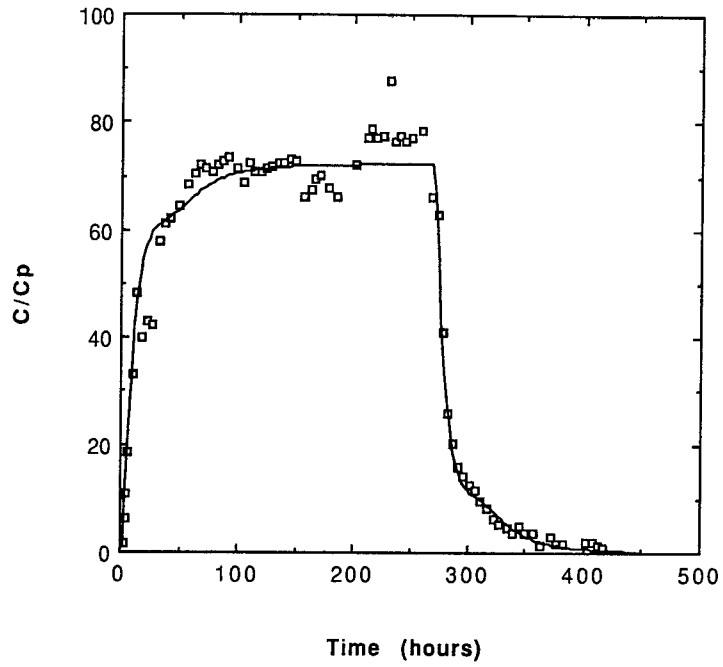


Figure 12.4. Bromide concentration breakthrough data of experiment Tracer11 observed at S1 (squares), and simulated concentration history (solid curve).

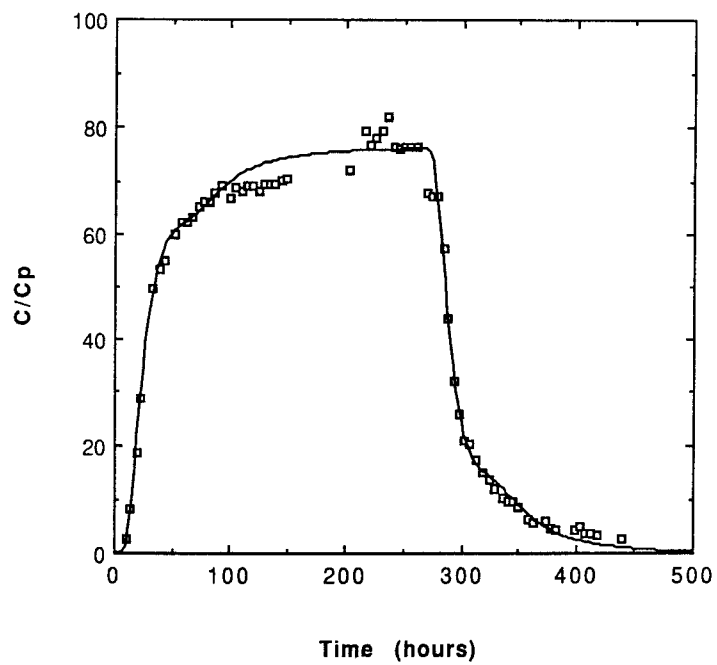


Figure 12.5. Bromide concentration breakthrough data of experiment Tracer11 observed at S2 (squares), and simulated concentration history (solid curve).

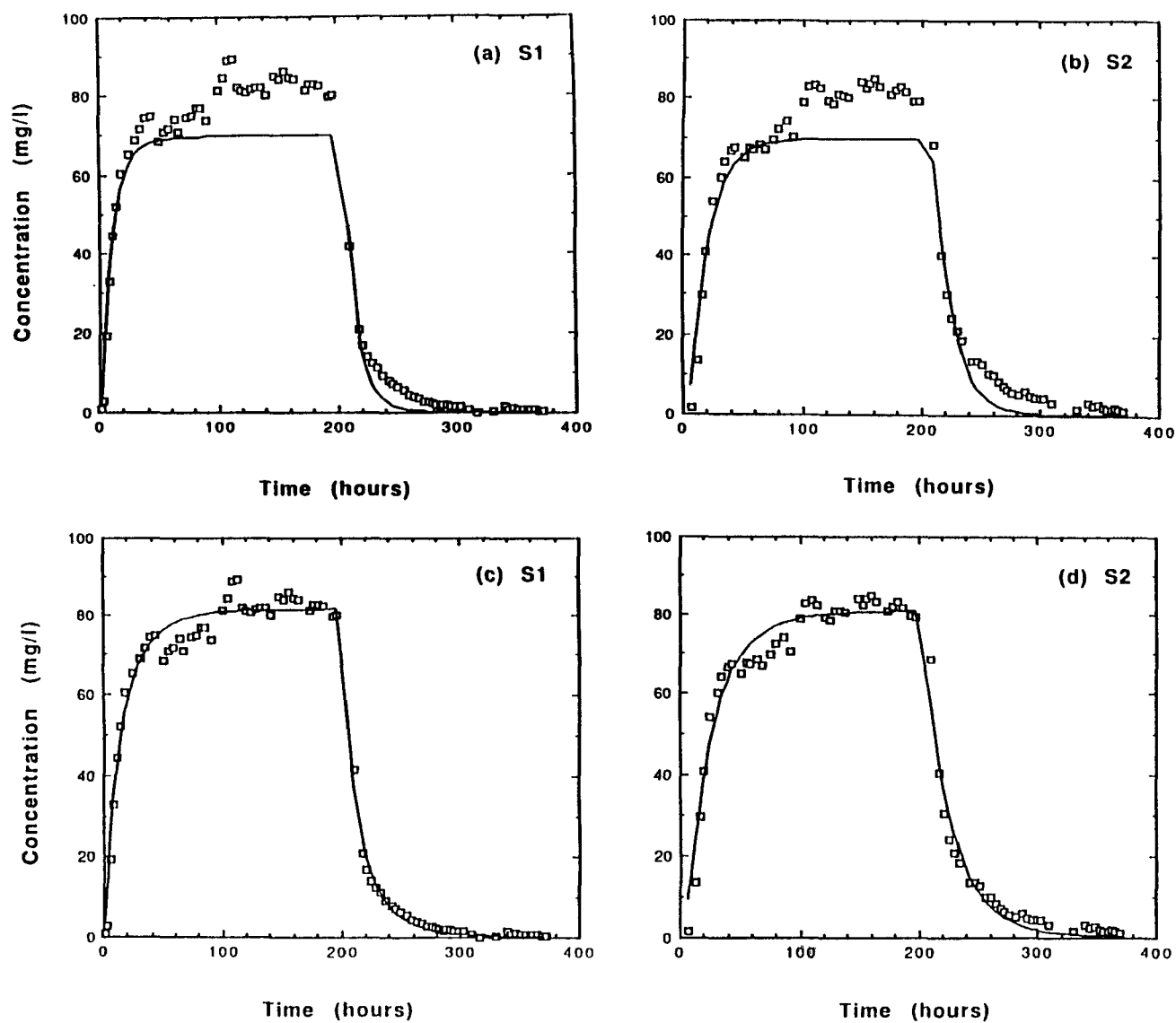


Figure 12.6. Curve matching with the two-parameter (V and D) classical advection-dispersion model to Tracer8 data observed at (a) S1, (b) S2, and with C_p as an additional fitting parameter, (c) S1, and (d) S2.

SECTION 13

BIOSTIMULATION AND BIOTRANSFORMATION MODELING

Lewis Semprini and Perry McCarty

INTRODUCTION

A non-steady-state model was developed for simulating the results of the field experiments. The model includes basic processes of microbial growth, utilization of the electron donor and electron acceptor, and the biotransformation of the chlorinated aliphatics as secondary substrates. Transport processes of advection, dispersion, and sorption in porous media are included in the model formulation.

Model simulations provide a quantitative means of evaluating the field results. The model also permits comparisons of field results with studies performed in the laboratory. Simulations of possible restoration scenarios can be made also using the calibrated model.

MODEL DEVELOPMENT

The non-steady-state model that was developed has features similar to those described by Molz et al. (1986b) and Borden and Bedient (1986). The basic features included in the model are summarized in Table 13.1. The contaminants and the electron donor (methane) and electron acceptor (oxygen) are assumed present as dissolved or sorbed onto the aquifer solids. The model was developed for several flow geometries, including linear (uniform) flow and radial flow. Based on the results of tracer simulations and 2-D modeling using RESSQ (discussed in Section 5), the flow between the injection wells and the monitoring wells was simplified to 1-D uniform. The model presented here and the resulting simulations are for the uniform flow case.

The model incorporates the basic microbial rate processes into the partial differential equations describing solute transport in porous media. Microbial growth and electron donor and acceptor utilization are modeled using Monod kinetics, assuming that rates are functions of aqueous substrate concentrations. The biomass is assumed to be an attached shallow biofilm that is fully-penetrated by the substrate, i.e., there are no substantial concentration gradients within the film. Sorption of components is modeled as either an equilibrium or non-equilibrium process.

The rates of microbial growth and decay are assumed functions of both electron donor and acceptor (Kissel et al., 1984; Molz et al., 1986b; Borden and Bedient, 1986):

$$\frac{dX_a}{dt} = X_a k Y \left(\frac{C_D}{K_{SD} + C_D} \right) \left(\frac{C_A}{K_{SA} + C_A} \right) - b X_a \left(\frac{C_A}{K_{SA} + C_A} \right) \quad (13-1)$$

where X_a = cell concentration (mg/l), k = maximum utilization rate (g donor/g cell-d), Y = yield coefficient (g cells/g donor), K_{SD} = donor saturation constant (mg donor/l), K_{SA} = acceptor saturation constant (mg acceptor/l), b = cell decay coefficient (d^{-1}), and C_D and C_A are the concentration of the appropriate electron donor and the electron acceptor (mg/l), respectively. The values of C_D and C_A are identical to local concentration in the advecting pore water, owing to the assumption of a shallow biofilm.

TABLE 13.1. BASIC FEATURES OF THE NON-STEADY-STATE BIOTRANSFORMATION MODEL

1-D Transport
Advection, Dispersion, Sorption
Linear, Radial, and Variable Volume Geometries
Monod Kinetics
Electron Donor and Electron Acceptor
Shallow Biofilm of Microorganisms
Sorption
Equilibrium
Non-Equilibrium
Secondary Substrate Biotransformation Kinetics
Monod Kinetics
Competitive Inhibition Kinetics
Boundary Conditions Which Permit Cyclic Pulsing of Methane and Oxygen

Rates of utilization of electron donor and acceptor are given by equations (13-2) and (13-3), respectively:

$$\frac{dC_D}{dt} = -k X_a \left(\frac{C_D}{K_{SD} + C_D} \right) \left(\frac{C_A}{K_{SA} + C_A} \right) \quad (13-2)$$

$$\frac{dC_A}{dt} = -k F X_a \left(\frac{C_D}{K_{SD} + C_D} \right) \left(\frac{C_A}{K_{SA} + C_A} \right) - d_c f_d b X_a \left(\frac{C_A}{K_{SA} + C_A} \right) \quad (13-3)$$

where F is the ratio of electron acceptor to electron donor utilization for the biomass synthesis (g acceptor/g donor), d_c = cell decay oxygen demand (g O_2 /g cells), and f_d is the fraction of cells that is biodegradable (McCarty, 1975). The DO demand from secondary substrate utilization was not included in equation (13-3), since the concentrations studied in the field test were much lower than those of the primary substrate.

Several different kinetic models were incorporated for the transformation of the chlorinated organics as secondary substrates. It was assumed the secondary substrates were oxidized by cometabolism, i.e., no energy for growth resulted. The simplest model used is the Monod model (McCarty, 1984):

$$\frac{dC_2}{dt} = -X_a k_2 \left[\frac{C_2}{K_{S2} + C_2} \right] \quad (13-4)$$

where k_2 = maximum utilization rate of the secondary substrate (g secondary/g cell-d), K_{S2} = secondary substrate saturation coefficient (mg secondary/l), and C_2 is the concentration of the secondary substrate.

The second model is that of competitive inhibition between a secondary substrate and the electron donor adapted from a multiple substrate model (Bailey and Ollis, 1986):

$$\frac{dC_2}{dt} = -X_a k_2 \left[\frac{C_2}{K_{S2} + C_2 + \frac{K_{S2}}{K_{SD}} C_D} \right] \quad (13-5)$$

With this model the rate of transformation of the secondary substrate would be inhibited by the presence of methane, the electron donor, as an alternative substrate. This inhibitory effect is represented by the last term in the denominator of equation 13-5. Inhibition increases with increasing C_D and decreasing K_{SD} .

The criteria of Rittmann and McCarty (1980) and Suidan et al. (1987) indicate that the assumption of a fully-penetrated biofilm without external or internal mass-transfer limitations, implied in the above formulations, is appropriate for the conditions of the field experiments. This permits a greatly simplified model. The assumption that the biomass is essentially all attached to aquifer material also appears appropriate (Harvey et al., 1984). Thus, transport of the microbial mass is not incorporated and equation (13-1) is directly used to model the change in microbial mass with time.

The 1-D uniform transport of the electron donor, electron acceptor, and the secondary substrate is governed by:

$$\frac{\partial C}{\partial t} + \frac{\rho_b}{\theta} \frac{\partial \bar{C}}{\partial t} = D_h \frac{\partial^2 C}{\partial x^2} - V \frac{\partial C}{\partial x} \quad (13-6)$$

where C is the concentration in the liquid phase (mg/l), \bar{C} is the concentration of the sorbed solute on the solid phase (mg/kg), D_h is the hydrodynamic dispersion coefficient (m^2/d), V is the average interstitial fluid velocity (m/d), x is the spatial coordinate (m), ρ_b is the bulk density of the solid matrix (kg/l), and θ is the porosity. Based on our laboratory studies, sorption onto the aquifer solids was modeled as linear and reversible, with the equilibrium sorbed-phase concentration given by:

$$\bar{C} = K_d C \quad (13-7)$$

where K_d is the partition coefficient (l/kg).

For the case of equilibrium sorption, substitution of equation (13-7) into (13-6) leads to the following transport equation in terms of the liquid-phase concentration:

$$R \frac{\partial C}{\partial t} = D_h \frac{\partial^2 C}{\partial x^2} - V \frac{\partial C}{\partial x} \quad (13-8)$$

where R is the retardation factor for the solute (Hashimoto et al., 1964):

$$R = 1 + \frac{\rho_b}{\theta} K_d \quad (13-9)$$

For the non-equilibrium case, the simple first-order linear nonequilibrium model was used:

$$\frac{d\bar{C}}{dt} = \alpha (K_d C - \bar{C}) \quad (13-10)$$

where α is the rate coefficient for mass transfer between the phases (d^{-1}). This simple model represents a reasonable approximation of more complex sorption models that include diffusive transfer between mobile and immobile zones (van Genuchten, 1985).

Substituting equation (13-10) into equation (13-6) yields:

$$\frac{\partial C}{\partial t} = D_h \frac{\partial^2 C}{\partial x^2} - V \frac{\partial C}{\partial x} - \frac{\rho_b}{\theta} \alpha (K_d C - \bar{C}) \quad (13-11)$$

Equations (13-10) and (13-11) must be solved to completely describe transport with non-equilibrium sorption.

The kinetic expressions for utilization of the electron donor and acceptor, and the biotransformation of the secondary substrate, are added to the transport equations. For the case of equilibrium sorption the rate expressions (13-2, 13-3, and 13-4 or 13-5) are added to equation (13-8):

$$\frac{\partial C_D}{\partial t} = \frac{D_h}{R_D} \frac{\partial^2 C_D}{\partial x^2} - \frac{V}{R_D} \frac{\partial C_D}{\partial x} - \frac{kX_a}{R_D} \left(\frac{C_D}{K_{SD} + C_D} \right) \left(\frac{C_A}{K_{SA} + C_A} \right) \quad (13-12)$$

$$\frac{\partial C_A}{\partial t} = \frac{D_h}{R_A} \frac{\partial^2 C_A}{\partial x^2} - \frac{V}{R_A} \frac{\partial C_A}{\partial x} - \frac{kFX_a}{R_A} \left(\frac{C_D}{K_{SD} + C_D} \right) \left(\frac{C_A}{K_{SA} + C_A} \right) - \frac{d_c f_d X_a}{R_A} \left(\frac{C_A}{K_{SA} + C_A} \right) \quad (13-13)$$

$$\frac{\partial C_2}{\partial t} = \frac{D_h}{R_2} \frac{\partial^2 C_2}{\partial x^2} - \frac{V}{R_2} \frac{\partial C_2}{\partial x} - \frac{k_2 X_a}{R_2} \left(\frac{C_2}{K_{S2} + C_2} \right) \quad (13-14)$$

Similar expressions were developed for the competitive inhibition and the non-equilibrium sorption cases.

For a semi-infinite system, the following initial and boundary conditions are applied:

$$C(x,0) = f(x) \quad (t = 0) \quad (13-15a)$$

$$-D_h \frac{\partial C}{\partial x} + VC = Vg(t) \quad (x = 0) \quad (13-15b)$$

$$\frac{\partial C}{\partial x}(L,t) = 0 \quad (x = L) \quad (13-15c)$$

where $f(x)$ can take several forms: a constant value spatially, or a value that varies with distance. To specify initial conditions, values must be estimated for the concentrations of microbial mass, electron donor, electron acceptor, and secondary substrate. The inlet is represented by a third- or flux-type boundary condition for mobile components in equation (13-15b); where the parameter $g(t)$ can take several forms, such as a constant value in time (as continuous feed), a pulse-type distribution, or a variable concentration distribution. Since the microbial mass is assumed immobile, a constant concentration boundary condition (first type) was used at $x = 0$. The outlet boundary condition used is that of a semi-infinite column of length L .

Numerical Method

For the equilibrium sorption case, a set of four nonlinear partial differential equations (13-1, 13-12, 13-13, 13-14), and in the nonequilibrium case a set of 8 equations, must be solved subject to the initial and boundary conditions given in equations (13-15a,b,c). The equations are coupled with as many as three of the dependent variables contained in an equation. Numerical methods are required to solve these equations. Methods for solving these types of equations are given by Molz et al. (1986b), Borden and Bedient (1986), and Speitel et al. (1987).

This model was formulated using the finite difference method that was solved by numerical integration. The method is similar to the one used by Borden and Bedient (1986). The method involves:

- 1) Discretization of the spatial terms on the right side of the equation using finite differences to produce a set of ordinary differential equations.
- 2) Simultaneous solution of the resulting sets of ordinary differential equations by numerical integration, using a fixed-step-size, fourth-order accurate, Runge-Kutta technique (Gear, 1971).

The Quick formulation (Leonard, 1979) was used for the spatial discretization, which significantly reduces the degree of numerical dispersion. The method uses central differences for the dispersion term and, for this 1-D case, a four-node formulation for the advection term given by:

$$\frac{dC_i}{dx} = \frac{C_{i-1} - \frac{1}{2}C_i - \frac{1}{3}C_{i+1} - \frac{1}{6}C_{i-2}}{\Delta x} \quad (13-16)$$

The solution is explicit in nature and easy to program and modify. The Runge-Kutta method of numerical integration was chosen since it executes significantly faster than other methods, while achieving sufficient accuracy (Gear, 1971). The Runge-Kutta routine solves the equations by stepping forward in time, using four internal steps for each whole time step. Concentrations of biomass, electron donor, electron acceptor, and the chlorinated aliphatic are updated at each internal time step. Thus, a simultaneous solution of the equations is achieved. The numerical code was written in FORTRAN, and the simulations were performed on an IBM-AT.

The solution can become unstable if too large a time step is taken. For the model simulations reported here, however, stability problems were encountered only when the biostimulated biomass accumulated to high concentrations in the node nearest the input boundary, resulting in very fast transformation rates. Decreasing the time step overcame this instability. For most simulations, stability was achieved when the time step, Δt , satisfied the criteria given in Bear (1979):

$$\Delta t < \left(\frac{\Delta x}{\left(\frac{2D_h}{\Delta x} + V \right)} \right) \quad (13-17)$$

To verify the numerical code, the numerical model was compared with analytical solutions to equation (13-8). A comparison was made between numerical and analytical solutions for example A1-2 in van Genuchten and Alves (1982) for the breakthrough of a short injected pulse at the outlet of a semi-infinite column. Agreement was excellent, with little numerical dispersion. Numerical simulations were also in excellent agreement with analytical results given in example C8-2 of van Genuchten and Alves (1982), which includes a first-order decay term and zeroth-order source term added to equation (13-8).

The numerical solution of equations (13-1), (13-12), (13-13), and (13-14) was checked by comparing: 1) the total steady-state biomass predicted by the model, and 2) the total biomass determined by kinetics and mass balance in a plug flow system. The plug flow analytical expression is given by

$$X_m = \frac{Y C_{A0} Q}{b} \quad (13-18)$$

where X_m represents the total steady-state biomass, C_{A0} is the input substrate concentration, and Q is the volumetric flow rate. Comparison at several different flow rates and substrate concentrations indicated deviations of less than 1%.

Simulations of the transport portion of the non-equilibrium sorption model were found to be in excellent agreement with the analytical solutions of Valocchi (1986) for the case of converging radial flow. These equations demonstrated that the numerical code solves correctly the set of coupled nonlinear partial differential equations.

MODEL SIMULATIONS OF BIOSTIMULATION EXPERIMENTS

Model simulations were compared with the results of biostimulation and biotransformation experiments presented in Section 6. The ability of the model to simulate the transient uptake of methane and DO observed in the field experiments was tested. Since the biotransformation of the chlorinated organics depends on the biosimulation of the methanotrophic biomass, simulations of the biotransformation of the chlorinated organics were attempted only after good matches were obtained to the biostimulation portions of the experiments.

Model Inputs

Model simulations of transient DO and methane concentration responses at the S1 and S2 observation wells assumed that the flow between the injection and monitoring wells can be represented by 1-D uniform flow. An analysis of the induced flow field created by the operating conditions was performed using RESSQ, a 2-D semi-analytical transport model (Javandel et al., 1984). Figure 13.1 illustrates the comparative distance traveled by injected fluid with time, along the flow path between injection and observation wells for the 2-D model (squares) and the 1-D model (line). While some deviation occurs close to the injection well, the velocity is relatively constant over much of the distance. Thus, the 1-D model appears adequate for these initial simulations.

Breakthroughs of injected bromide, methane, and DO during the early stages of the biostimulation experiments were used to estimate the average interstitial fluid velocity. Shown in Figure 13.2 is the model match of field observations at the S1 well. Consistent with the uniform flow assumption, the 1-D transport equation fits these data and the S2 data well using the same groundwater velocity of 2.9 m/d. The results confirm that these three constituents are not retarded with respect to fluid flow; thus, retardation factors for them were set to 1 in the model simulations. Hydrodynamic dispersion coefficients ranged from 0.6 m²/d for well S1 to 1.0 m²/d for well S2.

Model simulations are presented for two sets of field data, obtained from the first and second years' tests, termed Biostim1 and Biostim2, respectively (Section 6). The second year's test was started approximately eight months after methane and oxygen addition had been terminated in the first year's tests.

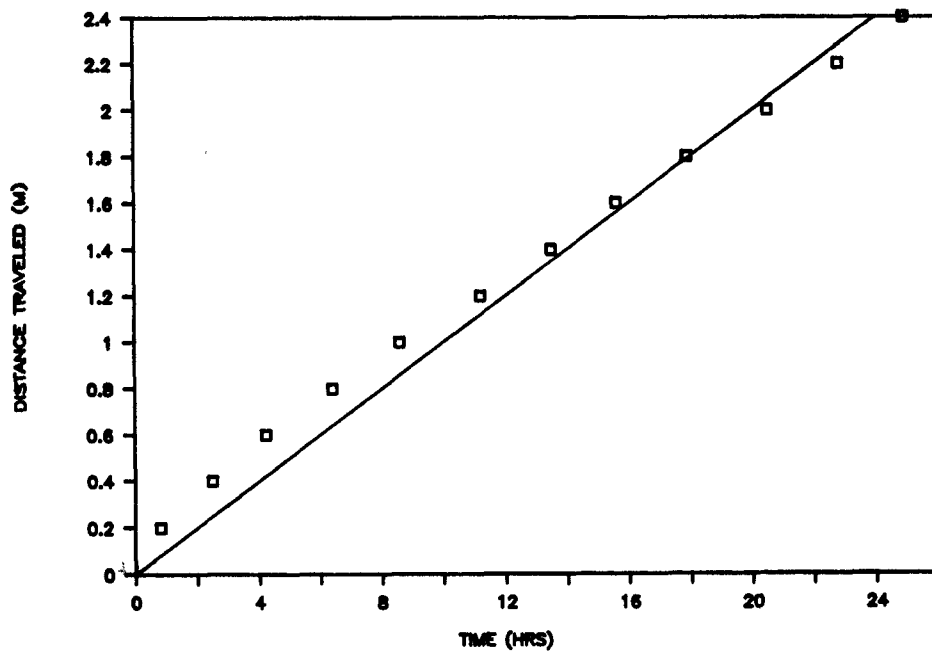


Figure 13.1. Arrival of fluid at distances along a direct path from the injection to observation wells under hydraulic conditions of the field experiment based on simulations using RESSQ.

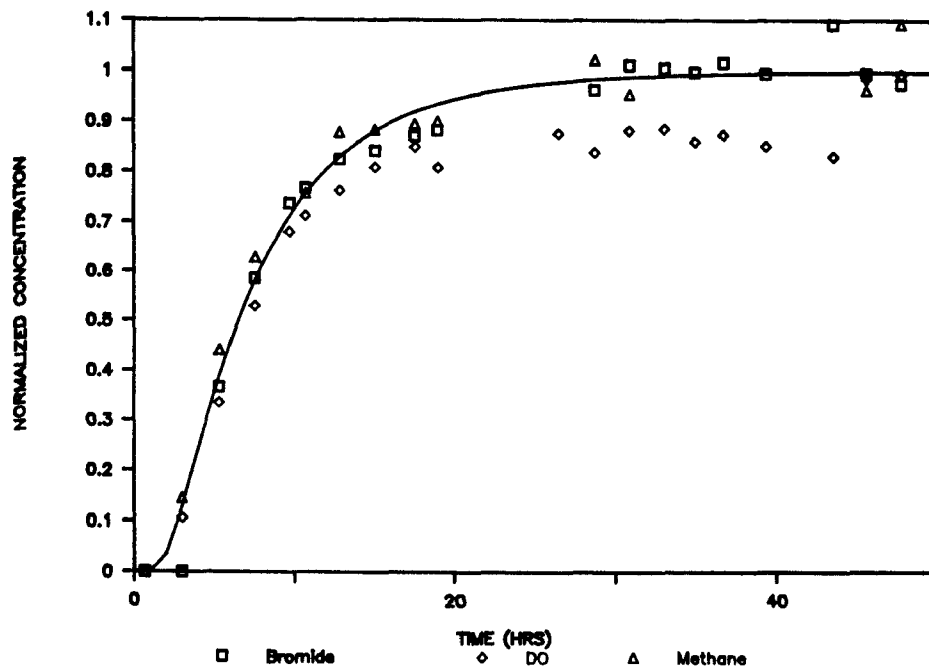


Figure 13.2. Breakthrough of bromide, methane, and DO at the S1 observation well and the fit to equation (13-4).

Table 13.2 lists the model input parameters, which were obtained by independent means of estimation to the extent possible, including: 1) measurement in the field or laboratory, 2) estimation based on literature values, or 3) adjustment within a range of literature values to obtain good model fit. A heuristic fitting procedure was used. Adjusted values were constrained within a reasonable range based on literature or theoretically derived values. As indicated in Table 13.2, dispersion coefficients lower than those derived from the fit to the complete breakthrough (Figure 13.2) were required to match the field response to alternate pulsing of DO and methane.

Table 13.3 contains operational data used in the model. The use of 24 nodes over an interval of 2.4 m was found to provide sufficient numerical accuracy. Time steps between 0.0025 d and 0.01 d were sufficient to maintain stability for simulations of 20 to 60 days.

Tables 13.2 and 13.3 show different input values of the dispersion coefficient, and initial microbial concentrations, were required to match responses at the S1 and S2 wells. Also, in the Biostim1 experiment, the injected fluid accounted for 90% and 80% of the fluid sampled at wells S1 and S2, respectively. The 10 to 20% dilution by native groundwater was incorporated into the 1-D simulation by adjusting the injection concentrations of methane and DO. Thus, separate simulations were required for the response at the S1 and S2 wells.

TABLE 13.2. INPUT PARAMETERS USED IN THE BIOSTIMULATION MODEL SIMULATIONS

Parameter	Biostim1	Biostim2	Value Basis	Literature Values	Refs.
V (m/d)	2.9	(S1) 2.9 (S2) 3.3	M	-	
D _h (m ² /d)	(S1) 0.165 (S2) 0.25	(S1) 0.165 (S2) 0.25	F	-	
k (g/g-d)	2.30	2.0	F	3.5-5 (32°C)	C
K _{SD} (mg/l)	5.5	1.0	F	0.2-0.3	A, B
K _{SA} (mg/l)	1.0	1.0	L	0.01-0.1	C, D
Y (mg/mg)	0.5	0.5	L	0.35-1.1	C, E, F, G
b (d ⁻¹)	0.15	0.10	F	0.15-0.4	E, F, G
F (mg/mg)	2.4	2.4	F	2.2-4	C, E, F
f _d	0.8	0.8	L	0.8	H
d _c (mg/mg)	1.42	1.42	L	1.42	H
R _d	1.00	1.00	M	-	
R _a	1.00	1.00	M	-	

M = measured; F = fitted; L = literature (held constant).

References: A, Ferenci et al., 1975; B, Harrison, 1973; C, Wilkinson et al., 1974; D, Morinaga et al., 1979a; E, Morinaga et al., 1979b; F, Whittenbury et al., 1970; G, Heijnen and Roels, 1981; H, McCarty, 1975.

TABLE 13.3. MODEL SETUP PARAMETERS

Parameter	Biostim1			Biostim2	
Total Simulation Length (m)	2.4			2.4	
Num. Nodes	24			24	
Δx (m)	0.1			0.1	
Δt (d)	0.01			0.0025	
<u>Initial Conditions</u>					
X_{ai} (mg/l)	(S1) 0.015 (S2) 0.035			1.13 ^a 1.7 ^a	
C_{Di} (mg/l)	0.0			0.0	
C_{Ai} (mg/l)	0.0			0.0	
<u>Injection Conc.</u>					
C_{Do} (mg/l)	(S1) 18.0 (S2) 16.5 ^b			(S1,S2) 20	
C_{Ao} (mg/l)	(S1) 31.0 (S2) 26.3 ^b			(S1,S2) 36	
<u>Pulse Interval</u>					
t_D (d)	0.01	(0-19.1 d) ^C	0.01	(0-1 d) ^C	
t_D (d)	0.17	(19.1-25 d)	0.02	(1-10 d)	
t_A (d)	0.02	(0-19.1 d)	0.04	(0-1 d)	
t_A (d)	0.34	(19.1-25 d)	0.03	(1-10 d)	

^aaverage value for the distributed concentration over the distance of 2.2 m.

^blower injection concentration to account for dilution by native groundwater.

^cexperimental interval over which the pulse length was used.

Simulation of the First Season's Test (Biostim1)

Figure 13.3 illustrates the simulation match for methane and DO concentration response at the S2 well for Biostim1. Here, dissolved methane and DO were injected continuously in short alternating pulses. The good simulation match demonstrates that the field response results from biostimulation of indigenous methane-utilizing bacteria. Initially the concentration of methane-utilizing bacteria was sufficiently low so that little uptake was observed. With biostimulation, an increase in the microbial concentration occurred, resulting in a marked decrease in methane and DO concentrations beginning at about 200 hrs. The simulated biomass increase with time is illustrated in Figure 13.4. A fairly uniform spatial increase in

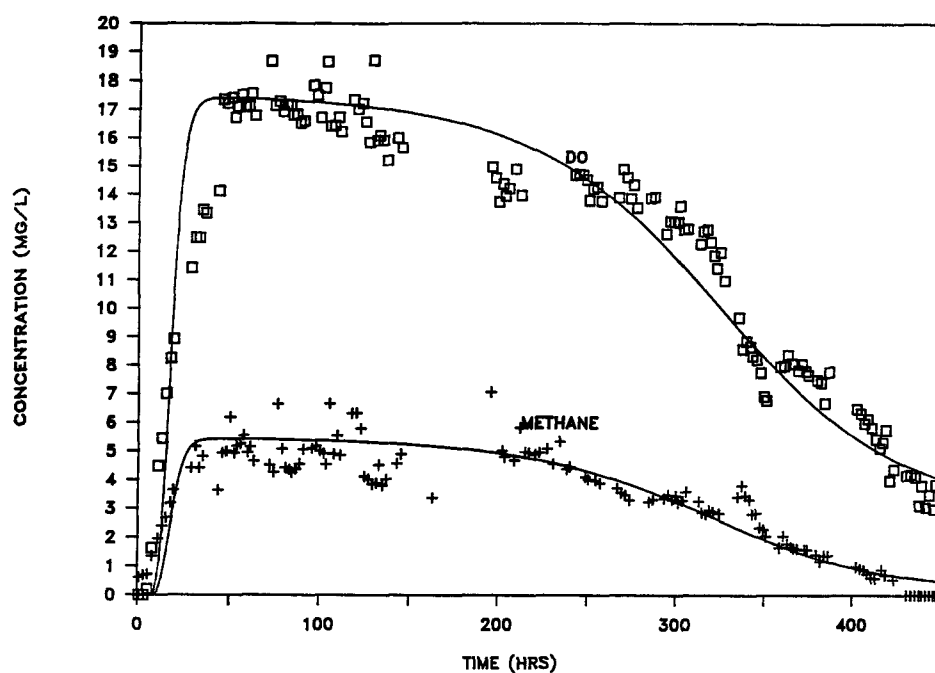


Figure 13.3. Model simulation and observed methane and DO response at the S2 observation well in the Biostim1 experiment.

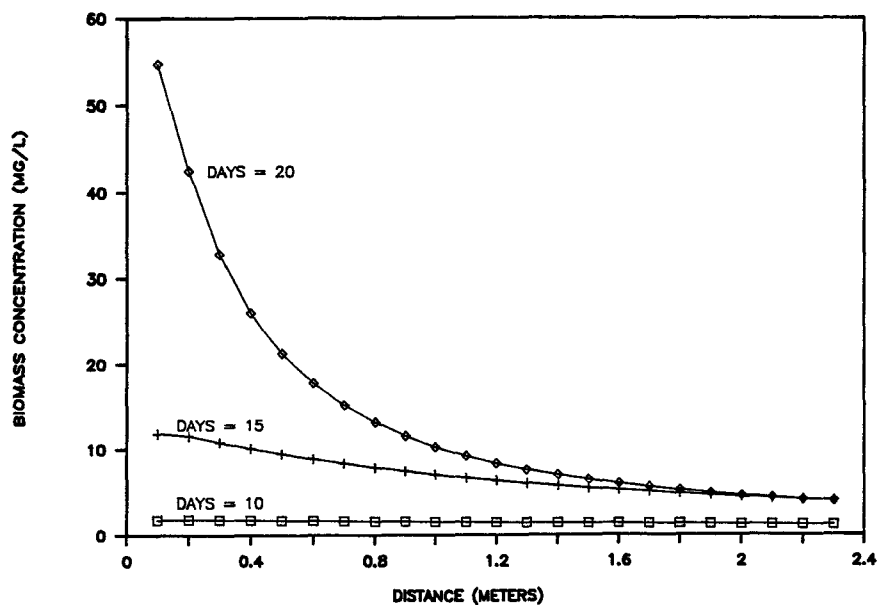


Figure 13.4. Snapshots of the predicted distribution of methane-utilizing biomass during Biostim1 experiment.

biomass is predicted during the first 10 days, during which methane was uniformly available through out the test zone. However, with time, the methane-utilizing biomass increases to a greater extent in closer proximity to the injection well as a result of rapid microbial growth.

The initial biomass concentration was unknown, and thus had to be treated as a major fitting parameter for the model. Other parameters affecting the lag time are k , b , K_{SD} , and F . These are basic rate coefficients for which average literature values were used initially, but slight adjustments were made subsequently to improve model fit. The adjusted values indicated in Table 13.2 are consistent with values measured in the laboratory or determined from theoretical considerations. Values for d_c and f_d were not adjusted. The good fit between model simulations and field results, using coefficients largely derived from basic studies, is encouraging.

Even the initial concentration of methane-utilizing biomass selected to obtain a reasonable simulation for data for S2 is reasonable, based upon acridine orange direct counts of bacterial numbers (Ghiorse and Balkwill, 1983) measured on aquifer solids from the test zone prior to biostimulation (Section 4). Assuming a methanotroph bacterial cell has a mass of 0.5×10^{-13} g, the best-fit initial biomass concentration of 0.035 mg/l is about one thousandth of the estimated enumerated concentration. This appears reasonable, since methanotrophs are expected to represent only a small portion of the total aquifer biomass.

Biomass estimates were also made to match the response at the S1 well (not shown). The best-fit initial biomass of 0.015 mg/l was quite similar to that used for S2 data, considering the heterogeneities in the system. All other parameters were left unchanged in achieving this value.

The fact that S1 and S2 simulations yielded good matches with field results using the same kinetic parameters is not unexpected since the types of methane-utilizers is not expected to vary greatly in the test zone. This is important since it suggests that the model, when calibrated with one set of field data, can be applied to other locations within the same aquifer system. The only parameter that then needs to be adjusted is the initial biomass concentration which is expected to vary spatially.

Pulsing of Electron Donor and Acceptor

The Biostim1 experiment was started with short alternating pulse cycles to simulate continuous injection of methane and DO. Based on model simulations (Figure 13.4), microbial growth would eventually become concentrated near the injection well; this would be undesirable, as it would increase the clogging potential and greatly reduce the desired uniform distribution of methanotrophic biomass in the stimulated zone. In order to reduce these potential problems, the methane and oxygen pulse cycle was increased, as discussed in Section 6.

After 458 hrs of injection, the pulse times of methane- and oxygen-containing injection water were increased from 0.01 and 0.02 d to 0.17 and 0.34 d, respectively. The responses at the S2 and S1 observation wells are illustrated in Figures 13.5 and 13.6, respectively. The simulation results are in good agreement with the field observations.

The DO data are more reliable for evaluations of system response to pulsing because methane concentrations were near the detection limit. The mean DO concentration at the S2 well increased from 3.5 mg/l before pulsing to 4.5 mg/l after pulsing. Both simulations and field data indicated a continued decrease in concentration with time. This predictably resulted from an increased oxygen demand from cell decay as biomass continued to increase in the test zone.

Simulation for the S1 well (Figure 13.6) shows less attenuation in the pulse heights than at S2, which is consistent with field observations and the analytical solutions of Valocchi and Roberts (1983). Greater microbial uptake with longer distance traveled also acts to attenuate the pulse heights at the S2 well.

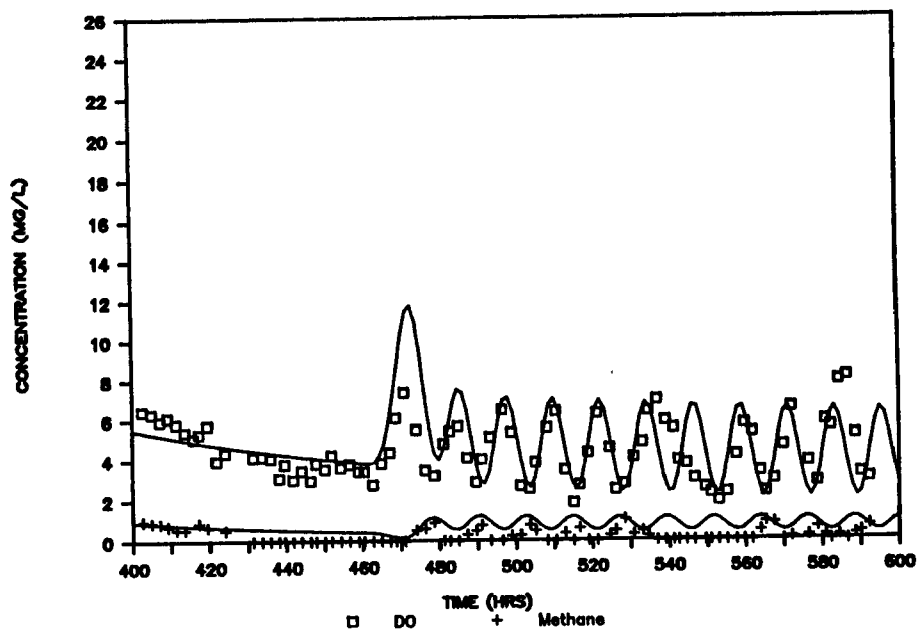


Figure 13.5. Model and field response at the S2 well resulting from the change from short to long alternating pulse cycles.

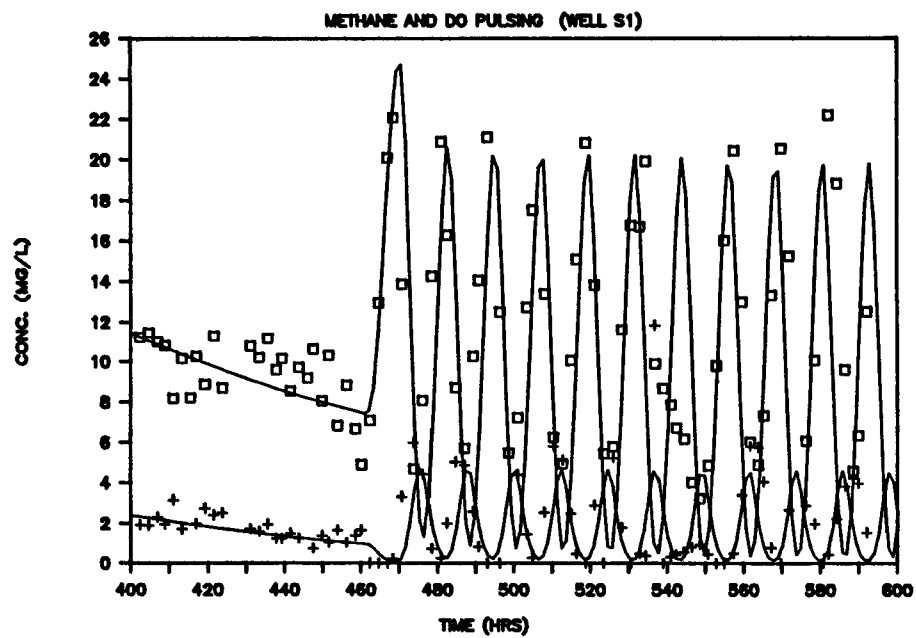


Figure 13.6. Model and field response at the S1 well resulting from the change from short to long alternating pulse cycles.

In order to obtain correct peak attenuations in simulations shown in Figures 13.5 and 13.6, the dispersivity had to be decreased by a factor of 4 below that obtained from a fit of the complete breakthrough data (Figure 13.2). However, this decrease in the dispersivity resulted in a somewhat sharper simulated initial breakthrough of methane and DO compared to the field results (Figure 13.3). This phenomenon was observed when simulating DO pulse experiments before biostimulation (Figure 5.16). The higher values of dispersivity required to fit the complete breakthrough curves perhaps result from fitting the 1-D macroscopic advection-dispersion equation with uniform flow to an aquifer that undoubtedly has vertical variations in hydraulic conductivity. On the other hand, pulsing in the test zone may reflect the response of a highly conductive zone of lower dispersivity, which conveys a larger portion of the sampled groundwater. Tracer and modeling studies by Molz et al. (1986a) support this hypothesis.

Figure 13.7 shows the growth with time of the simulated biomass concentration at a node in the region of the S2 observation well. Biomass concentration reaches a maximum concentration after injecting for 400 hrs (with short pulse cycles). The concentration then decreases due to cell decay as the decreasing amount of methane reaching that node can no longer support the resulting biomass. The initiation of longer pulses at 458 hrs results in a reestablishment of a higher biomass concentration since more methane then reaches this area.

Pulsing Effect on Biomass Distribution

Figure 13.8 presents a snapshot of the predicted spatial distributions of methane and DO during pulsing. Growth of biomass at that instant occurs primarily in the region 0.8 to 1.3 m and 1.5 to 2.2 m from the injection well, where the concentrations of both methane and oxygen overlap. In the next instant in time, the methane peak moves to the right, as does the location of the highest biomass growth rate.

For a given pulsing strategy, biomass would reach some steady-state level after a sufficiently long time. The near steady-state model distributions predicted to result from two different pulse cycle lengths after 120 days are shown in Figure 13.9. With alternate pulses of 4 and 8 hrs, most of the microbial mass would be located within the first meter of the test zone. Increasing the pulse length to 8 and 16 hrs is predicted to help distribute the biomass more uniformly over the test zone. The total biomass present (area under the curves) for this case is less, however, since more methane and oxygen reach the outer boundary and are removed from this particular system.

Simulation of Second Season's Test (Biostim2)

Biostimulation was achieved in the second season of field testing using the same methodology as in the previous year (Section 6). In the second year, methane and DO uptake was observed almost immediately after commencing biostimulation, which implies that a significant population of methanotrophs remained from the previous season of stimulation. Thus, the initial biomass in the simulation model had to be adjusted to fit this response. The initial biomass distribution was assumed to be that illustrated in Figure 13.9 (4 and 8 hr pulses), but reduced in concentration by first-order decay over the eight months of starvation. In addition, the use of rate parameters from the Biostim1 experiment (Table 13.2) did not yield as good matches, predicting more gradual decreases in methane and oxygen concentrations than were observed in the field.

Several rate parameters were adjusted to obtain a good match with second-season field observations, as summarized in Table 13.4. In the resulting comparison for the response at the S1 well shown in Figure 13.10, the more rapid uptake of methane and DO compared to the first year's results (Figure 13.3) is apparent. Both the simulation and the field observations show two peak methane concentrations within the first 60 hr, resulting from a planned increase in the methane injection pulse length after the first 24 hrs in order to supply more methane to the test zone. The model is able to simulate these transient conditions.

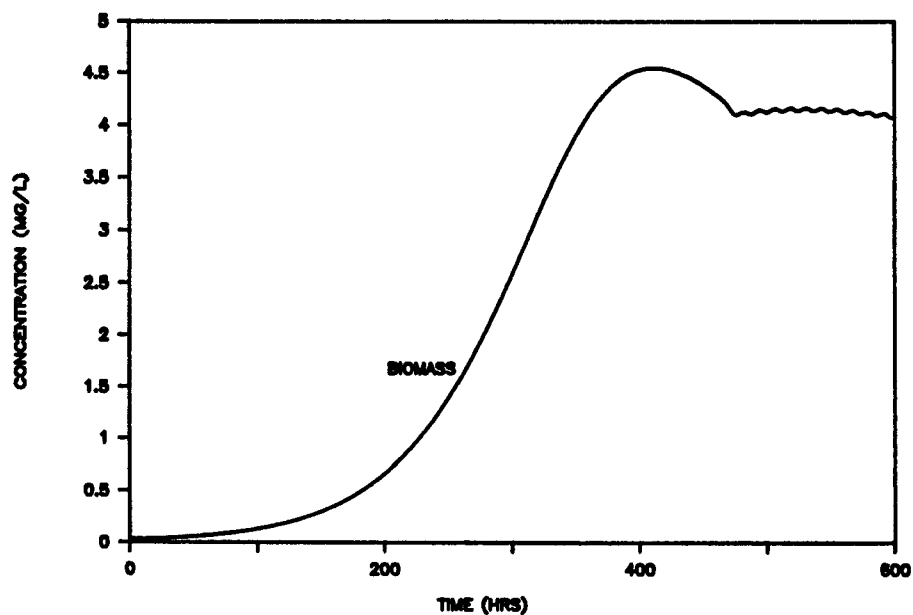


Figure 13.7. Predicted biomass concentration at the node 2.2 meters from the injection well due to biostimulation with short and long pulse cycles.

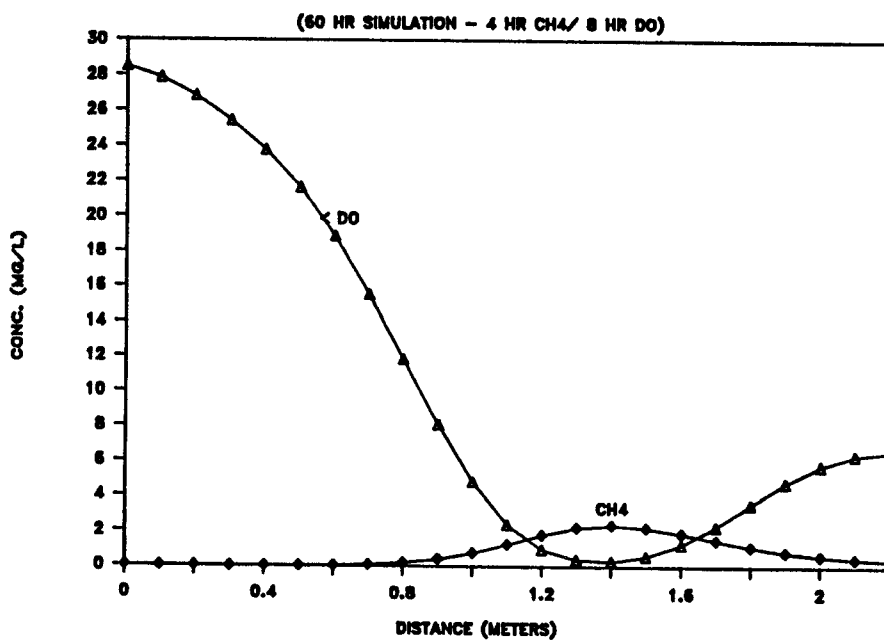


Figure 13.8. Snapshot of the predicted spatial distribution of DO and methane during a DO pulse cycle after a steady-state biomass is achieved.

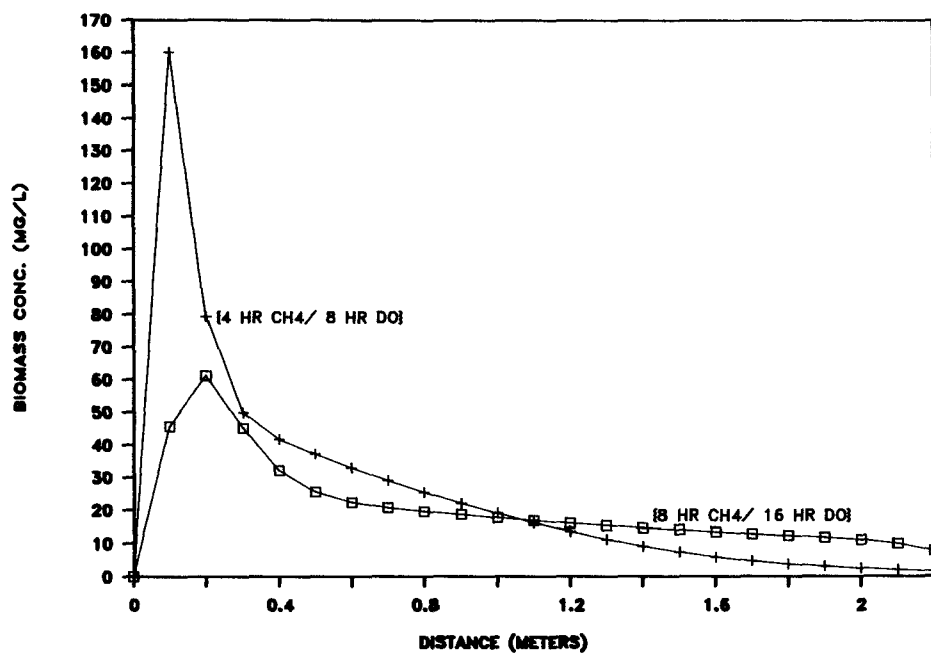


Figure 13.9. Predicted steady-state biomass distributions achieved at two different pulse cycle lengths.

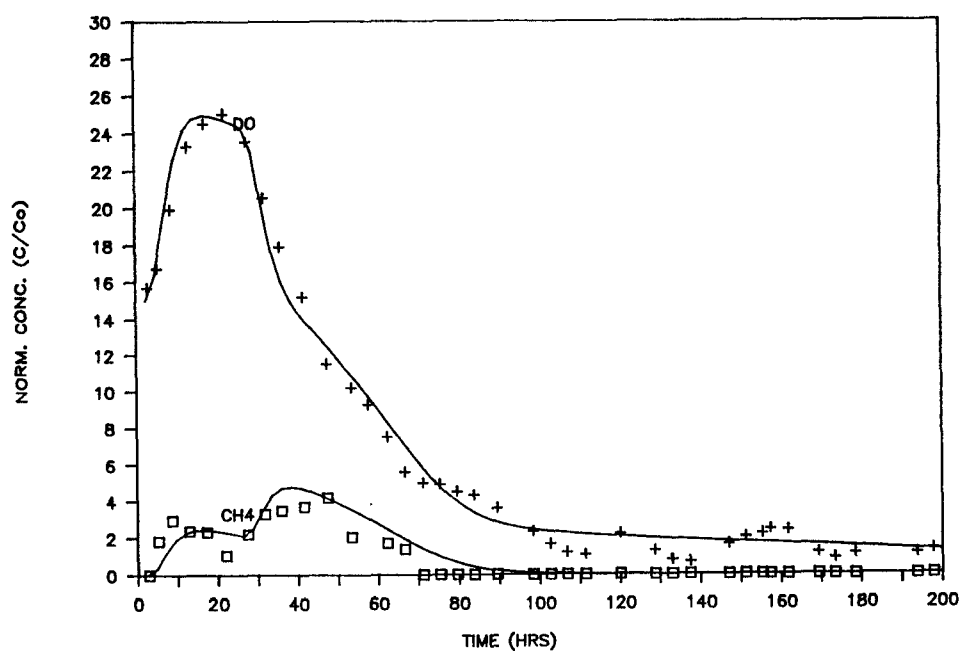


Figure 13.10. Simulated and observed DO and methane response at the S1 observation well during the Biostim2 experiment.

TABLE 13.4. COMPARISON OF ADJUSTED MODEL PARAMETERS FOR THE BIOSTIMULATION EXPERIMENTS (WELL S2)

	Biostim1 (First Year)	Biostim2 (Second Year)	Biostim3 (Third Year)
Initial Biomass (mg/l)	0.035	1.75 ^a	5.75 ^a
k (mg/mg-d)	2.3	2.0	2.0
K _{SD} (mg/l)	5.5	1.0	1.0
k/K _{SD} (l-mg/d)	0.42	2.0	2.0
b (d ⁻¹) (methane and DO)	0.15	0.10	0.10
b' (d ⁻¹) (no methane or DO)	0.01		

^a Average concentration over the 2.2-m simulated interval.

Simulations were also performed on the response at the S2 well (not shown). An initial biomass concentration 50% higher than that used in the S1 simulation was required, which is consistent with simulations of the first year's experiment. This consistency further supports the hypothesis that the S1 and S2 wells do not sample identical zones in the aquifer.

As indicated in Table 13.4, the initial average biomass was increased in the second-year simulation by a factor of 50 over the first year simulation. This represents approximately 6% of the predicted steady-state biomass at the end of the first year (Figure 13.9). The b' value listed in Table 13.4 was required to achieve this estimated 17-fold decrease in biomass over the 8 month resting period, and is substantially lower than the b value used under active biostimulation. During most of the 8 month period, oxygen was not present and, thus, a lower decay rate would be expected.

Table 13.4 also lists the rate coefficients for the two periods. In order to achieve the rapid decrease in methane to low concentrations as observed in the second season, K_{SD} was lowered by a factor of 5, while k was lowered only slightly from the first-year value. These changes resulted in an increase in the ratio of k to K_{SD} by a factor of 5. A lower b was found appropriate as well. These changes are more favorable for reducing methane rapidly to low concentrations, and perhaps reflect an evolution of methanotrophic capability towards a population with greater ecological advantage. A similar change in laboratory column study with acetate as primary substrate was noted by Bouwer and McCarty (1985).

Simulations of the Biostim3 experiment of the third season of field testing also were performed. Uptake of methane was observed to occur even more rapidly than in the second season. The simulations of the Biostim3 experiment match the field observations using the same kinetic parameters as in the second season. The initial microbial mass, however, had to be increased by a factor of 5 compared to that used in the second season simulation.

Summary of Biostimulation Simulations

Model simulations provided good matches to the observed transient uptake of methane and DO in the test zone. The matches indicate a mathematical model combining transport, utilization of the electron donor and acceptor, and microbial growth provide a good representation of the behavior observed in the field tests. This good agreement justifies adopting the simplifying assumption of uniform one-dimensional transport.

Simulations indicated that initial biomass of methane utilizing bacteria was a key fitting parameter. The initial biomass estimates were reasonable when compared with prestimulation microbial

enumerations. Increases in estimated initial biomass over the field seasons indicate that methanotrophic biomass stimulated in the previous year's experiments degraded only very slowly.

Kinetic parameters obtained from model matches are quite reasonable based on laboratory measured values and theoretical considerations. Thus, the model can be used with some confidence in simulating the biostimulation of methanotrophs in the field test.

MODEL SIMULATIONS OF BIOTRANSFORMATION EXPERIMENTS

Model simulations of the biotransformation of chlorinated aliphatics were compared with the results of the second and third seasons of field testing. The simulations were performed after the match to the DO and methane uptake was achieved in the biostimulation simulations previously discussed. The different kinetic models for biotransformation and sorption were evaluated to determine which models best described the behavior observed in the field.

Model Input Parameters

Tables 13.2 and 13.3 contain the model parameters used in the biostimulations. The additional parameters needed for the chlorinated aliphatic decomposition simulations are those for the sorption and biotransformation of the chlorinated aliphatics. The sorption parameters include the retardation factor, for the equilibrium sorption model, and the partition coefficient, K_d , and mass transfer coefficient α , for the first-order kinetic-model. Sorption parameters, lying within the range of values used to fit the breakthrough response of the organics before biostimulation, were used in the model simulations.

Both the Monod and competitive inhibition models for secondary substrate utilization required as inputs the k_2 and K_{S2} values for each compound. Literature values for the K_{S2} for each compound were not available. Laboratory-determined values for K_S , presented in Section 9, show a range for TCE from 0.1 to 0.9 mg/l. K_{S2} values used in the simulations ranged from 1 to 2 mg/l. Since the concentrations of the chlorinated aliphatics in the field studies ranged from 50 to 100 $\mu\text{g/l}$, these K_S values essentially reduce equation (13-4) to a second-order rate expression, where the ratio of k/K_{S2} , is a second-order rate parameter. It should be noted that in the competitive inhibition model (equation 13-5), the K_{S2} and K_{SP} values are used to determine the extent of methane inhibition. The K_{S2} values were adjusted to yield simulation responses to competitive inhibition similar to those observed in the field.

The maximum utilization rate, k_2 , for each compound was adjusted to obtain matches to the field observations. Use of different k_2 values was necessary depending on whether the Monod or competitive inhibition model was being used.

Results of Biotransformation Simulations

The initial simulations of the second season's biotransformation experiment (Biostim2) were performed using the Monod kinetic model (equation 13-4) and the equilibrium sorption transport model. Figure 13.11 shows simulations and field observations for the response of TCE, cis-DCE, and trans-DCE at the S1 observation well. The simulation corresponds to that for methane and oxygen shown in Figure 13.10. The model simulations are generally in good agreement with the observed transient decreases of the chlorinated organics in response to biostimulation of the methanotrophs. In obtaining a fit to the later time trans-DCE concentrations, the model underestimated transformation at early time.

Table 13.5 presents retardation and kinetic factors used in the simulations. The retardation factors are in the range of values determined in the transport experiments. The main parameter that was varied in these simulations was the maximum utilization rate (k_2), ranging from 0.007 d^{-1} for TCE, the most slowly degrading compound, to 0.15 d^{-1} for trans-DCE, the most rapidly degrading compound. The ratio of k_2/K_{S2} values of the chlorinated aliphatics to that of methane range from 0.0035 for the slowly degraded TCE, to 0.075 for the rapidly degraded trans-DCE.

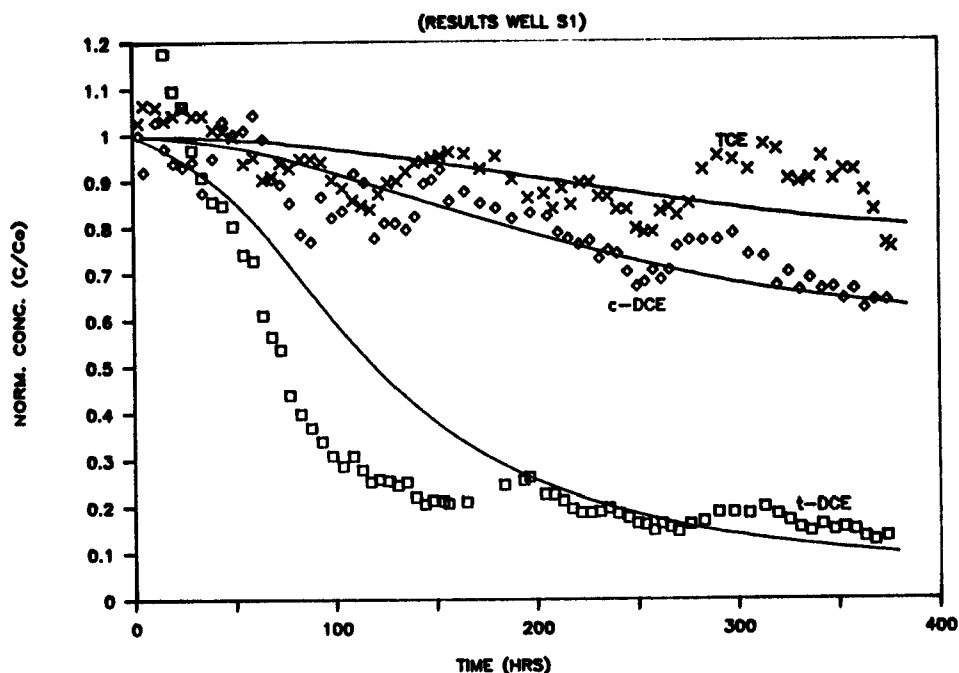


Figure 13.11. Simulation and field response of trans-DCE, cis-DCE, and TCE at the S1 well during the second season's biostimulation experiment (Biostim2). Simulations performed with the Monod kinetic model (equation 13-4) and the equilibrium sorption transport model.

TABLE 13.5. MODEL PARAMETERS FOR SIMULATION OF CHLORINATED ORGANICS IN BIOSTIM2 (Figure 13.11)

Compound	R	k (d ⁻¹)	k/K _S (l/mg-d)	Relative to Methane
Methane	1	2.0	2.0	1.0
trans-DCE	8	0.15	0.15	0.075
cis-DCE	8	0.018	0.018	0.009
TCE	12	0.007	0.007	0.0035

K_S value of 1 mg/l used for all the compounds.

These initial simulations strongly support the hypothesis of biotransformation due to biostimulation of methanotrophs. The different responses of the chlorinated organics to biostimulation results mainly from the compounds having different transformation rates. The similar responses of the model and the field results indicate that the processes incorporated into the model are representative of those occurring in the field. However, some salient differences remain.

The lack of fit of the trans-DCE simulation to the early time response suggests that the kinetically limited sorption model or competitive inhibition biotransformation model may more accurately represent the field behavior. Another possible explanation for the lack of fit is that the concentrations of trans-DCE in this experiment were improperly corrected for a large background concentration of 1,1-DCA, that was subsequently found to co-elute with t-DCE during GC analysis. If the actual concentration of 1,1-DCA was higher than assumed, then the actual extent of biotransformation of trans-DCE would have been underestimated. Model parameters that would better simulate the early time response also would predict greater removals at a later time than shown. This is consistent with the third season's field results. In the latter, the 1,1-DCA problem was eliminated.

Competitive inhibition of methane on transformation of the chlorinated organics, as well as rate-limited sorption-desorption kinetics, were strongly indicated in the third season's results. These data, therefore, provide a basis for evaluating the more complicated biotransformation models.

Figure 13.12 shows model simulations and the response of vinyl chloride, trans-DCE, and cis-DCE at the S2 well, due to biostimulation (Biostim3). In order to activate the large mass of methanotrophs initially present to degrade the chlorinated aliphatics, a lag period of 6 hrs was incorporated into the simulations. The simulations match the observed response quite well, especially for vinyl chloride and trans-DCE, the most rapidly degraded compounds. The simulations show that a rapid reduction of the aqueous-phase concentration occurs once the large initial methanotrophic population becomes activated. As time proceeds, nondegraded compounds from the sorbed phase are slowly released to the aqueous phase, resulting in a slow decrease in the aqueous-phase concentration. Thus, rate-limited desorption appears to be an important process.

For comparison purposes Figure 13.13 presents simulations for vinyl chloride, where sorption is modeled as an equilibrium process. All other parameters are those used in Figure 13.12 simulation. The simulations do not match either the initial rapid decrease in concentration nor the gradual decrease at later time. For the trans-DCE simulations (not shown), a similar response is obtained. However, for the more slowly transformed cis-DCE, it is difficult to determine which model provides a better fit to the data. Thus, it appears that the first-order rate model for sorption-desorption is a better choice for simulating field response, especially when the transformation rate is rapid.

Parameter inputs for the simulations shown in Figure 13.12 are presented in Table 13.6. Parameters include the sorption parameters of K_d and α , as well as biotransformation rate parameters of k_2 and K_{S2} for the chlorinated aliphatics.

Sorption parameters are in the range of values used to model transport experiments before biostimulation. Transformation rate parameters (k_2/K_{S2}) for vinyl chloride and trans-DCE were found to be in the range of those for methane. While vinyl chloride and trans-DCE had similar biotransformation rate and parameters, simulated and measured trans-DCE concentrations decreased more slowly. The main parameter causing the slower decrease in the simulations is the higher K_d value for trans-DCE. Thus, the more gradual decrease of trans-DCE appears to result from sorption interactions, rather than from a slower rate of transformation. The higher K_{S2} value for vinyl chloride compared to trans-DCE was used to match the competitive inhibition response, as will be discussed. The transformation rates used for cis-DCE and TCE are significantly lower than for vinyl chloride and trans-DCE.

Model Simulations of Competitive Inhibition Response

Transformation rates for trans-DCE, cis-DCE, and TCE (k_2/K_{S2}) used to simulate third-season field results are significantly higher than those from the the second season (Table 13.5). The higher rates are partly associated with the use of a competitive-inhibition biotransformation model and rate-limited desorption in the third year

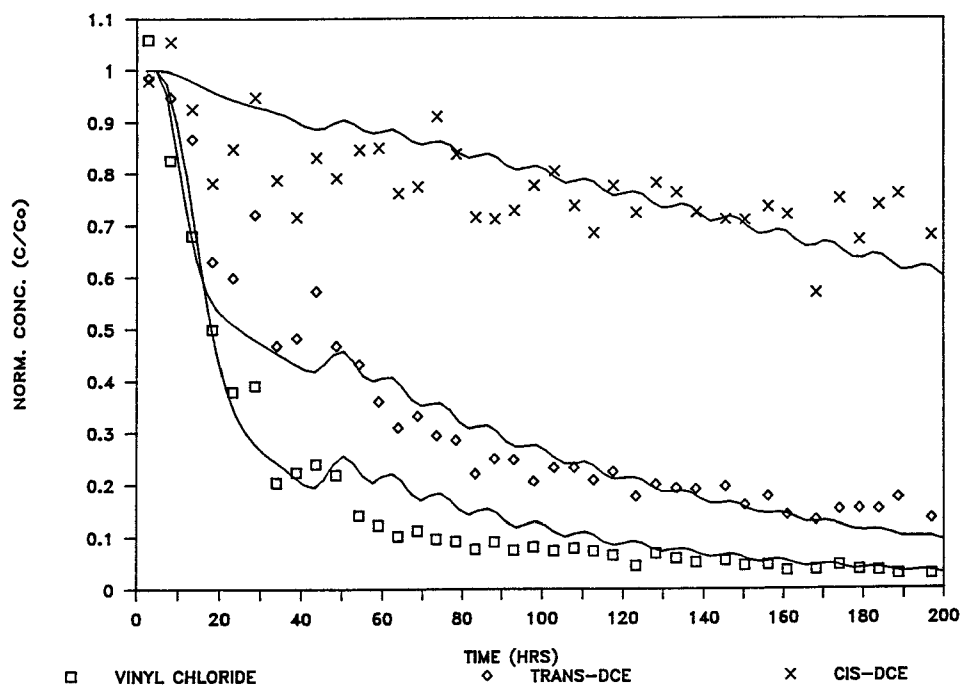


Figure 13.12. Simulations and field response of vinyl chloride, trans-DCE, and cis-DCE at the S2 well during the third season's biostimulation experiment (Biostim3). Simulations performed with the multiple substrate (inhibition) kinetic model (equation 13-5), and the non-equilibrium sorption model.

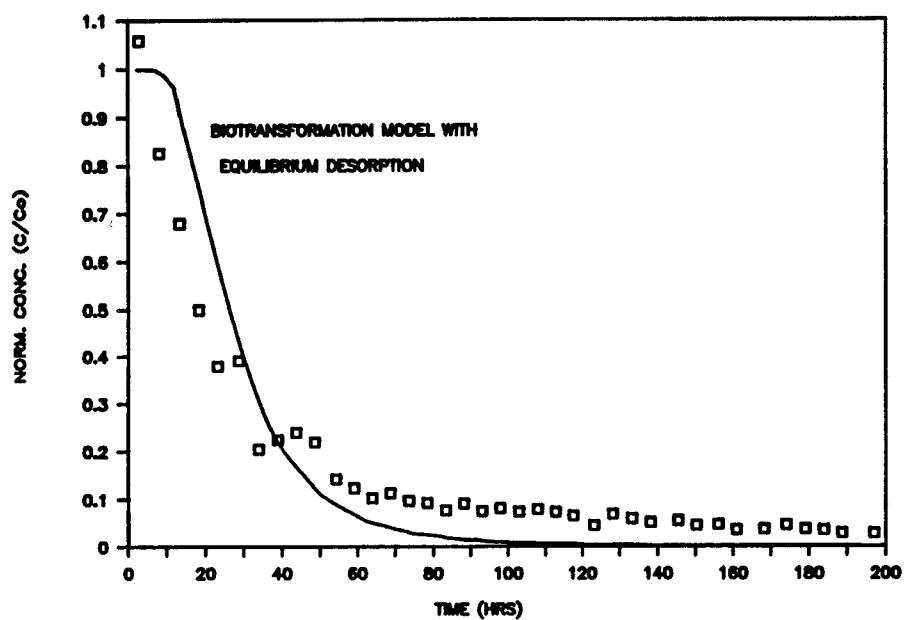


Figure 13.13. Simulation of vinyl chloride response at the S2 well using the equilibrium sorption model.

TABLE 13.6. MODEL PARAMETERS FOR SIMULATION OF CHLORINATED ORGANICS IN BIOTIM3 (Figure 13.12)

Compound	K_d (ml/g)	α (d ⁻¹)	k (d ⁻¹)	K_S (mg/l)	k/K_S (l/mg-d)
Methane	0.0	0.00	2.0	1.0	2.0
VC	0.40	0.33	2.0	2.0	1.0
trans-DCE	1.60	0.33	2.0	1.0	2.0
cis-DCE	1.90	0.33	0.10	1.0	0.1
TCE	2.25	0.33	0.015	1.0	0.025

The effects of competitive inhibition on the observed concentrations were most pronounced at the S1 well. Figure 13.14 shows both the simulated aqueous- and sorbed-phase concentrations of vinyl chloride at the S1 well. The rapid response of the system to methane pulses is apparent. The simulated aqueous-phase concentration response shows amplitude heights and a general concentration decrease (Figure 6.15), similar to those observed in the field experiments. Oscillations of the calculated concentration of VC in the sorbed phase in response to methane pulsing are greatly attenuated compared to those of the aqueous phase. This results from the slow transfer of the vinyl chloride from the sorbed phase to the aqueous phase, where biotransformation is assumed to occur. Simulations for trans-DCE were similar. By contrast, simulations using the equilibrium sorption model, Figure 13.15, show oscillations in aqueous vinyl chloride concentration were greatly attenuated, as instantaneous desorption greatly damped the aqueous-phase response to competitive inhibition. Simulations for the more strongly sorbed trans-DCE showed oscillations being even more attenuated when the equilibrium sorption model was used. The simulations, therefore, indicate that both the processes of competitive inhibition and rate-limited sorption-desorption strongly contribute to the responses observed in the field test.

The concentration oscillations, in response to competitive inhibition, become attenuated with transport through the test zone, as indicated by simulations of the S2 well (Figure 13.12). This results partly because methane concentrations are lower and more attenuated in that region. The combined processes of dispersion, sorption, and biotransformation also act to attenuate oscillations in the chlorinated organic concentrations.

The effects of reduction in competitive inhibition were simulated also for the transient experiments in which formate and methanol were substituted for methane. Model simulations, used in the design of these experiments, indicated that enhanced transformation would result if the compound that was substituted for methane did not inhibit the rate of transformation, but supplied reducing power to keep the MMO enzymes activated. The simulations assumed that biotransformations would proceed at a maximum rate (no inhibition) in the absence of methane. The simulation also assumed that methanotrophs would not grow when formate was substituted for methane.

The simulation of the response for trans-DCE at the S1 well to substitution of formate for methane is presented in Figure 13.16. The simulated response is similar to that observed in the field (Figure 6.18). Upon adding formate, oscillations in trans-DCE concentration stopped, and the concentration decreased to levels slightly lower than the best achieved when minimum methane conditions were present. The model assumption that maximum utilization rates would be achieved when formate was substituted for methane, appears to be correct, at least in the early stages of formate addition.

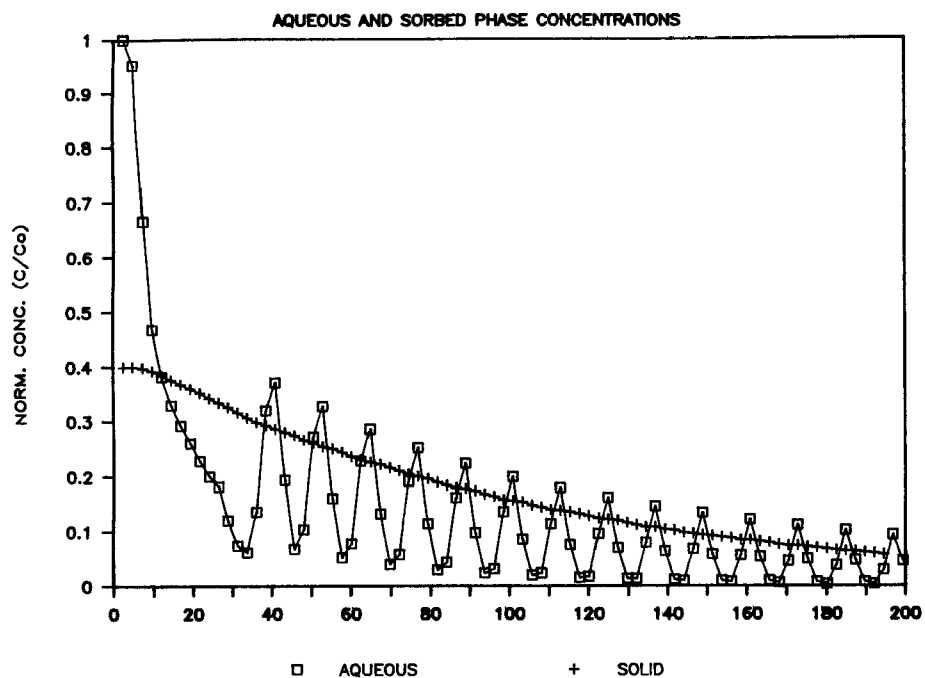


Figure 13.14. Simulation of the aqueous- and sorbed-phase vinyl chloride concentrations at the S1 well using the non-equilibrium sorption model. The field results are shown in Figure 6.15.

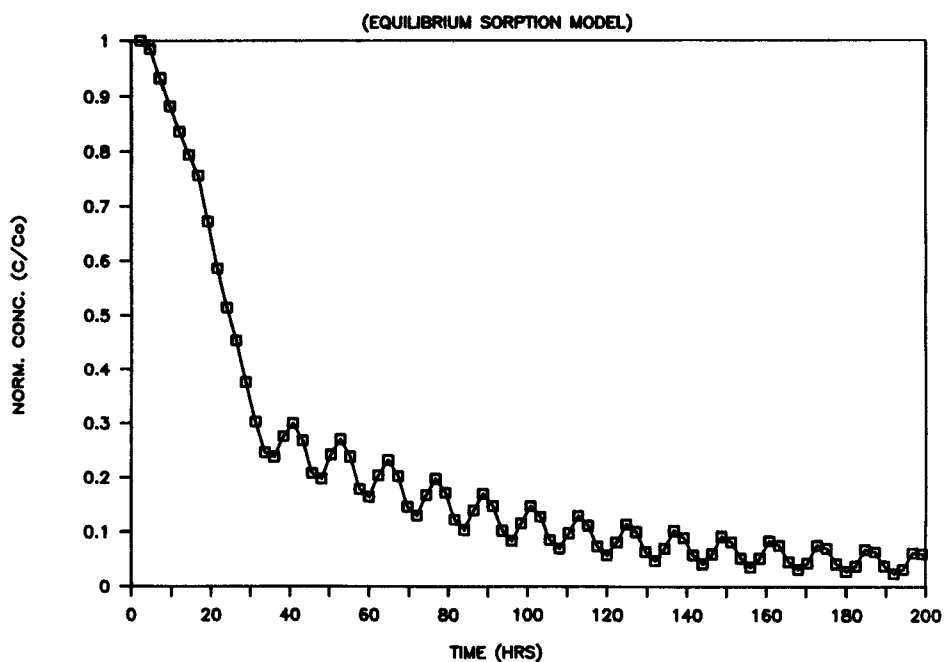


Figure 13.15. Simulation of the aqueous vinyl chloride response at the S1 well using the equilibrium sorption model.

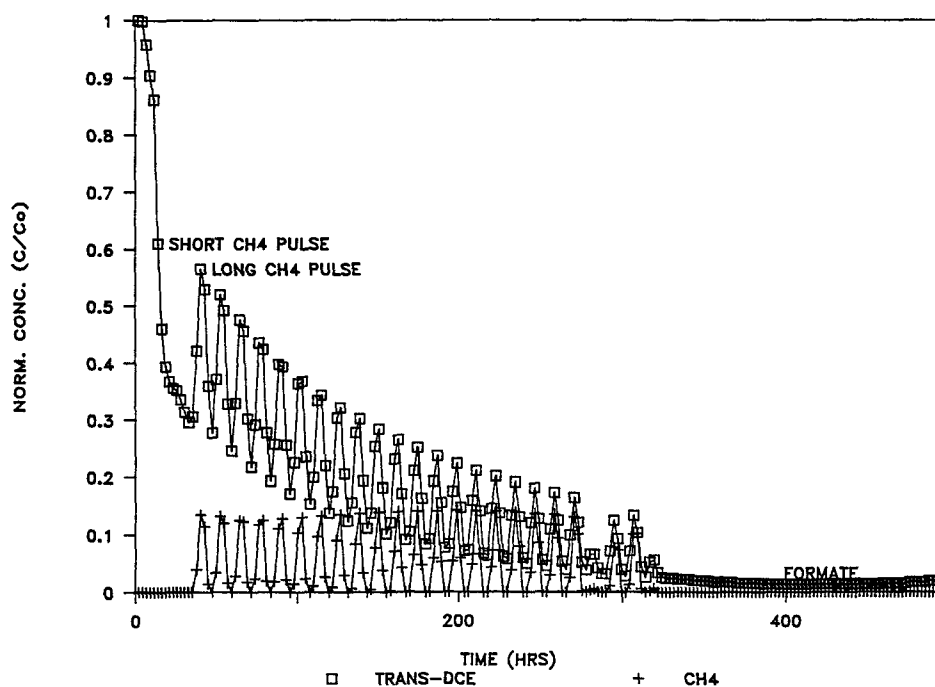


Figure 13.16. Simulation of the trans-DCE response at the S1 well to methane pulsing and formate substitution for methane. The field results are shown in Figure 6.18.

With prolonged formate addition, the field results and the model simulations differ, with a greater increase in concentration with time observed in the field. Since the simulations do include microbial decay, this process does not account for the greater decrease observed in the field. Processes not incorporated in the model may be occurring, such as the gradual deactivation of the MMO enzyme with prolonged formate addition or growth of a separate formate-using non-chlorinated aliphatic-degrading culture.

DISCUSSION

The agreement found between model simulations and field-test results demonstrates the usefulness of a model that incorporates fundamentals of microbial and transport processes. Since knowledge of these processes is incomplete, and basic rate and growth coefficients differ from one species of methanotrophs to another, some adjustment of these coefficients was necessary for a good match to field data. Also, some adjustment can be expected because of the simplifying assumptions made in model development, as well as due to the fact that aquifer heterogeneities make development of a perfect simulation model difficult. Experiments are currently underway in order to determine how well coefficients for rate and growth, as well as initial population levels, as determined in the laboratory using Moffett Field aquifer material, match the coefficients used to fit the field results. It is hoped this will remove some of the uncertainties and will provide an approach for better predicting field behavior.

Of particular interest are the parameter adjustments required in order to fit the first and second year's field results. The ratio of k/K_{SD} was increased by a factor of 5 in the second year's simulations. Bouwer and McCarty (1985) found ratios of k/K_{SD} to increase with time when modeling the aerobic utilization of acetate in a continuous flow laboratory column. Ratios increased by factors of 15 to 30 over a three-year period. They suggest either the development of a separate faster-degrading population or the slow

adaptation of the initial population as possible reasons for the changes in this system. Such changes are possible for the population of methanotrophs at Moffett Field. This may limit the usefulness of rate-coefficients derived from short-term laboratory studies, although the changes noted tend to lead to more efficient removals with time. Thus, short-term laboratory studies may tend to provide conservative estimates of treatment potential.

The 1-D representation for fluid flow from the injection to the observation wells appears to be adequate for estimating responses at the observation wells under the experimental conditions presented. Two-dimensional simulations would, however, be required for adequate modeling of the production well's response to biostimulation, or for determining the 2-D biomass distribution in the test zone. For the 1-D simulations that were performed, the velocity varies most near the injection well. Simulations also were performed using a variable volume element form of the 1-D model that fits the actual times of arrival more closely. This model indicates a distribution similar to the uniform-flow case of the microbial mass near the injection location, despite the higher predicted fluid velocities in that region. Matches to methane and DO response, and those of the chlorinated organics, were similar.

The different dispersivities required to fit the conditions of pulsing compared with near-continuous injection suggest significant aquifer heterogeneities were present, most likely in the vertical direction. This is an important limitation of any model, as it requires information about an aquifer that is difficult to obtain. More tracer studies here would be very useful, and would be required as inputs into 2-D or 3-D simulations as well. Advanced 2-D models that consider vertical heterogeneities may be useful, as demonstrated by Molz and Widdowson (1988).

The simulated responses of the chlorinated organics to biostimulation indicate that the organics are transformed at different rates depending on their chemical structure. The observation that the methanotrophic transformation rates of chlorinated alkenes increase with decreasing chlorine substitution agrees with the laboratory findings of Henson et al. (1987, 1988). Sorption of organics also plays an important role in the responses observed. Nevertheless, the observed responses can be closely matched by using a competitive inhibition model with rate-limited sorption and desorption. In this exercise, a simple model that incorporates relatively few input parameters was used to incorporate these processes. More information on the basic microbial processes is required to select the most appropriate inhibition model, and additional sorption studies are needed to determine if a more complex sorption model is required.

Model simulations also were performed to investigate the response of the system to hydrogen peroxide addition as a substitute for oxygen. This would permit addition of a higher methane concentration. However, simulations using the competitive inhibition model showed that little additional transformation would result if a higher methane concentration were added, even though a greater biomass would develop in the test zone. The higher methane concentration input this requires, inhibits more strongly transformation rates for the chlorinated aliphatic compounds. This simulated result is consistent with the field results from peroxide addition, discussed in Section 6, where no additional TCE transformation was observed when greater amounts of methane were added.

Simulations of field responses from switching the electron donor from methane to formate were quite good initially, but did not mimic the gradual increase in chlorinated aliphatic concentration observed in the field. More basic information on the microbial kinetics and ecology is required to model such transient changes.

The use of the 1-D model greatly simplified the simulations made. However, model parameters used to obtain fits to the field response probably reflect this 1-D simplification. For instance, the first-order mass transfer coefficient used in the sorption model may also include the effects of aquifer heterogeneities. The slow breakthrough of solute moving in a low conductivity zone would produce a similar response as slow sorptive release from the aquifer solids. Microbial process parameters, such as the appropriate saturation coefficient, K_s , for simulation would also be affected by such mass-transfer effect. Thus such parameters may be site- as well as model- and compound-specific.

The fact that the relatively simple 1-D non-steady-state model fit the field results so well when using typical coefficients for bacterial growth and decay, secondary utilization rates, and measured values of transport, dispersion, and sorption indicates that the understanding of the basic process underlying movement and fate are fairly well understood. The value of a basic model of this type is that it can be used with confidence to obtain reasonable predictions for other systems. The knowns and unknowns are better understood, thus making it easier to determine what information about a given system is most critical for evaluation. The 1-D model used here does have limitations, and 2-D and 3-D models can be applied where this is necessary to obtain the information required, assuming this is justified by the availability of sufficient knowledge of aquifer characteristics.

SECTION 14

IN-SITU BIOTRANSFORMATION METHODOLOGIES

Perry McCarty, Lewis Semprini, and Paul Roberts

In order to carry out successful bioremediation, a good understanding of the processes involved, and the development of appropriate methodologies for design and control, are necessary. This requires knowledge of the physical, chemical, and biological characteristics of the contaminated subsurface environment, and of the nature and distribution of contaminants. In addition, methods are needed for in-situ stimulation of the required population of microorganisms, for effecting their distribution to areas where needed, and for maintaining their transforming abilities.

PROTOTYPE SCENARIOS

For illustration of the requisite information, Figure 14.1 shows two possible remediation systems that might be used to degrade contaminants in the saturated zone of an aquifer. The system depicted in Figure 14.1a is designed to permit the injection and extraction of fluid in a zone that runs transverse to the natural flow of the groundwater. Methane, oxygen, and other nutrients that may be required by a native population of methanotrophs are dissolved in the injection water, which then is passed through the aquifer towards the extraction well. An above ground treatment system, such as air stripping, is used to remove contaminants contained in the extracted water. The treated water is used here as the injection water. This system would be capable of removing contaminants from the aquifer, even in the absence of bioremediation. The advantages of bioremediation are 1) more rapid removal of contaminants, and 2) destruction of that portion removed biologically.

In the absence of bioremediation, a single pass of injected water through the aquifer depicted in Figure 14.1a would displace the existing groundwater in its path and effect the removal of the dissolved portion of the contaminants there contained for above ground treatment. Thus, the originally contaminated aquifer water would be replaced with non-contaminated injection water. Then, the contaminants sorbed to the aquifer solids would begin to desorb into the injected water, in turn contaminating it. Injection of another pass of cleaned injection water, along with extraction, would displace the contaminated injection water as previously, and again in turn, the newly injected water would become contaminated through further desorption of contaminants from the solids. Through repeated injection and extraction, the contaminant eventually would be purged from the pore water and leached from the solids, and the aquifer would slowly become restored. The greater the degree to which the contaminants are sorbed, the larger the number of passes of injection water required, and the longer the time for cleanup.

With bioremediation, each pass of injected water might contain primary substrate and nutrients to stimulate the methanotrophic population, which in turn would oxidize a portion of the desorbed contaminants. Since the organisms essentially remain in place in the aquifer, contaminants could be decomposed as they desorb from the aquifer solids. The degradation would reduce the solution concentration, thus enhancing the rate of desorption. In the scheme shown, once the aquifer in the path of the extraction system is adequately cleaned, then the bioremediation system could be discontinued until more contaminated water moves into the treatment zone as a result of natural groundwater movement, and the treatment could be reinitiated. In this manner, down-gradient water users would be protected.

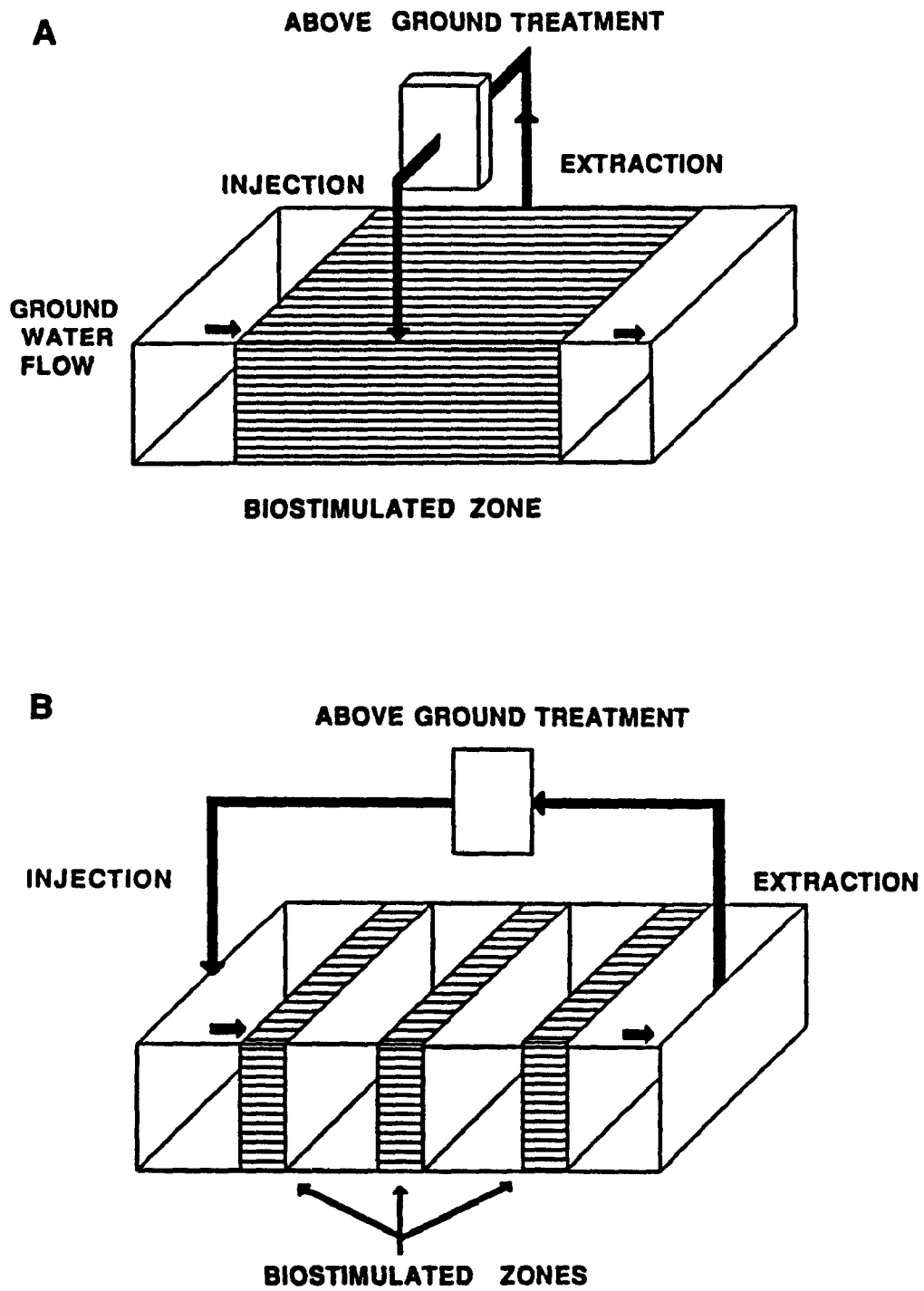


Figure 14.1. Two possible bioremediation systems.

An alternative scheme is illustrated in Figure 14.1b. Here, a series of biostimulated zones are developed that run transverse to the direction of groundwater movement. Once the biologically active zone is developed, then an injection and extraction system is operated in the direction of groundwater flow. This system is more efficient than the one illustrated in Figure 14.1a, but depends upon the ability of the methanotrophs to maintain activity during a period when they are not supplied with methane and oxygen.

Several other treatment schemes are possible, depending upon the given situation. However, the approaches illustrated in Figure 14.1 can be used to outline the characteristics of the system that need to be understood in order to carry out successful remediation as related to 1) the properties of the aquifer, 2) the distribution of contaminants, and 3) the design features of the treatment system.

Important physical characteristics of the aquifer include the composition of the aquifer materials, aquifer heterogeneity, transmissivity, dispersivity, and hydraulic gradient. These properties will provide information on direction and speed of groundwater flow, pumping requirements for injection and extraction, and the degree of certainty with which aquifer response to injection and extraction can be predicted and controlled.

Important chemical properties of the groundwater include pH, temperature, major inorganic ions, and presence of nutrients (N,P). These factors will indicate whether the environment is suitable for the growth of methanotrophs, and will allow some prediction to be made of reaction rates. Redox characteristics of importance are perhaps best characterized through analysis for dissolved oxygen, nitrate, nitrite, ammonia, Fe(II), Mn(II), and sulfide concentrations. The potential presence of organics that are readily biodegraded aerobically also needs to be known. Aquifers that are highly reduced, or contaminated with degradable organics may have a high oxygen demand that would affect the ability to maintain an aerobic system.

The nature, distribution, and concentrations of contaminants in the aquifer also must be known. The rates of transformation of halogenated alkanes and alkenes vary widely, depending on the degree of halogenation, the degree of sorption, and the concentration. Transformation is more efficient with high concentrations of contaminants; that is, a greater mass can be transformed per unit time per unit mass of organisms. However, if the concentration is too high, then inhibition may result. There is ample evidence that concentrations in the low mg/l range are not inhibitory, but just what concentrations need be of concern is not yet well established. Microorganisms that can degrade other contaminants present that are readily oxidized under aerobic conditions may also compete with methanotrophs for oxygen, and the possible presence of this condition needs to be established.

An important property of contaminants is their distribution in the aquifer, and in particular their partitioning between the aqueous and solid phases. Compounds that do not partition onto aquifer solids are not readily susceptible to biotransformation in an aquifer by the methanotrophic process if they are displaced by the injection of water containing the primary substrates for organism growth. It is the sorbed fraction for which this in-situ bioremediation process has the greatest potential, as this is the fraction that is most difficult to remove by the pump and treat method. Biotransformation lowers the aqueous concentration, thus increasing the driving force and hence rate of desorption. On the other hand, the greater the degree of sorption, the less will be the rate of biotransformation, because strong sorption causes low aqueous concentrations. The impact of sorption on treatment rate is thus complex; it appears that moderately sorbed contaminants are the most amenable to treatment by this bioremediation approach.

In-situ biotransformation is most attractive when indigenous bacteria are used, as this avoids the significant problem of injecting and distributing a population of contaminant-degrading bacteria. Indigenous organisms that can be stimulated by primary substrate injection tend to be hardy and competitive with other organisms in the environment where they are found. This might not be true of injected organisms. In addition, injection of non-indigenous organisms may raise questions about the potential environmental consequences. In order to use indigenous organisms it must be established that they 1) are present and distributed throughout the subsurface environment of interest, 2) can be stimulated to grow

through injection of primary substrates and required nutrients, and can survive in that environment, and 3) have the ability to transform the contaminants of concern once stimulated.

Given the above information, the feasibility of a bioremediation system can be evaluated for situations where the subsurface environment is reasonably homogeneous. This requires a suitable numerical model that considers 1) pumping and extraction efficiencies, power requirements, and associated advection and dispersion of water in the aquifer, 2) a strategy for injecting the primary substrate or electron donor for energy and growth (methane) and electron acceptor (oxygen) in a manner to achieve growth of methanotrophic bacteria throughout the treatment zone as uniformly as possible, and 3) the rates of bacterial growth, decay, primary substrate (electron donor and acceptor) utilization, contaminant oxidation, and contaminant desorption. It would be difficult to predict the effectiveness of a given treatment scheme without such a model because of the complex interactions between the many physical, chemical, and biological processes involved. A properly calibrated and verified model is thus an essential tool for evaluating possible bioremediation schemes.

CONTAMINATION CHARACTERIZATION

At any site it is important initially to identify the contaminants present and to quantify their spatial distribution. This is especially important when in-situ bioremediation is considered, since the rates of transformation can be compound-specific. The laboratory and field studies reported here demonstrate that the methanotrophic oxidation process is best suited for less chlorinated compounds such as vinyl chloride, trans-DCE, and cis-DCE, compared to more highly substituted compounds such as TCE and PCE. Currently the processes does not seem well suited for more chlorinated compounds such as PCE.

At some sites, however, anaerobic transformations may convert the more highly chlorinated compounds to less chlorinated products (Section 1). This may occur when there is co-contamination with hydrocarbons that can act as primary substrates for anaerobic growth. The remediation effort could take advantage of these transformations, especially if the less chlorinated transformation products have become spatially separated from the more chlorinated parent compounds. Due to sorption processes, spatial separation would be anticipated since the less chlorinated products tend to be less retarded (Sections 5 and 8) and, therefore, would move down-gradient faster.

Core samples for laboratory studies should be obtained from the contaminated zone where the in-situ treatment process is most likely to be applied, using aseptic techniques to prevent contamination by surface microorganisms. In the laboratory, aseptic procedures should be used to obtain uncontaminated center core material from microbiological analysis, construction of laboratory cores, and sorption studies, as described in Section 10.

Evaluating the feasibility of in-situ remediation of contamination at a specific site requires controlled laboratory studies. The laboratory work presented in Sections 8, 9, 10, and 11 represents different types of methods that can be applied.

COMPARISON OF LABORATORY AND FIELD RESULTS

As summarized in Section 2, the laboratory and field results of this work agreed quite well. The mixed culture studies (Section 9), the batch column study (Section 10), and the continuous column study (Section 11) all demonstrated that indigenous methanotrophs were present in the test zone, and that they could be easily biostimulated. The batch and continuous flow columns, and the field study showed agreement between the lag times before methane consumption was observed.

The three types of microbial studies also demonstrated that TCE was degraded by the stimulated methanotrophs, consistent with the field results. The degree of transformation achieved in the batch and continuous flow columns also agreed quite well with the field observations. These studies also demonstrated further that less chlorinated compounds--including vinyl chloride, 1,2-DCA, and trans-DCE--would

be degraded more rapidly than TCE. The degree of transformation of trans-DCE observed in the continuous flow column was essentially identical to that observed in the field experiment.

These studies also provided qualitative information that agreed with field observations. The studies indicated that methane probably inhibited transformation rates, as increased methane concentration did not enhance the rates of transformation of the target compounds.

The batch and continuous soil columns, like the field, are complex systems, in which numerous processes occur simultaneously. Thus, the determination of rate parameters from these systems requires the application of models, as was performed for the field results (Section 13). Limited modeling has been performed on these laboratory data. A preliminary model simulation of the response of the continuous flow column to biostimulation (Figure 11.3) was made. The simulation and the laboratory results agreed quite well using the same parameters as the field test simulations (Table 13.2). Thus, for this one case, parameters derived from the model fit to laboratory column data would be expected to give reasonable results when used in the reverse direction to predict field behavior.

It is also important to compare parameter estimates that are derived from simple, quantitative measurements with well-defined systems with the field results. Comparisons between field results and the sorption study (Section 8) and the mixed and pure culture study microbial study (Section 9) are summarized below.

Sorption Studies

Sorption studies determined the extent and rates of partitioning of contaminants onto the aquifer solids. Both sets of information are important in determining the response of a system to bioremediation. The K_d values for the synthesized bulk sample shown in Table 8.3 are in qualitative agreement with the response in the field based on retardation estimates given in Tables 5.4 and 5.5. The laboratory and field data both show the following rank order in retardation: TCE > trans-DCE and cis-DCE > VC.

Retardation estimates based on the laboratory K_d data differed, depending on the solids sample that was used. A retardation value of 8 was obtained for TCE when using the bulk Moffett solids obtained from the test zone, which is in fairly good agreement with the estimate of 12 inferred from field data. The synthesized bulk solids, using samples from outside the test zone, give a much higher retardation value of 40. Estimated retardation factors for vinyl chloride, cis-DCE, and trans-DCE were factors of 2 to 3 greater using the synthesized bulk solids compared to the field estimates.

These results stress the importance of obtaining representative samples from the test zone. In our case, the presence of loose gravel and cobbles made it difficult to obtain large intact cores from the test zone. Even when care was taken to use a synthesized bulk sample with the same particle size distribution as in the cores from the test zone, different K_d values resulted.

The sorption rates determined from laboratory sorption studies agree quite well with those used to model the field response. The first order sorption rate parameter that was estimated with the laboratory data (0.4 to 0.6 d^{-1}) agrees quite well with the value of 0.33 d^{-1} used in model simulations (Table 13.6). The lower value used in the model most likely incorporates other factors not explicitly accounted for in the model resulting from aquifer heterogeneities.

This ability to incorporate sorption rate effects using a simple model will prove useful in determining the response of a contaminated aquifer to bioremediation or other treatment measures, system such as pump-and-treat. The first-order sorption model was used in our work in the design of the two step concentration injection experiment for vinyl chloride. Simulations performed prior to the experiments indicated that the approach to steady-state conditions could be expedited by first injecting at a concentration of $100\text{ }\mu\text{g/l}$ for the first 3.5 days and then lowering the concentration to $50\text{ }\mu\text{g/l}$. The simulated concentrations of the liquid and solid phases at the S2 well are shown in Figure 14.2. Upon reducing the injection concentration to $50\text{ }\mu\text{g/l}$, the computed aqueous concentration rapidly approached the injection

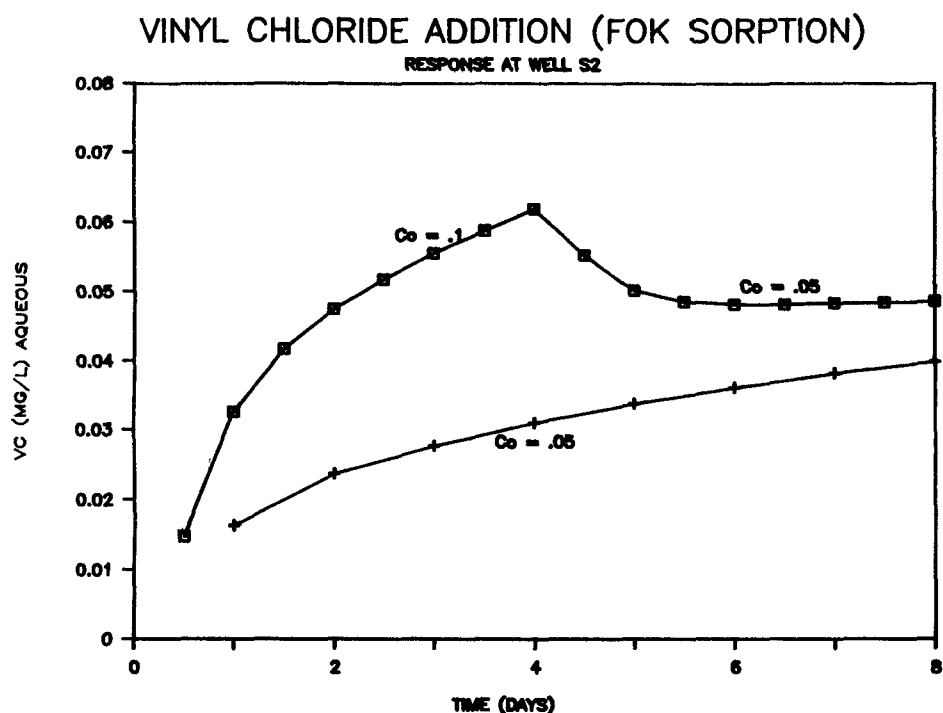


Figure 14.2. Simulation of the aqueous phase (boxes) and sorbed phase (crosses) concentrations of vinyl chloride at the S2 well resulting from a two concentration step addition of vinyl chloride.

concentration; due to slow sorption, the solid phase concentration shows a gradual approach to equilibrium. The rapid approach to steady-state aqueous concentration was later demonstrated in the field experiment (Figure 5.12).

Transformation Rates

The mixed and pure culture studies provide quantitative data on the rates of TCE transformation which can be compared with values obtained independently from the model fit to the field observations. As discussed in Section 9, the rates were dependent on growth and incubation conditions. Rates of TCE transformation by mixed cultures based on k/K_s values (Table 9.1) ranged from 0.01 to 0.046 l/mg-d. The model fit to the field response yielded a rate of 0.015 l/mg-d, which is within the range of laboratory estimates. It is important to note that the laboratory estimates are based on the total mixed culture biomass, while the model-fitted rate is based only on the estimated methanotrophic biomass. The model-fitted estimate therefore agrees more closely with the lower laboratory values. The model-fitted rate is also in the range of low values for the pure culture, 0.01 l/mg-d, where EDTA was not added (Table 9.4).

The agreement between the laboratory rates and model-fitted rate values to the field results is, however, quite remarkable considering the differences between the laboratory and the field systems, and the multiple parameters involved. Using the laboratory derived rate parameters, the model would have yielded predictions for TCE transformation that would be in the range of those observed in the field. These results indicate there is real promise of success using laboratory derived rate parameters in models used for estimating the response of a system to bioremediation.

MODEL SIMULATIONS OF RESTORATION SCENARIOS

Models such as the one described in Section 13 can be used as a tool in evaluating different restoration scenarios. Basic rate parameters derived from the laboratory studies can be used as inputs for the simulations. A modeling exercise would then permit evaluation of different restoration scenarios for a given situation.

Modeling exercises were performed for the two treatment scenarios shown in Figure 14.1. The first exercise represents the scheme shown in Figure 14.1a, where treatment is applied over the complete section of the aquifer. The first case simulates the restoration of an aquifer contaminated with a compound that can be rapidly degraded by methanotrophs and is sorbed to a moderate extent ($R = 12$). The simulations assumed that methane inhibits the rate of transformation, and that sorption and desorption are rate-limited processes. Model parameters used were those for trans-DCE given in Table 13.6 and those for methanotrophs given in Table 13.2. The simulation compares the in-situ bioremediation method to the pump-and-treat remediation method. For the pump-and-treat case, groundwater was extracted and treated at the surface, and reinjected. For the in-situ bioremediation, groundwater was extracted, saturated with methane and oxygen at the surface, and reinjected without removing the contaminants at the surface.

Figure 14.3 shows the results of the model simulations, where the extraction well concentration history is shown. Cases for bioremediation using both long (10 and 15 days) and short (5 and 10 days) alternating pulses of methane and oxygen are shown. The most effective treatment results with long alternating pulses that distribute methanotrophic growth throughout the treatment zone. The time for aquifer restoration is reduced by a factor of three compared to the pump-and-treat case. An additional benefit of the bioremediation is that all the contaminants are degraded in the subsurface.

The results of another modeling exercise is illustrated in Figure 14.4. The simulation represents a multiple-zone scheme similar to that shown in Figure 14.1b. The scheme is proposed for the treatment of more slowly degrading compounds, such as TCE. The simulation was performed using a biotransformation rate coefficient for TCE derived from the field and laboratory experiments. A comparison is illustrated between the pump-and-treat system with and without biostimulation, but each employing reinjection of the extracted water. Similar hydraulic conditions were used in both cases, and sorption-desorption was assumed to be rate-limited, as indicated by the field and laboratory studies. For the case of pump-and-treat, groundwater was assumed to be surface treated and reinjected. Then biostimulation was added, three zones are stimulated, each having a methanotrophic biomass equivalent to that achieved in our studies.

Biostimulation is estimated to significantly decrease both the time for aquifer restoration and the amount of contaminant that must be treated at the surface. For the case illustrated, about 3/4 of the TCE would be biodegraded in-situ. For more rapidly degraded compounds, such as vinyl chloride and trans-DCE, restoration should occur even faster.

These simulated scenarios are intended as illustrative exercises only. Any real applications would of course necessitate careful site characterization of the kinds undertaken in this research and summarized above in this section.

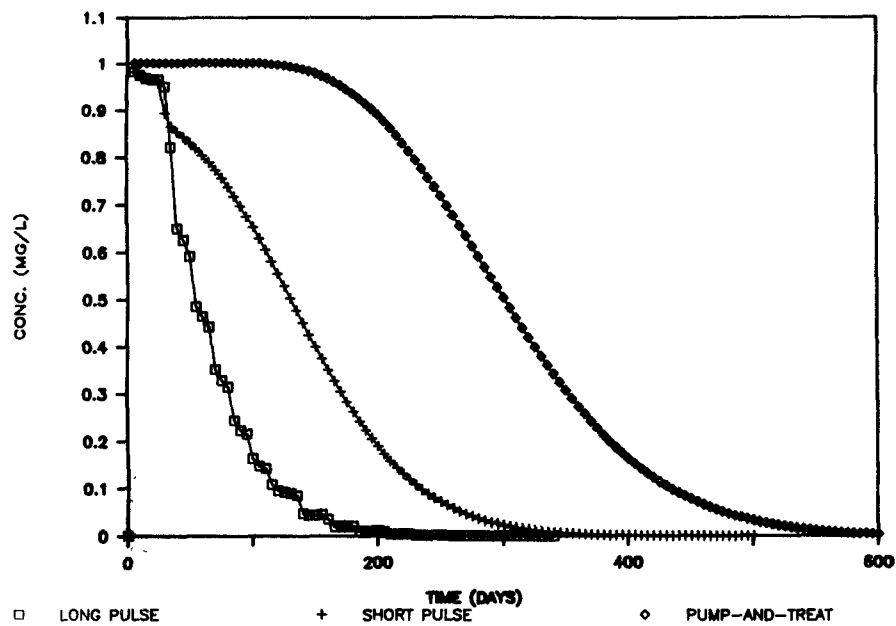


Figure 14.3. Comparison of bioremediation versus pump-and-treat of rapidly degrading, moderately sorbed compounds, such as trans-DCE, based upon the scheme illustrated in Figure 14.1a.

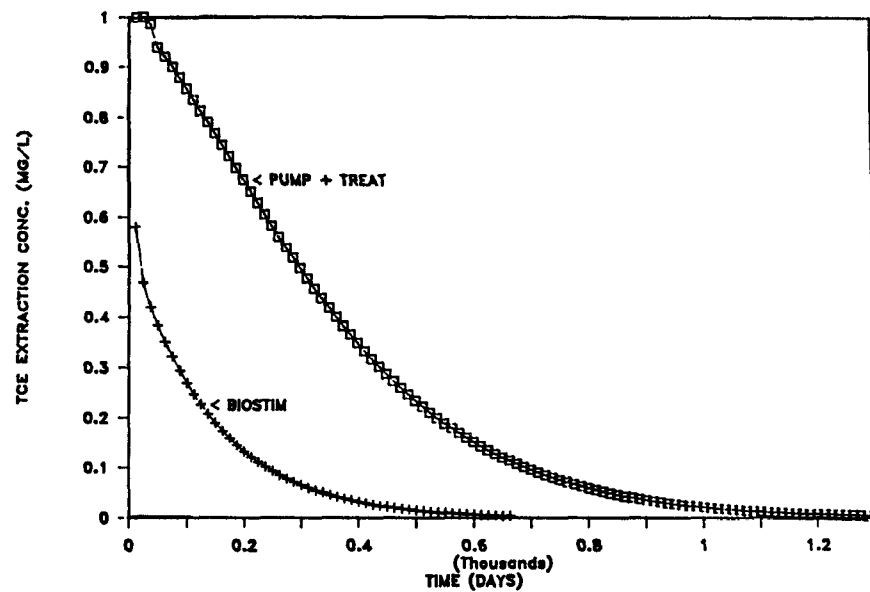


Figure 14.4. Comparison of bioremediation versus pump-and-treat remediation of TCE contamination with and without biostimulation based upon the scheme illustrated in Figure 14.1b.

REFERENCES

- Anthony, C. 1975. The Biochemistry of Methylophilic Bacteria. *Sci. Prog. (London)* 62:167-206.
- Anthony, C. 1979. The Prediction of Growth Yield of Methylophilic Bacteria. *J. Gen. Microbiol.* 104:91-104.
- Anthony, C. 1982. The Biochemistry of Methylophilic Bacteria. Academic Press, Inc., London.
- Atwater, B. F., C. W. Hedel, and E. J. Helley. 1977. Late Quaternary Depositional History, Holocene Sea-Level Changes, and Vertical Crustal Movement, Southern San Francisco Bay, California. U.S.G.S Prof. Paper 1014, Washington, D.C.
- Bailey, J. E., and D. F. Olis. 1986. Biochemical Engineering Fundamentals, 2nd ed. McGraw-Hill, Inc., New York.
- Ball, W.P., and P.V. Roberts. 1985. Rate-Limited Sorption of Halogenated Aliphatics onto Sandy Aquifer Material. Experimental Results and Implications for Solute Transport. Presented at Fall Meeting of the American Geophysical Union, AGU, San Francisco, December.
- Ball, W.P., and P.V. Roberts. 1987. Sorption Kinetics of Synthetic Organic Chemicals in Sandy Aquifer Material. Presented at 1987 Annual Meeting, Geological Society of America, Phoenix, AZ, October.
- Ball, W. P., C. Buehler, T. C. Harmon, D. M. Mackay, and P. V. Roberts. 1989. Characterization of a Sandy Aquifer Material at the Grain Scale. Submitted to *J. Contaminant Hydrol.*
- Barrio-Lage, G., F. Z. Parsons, R. S. Nassar, and P. A. Lorenzo. 1986. Sequential Dehalogenation of Chlorinated Ethenes. *Env. Sci. Technol.* 20:96-99.
- Bear, J. 1972. Dynamics of Fluids in Porous Media. American Elsevier, New York.
- Bear, J. 1979. Hydraulics of Groundwater. McGraw-Hill, New York.
- Beebe, R. A., J. B. Beckwith, and J. M. Honig. 1945. The Determination of Small Surface Areas by Krypton Adsorption at Low Temperature. *J. Am. Chem. Soc.* 67:1554-1558.
- Belay, N., and L. Daniels. 1987. Production of Ethane, Ethylene, and Acetylene from Halogenated Hydrocarbons by Methanogenic Bacteria. *Appl. Environ. Microbiol.* 53:1604-1610.
- Borden, R. C., and P. B. Bedient. 1986. Transport of Dissolved Hydrocarbons Influenced by Oxygen-Limited Biodegradation. 1. Theoretical Development. *Water Resour. Res.* 2(13):1973-1982.
- Bouwer, H. 1978. Groundwater Hydrology. McGraw-Hill Book Company, New York.
- Bouwer, E. J., and P. L. McCarty. 1983. Transformation of 1- and 2-Carbon Halogenated Aliphatic Organic Compounds under Methanogenic Conditions. *Appl. Environ. Microbiol.* 45:1286-1294.

- Bouwer, E. J., and P. L. McCarty. 1985. Utilization Rates of Trace Halogenated Organic Compounds in Acetate-Grown Biofilms. *Biotechnol. Bioeng.* 27:1564-1571.
- Bouwer, E. J., B. E. Rittmann, and P. L. McCarty. 1981. Anaerobic Degradation of Halogenated 1- and 2-Carbon Organic Compounds. *Env. Sci. Technol.* 15:596-599.
- Bowker, A. H., and G. J. Lieberman. 1972. *Engineering Statistics*. Prentice-Hall, Englewood Cliffs, NJ.
- Brigham, W. E. 1974. Mixing Equations in Short Laboratory Cores. *Soc. Pet. Eng. J.* 14:91-99.
- Brock, T. D., D. W. Smith, and M. T. Madigan. 1984. *Biology of Microorganisms*, 4th ed. Prentice-Hall, Englewood Cliffs, NJ.
- Brunauer, S., P. H. Emmett, and E. Teller. 1938. Adsorption of Gases in Multimolecular Layers. *J. Am. Chem. Soc.* 60:309-319.
- Burlinson, N. E., L. A. Lee, and D. H. Rosenblatt. 1982. Kinetics and Products of Hydrolysis of 1,2-Dibromo-3-Chloropropane. *Env. Sci. Technol.* 16(9):627-632.
- Canonie Engineers. 1983. Subsurface Hydrogeologic Investigation, Mountain View Facility. Project CES 82-023, June.
- Carter, D. L., M. D. Heilman, and C. L. Gonzalez. 1965. Ethylene Glycol Monoethyl Ether for Determining Surface Area of Silicate Minerals. *Soil Sci.* 100:356-360.
- Chrysikopoulos, C. V., P. V. Roberts, and P. K. Kitanidis. 1989. One-Dimensional Solute Transport in Porous Media with Well-to-Well Recirculation: Application to Field Experiments. Submitted to *Water Resour. Res.*
- Coats, K. H., and B. D. Smith. 1964. Dead-End Pore Volume and Dispersion in Porous Media. *Soc. Pet. Eng. J.* 4(1):73-84.
- Colby, J., D. I. Stirling, and H. Dalton. 1977. The Soluble Methane Mono-Oxygenase of *Methylococcus capsulatus* (bath). Its Ability to Oxygenate *n*-Alkanes, *n*-Alkenes, Ethers, and Alicyclic, Aromatic, and Heterocyclic Compounds. *Biochem. J.* 165:395-402.
- Colby, J. H., H. Dalton, and R. Whittenbury. 1979. Biological and Biochemical Aspects of Microbial Growth on Cl Compounds. *Annu. Rev. Microbiol.* 33:481-517.
- Crank, J. 1975. *The Mathematics of Diffusion*, 2nd ed. Oxford University Press, Oxford.
- Criddle, C. S., J. Dewitt, and P. L. McCarty. 1989. Biotransformations of Carbon Tetrachloride by Stationary Phase *Escherichia coli* K-12 under Different Electron Acceptor Conditions. Submitted to *Appl. Environ. Microbiol.*
- Curtis, G.P. 1984. Sorption of Hydrophobic Organic Solutes onto Aquifer Materials: Comparisons Between Laboratory Results and Field Observations. M.S. Thesis, Stanford University, Stanford, CA.
- Curtis, G. P., P. V. Roberts, and M. Reinhard. 1986. A Natural Gradient Experiment on Solute Transport in a Sand Aquifer: IV. Sorption of Organic Solutes and Its Influence on Mobility. *Water Resour. Res.* 22(13):2059-2067.
- Dennis, J. E., D. M. Gay, and R. E. Welsch. 1981. An Adaptive Nonlinear Least-Squares Algorithm. *ACM Trans. Math. Software* 7(3):369-383.

- Donaldson, J. R., and R. V. Tryon. 1983. Nonlinear Least-Squares Regression Using STARPAC: The Standards Times Series and Regression Package. National Bureau of Standards Tech. Note 1068-2, Boulder, CO.
- Donaldson, J. R., and R. B. Schnabel. 1987. Computational Experience with Confidence Regions and Confidence Intervals for Nonlinear Least Squares. *Technometrics* 29(1):67-93.
- Ferenci, T., T. Strom, and J. R. Quayle. 1975. Oxidation of Carbon Monoxide and Methane by *Pseudomonas methanica*. *J. Gen. Microbiol.* 91:79-91.
- Fogel, M. M., A. R. Taddeo, and S. Fogel. 1986. Biodegradation of Chlorinated Ethenes by a Methane-Utilizing Mixed Culture. *Appl. Environ. Microbiol.* 51:720-724.
- Freeze, R. A., and J. A. Cherry. 1979. *Groundwater*. Prentice-Hall, Inc., New York.
- Fried, J. J., and M. A. Combarous. 1971. Dispersion in Porous Media. *Adv. Hydrosol.* 7:169-281.
- Gaines, G.L., Jr., and P. Cannon. 1960. On the Energetics of Physically Adsorbed Films, with Particular Reference to the Use of Krypton for Surface Area Measurement. *J. Phys. Chem.* 62:997-1000.
- Gear, C. W. 1971. *Numerical Initial Value Problems in Ordinary Differential Equations*. Prentice-Hall, Englewood Cliffs, NJ.
- Ghiorse, W. C., and D. L. Balkwill. 1983. Enumeration and Morphological Characterization of Bacteria Indigenous to Subsurface Environments. *Dev. Indust. Microbiol.* 24:213-224.
- Goltz, M. N. 1986. Three-Dimensional Analytical Modeling of Diffusion-Limited Solute Transport. Ph.D. Dissertation, Stanford University, Stanford, CA.
- Goltz, M. N., and P. V. Roberts. 1986a. Three-Dimensional Solutions for Solute Transport in an Infinite Medium with Mobile and Immobile Zones. *Water Resour. Res.* 22(7):1139-1148.
- Goltz, M. N., and P. V. Roberts. 1986b. Interpreting Organic Transport Data from a Field Experiment Using Physical Nonequilibrium Models. *J. Contaminant Hydrol.* 1:77-93.
- Golub, G. H., and V. Pereya. 1973. The Differential of Pseudo-Inverses and Non-Linear Squares Problems Whose Variables Separate. *SIAM J. Numer. Anal.* 10:413-432.
- Gossett, J.M. 1985. Anaerobic Degradation of C1 and C2 Chlorinated Hydrocarbons. U.S. Air Force Report ESL-TR-85-38. National Technical Information Service, Springfield, VA.
- Graydon, J. W., K. Grob, F. Zuercher, and W. Giger. 1983. Determination of Highly Volatile Organic Water Contaminants by the Closed-Loop Gaseous Stripping Technique Followed by Thermal Desorption of the Activated Carbon Filters. *J. Chromatogr.* 285:307-318.
- Gregg, S. J., and K. S. W. Sing. 1982. *Adsorption, Surface Area and Porosity*. Academic Press, New York.
- Griesbaum, K., R. Kibar, and B. Pfeffer. 1975. Synthese und Stabilität von 2,3-Dichlorooxiranen. *Liebigs Ann. Chem.* 214-224.
- Hanson, R. S. 1980. Ecology and Diversity of Methylophilic Organisms. *Adv. Appl. Microbiol.* 26:3-39.
- Hantush, M. S., and C. E. Jacob. 1955. Nonsteady Radial Flow in an Infinite Leaky Aquifer. *Am. Geophys. Un. Trans.* 36:95-100.

- Harding Lawson Associates (HLA). 1986. Technical Memorandum: Short- and Long-Term Aquifer Tests. Remedial Investigation/Feasibility Study, Middlefield-Ellis-Whisman Area, Mountain View, CA. Report for U.S. EPA, Region 9, HLA Job No. 17,580,012.02.
- Harrison, D. E. F. 1973. Studies on the Affinity of Methanol- and Methane-Utilizing Bacteria for Their Carbon Substrates. *J. Appl. Bacteriol.* 36:301-308.
- Harrocks, D. L. 1974. Applications of Liquid Scintillation Counting. Academic Press, New York.
- Harvey, R. W., R. L. Smith, and L. George. 1984. Effect of Organic Contamination upon Microbial Distributions and Heterotrophic Uptake in a Cape Cod, Mass. Aquifer. *Appl. Environ. Microbiol.* 48:1197-1202.
- Hashimoto, I., K. B. Deshpande, and H. C. Thomas. 1964. Peclet Numbers and Retardation Factors for Ion Exchange Columns. *Ind. Eng. Chem. Fund.* 3(3):213-218.
- Hayat, M. A. 1981. Fixation for Electron Microscopy. Academic Press, Inc., New York.
- Heijnen, J. J., and J. A. Roels. 1981. A Macroscopic Model Describing Yield and Maintenance Relationships in Aerobic Fermentation Processes. *Biotechnol. Bioengin.* 23:739-763.
- Henderson, J. E., G. R. Peyton, and W. H. Glaze. 1986. A Convenient Liquid-Liquid Extraction Method for the Determination of Halomethanes in Water at the ppb Level. In: Identification and Analysis of Organic Pollutants in Water, L. H. Keith, ed. Ann Arbor Science Publishers, Ann Arbor, MI. pp. 105-112.
- Henry, S. M., and D. Grbić-Galić. 1986. Aerobic Degradation of Trichloroethylene (TCE) by Methylophils Isolated from a Contaminated Aquifer. Abstr. Q-64, Annu. Meet. Am. Soc. Microbiol. p. 294.
- Henry, S. M., and D. Grbić-Galić. 1987. Variables Affecting Aerobic TCE Transformation by Methane-Degrading Mixed Cultures. Abstr. #401, Soc. Environ. Toxicol. Chem. Eighth Annual Meeting. p. 207.
- Henry, S. M., F. Thomas, and D. Grbić-Galić. 1988. Electron Microscopy Studies of TCE-Degrading Groundwater Bacteria. Abstr. #2261, Soc. Environ. Toxicol. Chem. Ninth Annual Meeting. p. 74.
- Henschler, D., W. R. Hoos, H. Fetz, E. Dallmeier, and M. Metzler. 1979. Reactions of Trichloroethylene Epoxide in Aqueous Systems. *Biochem. Pharmacol.* 28:543-548.
- Henson, J. M., M. V. Yates, and J. W. Cochran. 1987. Metabolism of Chlorinated Aliphatic Hydrocarbons by a Mixed Bacteria Culture Growing on Methane. Abstr. Q-97, Annu. Meet. Am. Soc. Microbiol. p. 298.
- Henson, J. M., M. V. Yates, J. W. Cochran, and D. L. Shackelford. 1988. Microbial Removal of Halogenated Methanes, Ethanes, and Ethylenes in an Aerobic Soil Exposed to Methane. *FEMS Microbiol. Ecol.* 53:193-201.
- Higgins, I. J., R. C. Hammond, F. S. Sariaslani, D. J. Best, M. M. Davies, S. E. Tryhorn, and F. Taylor. 1979. Biotransformation of Hydrocarbons and Related Compounds by Whole Organism Suspensions of Methane-Grown *Methylosinus trichosporium* OB3b. *Biochem. Biophys. Res. Comm.* 84(2):671-677.
- Higgins, I. J., D. J. Best, R. C. Hammond, and D. Scott. 1981. Methane-Oxidizing Microorganisms. *Microbiol. Rev.* 45:556.

- Hopkins, G. D., L. Semprini, P. V. Roberts, and D. M. Mackay. 1988. An Automated Data Acquisition System for Assessing in-situ Biodegradation of Chlorinated Aliphatic Compounds. Proc. of the Second Outdoor Conference on Groundwater Monitoring and Aquifer Restoration, NWWA, Las Vegas, Nevada, May.
- Horvath, A. L. 1982. Halogenated Hydrocarbons. M. Dekker, New York.
- Horvath, R. S. 1972. Microbial Co-Metabolism and the Degradation of Organic Compounds in Nature. Bact. Rev. 36:146-155.
- Hou, C. T. 1984a. Microbiology and Biochemistry of Methylotrophic Bacteria. In: Methylotrophs: Microbiology, Biochemistry, and Genetics, C. T. Hou, ed. CRC Press, Inc., Boca Raton, FL. pp. 1-53.
- Hou, C. T. 1984b. Other Applied Aspects of Methylotrophs. In: Methylotrophs: Microbiology, Biochemistry, and Genetics, C. T. Hou, ed. CRC Press, Inc., Boca Raton, FL. pp. 145-180.
- Hou, C. T., R. N. Patel, A. I. Laskin, and N. Barnabe. 1979a. Microbial Oxidation of Gaseous Hydrocarbons: Epoxidation of C2 to C4 n-Alkenes by Methylotrophic Bacteria. Appl. Environ. Microbiol. 38:127-134.
- Hou, C. T., R. Patel, A. I. Laskin, N. Barnabe, and I. Marczak. 1979b. Microbial Oxidation of Gaseous Hydrocarbons: Production of Methyl Ketones from Their Corresponding Secondary Alcohols by Methane- and Methanol-Grown Microbes. Appl. Environ. Microbiol. 38:135-142.
- Hutzler, N. J., J. C. Crittenden, J. S. Gierke, and A. J. Johnson. 1986. Transport of Organic Compounds with Saturated Groundwater Flow: Experimental Results. Water Resour. Res. 22:285-295.
- Janssen, D. B., G. Grobбен, and B. Witholt. 1987. Toxicity of Chlorinated Aliphatic Hydrocarbons and Degradation by Methanotrophic Consortia. Proc. 4th European Congress on Biotechnology, 1987. Vol. 3, pp. 515-519.
- Javandel, I., C. Doughty, and C. Tsang. 1984. Groundwater Transport: Handbook of Mathematical Models. Water Resources Monograph Series 10, Amer. Geophys. Union, Washington, D.C.
- Johns, R. A., L. Semprini, and P. V. Roberts. 1989. Estimating Aquifer Properties by Regression Analysis of Pump Test Response Data. Submitted to Ground Water.
- Kennedy, S. I. T., and C. A. Fewson. 1968. Enzymes of the Mandelate Pathway in Bacterium NCIB 8250. Biochem. J. 107:497-506.
- Kissel, J. C., P. L. McCarty, and R. L. Street. 1984. Numerical Simulation of Mixed-Culture Biofilm. J. Env. Eng. (ASCE) 110(2):393-411.
- Kreft, A., and A. Zuber. 1978. On the Physical Meaning of the Dispersion Equation and Its Solutions for Different Initial and Boundary Conditions. Chem. Eng. Sci. 33:1471-1480.
- Lapidus, L., and N. R. Amundson. 1952. Mathematics of Adsorption in Beds: The Effect of Longitudinal Diffusion in Ion Exchange and Chromatographic Columns. J. Phys. Chem. 56:984-988.
- Large, P. J., and J. R. Quayle. 1963. Enzyme Activities in Extracts of *Pseudomonas* AM1. Biochem J. 87:386-396.

- Lee, M. D., J. M. Thomas, R. C. Borden, P. B. Bedient, C. H. Ward, and J. T. Wilson. 1988. Bioremediation of Aquifers Contaminated with Organic Compounds. *CRC Crit. Rev. in Environ. Control* 18(1):29-89.
- Leonard, B. P. 1979. A Stable and Accurate Modeling Procedure Based on Quadratic Upstream Modeling. *Comput. Methods Appl. Mech. Eng.* 19:59-98.
- Liebler, D. C., and F. P. Guengerich. 1983. Olefin Oxidation by Cytochrome P-450: Evidence for Group Migration in Catalytic Intermediates Formed with Vinylidene Chloride and t-1-Phenyl-1-Butene. *Biochemistry* 22:5482-5489.
- Lindstrom, F. T., R. Haque, V. H. Freed, and L. Boersma. 1967. Theory on the Movement of Some Herbicides in Soils, Linear Diffusion and Convection of Chemicals in Soils. *Env. Sci. Technol.* 1(7):561-565.
- Little, C. D., A. V. Palumbo, S. E. Herbes, and D. M. Genung. 1987a. Stimulation of Trichloroethylene Biodegradation in Ground Water Samples. *Abstr. Q-105, Annu. Meet. Am. Soc. Microbiol.*, p 299.
- Little, C. D., A. V. Palumbo, S. E. Herbes, M. E. Lidstrom, R. L. Tyndall, and P. J. Gilmer. 1987b. Trichloroethylene Biodegradation by a Methane-Oxidizing Bacterium. *Abstr. 402, Annu. Meet. Soc. Environ. Toxicol. Chem.* p. 207.
- Little, C. D., A. V. Palumbo, S. E. Herbes, M. E. Lidstrom, R. L. Tyndall, and P. J. Gilmer. 1988. Trichloroethylene Biodegradation by a Methane-Oxidizing Bacterium. *Appl. Environ. Microbiol.* 54:951-956.
- Mackay, D., and W. Y. Shiu. 1981. A Critical Review of Henry's Constants for Chemicals of Environmental Interest. *J. Phys. Chem. Ref. Data* 10:1175-1199.
- Mackay, D. M., W. P. Ball, and M. G. Durant. 1986. Variability of Aquifer Sorption Properties in a Field Experiment on Groundwater Transport of Organic Solutes: Methods and Preliminary Results. *J. Contaminant Hydrol.* 1:119-132.
- March, J. 1985. *Advanced Organic Chemistry*. John Wiley & Sons, New York. pp. 804-805.
- McCarty, P. L. 1965. Thermodynamics of Biological Synthesis and Growth. In: *Proceedings of Second International Water Pollution Research Conference, Tokyo*. Pergamon Press, New York.
- McCarty, P. L. 1975. Stoichiometry of Biological Reactions. *Progress in Water Technology* 7(1): 157-172.
- McCarty, P. L. 1984. Application of Biological Transformation in Groundwater. *Proc. Second Int. Conf. on Ground Water Quality, Tulsa, OK, March 27*.
- McCarty, P.L. 1988. Bioengineering Issues Related to in-situ Remediation of Contaminated Soils and Groundwater. In: *Environmental Biotechnology*, G. S. Omenn, ed. Plenum Publishing Corp., New York.
- McCarty, P. L., M. Reinhard, and B. E. Rittmann. 1981. Tracer Organics in Groundwater. *Environ. Sci. Technol.* 15:40-51.
- McKinney, L. L., E. H. Uhing, J. L. White, and J. C. Picken. 1955. Autoxidation Products of Trichloroethylene. *J. Agric. Food Chem.* 3:413-419.

- Miller, C. T., and W. J. Weber. 1986. Sorption of Hydrophobic Organic Pollutants in Saturated Soil Systems. *J. Contaminant Hydrol.* 1:243-261.
- Miller, R. E., and F. P. Guengerich. 1982. Oxidation of Trichloroethylene by Liver Microsomal Cytochrome P-450: Evidence for Chlorine Migration in a Transition State Not Involving Trichloroethylene Oxide. *Biochemistry* 21:1090-1097.
- Molz, F. J., O. Güven, J. G. Melville, R. D. Crocker, and K. T. Matteson. 1986a. Performance, Analysis, and Simulation of a Two-Well Tracer Test at the Mobile Site. *Water Resour. Res.* 22(7):1031-1037.
- Molz, F. J., M. A. Widdowson, and L. D. Benefield. 1986b. Simulation of Microbial Growth Dynamics Coupled to Nutrient and Oxygen Transport in Porous Media. *Water Resour. Res.* 22(8):1207-1216.
- Molz, F. J., and M. A. Widdowson. 1988. Internal Inconsistencies in Dispersion-Dominated Models That Incorporate Chemical and Microbial Kinetics. *Water Resour. Res.* 24(4):615-619.
- Morinaga, Y., S. Yamanaka, K. Takinami, and Y. Hirose. 1979a. Optimum Feeding Proportion of Methane and Oxygen in Cultivation of the Obligate Methane-Utilizing Bacterium, *Methylobacterium flagellata*, in Batch Culture. *Agricult. Biol. Chem.* 43:2447-2451.
- Morinaga, Y., S. Yamanaka, K. Takinami, and Y. Hirose. 1979b. Methane Metabolism of the Obligate Methane-Utilizing Bacterium, *Methylobacterium flagellata*, in Methane-Limited and Oxygen-Limited Chemostat Culture. *Agricult. Biol. Chem.* 43:2453-2458.
- Nation, J. L. 1983. A new Method Using Hexamethyldisilazane for preparation of soft insect tissues for scanning electron microscopy. *Stain Tech.* 58:347-351.
- Nelson, M. J. K., S. O. Montgomery, E. J. O'Neill, and P. H. Pritchard. 1986. Aerobic Metabolism of Trichloroethylene by a Bacterial Isolate. *Appl. Environ. Microbiol.* 52:383-384.
- Nelson, M. J. K., S. O. Montgomery, W. R. Mahaffey, and P. H. Pritchard. 1987. Biodegradation of Trichloroethylene and the Involvement of an Aromatic Biodegradative Pathway. *Appl. Environ. Microbiol.* 53:949-954.
- Nelson, M. J. K., S. O. Montgomery, and P. H. Pritchard. 1988. Trichloroethylene Metabolism by Microorganisms That Degrade Aromatic Compounds. *Appl. Environ. Microbiol.* 54:604-606.
- Nkedi-Kizza, P., J. W. Biggar, M. Th. van Genuchten, P. J. Wierenga, H. M. Selim, J. M. Davidson, and D. R. Nielsen. 1983. Modeling Tritium and Chloride 36 Transport Through an Aggregated Oxisol. *Water Resour. Res.* 19(3):691-700.
- Norris, J. R., and H. Swain. 1971. In: *Methods in Microbiology*, Vol 5A, J. R. Norris and D. W. Ribbons, eds. Academic Press, London. pp. 105-133.
- Oliveira, L., A. Burns, T. Bisalputra, and K. Yang. 1983. The Use of Ultra-Low Viscosity Medium (VCD/HXSA) in the Rapid Embedding of Plant Cells for Electron Microscopy. *J. Microscopy* 132(2):195-202.
- Parsons, F. and G. B. Lage. 1985. Chlorinated Organics in Simulated Groundwater Environments. *J. Am. Water Works Assoc.* 77(5):52-59.
- Patel, R. N. 1984. Methane Monooxygenase from *Methylobacterium* sp. Strain CRL-26. In: *Microbial Growth on C1 Compounds: Proceedings of the 4th International Symposium*, R. L. Crawford and R. S. Hanson, eds. American Society for Microbiology, Washington, D.C. pp. 83-90.

- Patel, R. N., C. T. Hou, A. I. Laskin, A. Felix, and P. Derelanko. 1979. Microbial Oxidation of Gaseous Hydrocarbons. II. Hydroxylation of Alkanes and Epoxidation of Alkenes by Cell-Free Particulate Fractions of Methane-Utilizing Bacteria. *J. Bacteriol.* 139: 675-679.
- Patel, R. N., C. T. Hou, A. I. Laskin, and A. Felix. 1982. Microbial Oxidation of Hydrocarbons: Properties of a Soluble Methane Monooxygenase from a Facultative Methane-Utilizing Organism *Methylobacterium* sp. Strain CRL-26. *Appl. Environ. Microbiol.* 44:1130-1137.
- Press, F., and R. Siever. 1974. *Earth*. Freeman & Co., San Francisco.
- Prior, S. D., and H. Dalton. 1985. The Effect of Copper Ions on Membrane Content and Methane Monooxygenase Activity in Methanol-Grown Cells of *Methylococcus capsulatus* (bath). *J. Gen. Microbiol.* 131:155-163.
- Quayle, J. R. 1972. The Metabolism of One-Carbon Compounds by Microorganisms. *Adv. Microb. Physiol.* 7:119-203.
- Rao, P. S. C., D. E. Rolston, R. E. Jessup, and J. M. Davidson. 1980. Solute Transport in Aggregated Porous Media: Theoretical and Experimental Evaluation. *Soil Sci. Soc. Am. J.* 44:1139-1146.
- Rasmuson, A., and I. Neretnieks. 1980. Exact Solution of a Model for Diffusion in Particles and Longitudinal Dispersion in Packed Beds. *AIChE J.* 26(4):686-690.
- Raymond, R. L. 1974. Reclamation of Hydrocarbon Contaminated Groundwaters. United States Patent Office, Pat. No. 3,846,290, Nov. 5, 1974.
- Raymond, R. L., V. W. Jamison, and J. O. Hudson. 1976. Beneficial Stimulation of Bacterial Activity in Groundwaters Containing Petroleum Products. *AIChE Symp. Series* 73:390.
- Rittmann, B. E., and P. L. McCarty. 1980. Model of Steady-State Biofilm Kinetics. *Biotechnol. Bioeng.* 22:2343-2357.
- Roberts, P. V., and D. M. Mackay, eds. 1986. A Natural Gradient Experiment on Solute Transport in a Sand Aquifer. Technical Report No. 292, Department of Civil Engineering, Stanford University, Stanford, CA.
- Roberts, P. V., P. L. McCarty, M. Reinhard, and J. Schreiner. 1980. Organic Contaminant Behavior During Groundwater Recharge. *J. WPCF* 52:161-172.
- Roberts, P. V., M. N. Goltz, and D. M. Mackay. 1986. A Natural Gradient Experiment on Solute Transport in a Sand Aquifer. III. Retardation Estimates and Mass Balances for Organic Solutes. *Water Resour. Res.* 22(13):2047-2058.
- Roels, J. A. 1983. *Energetics and Kinetics in Biotechnology*. Elsevier Biomed Press, New York.
- Schwarzenbach, R. P., and J. Westall. 1981. Transport of Non-Polar Organic Compounds from Surface Water to Groundwater. *Env. Sci. Technol.* 15(11):1360-1367.
- Semprini, L., P. V. Roberts, G. D. Hopkins, and D. M. Mackay. 1988. A Field Evaluation of in-situ Biodegradation for Aquifer Restoration. EPA/600/S2-87/096. NTIS No. PB 88-130 257/AS. Springfield, VA.
- Semprini, L., P. V. Roberts, G. D. Hopkins, and P. L. McCarty. 1989. A Field Evaluation of in-situ Biodegradation Methodologies for Aquifer Contaminated with Chlorinated Aliphatic Compounds:

Part 2: The Results of Biostimulation and Biotransformation Experiments. Submitted to Ground Water.

- Siegrist, H., and P. L. McCarty. 1987. Column Methodologies for Determining Sorption and Biotransformation Potential for Chlorinated Aliphatic Compounds in Aquifers. *J. Contaminant Hydrol.* 2:31-50.
- Sing, K. S. W., and D. Swallow. 1960. Krypton Adsorption and Surface Area of Silica. *J. Appl. Chem.* 10:171-175.
- Speitel, G. E., Jr., K. Dovantzis, and F. A. DiGiano. 1987. Mathematical Modeling of Bioregeneration of GAC Columns. *J. Env. Eng. (ASCE)* 113(1):32-48.
- Stehfest, H. 1970. Algorithm 368 Numerical Inversion of Laplace Transforms. *J. ACM* 13(1):47-49.
- Stirling, D. I., and H. Dalton. 1979. The Fortuitous Oxidation and Cometabolism of Various Carbon Compounds by Whole-Cell Suspensions of *Methylococcus capsulatus* (bath). *FEMS Microbiol. Lett.* 5:315-318.
- Stirling, D. I., J. Colby, and H. Dalton. 1979. A Comparison of the Substrate and Electron-Donor Specificities of the Methane Monooxygenase from Three Strains of Methane-Oxidizing Bacteria. *Biochem. J.* 177:361-364.
- Suidan, M. T., B. E. Rittmann, and U. K. Traegner. 1987. Criteria Establishing Biofilm Kinetic Types. *Water Resour. Res.* 21(4):491-498.
- Tonge, G. M., D. E. F. Harrison, and I. J. Higgins. 1975. Properties and Partial Purification of the Methane-Oxidizing Enzyme System from *Methylosinus trichosporium*. *FEBS Lett.* 58:293-299.
- U.S. Environmental Protection Agency. 1984. National Revised Primary Drinking Water Regulations, Volatile Synthetic Organic Chemicals in Drinking Water; Proposed Rulemaking. *Fed. Reg.* 49:24329-24355.
- U.S. Environmental Protection Agency. 1985. National Primary Drinking Water Regulations; Volatile Synthetic Organic Chemicals. Final Rule 40 CFR 141. *Fed. Reg.* 50:46880-46901.
- Valocchi, A. J. 1986. Effect of Radial Flow on Deviation from Local Equilibrium During Sorbing Solute Transport through Homogeneous Soils. *Water Resour. Res.* 22:1693-1701.
- Valocchi, A. J., and P. V. Roberts. 1983. Attenuation of Groundwater Contaminant Pulses. *J. Hydrol. Eng. (ASCE)* 109(12):1665-1682.
- van Genuchten, M. Th. 1981. Non-Equilibrium Transport Parameters from Miscible Displacement Experiments. Research Report 119, U.S. Salinity Lab., Riverside, CA.
- van Genuchten, M. Th. 1985. A General Approach for Modeling Solute Transport in Structured Soils. In: *Hydrogeology of Rocks of Low Permeability*, Proc. 17th Int. Congress, Int. Association of Hydrogeologists, Tucson, AZ, January.
- van Genuchten, M. Th., and W. J. Alves. 1982. Tech. Bull. No. 1661, U.S. Department of Agriculture. p. 151.
- van Genuchten, M. Th., and P. J. Wierenga. 1976. Mass Transfer Studies in Sorbing Porous Media: I. Analytical Solutions. *Soil Sci. Soc. Am. J.* 40(4):473-480.

- van Genuchten, M. Th., J. M. Davidson, and P. J. Wierenga. 1974. An Evaluation of Kinetic and Equilibrium Equations for the Prediction of Pesticide Movement through Porous Media. *Soil Sci. Soc. Am. Proc.* 38:29-35.
- Vogel, T. M., and P. L. McCarty. 1985. Biotransformation of Tetrachloroethylene to Trichloroethylene, Dichloroethylene, Vinyl Chloride, and Carbon Dioxide under Methanogenic Conditions. *Appl. Environ. Microbiol.* 49:1080-1083.
- Vogel, T. M. and P. L. McCarty. 1987. Abiotic and Biotic Transformations of 1,1,1-Trichloroethane under Methanogenic Conditions. *Env. Sci. Techn.* 21:1208-1213.
- Vogel, T. M., C. S. Criddle, and P. L. McCarty. 1987. Transformations of Halogenated Aliphatic Compounds. *Env. Sci. Techn.* 21(8):722-736.
- Webster, J. J., G. J. Hampton, J. T. Wilson, W. C. Ghiorse, and F. R. Leach. 1985. Determination of Microbial Cell Numbers in Subsurface Samples. *Ground Water* 23(1):17-25.
- Westrick, J. J., J. W. Mello, and R. F. Thomas. 1984. The Groundwater Supply Survey. *J. Am. Water Works Assoc.* 76(5):52-59.
- Whittenbury, R., K. C. Phillips, and J. F. Wilkinson. 1970. Enrichment, Isolation, and Some Properties of Methane-Utilizing Bacteria. *J. Gen. Microbiol.* 24:225-233.
- Wilkinson, T. G., H. H. Topiwala, and G. Hamer. 1974. Interactions in a Mixed Bacterial Population Growing on Methane in Continuous Culture. *Biotechnol. Bioeng.* 16:41-59.
- Wilson, J. T., and B. H. Wilson. 1985. Biotransformation of Trichloroethylene in Soil. *Appl. Environ. Microbiol.* 29:242-243.
- Wilson, J. T., J. F. McNabb, D. L. Balkwill, and W. C. Ghiorse. 1983. Enumeration and Characterization of Bacteria Indigenous to a Shallow Water Table Aquifer. *Ground Water* 21(2):134-141.
- Wilson, J. T., L. F. Leach, M. J. Henson, and J. N. Jones. 1986. In-situ Bioremediation as a Ground-Water Remediation Technique. *Ground Water Monit. Rev.*, Fall. p 56.
- Wilson, J. T., S. Fogel, and P. V. Roberts. 1987. Biological Treatment of Trichloroethylene in situ. In: *Proceedings: Symposium on Groundwater Contamination, ASCE National Convention, Atlantic City, NJ, April 27-30.*
- Wolfe, R. S., and I. J. Higgins. 1979. Microbial Biochemistry of Methane--a Study in Contrasts. *Int. Rev. Biochem.* 21:267-300.
- Wu, S-C., and P. M. Gschwend. 1986. Sorption Kinetics of Hydrophobic Organic Compounds to Natural Sediments and Soils. *Env. Sci. Techn.* 20:717-725.
- Wu, S-C., and P. M. Gschwend. 1988. Numerical Modeling of Sorption Kinetics of Organic Compounds to Soil and Sediment Particles. *Water Resour. Res.* 24:1373-1383.